UNIVERSITY OF LONDON THESIS

Degree PhD Year 2007 Name of Author POWELL, Howell William Robert

INVESTIGATING BRAIN STRUCTURE AND FUNCTION IN TEMPORAL LOBE EPILEPSY

Howell William Robert Powell, MA MBBS MRCP

DEPARTMENT OF CLINICAL AND EXPERIMENTAL EPILEPSY,

INSTITUTE OF NEUROLOGY, UNIVERSITY COLLEGE LONDON

THESIS SUBMITTED TO THE UNIVERSITY OF LONDON FOR THE DEGREE OF DOCTOR OF PHILOSOPHY, 2006

ProQuest LLC
789 East Eisenhower Parkway
P.O. Box 1346
Ann Arbor, MI 48106-1346

PERSONAL CONTRIBUTION

I, Robert Powell, confirm that the work presented in this thesis is my own. Where information has been derived from other sources, I confirm that this has been indicated in the thesis. Although the work reflects the contributions of a team of researchers, I have outlined my individual contribution below.

I was responsible for recruitment and data acquisition on all subjects studied. I performed all data analyses described in the thesis and was responsible for archiving the data. I performed all statistical analyses and was responsible for producing all the figures and graphical presentation of the data. All results and interpretations were presented by myself and developed following discussions at regular supervision meetings.

ABSTRACT

Background

Anterior temporal lobe resection (ATLR) is increasingly used in the treatment of patients with refractory temporal lobe epilepsy (TLE). Complications of surgery include a decline in language and memory abilities, and visual field defects. The principal aim of this thesis was to use magnetic resonance imaging (MRI) techniques to improve the planning of effective surgical treatment for patients with TLE by using functional MRI to localise areas in the brain involved in language and memory function, and MR-tractography to investigate the structural connections of these areas and those involved in visual function.

Methods

Ten control subjects underwent tractography to study the connections of the medial temporal lobe (MTL). Two patients underwent tractography pre- and post-operatively to look at the trajectory of the optic radiation. For the memory studies we scanned 10 control subjects and 15 presurgical patients with refractory TLE. For the combined language fMRI and tractography study, 10 control subjects and 14 patients with hippocampal sclerosis underwent both fMRI and tractography. All scans were performed on a 1.5T GE Signa Horizon scanner.

Findings

The connections of the MTL were identified in a group of control subjects. The optic radiation was mapped preoperatively and shown to be disrupted following ATLR in a patient with a visual field defect. A material-specific lateralisation of memory encoding activation was demonstrated in control subjects with reduced ipsilateral activation in patients with TLE. Increased ipsilateral hippocampal activation correlated with better preoperative memory function and with greater postoperative memory decline. fMRI and tractography were combined to study the structural connections of functional language areas in controls and TLE patients, demonstrating reduced left sided and increased right hemisphere connections in left TLE patients, findings that reflected the pattern of functional activation.

INVESTIGATING BRAIN STRUCTURE AND FUNCTION IN TEMPORAL LOBE EPILEPSY

TABLE OF CONTENTS

TABLES

FIGURES

ABBREVIATIONS

ADC	Apparent diffusion coefficient
AED	Antiepileptic drug
AI	Asymmetry index
ANOVA	Analysis of variance
ATLR	Anterior temporal lobe resection
BA	Brodmann area
BOLD	Blood oxygenation level-dependent
CA	Cornu Ammonis
CCEP	Cortico-cortical evoked potentials
CNS	Central nervous system
CPS	Complex partial seizure
CSF	Cerebrospinal fluid
CT	Computed tomography
DNET	Dysembryoplastic neuroepithelial tumour
DTI	Diffusion tensor imaging
DWI	Diffusion weighted imaging
ECG	Electrocardiogram
ECS	Electrocortical stimulation
EEG	Electroencephalography
EPI	Echo planar imaging
FA	Fractional anisotropy
FE	Frequency encoding
fMRI	Functional magnetic resonance imaging
FMT	Fast marching tractography
FWHM	Full width half maximum
GCD	Granule cell dispersion
GTCS	Generalised tonic-clonic seizures

HERA	Hemispheric encoding/retrieval asymmetry
HIPER	Hippocampal encoding/retrieval
HRF	Haemodynamic response function
HS	Hippocampal sclerosis
IAT	Intracarotid amytal test
ICEES	International Classification of the Epilepsies and Epileptic Syndromes
ICES	International Classification of Epileptic Seizures
IFG	Inferior frontal gyrus
IGE	Idiopathic generalized epilepsy
ILAE	International League Against Epilepsy
LGB	Lateral geniculate body
MCD	Malformations of cortical development
MD	Mean diffusivity
MFG	Middle frontal gyrus
MNI	Montreal Neurological Institute
MRI	Magnetic resonance imaging
MTL	Medial temporal lobe
MTLE	Medial temporal lobe epilepsy
NMR	Nuclear magnetic resonance
OR	Optic radiation
PD	Proton density
PDF	Probability density function
PE	Phase encoding
PET	Positron emission tomography
PFC	Prefrontal cortex
PHG	Parahippocampal gyrus
PICo	Probabilistic index of connectivity
RCI	Reliable change index

RF	Radiofrequency
ROI	Region of interest
SLF	Superior longitudinal fasciculus
SNR	Signal to noise ratio
SPECT	Single photon emission computed tomography
SPM	Statistical parametric mapping
SPS	Simple partial seizure
SS	Slice selection
STG	Superior temporal gyrus
SVC	Small volume correction
TE	Echo time
TR	Repetition time
TLE	Temporal lobe epilepsy
VBM	Voxel based morphometry
VFD	Visual field defect
WHO	World Health Organisation

ORIGINAL ARTICLES

Powell HWR, Guye M, Parker GJM, Symms MR, Boulby PA, Koep MJ, Barker GJ, Duncan JS. Noninvasive in vivo demonstration of the connections of the human parahippocampal gyrus. **Neuroimage** 2004;22:740-747.

Powell HWR, Koepp MJ, Symms MR, Boulby PA, Salek-Haddadi A, Thompson PJ, Duncan JS, Richardson MP. Material-specific lateralization of memory encoding in the medial temporal lobe: blocked versus event-related design. **Neuroimage** 2005;27:231-239.

Powell HWR, Parker GJM, Alexander DC, Symms MR, Boulby PA, Wheeler-Kingshott CA, Barker GJ, Koepp MJ, Duncan JS. MR tractography predicts visual field defects following temporal lobe resection. **Neurology** 2005;65:596-599.

Powell HWR, Parker GJM, Alexander DC, Symms MR, Boulby PA, Wheeler-Kingshott CA, Barker GJ, Noppeney U, Koepp MJ, Duncan JS. Hemispheric asymmetries in language-related pathways: a combined functional MRI and tractography study. **Neuroimage** 2006;32:388-399.

Powell HWR, Parker GJM, Alexander DC, Symms MR, Boulby PA, Wheeler-Kingshott CA, Barker GJ, Koepp MJ, Duncan JS. Abnormalities of language networks in temporal lobe epilepsy. **Neuroimage** 2007;36:209-221.

Powell HWR, Richardson MP, Symms MR, Boulby PA, Thompson PJ, Duncan JS, Koepp MJ. Reorganisation of verbal and non-verbal memory in temporal lobe epilepsy. **Epilepsia** 2007.

Powell HWR, Richardson MP, Symms MR, Boulby PA, Thompson PJ, Duncan JS, Koepp MJ. Preoperative fMRI predicts memory decline following anterior temporal lobe resection. Submitted to **J Neurol Neurosurg Psychiatry** 05/07.

REVIEW ARTICLES

Powell HWR, Koepp MJ, Richardson MP, Symms MR, Thompson PJ, Duncan JS. The application of functional MRI of memory in temporal lobe epilepsy: a clinical review. **Epilepsia** 2004;45:855-863.

Powell HWR, Duncan JS. Functional magnetic resonance imaging for assessment of language and memory in clinical practice. **Curr Opin Neurol** 2005;18:161-166.

ABSTRACTS

Powell HWR, Guye M, Parker GJM, Symms MR, Boulby PA, Koep MJ, Barker GJ, Duncan JS. Noninvasive in vivo demonstration of the connections of the human parahippocampal gyrus. International League Against Epilepsy, British Chapter, Manchester 2003. Book of abstracts p26.

Powell HWR, Guye M, Parker GJM, Symms MR, Boulby PA, Koep MJ, Barker GJ, Duncan JS. Noninvasive in vivo demonstration of the connections of the human parahippocampal gyrus. **Epilepsia** 2003;44(suppl 9):257. American Epilepsy Society Meeting, Boston.

Powell HWR, Richardson MP, Thompson PJ, Symms MR, Duncan JS, Koepp MJ. Reorganisation of verbal and non-verbal memory in unilateral temporal lobe epilepsy: An event-related study. **Neuroimage** 2004;22(suppl 1):S34. Human Brain Mapping Meeting, Budapest.

Powell HWR, Richardson MP, Thompson PJ, Symms MR, Duncan JS, Koepp MJ. Reorganisation of verbal and non-verbal memory in unilateral temporal lobe epilepsy: An event-related study. **Epilepsia** 2004;45(suppl 7):292. American Epilepsy Society meeting, New Orleans.

Powell HWR, Koepp MJ, Symms MR, Boulby PA, Salek-Haddadi A, Thompson PJ, Duncan JS, Richardson MP. Material-specific lateralization of memory encoding in the medial temporal lobe: blocked versus event-related design. **Neurology** 2005; American Academy of Neurology meeting, Miami.

Powell HWR, Parker GJM, Alexander DC, Symms MR, Boulby PA, Wheeler-Kingshott CA, Barker GJ, Koepp MJ, Duncan JS. MR tractography predicts visual field defects following temporal lobe resection. **J Neurol Neurosurg Psychiatry** 2005;76:1319. Association of British Neurologists, Spring Meeting, Belfast.

Powell HWR, Parker GJM, Alexander DC, Symms MR, Boulby PA, Wheeler-Kingshott CA, Barker GJ, Koepp MJ, Duncan JS. MR tractography predicts visual field defects following temporal lobe resection. International Leaugue Against Epilepsy, British Chapter, Belfast 2005. Book of abstracts, p61.

Powell HWR, Parker GJM, Alexander DC, Symms MR, Boulby PA, Wheeler-Kingshott CA, Barker GJ, Noppeney U, Koepp MJ, Duncan JS. Combined fMRI and tractography reveal asymmetries in language pathways. **Proc Intnl Soc Magn Res** 2005;13:174. ISMRM meeting, Miami.

Powell HWR, Parker GJM, Alexander DC, Symms MR, Barker GJ, Koepp MJ, Duncan JS. Diffuse language pathway abnormalities in temporal lobe epilepsy. European Congress on Epileptology, Helsinki 2006. Book of abstratcts, p152.

Powell HWR, Parker GJM, Alexander DC, Symms MR, Barker GJ, Koepp MJ, Duncan JS. Diffuse language pathway abnormalities in temporal lobe epilepsy. International Leaugue Against Epilepsy, British Chapter, Newcastle 2006. Book of abstracts, p26.

Powell HWR, Richardson MP, Symms MR, Boulby PA, Thompson PJ, Duncan JS, Koepp MJ. Preoperative fMRI predicts memory decline following anterior temporal lobe resection. International Leaugue Against Epilepsy, British Chapter, Newcastle 2006. Book of abstracts, p27.

Powell HWR, Richardson MP, Symms MR, Boulby PA, Thompson PJ, Duncan JS, Koepp MJ. Preoperative fMRI predicts memory decline following anterior temporal lobe resection. **J Neurol Neurosurg Psychiatry** *in press*. Association of British Neurologists, Autumn Meeting, London, 2006. Book of abstratcts, p30.

Powell HWR, Parker GJM, Alexander DC, Symms MR, Barker GJ, Koepp MJ, Duncan JS. Diffuse language pathway abnormalities in temporal lobe epilepsy. **J Neurol Neurosurg Psychiatry** *in press*. Association of British Neurologists, Autumn Meeting, London, 2006. Book of abstratcts, p78.

ACKNOWLEDGEMENTS

It has been a pleasure to work as part of the Department of Clinical and Experimental Epilepsy during my period of research and I am grateful to a number of people who have helped make this such an enjoyable and rewarding experience. Professor John Duncan provided direction, encouragement, clarity of vision and humour throughout. He provided me with opportunities to present my work at international meetings and I am especially grateful for his support and help with future career plans.

Both my supervisors became good friends during the course of this study. Dr Matthias Koepp, my principal supervisor, could not have been more approachable, was always available for discussion and was a consistent source of helpful advice and ideas. His enthusiasm and ability to see the bigger picture were of great help when problems arose. Dr Mark Symms, my co-supervisor, was responsible for developing all the acquisition sequences used in this work. From day one, when he showed me how turn on my Sun workstation, he was always on hand to help with a number of methodological problems and was a source of expertise in both MR physics and anti-Welsh humour.

Dr Phil Boulby spent many hours patiently solving problems and developed the high resolution sequences for use with the fMRI. I will be in touch with him as soon as I need a good accountant. Dr Mark Richardson was a great help in getting me started with fMRI; providing helpful advice with designing the fMRI paradigms, SPM analysis and results interpretation. Dr Pam Thompson performed all the patient neuropsychological assessments and was a source of insightful comments when writing up the findings.

Dr Geoff Parker developed the tractography algorithms used in this thesis and I am grateful to him for taking the time to come down to London from Manchester to install these and train me in their use. Professor Gareth Barker, Dr Danny Alexander and Dr Claudia Wheeler-Kingshott all made valuable methodological contributions to the diffusion tensor imaging and helpful comments with manuscripts, and I am grateful to Peter Gilford for IT assistance.

The patients were generously referred by Professor Ley Sander, Professor Simon Shorvon, Dr Sanjay Sisodiya, Dr Shelagh Smith and Dr Matthew Walker and expertly operated on by Mr William Harkness and Mr Andrew McEvoy, consultant Neurosurgeons at the National Hospital for Neurology and Neurosurgery.

It was always a pleasure to work with, and to do as I was told by the radiographers at the National Society for Epilepsy, Philippa Bartlett, Jane Burdett, Penny Hitchins and Elaine Williams, and to share an office with all the other research fellows at Chalfont and Queen Square. In particular I am grateful to Afraim Salek-Haddadi who guided me through SPM during the course of my first year and wrote a number of time-saving matlab scripts.

I am extremely grateful to all the patients and control subjects who volunteered enthusiastically to give up their time in order to participate in these studies. Their contribution to this work is greatest of all and it would not have been possible without their selflessness.

Funding for this project was provided by a Wellcome Trust Programme Grant.

Final thanks go to my family for their continued support and for giving me the reason to leave work on time every day; to my wife Nicola who has endured stoically a period of reduced family income, offering encouragement and understanding throughout, and my daughter Bethan for laughing at me on a daily basis.

CHAPTER I BACKGROUND

1.1 EPILEPSY

1.1.1 Definition

Epilepsy is the commonest serious neurological condition, affecting all ages, races and social classes. It is distributed worldwide with an overall incidence of around 50 cases per 100,000 persons per year in developed societies (1) and 100 per 100,000 in developing countries (2). The prevalence is about 5-10 cases per 1000 persons, with a lifetime prevalence of seizures of 2 to 5% (3).

An epileptic seizure is a transient event experienced by a subject as a result of an abnormal paroxysmal discharge of cerebral neurones. Epilepsy by definition is the continuing tendency to have such seizures and arises secondary to a variety of pathologic processes. Seizures have a wide range of clinical manifestations and classification of epilepsy has proved challenging.

1.1.2 Seizure classification

There are many reasons why seizure classification is important, both for the individual patient and for the advancement of knowledge of epilepsy. It allows communication within both the clinical and research setting and is also important for the diagnosis, prognosis and choice of treatment for any particular patient. Accurately identifying the type of seizures is the first step towards diagnosis in a patient with epileptic seizures. Classically, two seizure types have been recognised: those arising from focal cortical disturbances and those characterised by synchronous discharge of both hemispheres. These correspond to partial and generalised seizures and can be differentiated both clinically and by their electroencephalographic (EEG) findings. This division formed the basis of the revised International Classification of Epileptic Seizures (ICES), introduced by the International League Against Epilepsy (ILAE) in 1981 (4) (Table 1.1). This classification divides seizures into partial and generalised, with partial seizures subsequently divided further into 'simple' and 'complex', depending on whether consciousness is retained or lost.

In most surveys, partial seizures appear to be the most common seizure type, with complex partial and secondarily generalised seizures comprising around 60% of prevalent cases, primary generalised tonic-clonic seizures about 30%, and generalised absence and myoclonus less than 5% (3). These however

may be biased, being largely based on populations of patients with relatively severe epilepsy, including large numbers with focal epilepsy. For less severe cases it is often more difficult to determine clinically and electroencephalographically whether it is of primary generalised or focal type.

1.1.3 Syndromic diagnosis of epilepsy

Seizure diagnosis alone cannot however provide accurate guidance on treatment, severity of disease and prognosis. An advance in modern epileptology has been the recognition of epileptic syndromes and diseases, each with different causes and prognoses, and requiring different short and long term management. The fact that epilepsy is not a single disease entity is recognised by the World Health Organization (WHO) Dictionary of Epilepsy (5), which gives this definition:

'Epilepsy is a chronic brain disorder of various aetiologies characterised by recurrent seizures due to excessive discharge of cerebral neurones (epileptic seizures), associated with a variety of clinical and laboratory manifestations. Single or occasional epileptic seizures (such as febrile convulsions and the seizures of puerperal eclampsia) as well as those occurring during an acute illness should not be classified as epilepsy.'

The Commission on Classification and Terminology of the ILAE simply describes epilepsy as:

'.... two or more seizures.'

Such broad definitions reveal the diagnostic inaccuracy of the term 'epilepsy', and the usefulness of a syndromic diagnosis.

'An epileptic syndrome is a cluster of seizures, other symptoms, physical signs and laboratory findings, which are associated in a non-fortuitous manner' (6).

Identification of an epileptic syndrome requires specific clinical information, including age of onset, seizure manifestations, precipitating factors, associated central nervous system (CNS) symptoms and signs, severity, and course. Findings from other investigations such as EEG and brain imaging also contribute.

The International Classification of the Epilepsies and Epileptic Syndromes (ICEES) (1989) (6) attempted to provide such a syndromic classification and recognises the heterogeneity of epilepsy. It specified over 40 distinct types of syndromes, classified both according to seizure type and aetiology. However this is

problematic due to overlap between syndromes, inadequate definitions of syndromes and the complexity of the classification. A Task Force for the classification and terminology concluded that the classification would need to be reviewed periodically based upon emerging new information and problems identified through use and it is anticipated that progress in the understanding of the basis of the epilepsies will lead to a revision of the current classification. The Task Force also proposed that the terms partial and localisation-related be replaced with 'focal' (7).

1.1.4 Aetiology

In the 1989 ILAE classification, both focal and generalised epilepsies and syndromes are divided according to aetiology into idiopathic, symptomatic and cryptogenic varieties. Idiopathic epilepsies are not associated with structural brain lesions, neurological abnormalities other than seizures, or cognitive impairment. Conversely, in symptomatic epilepsy, seizures are the consequence of a focal brain abnormality. Cryptogenic epilepsies are those in which a symptomatic aetiology is suspected but the aetiology is not known. The advances in neuroimaging over the past decade have allowed identification of an increasing number of underlying aetiologies and thus decreased the proportion of epilepsies and epilepsy syndromes considered to be cryptogenic. The 2001 Task Force proposed that the term cryptogenic be replaced by 'probable symptomatic epilepsy syndrome' to refer to syndromes believed to be symptomatic, but in which no aetiology has been identified (7).

Epilepsy may develop for a number of reasons with brain trauma, CNS infections, cerebrovascular disease and brain tumours all increasing the incidence of epilepsy. The aetiology varies considerably according to age. Onset of epilepsy during adult life is more commonly associated with an underlying neurological disorder than is the case with epilepsies developing in childhood. The aetiologies underlying focal epilepsy also vary according to geography, for example endemic infections such as neurocysticercosis are the commonest cause of epilepsy in parts of South America but are virtually unknown in Europe (8).

Any condition causing cortical disruption may lead to seizures. The aetiology may be multifactorial, with patients with an inherited predisposition more prone to the development of acquired conditions. A prospective cohort population-based study of patients with newly-diagnosed epilepsy in the United

Kingdom reported that the aetiology was cerebrovascular disease in 15%, cerebral tumour in 6%, alcohol-related in 6% and post-traumatic in 3% of patients (9). Notably, seizures were classed as cryptogenic in 62% of cases. Other neuropathological lesions associated with chronic epilepsy, including hippocampal sclerosis and malformations of cortical development will be considered in more detail in the next chapter.

Although the majority of epilepsies lack an overt genetic cause, underlying genetic contributions to aetiology have been estimated to be present in about 40% of patients with epilepsy (10), and are particularly important in the idiopathic generalised epilepsies (IGE). There are over 200 Mendelian diseases which include epilepsy as part of the phenotype although these account for less than 1% of all epilepsies (10). Many of these, such as tuberous sclerosis, are associated with structural lesions although several families exhibiting idiopathic epilepsy transmitted in a Mendelian manner have recently been found to have mutations in single genes. They are all dominantly inherited and all but one code for ion channels, underlying the importance of these signalling proteins in determining the excitability of neuronal circuits (11). The theory of a genetically determined increased excitability of neuronal circuits provides an attractive explanation why otherwise normal individuals should develop unprovoked seizures without an identifiable locus of onset.

Although this pattern of Mendelian inheritance is rare, first degree relatives of patients with IGE have a roughly two- to threefold elevated risk of being affected (12). Twin studies in developed countries have shown monozygotic concordance rates greater than 40% (13) although this was lower when attention was restricted to relatives with the same syndromic diagnosis. Where these patterns of complex inheritance exist the interaction of certain susceptibility genes with environmental factors is likely to be important. At present a number of large families with many affected members are currently under investigation and it is likely that further genes will be identified, some of which will be responsible for monogenic epilepsy and others that turn out to be epilepsy susceptibility genes.

Table 1.1 International Classification of Seizures (Commission on Classification and Terminology of the International League Against Epilepsy, 1981). Modified version.

Partial seizures beginning locally

Simple (consciousness not impaired)
- With motor symptoms
- With somatosensory or special sensory symptoms
- With autonomic symptoms
- With psychic symptoms

Complex (with impairment of consciousness)
- Beginning as simple partial seizure (progressing to complex seizure)
- Impairment of consciousness at onset
  a) Impairment of consciousness only
  b) With automatism

Partial seizures becoming secondarily generalised

Generalised seizures

Absence seizures
- Typical
- Atypical

Myoclonic seizures

Clonic seizures

Tonic seizures

Tonic-clonic seizures

Atonic seizures

1.2 TEMPORAL LOBE EPILEPSY

1.2.1 Introduction

The proportion of focal epilepsy with seizures believed to originate in the temporal lobe is about 60-70%. Temporal lobe epilepsy (TLE) is characterised by recurrent simple and complex partial seizures, of which a number of subclassifications exist. Some of these are rather complex, but the most widely accepted and useful distinction is between mesiobasal and lateral neocortical types. There is considerable overlap between the clinical features of these two and spread from lateral to medial cortex, and vice versa, is common. Medial TLE is by far the more frequent of the two and the commonest underlying pathology is hippocampal sclerosis (HS), also known as medial temporal sclerosis or Ammon's Horn sclerosis. This pathology is associated with febrile convulsions in childhood, and patients typically have medically refractory seizures but a predictably good outcome following anterior temporal lobe resections (ATLR).

1.2.2 Hippocampal structure and connections

The hippocampal formation is located in the medial part of the temporal lobe, lying on the floor of the temporal horn of the lateral ventricle. The hippocampus proper is composed of the four CA (Cornu Ammonis) subregions, CA 1-4, whereas the hippocampal formation includes the dentate gyrus, the CA subfields and subiculum (Figure 1.1). All hippocampal components are composed of simple three layered allocortex, which differentiates them from surrounding six layered medial temporal neocortex. The ventricular surface of the hippocampus is a layer of white matter called the alveus which is continuous with the fornix posteriorly and contains afferent and efferent axons. Adjacent to these lies the parahippocampal gyrus (PHG), which includes the entorhinal cortex, both of which are functionally related to the hippocampus (14).

The major input to the hippocampus is from the entorhinal cortex, via the perforant path to the dentate gyrus. From here, the dentate granule cells project to the CA3 field of the hippocampus via efferent mossy fibres. The CA3 pyramidal cells in turn project to the CA1 field. The neurotransmitter of these pathways is glutamate. Much of the input from the CA1 field is sent on to the subiculum which projects,

amongst other areas to the entorhinal cortex, creating a loop involving the hippocampus (Figure 1.6, page 100) (14).

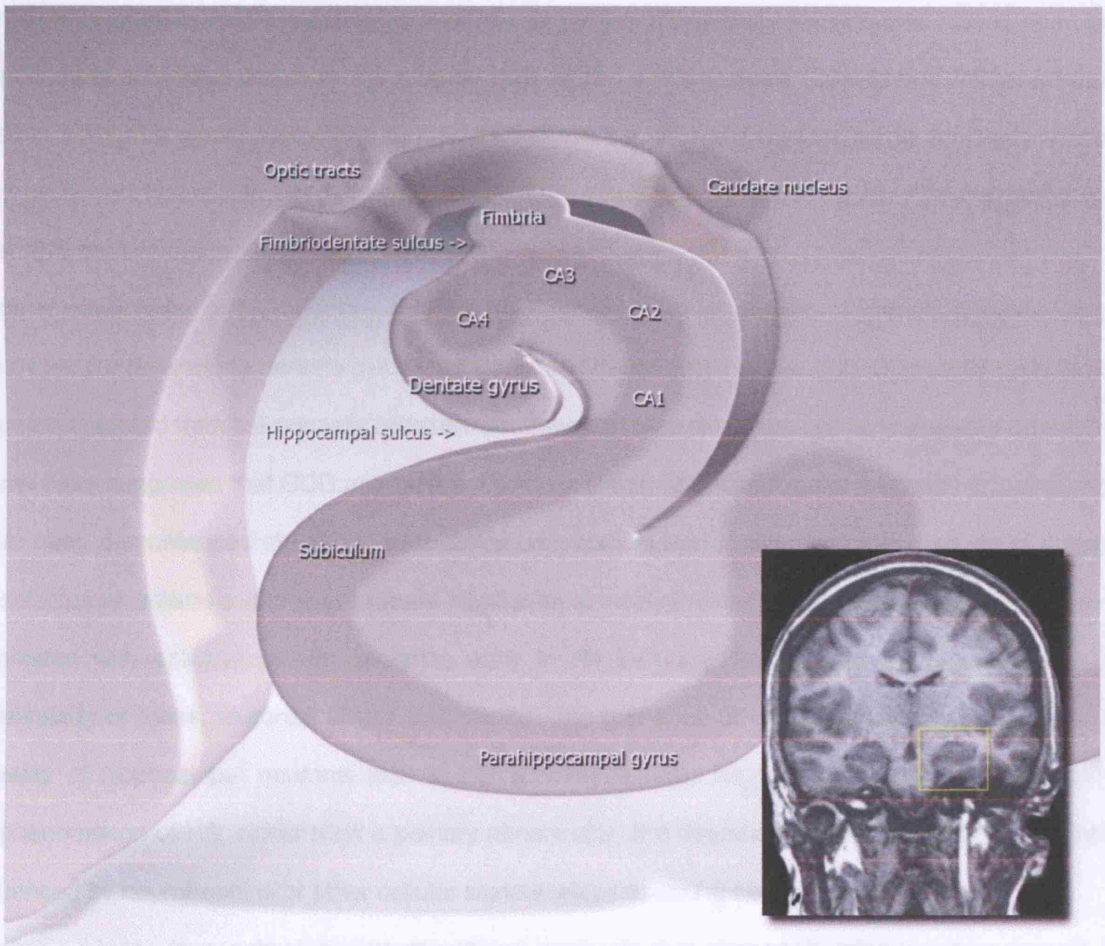

Figure 1.1 Structure of the hippocampus

1.2.3 Aetiology and pathology

1.2.3.1 Hippocampal sclerosis

HS is the commonest pathologically confirmed lesion in chronic TLE, and the expansion of surgical treatment of this type of epilepsy has resulted in increasing interest in HS (15). HS is typically unilateral and diffuse (16), affecting either hemisphere equally (17), although damage can be more localised, with the hippocampal body the most frequently affected region. If bilateral hippocampal atrophy is seen it is

often asymmetrical, with greater cell loss on the epileptogenic side (18). The classical pattern of cell loss seen in histological sections is of selective loss of pyramidal cells in the CA1 subfield and in the hilar region (including CA4 pyramidal cells) with accompanying astrocytic gliosis (19). Pyramidal cells of CA2 and dentate granule cells appear more resistant. In severe HS almost total neuronal loss is seen in all hippocampal subfields, including the granule cells of the dentate gyrus (20). In end folium sclerosis, seen in 3-4% of surgical cases, damage is centered on the hilus and dentate gyrus. It is important as it may be undetectable with neuroimaging, associated with a later onset of epilepsy and a worse post-operative seizure outcome (21).

Another observation in HS specimens is the disorganisation or dispersion of granule cells (GCD) into the molecular layer of the dentate gyrus, first described in detail by Houser (22). Dispersed granule cells appear separated from the normally compact cell layer and as a result the cell layer appears broadened. Some have suggested that GCD represents a primary abnormality of neuronal migration (23) and cases have been demonstrated of GCD in association with cortical malformations in the absence of a history of seizures or sclerosis and with bilateral hippocampal involvement (24). GCD has been shown to be correlated with epileptic events occurring early in life including febrile seizures (25) suggesting a vulnerability of these neurones at this time period. The presence of GCD also correlates well with the severity of hippocampal neuronal loss in HS specimens (26), suggesting that GCD represents an epiphenomenon of HS, rather than a primary abnormality, the migration of granule cells perhaps being influenced by neurotrophins or other cellular signals released during seizures (25).

Further evidence from animal models of epilepsy suggests that abnormally migrated granule cells are newly generated cells, neurogenesis being stimulated by the seizures (27). Studies have also confirmed that regeneration also occurs in human adult granule cells (28) and neuronal progenitor cells have been isolated from the dentate gyrus (29). It may be that this pool of precursor cells have important physiological functions, for example in memory and learning, but following stimulation by seizures, an increased rate of granule cell neurogenesis occurs leading to the abnormal cell localisation and reorganisation observed in HS (20).

Another neuropathological feature recognized in both rat models and humans and believed to be a key event in the development of chronic seizures, is the aberrant axonal reorganisation, or sprouting of

mossy fibres, the excitatory, glutamatergic axons of the dentate gyrus (30). More recent experimental findings however, in which mossy fibre sprouting is prevented, suggest that it is not an essential process to the generation of spontaneous recurrent seizures (31). Other theories involve alterations of neurotransmitter systems and inhibitory interneuronal populations (20), leading to a shifting of balance between excitation and inhibition towards excitation.

While the typical picture of HS is well established, the question of its aetiology, natural history and relationship to seizure genesis continues to be addressed. There is a strong association between the development of HS and a history of prolonged childhood febrile convulsions (32;33). This has led to the hypothesis that an initial precipitating injury irreversibly damages or alters the hippocampus and acts as a template for the progression to HS following a 'latent' interval. Furthermore the severity or degree of HS correlates with an earlier age of onset of seizures (34).

Other evidence suggests that an underlying malformation of the hippocampus predisposes to both HS and febrile convulsions. Evidence from neuroimaging has suggested subtle hippocampal malformations as a cause of familial febrile convulsions and subsequent hippocampal sclerosis (35), and HS has also been reported in patients in association with isolated malformations of the hippocampus (36). Other studies have demonstrated the coexistence of HS with subtle cytoarchitectural malformations in the neocortex, also called microdysgenesis (37). It is possible that these epileptogenic extra-hippocampal lesions 'kindle' the hippocampal neuronal loss, leading to the development of HS.

1.2.3.2 Malformations of cortical development

Malformations of cortical development (MCD) originate during intrauterine development as a result of a disturbance of the normal migration and differentiation of nerve cells from the germinal matrix to the cortex and result in a wide spectrum of structural abnormalities. As imaging techniques improve, MCDs are being increasingly recognized as an important cause of epilepsy (38). In subtle cases, such as patients with subependymal heterotopias or discreet areas of focal cortical dysplasia, seizures may be the only clinical sign, while patients with more severe MCD, e.g. lissencephaly or schizencephaly may have additional physical or learning disabilities. Dysembryoplastic neuroepithelial tumours (DNET)

typically present with medically refractory focal epilepsy starting in childhood. Lesions are commonly located in the MTL and are associated with good outcome following surgery (39).

1.2.4 Clinical features of MTLE

1.2.4.1 Seizure characteristics

These seizures can take the form of simple partial (aura alone with clear consciousness), or more commonly complex partial seizures (40). They tend to have a more gradual onset, slower evolution and longer duration (2-10 minutes) than extra-temporal complex partial seizures and typically consist of three components (41).

1.2.4.1.1 Aura

An aura can occur in isolation as a simple partial seizure (SPS) or as the initial manifestation of a complex partial seizure (CPS). It typically comprises visceral, cephalic, gustatory, dysmnestic, affective, perceptual or autonomic symptoms. Ascending epigastric sensations are particularly common. Autonomic symptoms, if present, include changes in skin colour, blood pressure, heart rate, and pupil size. There is usually no or severely reduced speech, but occasionally repetitive vocalisation with formed words may occur. Of affective symptoms, fear is the commonest and can be very intense; its occurrence is thought to indicate amygdala involvement. Other affective symptoms occurring in TLE include depression, anger and irritability.

1.2.4.1.2 Motor arrest

Motor arrest, or the 'motionless stare', is a prominent feature of progression of the aura (SPS) to a CPS. When the aura is short, this is often the first manifestation of the seizure noticed by eyewitnesses.

1.2.4.1.3 Automatism

Automatisms are semi-purposeful involuntary motor activity occurring during the state of clouding of consciousness either in the course of, or after, an epileptic seizure. Automatisms in TLE are typically less violent than in frontal lobe seizures, and are usually oro-alimentary (e.g. lip-smacking, chewing,

swallowing) or gestural (e.g. fumbling, fidgeting, repetitive motor actions, undressing, walking, and sexually-directed actions). They can sometimes be prolonged or semi-purposeful, e.g. rearranging items on a desk. Limb automatisms are usually ipsilateral to the focus, with contralateral dystonic posturing. Generally, vocalisation of identifiable words suggests a non-dominant seizure focus.

Post-ictal confusion and headache are common and if dysphasia is present after the seizure, this is a useful lateralising sign indicating seizure origin in the dominant temporal lobe. Another useful lateralising sign in the post-ictal phase is nose-rubbing which is ipsilateral to the focus in 90% of cases (42). Amnesia is almost invariable even though a patient may not recognize that consciousness was fully lost, and psychiatric or behavioural disturbances may accompany the epilepsy. Secondary generalisation is much less common than in extratemporal lobe epilepsy (particularly frontal lobe epilepsy), but psychiatric or behavioural disturbances are more common.

1.2.4.2 Memory impairment in MTLE

People with epilepsy have an increased risk of cognitive impairments and memory difficulties are the most frequently reported and assessed cognitive problem in TLE patients. The hippocampus and related medial temporal lobe (MTL) structures are critical for the encoding of episodic declarative memory for subsequent long term storage (43). Studies from amnesic patients and targeted lesions in animals have provided evidence for a dissociation in function between the dominant (usually the left) MTL, mediating verbal memory (44) and non-dominant (usually the right) MTL mediating non-verbal or visual memory (45). As a result left sided TLE is typically characterised by verbal memory deficits (46) and right sided TLE by non-verbal, or visuo-spatial (47;48) memory deficits.

A number of factors may contribute to the memory deficits seen in epilepsy. These include the underlying pathological lesion which may be stable or progressive and tend to cause irreversible impairment, and functional changes such as interictal discharges, ongoing seizures and anti-epileptic medications, the effects of which are potentially reversible (49). Some studies have suggested that cognition is already affected at disease onset, suggesting that the underlying disease causes a baseline cognitive deficit (50) which may then change in the long term course of the disease. The 'cause' of the epilepsy may be confused as a predictor with 'age at onset', given that the onsets of epilepsy disorders

due to different causes peak in different age groups. When grouped according to age of onset, patients with onset in early childhood had worse memory (51).

A longitudinal study looking at a large number of medically and surgically treated TLE patients found that chronic TLE was associated with progressive memory impairment (52). Surgery, particularly if unsuccessful, accelerated the decline, however memory decline may be stopped if seizures were fully controlled. In another study of a large group of patients with severe epilepsy, the presence of generalised tonic-clonic seizures was the strongest predictor of cognitive decline, while periods of seizure remission were associated with a better cognitive outcome (53).

Early neuropsychological assessment of these patients is advisable, both in aiding diagnosis and to help identify any cognitive difficulties which may exist in order to set realistic employment and educational goals. Furthermore, when difficulties are found it may be possible to devise strategies to minimise the detrimental impact which that deficit may have on functioning in daily life.

1.2.4.3 Psychiatric problems in MTLE

A number of TLE patients develop psychiatric disorders, most commonly depression, anxiety and psychotic disturbances. These can be classified according to how they relate in time to seizure occurrence, i.e. ictal, peri-ictal or inter-ictal.

1.2.4.3.1 Ictal

Anxiety, depression and hallucinations can occur as a direct manifestation of a seizure. These are usually brief and stereotyped and treatment is aimed at adequate seizure control.

1.2.4.3.2 Peri-ictal

Pre-ictal mood changes can last a few hours, and sometimes up to a few days before a seizure and are usually relieved by the seizure. Post-ictal psychiatric disturbances are more likely to occur following clusters of seizures, generalised seizures or status epilepticus.

Post-ictal confusion is characterised by impaired awareness/consciousness and diffuse EEG slowing without ictal discharges. These episodes are usually brief and common after complex partial or

generalised tonic-clonic seizures. Aggressive behaviour may occur and is usually undirected or resistive and the patient is likely to be amnesic for the event.

Post-ictal depression can last longer than other post-ictal states (up to two weeks). Symptoms range from mild to severe and may involve suicidal behaviour. It has been reported to occur more commonly with right-sided temporal or frontal foci (54). Post-ictal anxiety and mania are less common and shorter in duration.

The prevalence of post-ictal psychosis has been estimated to be 6-10% in patients with epilepsy, and is usually seen in TLE (55). It typically occurs after a cluster of complex partial seizures and there is usually a period of lucidity (12-72 hours), prior to the onset of psychosis. The psychotic symptoms include delusions, hallucinations, thought disorder or mania, which are usually transient but can last several weeks. It has also been reported that some patients with recurrent episodes of post-ictal psychosis may develop an inter-ictal psychosis (56). Mechanisms are unknown but may be related to transient neurochemical changes as a result of seizures. Treatment of acute post-ictal psychosis may require short courses of benzodiazepines or antipsychotics. Improving seizure control would be the long-term goal.

1.2.4.3.3 Inter-ictal

Depression is the commonest psychiatric disorder seen in epilepsy, occurring in up to 40% of patients (57) and is more common in TLE than in generalised epilepsy. Presentation can be with typical depressive symptoms including persistent low mood, anhedonia, loss of interest and biological symptoms of sleep or appetite disturbance, however some patients can present with atypical symptoms, referred to as inter-ictal dysphoric disorder (58). This is characterised by chronic intermittent dysthymia, irritability and anxiety symptoms. Treatment for depression includes psychological interventions such as counselling, psychotherapy or cognitive/behaviour therapy if appropriate. For more severe depression, antidepressant medications are needed but should be used cautiously because of the potential risk of lowering seizure threshold. Overall selective serotonin reuptake inhibitors are less likely to be epileptogenic than tricyclic antidepressants.

Inter-ictal anxiety disorders, such as panic disorder, generalised anxiety, agoraphobia, social phobia and obsessive compulsive disorder can occur in TLE, especially with left-sided foci. Psychosocial difficulties, social stigma and unpredictable seizures may also contribute to anxiety symptoms.

The prevalence of inter-ictal psychosis is reported to be 4-10% in patients with epilepsy, and is mainly seen in TLE (59). It is a chronic disorder and clinically resembles chronic schizophrenia. The onset of the psychosis is variable but usually occurs after many years of epilepsy (more than ten years). The risk factors that have been reported are early age of onset of epilepsy, bilateral temporal foci and a refractory course. It has been more commonly associated with left-sided epileptic focus (60). Treatment with antipsychotic medications is usually long term. The atypical antipsychotic drugs are potentially less likely to reduce seizure threshold (with the exception of clozapine) or cause extrapyramidal side effects. Lower doses than those used in primary schizophrenia seem to be effective. Psychosocial support and family education are also important.

1.2.5 EEG features of MTLE

The most common interictal EEG abnormalities seen in MTLE are anterior or mid-temporal spikes. Other changes include intermittent or persisting slow activity over the temporal lobes. These changes can be bilateral in about one-third of cases, but are usually more marked ipsilateral to the focus. While the ictal EEG would be expected to demonstrate abnormalities, seizures may occur without scalp EEG changes in 10-30% of cases (61). A number of different abnormalities may occur, including runs of spike discharges or fast activity, generalised or focal desynchronisation (flattening), bilateral synchronous spikes, localised spike-wave complexes, and rhythmic slow activity (61). Postictally, the EEG may exhibit focal or generalised slow activity or return rapidly to normal. The spike discharges may be localised over the area of focal onset or may occur widely. Bilateral temporal spikes may commonly occur in TLE and rapid spread of seizure activity may lead to the initial scalp EEG changes appearing contralateral to seizure onset. Diffuse spike, spike-wave, or slow activity may develop in a partial seizure, especially with secondary generalization. Scalp EEG changes during simple partial seizures are less common, and are said almost never to occur with psychic or visceral seizures (61). The commonest

abnormality observed during simple partial seizures is a run of fast activity progressively increasing in amplitude and slowing in frequency, followed by slow or spike-wave activity.

1.2.6 Imaging features of MTLE

The superiority of magnetic resonance imaging (MRI) over computed tomography (CT) scanning in terms of sensitivity and specificity for identifying the aetiology of epilepsy is well established. Structural lesions that underlie focal epilepsy may now be identified in 70% of newly diagnosed patients and up to 85% of those with medically refractory partial seizures who are candidates for surgical treatment (62). The most common abnormality is HS which is demonstrated by unilateral decrease in hippocampal volume on coronal T1 weighted images and increase in signal on T2-weighted MRI scans (63;64). The hippocampus is a curved structure and is best visualized in two planes: along its long axis and orthogonal to this. These imaging planes may be readily determined on a sagittal scout image: the axial plane being in the line joining the base of the splenium of the corpus callosum to the inferior, posterior border of the frontal lobe, and the coronal plane being perpendicular to this, parallel to the anterior border of the brainstem. Studies have shown that ipsilateral hippocampal atrophy is a good prognostic feature for seizure control following ATLR (65).

Patients being considered for surgical treatment merit the most sophisticated MR imaging available. Von Oertzen and colleagues demonstrated how standard MRI is inadequate for patients with refractory focal epilepsy (66). They found the sensitivity for focal lesions of standard MRI reported by non-experts to be 39%, but this rose to 91% when an epilepsy MRI protocol was employed and the images were reported by expert neuroradiologists.

A typical presurgical MR protocol would be:

a) A T1-weighted volume acquisition that is acquired in an oblique coronal orientation, orthogonal to the long axis of the hippocampi, and covers the whole brain in 0.9 mm partitions. This sequence produces approximately cubic voxels, allowing for reformatting in any orientation, subsequent measurement of hippocampal morphology and volumes, and for three-dimensional reconstruction and surface rendering of the brain;

b) Oblique coronal spin-echo sequence, with proton density (TE = 30), heavily T2-weighted (TE = 90 or 120) and FLAIR acquisitions that are orientated perpendicular to the long axis of the hippocampus, to demonstrate any increase in T2-weighted signal intensity.

Quantitative MRI studies can increase the sensitivity of assessment of hippocampal atrophy. The technique of hippocampal volumetry has been around for over a decade (67;68) and reliably identifies hippocampal atrophy which correlates well with neuronal loss, particularly in the CA1 sub-region (69). In addition the severity of hippocampal atrophy on the side of the language dominant hemisphere is an important determinant of impairment of verbal memory following hippocampal resection. The more severe the atrophy pre-operatively, the less likely it is that there will be a significant decline of verbal memory after surgery (70). The measurement of T2 relaxation time allows a quantitative determination of T2-weighted signal changes, and has been shown to be a useful identifier of hippocampal pathology, with marked elevations being associated with HS and intermediate values being seen in patients without qualitative MRI evidence of HS (71). In this study, contralateral abnormalities were also seen in about 30% of cases with clear cut HS. Measurement of regional abnormalities of HT2 along the length of the hippocampus, used in combination with volumetric data, may provide further refinement to the MRI assessment of HS (72).

The effects of chronic epilepsy on the brain, and in particular hippocampal volume can be addressed by longitudinal studies. A prospective, longitudinal follow-up study of patients with chronic epilepsy with serial MRI scans 3.5 years apart showed that cortical atrophy was a common development in chronic epilepsy, and may be widespread and remote from the putative epileptic focus (73). The increased risk of cerebral atrophy in epilepsy was not related to a history of documented seizures and risk factors for atrophy were age and multiple antiepileptic drug exposure. In two other studies, performed using considerably smaller samples, hippocampal volume loss in TLE patients over a 3.5 year period was correlated with number of seizures (74), and seizure free patients showed no change in hippocampal volume (75), suggesting seizure-associated hippocampal damage.

New MRI acquisitions, such as diffusion tensor imaging (76), whole brain T2 mapping (77), magnetization transfer imaging (78), and double inverse recovery imaging (79), can identify abnormalities that are not revealed on conventional MRI studies. Positron emission tomography (PET)

with flurorodeoxyglucose (80;81), and with specific ligands such as flumazenil (82-85), and detection of seizure-related haemodynamic changes using ictal single photon emission computed tomography (SPECT) scans (86;87) may be more sensitive in some patients when MRI is unremarkable, but do not confer specificity of aetiological diagnosis (62).

1.2.7 Clinical and EEG features of neocortical TLE

The clinical and EEG features of medial and lateral TLE overlap considerably (88). There is no association between febrile convulsions and lateral TLE and there is usually a detectable underlying structural pathology. The commonest are glioma, angioma, hamartoma, dysembryoblastic neuroepithelial tumour, other benign tumours, malformation of cortical development, and post traumatic change.

Clinically the seizures are again characterised by aura and automatisms. Consciousness tends to be preserved for longer than in a typical medial temporal seizure. The typical aura includes hallucinations of visual, auditory, gustatory, or olfactory forms depending on the exact location of seizure origin, or illusions of size (micropsia and macropsia), shape, weight, distance, or sound. Affective or psychic auras occur but are less common than in MTLE. The automatisms can be unilateral and have more prominent motor manifestations than in MTLE. Post-ictal phenomena such as amnesia and psychiatric accompaniments are equally common in both medial and lateral TLE.

The EEG changes most commonly seen are interictal spikes over the temporal region, maximal over the lateral convexity rather than the inferomedial electrodes. MRI will reliably demonstrate any structural lesions but hippocampal volumes and T2 measurements are usually normal.

1.3 EPILEPSY SURGERY

The majority of patients with epilepsy will respond to pharmacological treatment, with around two thirds becoming seizure-free on first line anti epileptic drugs (AEDs). The impact of newer AEDs, while having excellent results in individual patients, has only resulted in an additional 2-3% of patients previously refractory to medical treatment becoming seizure-free (89). This type of treatment however is only symptomatic, preventing seizures from occurring without treating the underlying disorder. For patients with focal epilepsy refractory to medical treatment, the possibility of epilepsy surgery should be considered.

1.3.1 History

It was in the late nineteenth century that epilepsy surgery as we know it came into practice. The work of Hughlings Jackson in identifying that particular brain areas were associated with certain seizure characteristics led Victor Horsley to perform the first successful surgical procedures for lesions associated with epilepsy. Horsley stressed that it was only through the careful examination of diagnosis, surgical procedure and outcome that progress could be made, principles which remain relevant today.

The development of the EEG in the 1930s enabled neurophysiologists to delineate the patterns of brain activity related to epilepsy and in the late 1930s, Penfield became one of the first to operate on the basis of EEG evidence alone (90). Before this, surgery had mainly been performed for epilepsy associated with a known, often post-traumatic lesion. The improvements since in the techniques used to localise seizure foci, including EEG, video telemetry and most notably the rapid development of neuroimaging techniques seen over the past decade have significantly improved the outcome of epilepsy surgery.

1.3.2 Modern epilepsy surgery

These days a wide range of surgical procedures are carried out in a large number of centres. Among them are lesionectomies, *en bloc* temporal lobe resection, anterior temporal lobe resection, hemispherectomy and extratemporal cortical resection. Selection of patients is based on the principles that they have drug resistant seizures of a frequency and severity to cause social and/or medical

disability, that the risk-benefit of surgery is acceptable, and that there is convergent data from different investigative modalities pointing towards localisation of the epileptogenic zone.

In general the presurgical evaluation consists of clinical history and seizure pattern, neuropsychometry, electrophysiology and neuroimaging. The chances of a good outcome depend on the concordance of the results of the above investigations and any discordant result markedly reduces the chances of a good outcome. Electrophysiology consists of scalp EEG and video telemetry. Intracranial EEG recordings may be required if there are discordant test results using non-invasive techniques, if there is inadequate localisation or lateralisation, or if pre-operative mapping of eloquent cortex is required. Between 5 and 20% of patients being operated upon in the UK will have such studies although the proportion is falling with improved neuroimaging.

One of the most important factors in determining a favourable outcome after surgery is the detection of a known lesion related to the seizure focus (91). Recent advances in neuroimaging techniques, in particular high resolution MRI, have been most important in finding these lesions (62). Functional imaging with PET (82) and SPECT (92), performed both interictally and ictally, often provide additional information in the detection of the seizure focus, particularly in cases where the MRI is normal or unclear.

1.3.3 Presurgical evaluation

1.3.3.1 Neuropsychology

Neuropsychology has played a prominent role throughout the modern era of epilepsy surgery. This is due mainly to the importance of the temporal lobes in memory function. Bilateral temporal lobe resection is associated with profound anterograde amnesia while unilateral resections may be associated with material-specific memory dysfunction. The traditional view is that the dominant temporal lobe (usually the left) is important for verbal memory processing (44) and the non-dominant temporal lobe (usually the right) for non-verbal or visual memory processing (45). The aetiology and underlying pathology however play a role in determining the nature and extent of pre- and post-operative neuropsychological deficits (93).

The principal role of baseline neuropsychology assessment is in:

a) identifying those at risk of post-operative amnesia

b) providing data on lateralisation and localisation of cerebral disturbance

c) predicting the impact of surgery on memory

d) providing evidence for cerebral reorganisation.

Neuropsychological performance has been related to surgical outcome. Patients with more focal neuropsychological deficits and less overall cognitive impairment should be expected to have better outcomes with respect to seizure frequency, given the absence of evidence of dysfunction extending beyond the resection zone. Neuropsychology can also contribute in evaluating the risk-to-benefit ratio of surgical resection. Patients at high risk of a significant memory decline can be counselled pre-operatively and can be trained in compensatory strategies prior to the surgery when appropriate.

1.3.3.2 Sodium amytal testing

The intracarotid amytal test (IAT) plays a role in the presurgical assessment of TLE in some centres. Its uses are in assessing the capacity of the contralateral temporal lobe to maintain useful memory functions, thus guarding against a severe post-operative amnesic syndrome, and as a means of lateralising language function. The procedure involves the injection of sodium amytal into one carotid artery via a catheter in the femoral artery. This inactivates the corresponding hemisphere for around 10 minutes thus crudely mimicking the effects of surgery on the MTL structures. The activity of the sodium amytal is monitored by the presence of a contralateral hemiplegia and unilateral slow wave activity on the EEG. During this time the patient is presented with a series of items to name and remember. When the side ipsilateral to the pathology is injected, normal memory function is expected but injection of the contralateral side is expected to result in impaired memory function due to the combined disruptive effects of the pathology on the one side and the amytal on the other. Therefore if poor IAT memory performance is obtained after injection ipsilateral to the seizure focus, the patient may be at risk of postoperative amnesia, given the implication of additional contralateral temporal lobe impairment.

Sabsevitz et al looked at outcome following left ATLR in patients with both expected (i.e. better memory performance after ipsilateral injection) and unexpected (i.e. better memory performance after contralateral injection) memory asymmetry scores on IAT testing (94). They found that patients with

reversed asymmetry were at a higher risk of memory decline and had poorer seizure outcome in comparison with patients with expected asymmetry scores. A more recent study demonstrated that unexpected asymmetry was associated with a worse surgical outcome following right ATLR but not following left ATLR (95). There was however a much higher incidence of unexpected asymmetry in the left TLE patients (36% compared to 8%) suggesting that assessment of memory with IAT was limited by language confounds in left TLE patients. In this study IAT memory asymmetry did not predict postoperative verbal memory decline.

IAT memory performance has been shown to be associated with a variety of quantitative measures of hippocampal structure. Patients with severe hippocampal cell loss (96) and those with greater hippocampal volume asymmetries on MRI measurement (97) are more likely to fail the IAT after injection contralateral to the seizure onset.

While still commonly used, the IAT has considerable disadvantages, not least the fact that it is an expensive, invasive procedure with potentially serious complications. Doubts also exist about its reliability and validity in predicting post-operative amnesia. In contrast to the traditional neuropsychological assessment, which relies on standardised tests of cognitive abilities and yields results that are easily validated, the IAT differs significantly among institutions. Differences exist between centres in the testing protocol used, choice of behavioural stimuli, dosage and administration of amytal, all of which can lead to variations in the results (98). The IAT is also poor at predicting verbal memory decline as deactivation of the language dominant hemisphere will cause increased errors on verbal memory testing (95).

1.3.4 Surgical outcome

The efficacy of epilepsy surgery has been demonstrated in a number of studies, most notably in a randomised controlled trial of surgery versus pharmacological treatment in patients with poorly controlled TLE (99). Outcome of surgery varies considerably however and when assessing it the key issues are the selection of candidates and the type of outcome measurement used. Patients with TLE, a resectable lesion on MRI and fully concordant electro-clinical and neuropsychological data have a 70-80% chance of becoming seizure-free. At the other end of the spectrum patients with frontal lobe

epilepsy, no definite pathology and poorly congruent data may have a less than 10% chance of becoming seizure-free. Another complicating factor is the lack of agreement on type of outcome measurement used between centres. Some centres classify patients with an aura as seizure free while others only consider patients completely free from any seizure manifestations as seizure free. Other outcome measurements of use in those not rendered seizure free may be percentage reduction in seizure frequency and quality of life measurements. Some problems with Engel's widely used classification system has led to a revised scheme being suggested by the ILAE commission on classification which will hopefully improve the possibilities for comparisons to be made between centres (100).

Table 1.2 Classification of seizure outcome following surgery (from ILAE commission on Neurosurgery report , 2001)

Outcome classification	Definition
1	Completely seizure free; no auras
2	Only auras; no other seizures
3	One to three seizure days per year; +/- auras
4	Four seizure days per year to 50% reduction of baseline seizure days; +/- auras
5	Less than 50% reduction of baseline seizure days to 100% increase of baseline seizure days; +/- auras
6	More than 100% increase of baseline seizure days; +/- auras

1.3.5 Surgical complications

The unwanted side effects of epilepsy surgery can be divided into three categories; neurological, psychological and psychiatric.

1.3.5.1 Neurological

Visual field defects occur in approximately 10% of patients following ATLR and in 5% are severe enough to render the patient ineligible for a driving license, despite being seizure free (101). These most commonly take the form of a superior homonymous quadrantanopia and are due to the disruption of Meyer's loop, the anterior part of the optic radiation. More serious complications occur less frequently, with most studies reporting a risk between 1 and 5%. These include intracranial infection, haemorrhages, severe neurological deficits, e.g. hemiparesis, and occasionally death. Although the risks of these events are likely to decrease over time with improvements in surgical techniques, they must be factored into the evaluation of the overall effectiveness of surgery.

1.3.5.2 Psychological

MTL structures have long been associated with memory functioning and surgical resection is known to cause reduced memory function in some cases. The study of patients following temporal lobe surgery has provided considerable evidence supporting the critical role that the hippocampi play in memory functioning (102). One of the most famous cases is that of the devastating amnesia suffered by the patient HM following an extensive bilateral temporal lobe resection. Although his ability to retrieve information learnt prior to surgery was unaffected and general intellectual function and personality remained intact, he was unable to learn any new information. Scoville and Milner went on to report the results of memory tests carried out on 10 patients who had undergone bilateral temporal lobe resections, finding that all those whose resections were extensive enough to damage the hippocampus displayed a clear and persistent disturbance of recent memory, and that the extent of the resection seemed to be related to the memory disturbance (103). These results effectively ended the practice of bilateral temporal lobe resections for the relief of epilepsy and psychiatric symptoms.

Although rare, some patients have sustained a severe anterograde amnesic syndrome following a unilateral ATLR. Most of these however have subsequently been found to have evidence of contralateral hippocampal pathology, either on postoperative EEG (104), post-mortem pathological findings (105) or postoperative volumetric MRI (106). Conversely, there has been a report of a patient with bilateral hippocampal damage and normal memory functioning (107). The abnormality was however clearly congenital suggesting an ability of the brain to successfully reorganise memory functions provided the hippocampal damage occurs early enough in life. These rare cases highlight the important role that the aetiology of the seizure disorder has in determining the nature of the associated neuropsychological deficit. In a review of unexpected cases of amnesia following unilateral temporal lobe surgery, Kapur and Prevett emphasised the importance of ictal semiology and neuropsychology in localising the seizure focus, and of interpreting the neurophysiological findings in the context of other investigations (108).

As unilateral temporal lobe surgery gained recognition as an effective treatment for refractory epilepsy, material-specific memory deficits following surgery have been increasingly recognised. The decline in verbal memory following surgery to the language-dominant hemisphere has been consistently reported and studied (109), along with deficits in topographical memory following non-dominant ATLR (110).

Two different models of hippocampal function have been proposed to explain memory deficits following unilateral ATLR; hippocampal reserve and functional adequacy (111). According to the hippocampal reserve theory, postoperative memory decline depends on the capacity or reserve of the contralateral hippocampus to support memory following surgery, while the functional adequacy model suggests that it is the capacity of the hippocampus that is to be resected that determines whether changes in memory function will be observed. Evidence from baseline neuropsychology (112), the IAT (113), histological studies of hippocampal cell density (96) and MRI volumetry (70) has suggested that of the two, it is the functional adequacy of the ipsilateral MTL, rather than the functional reserve of the contralateral MTL that is most closely related to the typical material specific memory deficits seen following ATLR.

Memory decline is not an inevitable consequence of temporal lobe surgery. Accurate prediction of likelihood and severity of post-operative memory decline is necessary to make an informed decision regarding surgical treatment. Much work has been focused on the identification of prognostic indicators

for risk of memory loss after ATLR. The severity of HS on MRI is an important determinant, being inversely correlated with a decline in verbal memory following left ATLR, with less severe HS increasing the risk of memory decline (70). Preoperative memory performance has been related to degree of postoperative memory impairment, with better performance increasing the risk of memory decline (112;114;115). Recently, functional MRI (fMRI) has also been shown to be a potential predictor of post-operative material-specific memory decline following ATLR (see section 1.6). Memory decline has also been found to correlate inversely with the severity of HS in the resected hippocampus, with patients with more severe HS having less memory decline (116;117). Baxendale and colleagues showed that the volume of hippocampal remnant left *in situ* significantly correlated with postoperative memory change with smaller remnants of hippocampal volumes correlated with a greater decrease in memory postoperatively (118). These risk factors reflect the functional integrity of the resected temporal lobe and suggest that patients with residual memory function in the pathological hippocampus are at greater risk of memory impairment post-operatively. However another study demonstrated that bilateral hippocampal atrophy in the presence of left TLE is associated with worse verbal memory before and after ATLR than in those patients with unilateral hippocampal atrophy, suggesting that the capacity of the contralateral MTL to maintain memory function is also of importance (119).

Positive changes in neuropsychological functions may also occur following temporal lobe surgery. These occur probably in part to cessation of seizures and also due to reduction in doses of antiepileptic drugs. Generally, improvements are greatest in functions subserved by the hemisphere contralateral to the site of resection and are seen primarily in patients who become seizure-free (120). Finally, it is worth comparing the documented cognitive risk factors associated with temporal lobe surgery with those for other types of neurosurgery, for which the frequency and severity of cognitive impairment are much less well established. Consequently the degree of informed consent is greater and counselling patients regarding the attendant risks can be done with more confidence.

1.3.5.3 Psychiatric

Psychiatric assessment prior to surgery is mandatory in order to document evidence of psychiatric conditions that may require separate interventions and to identify patients who may need additional

psychiatric support post-operatively. The prevalence of psychiatric conditions, such as affective disorders, anxiety disorders and psychosis is high in patients with medically refractory TLE both before and after surgical treatment. Studies have shown that while presurgical psychiatric conditions may be resolved or diminished following ATLR, new psychiatric problems appeared in up to one third of patients (121), although there is also an incidence of new psychiatric probs in those who do not have surgery.

Many of these experienced a transitory mood disorder which cleared up by the time they had neuropsychological re-evaluation one year after surgery. Theories for this include disrupted functioning within temporal lobe structures involved in emotion (122), 'forced normalisation' causing affective disorders through the suppression of the antidepressant effects of seizures, or because patients respond negatively to increased expectations once seizures have been abolished or reduced (122). Although the relation between seizure control and psychiatric symptoms shortly after surgery is still an open question, seizure free status is recognised to be the most powerful predictor of improved psychiatric and psychosocial adjustment outcome later in the postoperative course (123;124).

Psychotic disorders are less likely to change after surgery (125), a finding which has led to the general practice of not offering surgical treatment to patients with epilepsy and psychotic disorders. Psychosis may however present for the first time after surgery and it has been suggested that it is more common following right-sided surgery. This tends to pursue a chronic interictal course although there are reports of the de novo occurrence of postoperative postictal psychosis following ATLR, in occurrence with seizure recurrence contralateral to the resection (126). The occurrence of episodes of postictal psychosis preoperatively is not a contraindication for temporal lobe surgery.

In conclusion, it is worth noting that, when comparing the long term psychosocial outcomes of patients who underwent ATLR compared with medically managed patients, surgery was shown to have a significant positive impact in terms of employment, independent living, driving and financial independence (127).

1.4 MAGNETIC RESONANCE IMAGING

1.4.1 Basic MR physics

1.4.1.1 Nuclear magnetic resonance

Magnetic resonance imaging (MRI) relies on the the phenomenon of nuclear magnetic resonance (NMR), discovered by Block and Purcell in the 1940s, and developed as an imaging technique by Lauterbur and Mansfield in the early 1970s. Nuclei possess the intrinsic properties of charge and spin, and the spinning motion of this charge induces a local magnetic field. This nuclear magnetic moment can be thought of as a small magnet. The signal measured during MRI arises from particular atomic nuclei that contain an odd number of nuclear spins, and due to its abundance in the human body the strongest signal is obtained from the hydrogen nucleus. In an externally applied magnetic field B_0 the magnetic moments of the hydrogen nuclei align either parallel or anti-parallel with B_0. The presence of B_0 causes the hydrogen nucleus to revolve, or precess around the field direction at a frequency directly proportional to the field strength B_0. This frequency is known as the Larmor frequency, ω_0.

$$\omega_0 = \gamma \mathbf{B_0}$$

where ω_0 = the precessional frequency of the magnetic dipole of the spinning nucleus in radians per second, B_0 = field strength in Tesla, and γ = the gyro-magnetic ratio for the nucleus in question in radians per second per Tesla.

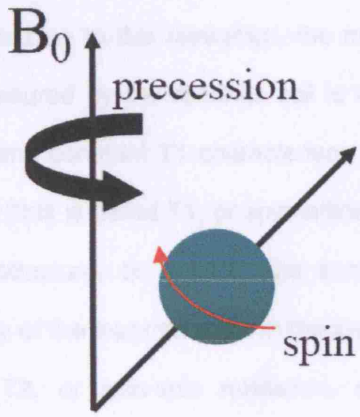

Figure 1.2 Spin and precession of a single proton.
The proton possesses the intrinsic property of spin (red arrow). In an external magnetic field, the proton precesses (black curved arrow) around the longitudinal magnetisation vector (B_0).

Quantum mechanics tells us that in an applied magnetic field the proton can only have two possible energy states, either parallel or anti-parallel to the field. When parallel to the field, the energy will be lower than when against the field. In equilibrium more protons are in the low energy state (i.e. aligned with the field) than the high energy state (i.e. against the field). The sum of all the individual magnetic moments precessing around B_0 can be reduced to a single bulk magnetisation vector, M aligned along B_0. The magnetisation can be described using a coordinate system, with the z-axis running in the direction of the magnetic field. It can be difficult to visualise the net magnetisation M within the laboratory frame of reference. For this reason M can be viewed in a frame rotating with respect to the laboratory frame, known as the rotating frame; an x-y axis that roates about z at the Larmor frequency.

At equilibrium M lies along the direction of B_0 (the z axis). If we apply a radiofrequency (RF) pulse B_1 perpendicular to B_0 we can induce protons to be excited from the low to the high energy state. To achieve this, the frequency of B_1 should be the same as the Larmor frequency (i.e. 64 MHz for a proton in a 1.5T field). This resonance has the effect of tilting M away from the z axis towards the transverse (x-y) plane. The degree to which M is tilted (flip angle) can be controlled by changing the length or strength of the RF pulse. A 90^0 flip angle causes M to be rotated into the x-y plane. This oscillating magnetic field induces a voltage in a receiver coil and it is this transverse component that gives rise to the detectable MR signal.

Following excitation the hydrogen nuclei gradually return to their original energy state and M returns to its original position along the z axis. Due to this relaxation, the measured signal gradually decays to zero. The decrease in voltage measured by the receiver coil is the free induction delay signal. The longitudinal relaxation exponential time constant T1 characterises the recovery of the z-component of the magnetisation after a RF pulse. This is called T1, or spin-lattice relaxation, as the absorbed energy is dissipated to the surrounding structure, or 'lattice'. The transverse relaxation exponential time constant T2 characterises the decay of the magnetisation in the x-y plane and occurs at a different rate to T1 relaxation. This is called T2, or spin-spin relaxation, as energy is exchanged between neighbouring hydrogen nuclei. The exchange of energy during relaxation causes the spins' rotation to become out of phase, or desynchronised, reducing the coherence of the transverse magnetisation. This

dephasing represents an added mechanism of loss of transverse magnetisation and may occur without T1 relaxation. T2 relaxation will always be faster than T1.

The static magnetic field is rarely homogenous, due to technical and sample factors. The consequence of this is that the nuclei will have a slightly different resonant frequency and become out of phase, leading to a net loss of transverse magnetisation. This decay is characterised by the exponential time constant T2*, which is usually faster than T2, and may be affected by any field inhomogeneity caused by the properties of the sample.

1.4.1.2 Spin and gradient echo pulse sequences

The spin echo sequence is routinely used in MRI and involves the use of a second 180^0 RF pulse to refocus the dephasing of nuclei due to inhomogeneities in the magnetic field (Figure 1.3). In the basic sequence a 90^0 pulse is used to produce transverse magnetisation along the *x* axis. This dephases due to local field inhomogeneities. At time *t* (TE/2), a 180^0 pulse then flips the spins from the *x* axis to the *–x* axis. The spins continue to precess in the same direction and at the same speed as before the 180^0 pulse was applied, leading to rephasing of the transverse magnetisation. The spins totally rephase at a time *2t* to produce a spin echo signal which can be detected. The time *2t* is called the echo time TE. Although the 180 pulse cancels out the effects of T2*, the recovered signal at the echo is less than its original height. This is due to T2-relaxation, the second contributor to magnetisation dephasing, which cannot be refocused with a spin-echo as it results from spatial and temporal variations in the intrinsic magnetic environment of each nucleus.

Echoes can also be formed without 180^0 pulses by using magnetic field gradients to rephase the protons dephased by the initial RF pulse. Again the rephasing leads to a signal which can be detected by the receiver coil, and this is called a gradient echo. In this type of sequence, lower flip angles can be used leading to faster recovery of longitudinal magnetisation allowing the use of a shorter repetition time, TR (the time between consecutive 90^0 pulses). Gradient echo imaging is therefore frequently used in fast imaging sequences but is susceptible to magnetic field inhomogeneities. These inhomogeneities may be the result of either intrinsic defects in the magnet itself or of susceptibility-induced field distortions produced by tissue or haemoglobin.

1.4.1.3 Image contrast

The contrast in an image is based on differences in signal intensity. A number of different factors affect the signal intensity from a particular tissue, including the T1 and T2 relaxation times, and the proton density (PD) of the tissue, determined by the relative number of protons per unit volume. The exact composition of the tissue also affects T1 and T2 relaxation times, for example protons in water have a longer T1 than those in fat. An image said to be T1-weighted is one where the difference in signal intensity between tissues, i.e. the tissue contrast, is mainly due to their differences in T1 relaxation times.

The relative contribution of T1, T2 and PD, and as a result the appearance of the image, may be manipulated by controlling the parameters of the spin echo pulse sequence, in particular the echo time, TE and the repetition time, TR. Different combinations of TR and TE will produce different degrees of contrast between tissues. Changing the TR changes the contrast between tissues with different T1 relaxation times while changing TE will change the contrast between tissues with different T2s. A short TE and a short TR produces images which are T1-weighted, a long TE and a long TR produces images which are T2-weighted, and a short TE and long TR gives PD weighting.

1.4.1.4 Image formation

Creating an image requires the use of additional magnetic fields (gradient fields) to spatially encode the protons and employs the fact that the resonance frequency (or Larmor frequency) of protons is directly proportional to the magnetic field. A gradient field varies the magnetic field across the object and the Larmor frequencies of the protons will therefore be determined by their location along the gradient. The combination of the RF pulse and gradient fields, applied at very specific times, is used to obtain slice selection (SS), frequency encoding (FE) and phase encoding (PE) as desired. The application of an RF pulse of the appropriate frequency and bandwidth in the presence of a slice select gradient excites a small slice of the sample, allowing the sample to be studied slice by slice.

Within each slice, the signal coming from it must be located along both axes of the image. For this spatial encoding, locations are encoded along one axis by frequency and along the second axis by phase. FE is done by the application of a gradient (known as the read gradient) during data acquisition.

Protons at different positions experience slightly different local fields and therefore the resulting signals have different frequencies. Finally a gradient is applied along the orthogonal axis to achieve PE. This gradient is usually applied after the RF pulse and slice select gradient but before data acquisition. Protons at different positions experience slightly different local fields and therefore precess at different rates. When the gradient is switched off, the precessional frequency of the protons returns to the Larmor frequency. By the end of the gradient however they have rotated through different angles, and have different phases. If the acquisition is repeated with different phase encode gradient strengths the way in which phase changes with gradient strength is unique to protons in a particular position. A pulse sequence diagram can be used to show all the gradients and RF pulses used to produce an image.

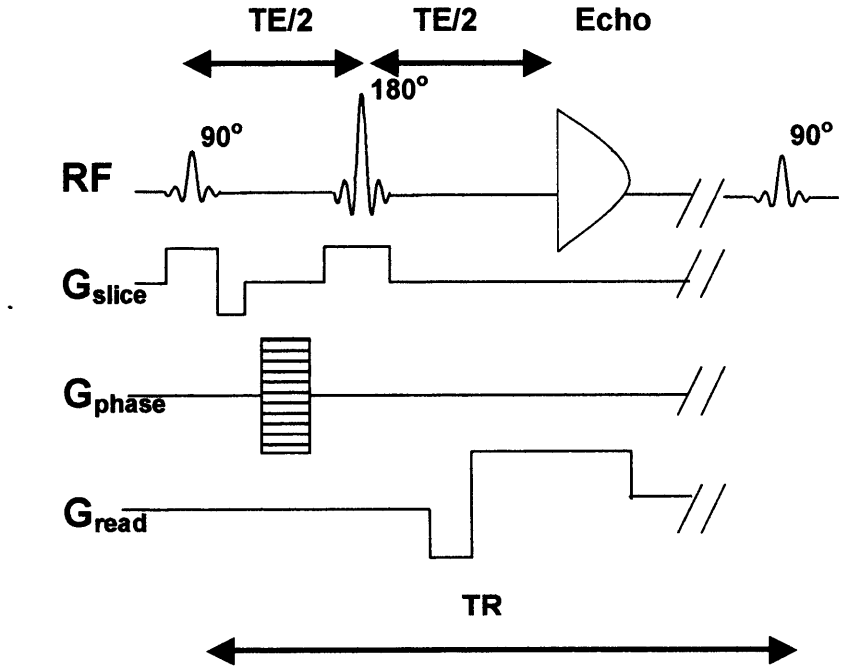

Figure 1.3 Pulse sequence diagram from a spin echo sequence
The repetition time (TR) is the interval between two successive pulse cycles in milliseconds (ms) and the echo time (TE) is the time taken from the application of the RF pulse to the measurement of the MR signal in ms. A combination of three gradient fields; slice selection (SS, G_{slice}), frequency encoding (FE, G_{read}) and phase encoding (PE, G_{phase}), are used to spatially encode the protons.

The spatially encoded MR signal needs to be Fourier transformed to produce an image. Fourier transformation is a mathematical manipulation that allows the signal to be converted from the time domain to the frequency domain. Prior to Fourier transformation the raw data lies in a matrix called k-space. All points in k-space contain data from all locations in an MR image. Points near the centre of k-space have low spatial frequencies and convey the overall form of the image. Points at the periphery of k-space have high spatial frequencies and convey the fine edge detail of the image, but have little effect on image contrast. In order to use the Fourier transform to produce an image a certain amount of k-space needs to be sampled. This can be done via a number of different paths, or trajectories. The representations of image resolution and field of view are inversely related for physical image space, compared to k-space; therefore sampling a larger area of k-space leads to increased spatial resolution in the image, whereas decreasing the distance between points of k-space increases the image field of view.

1.4.1.5 Voxels

The discrete nature of the acquisition in k-space using step-wise gradient increases means that, after Fourier Transformation, the image is represented by a grid of small cubes called voxels. Within each voxel, the protons experience the same frequency and phase encoding and the signal from a voxel is the sum of all the protons within it. The resolution of an image depends on the size of the voxels, which is determined by the step size of the gradients. To get a typical 128 x 128 matrix, FE is done at 128 points for each PE step, and a total of 128 PE steps are carried out. This produces 128 lines of data, each one of 128 points. Reducing the number of steps leads to an increased voxel size. Larger voxels have greater signal to noise but are more likely to encompass protons from different tissues with different behaviour, which could cause a misleading signal (known as the partial volume effect). Signal to noise is proportional to voxel volume and to the square root of the number of PE steps.

1.4.1.6 Echo planar imaging

The commonly used spin-echo sequences can take up to minutes to acquire each slice. Improving the speed of MRI acquisition was important for imaging dynamic processes and the introduction of echo

planar imaging (EPI) sequences meant that it was theoretically possible to obtain a whole brain image in a fraction of a second. The major difference between EPI and other MR imaging sequences is the way in which the data is sampled. Typical spin-echo and gradient-echo sequences sample a single line of k-space after each RF pulse whereas a fast sequence such as EPI samples all lines of k-space after a single RF excitation. EPI therefore greatly reduces imaging time and makes it an ideal sequence for dynamic MRI techniques such as fMRI.

The main technical problem when using EPI sequences, especially within the temporal lobes, is that of susceptibility artefact. Ideally in the absence of an applied gradient, the magnetic field would be homogenous throughout the bore of an MRI scanner. Unfortunately the different magnetic properties of bone, tissue and air introduce inhomogeneities in the field when a head is introduced into the bore. Brain regions closest to borders between sinuses and brain or bone and brain are most affected and therefore especially likely to suffer geometric distortions or signal loss (128).

Geometric distortions of the EPI data make it difficult to directly overlay fMRI activations directly on co-registered high-resolution scans. They can be unwarped using techniques that map the local field in the head (129), though it has been shown that approaches of this kind can introduce extra noise into the corrected EPI data (130). Alternative acquisition sequences that do not experience geometric distortions are available (131) though these rarely have the temporal resolution or high signal to noise ratio (SNR) per unit time of EPI.

The second artefact in EPI data is more serious, as signal loss leads to sensitivity loss which is unrecoverable by image processing techniques. Some of these artefacts can be corrected by shimming, a process whereby the static magnetic field is made more homogenous over the region of interest (128). Some will remain however, leading to distortion and dropout in echo-planar images. Other approaches to removing dropout often involve acquiring extra images, leading to a loss of temporal resolution (132), but more recent work has shown that dropouts and distortions can be reduced without incurring time penalties if regions of reduced spatial extent are imaged (133).

1.4.1.7 fMRI and the BOLD contrast

fMRI is performed using T2*-weighted EPI and makes use of the differing magnetic properties of oxygenated and deoxygenated haemoglobin, the protein responsible for oxygen transport found within red blood cells. Deoxyhaemoglobin is a paramagnetic molecule and causes local field inhomogeneity, increasing the effects of T2* and thus shortening the decay in transverse magnetization. Conversely oxyhaemoglobin is diamagnetic and has little effect on MR images. On heavily T2*-weighted sequences, changing the ratio of oxy- to deoxyhaemoglobin was shown to produce detectable contrast changes in blood vessels and in their surrounding tissues (134). This was termed the blood oxygenation level-dependent (BOLD) effect.

The BOLD signal is complex and has a number of key components; the neuronal response to a stimulus; the relationship between the neuronal activity and the haemodynamic response (neurovascular coupling); the haemodynamic response itself; and the way this response is detected by the MRI scanner. It is no longer felt to be the spiking of neurons that is of primary importance in determining these changes. Recent evidence suggests that the BOLD effect mainly represents synaptic activity, referred to as local field potentials (135). Increased activity is associated with increased oxygen and glucose usage in those areas. There is therefore an initial decrease in oxygen concentration followed by a compensatory increase in local blood flow that exceeds demand, leading to an increased blood oxygenation in the local capillaries and draining veins (136). This alters the ratio of oxy- and deoxyhaemoglobin and provides the BOLD signal typically measured in fMRI experiments. The dynamics of the neurovascular response mean that the BOLD reponse takes a number of seconds to evolve and the time course of this neurovascular response must be accounted for in the statistical analysis of fMRI time series. As blood occupies only a small fraction of grey matter, BOLD signal changes are of the order of a few percent at best. These small signal changes require the implementation of sophisticated image processing and analysis techniques to ensure that observations reflect true BOLD signal and not noise.

1.4.2 Statistical analysis of fMRI data

In fMRI experiments inferences are made about differences in regional brain activity between different conditions or states. The analysis of fMRI data begins with a series of preprocessing steps, the aims of which include correcting for motion and ensuring that the data conforms to a known anatomical space, and this is followed by the creation of a statistical model in order to draw inferences about differences in regional brain activity between different conditions or states. A number of different packages exist for carrying out these steps including statistical parametric mapping (SPM) (137).

1.4.2.1 Spatial preprocessing

1.4.2.1.1 Realignment

A typical fMRI data series consists of a number of 3D whole brain volumes, with one volume for each time point. Head motion can give rise to artefactual changes in signal intensity over a time series and therefore the first preprocessing step involves realigning the imaging time series to a common reference frame to correct for subject movement during scanning. This removes variance from the time series which would either be attributable to error (hence decreasing sensitivity) or to evoked effects, in the case of stimulus-correlated motion.

1.4.2.1.2 Normalisation

After realignment the data is transformed into standard anatomical space. This is known as spatial normalisation and allows group analyses to be performed and permits data reporting within a standardized reference co-ordinate system. The first step is to use the functional mean image (produced during the realignment step) and warp it directly to the SPM EPI template that already conforms to a standard anatomical space (138). The resulting transformation parameters are then applied to every image in the time course.

1.4.2.1.3 Smoothing

Smoothing is a process by which data points are averaged with their neighbours in a series, such as a time series, or image. This has the effect of blurring the sharp edges in the smoothed data. Smoothing

in SPM is carried out by applying a Gaussian kernel of known width to each voxel. It is usual to describe the width of the Gaussian with another related measure, the Full Width at Half Maximum (FWHM). The FWHM is the width of the kernel, at half of the maximum of the height of the Gaussian. Spatial smoothing is primarily carried out to increase signal to noise and to meet the assumptions of Gaussian field theory (see later). Smoothing is also necessary in order to perform comparisons across subjects so that homologies in functional anatomy that exist over subjects may be detected.

1.4.2.2 The general linear model

The statistical analysis performed by SPM is a univariate one, done by testing for experimentally-induced effects at each voxel independently and simultaneously using the General Linear Model. Firstly it does an analysis of variance separately at each voxel. It then makes t-statistics from the results of this analysis and works out a Z score equivalent for the t-statistic, before making an image of the t-statistics, i.e. a statistical parametric map. Finally, an inference is drawn from this SPM, reliably locating voxels where an effect is present while guarding against false positives, and the significance value takes account of the multiple comparisons in the image.

SPM uses much of the same underlying mathematics as other statistics packages and commonly used statistical tests such as linear regression, t-tests and analysis of variance (ANOVA) are all special cases of the general linear model used by SPM. This model explains variation in the response variable (i.e. the measured data for a given voxel) Y, in terms of a combination of the explanatory variables (or regressors) x;

$$Y_j = x_{j1}\beta_1 + \ldots + x_{jl}\beta_l + \ldots + x_{jL}\beta_L + \varepsilon_j$$

where β are unknown parameters, corresponding to each of the explanatory variables for Y, and ε are the residual errors.

This model can be expressed as a matrix;

$$\mathbf{Y = X\beta + \varepsilon}$$

Where **Y** is the data matrix, **X** is the design matrix (which has one row per observation (i.e. each scan) and one column per model parameter) and ε is the error matrix. β is the matrix of parameters that need to be estimated that best fit the data and this is done by least squares.

The design matrix **X** is displayed graphically by SPM and consists of a number of columns, each one corresponding to some effect that has been built in to the experiment. The relative contribution of each of these columns to the experimental variance (i.e. the parameter estimate for each column) is assessed by using least squares of the residuals. We can test the null hypothesis that there is no relationship between our experimental model and the voxel data by calculating t-statistics for specific linear combinations or 'contrasts' of parameter estimates, by dividing the contrast of parameter estimates by the standard error of that contrast. The standard error can be worked out using the remaining error, matrix ε above and is the variance of the residuals about the least squares fit. After calculating the t-statistic, SPM converts the t-statistics to Z scores. The Z scores are the numbers from the unit normal distribution that would give the same p value as the t-statistic.

fMRI time series are filtered to remove any low-frequency noise due, for example to scanner drift. The regressors are convolved with the haemodynamic response function (HRF) of the BOLD effect in order to account for the sluggish nature of the response. Because the data are typically correlated from one scan to the next the scans can not be treated as independent observations. The general linear model accounts for these autocorrelations by imposing a temporal smoothing function on the time-series.

1.4.2.3 Thresholding and random field theory

The null hypothesis for a particular statistical comparison will be that there is no change anywhere in the brain. Because each SPM map has so many statistics (i.e. one for each voxel) even if the null hypothesis is true, we can be sure that some of these will appear to be significant at standard statistical thresholds such as $p<0.05$ or $p<0.01$, giving a number of false positives. This is the problem of multiple comparisons and a correction is required for the number of statistical tests performed.

One method for dealing with this problem is the Bonferroni correction, where the p value threshold is divided by the number of tests performed. In most cases however this will be considerably too conservative. This is because, for most SPMs, the Z scores at each voxel are highly correlated with their

neighbours. Instead the correction used by SPM is based on Gaussian field theory, which takes into account the fact that neighbouring voxels are not independent by virtue of the spatial smoothing performed. This correction is similar to a Bonferroni correction for multiple comparisons but less conservative provided that the data are sufficiently smooth. If however activation has been predicted in a particular brain region, an appropriate search volume can be specified and an appropriate correction can be made for this volume (small volume correction).

1.4.2.4 fMRI experimental design

1.4.2.4.1 Blocked experimental design

Many functional imaging experiments have used blocked design paradigms looking for regions of the brain showing greater activation during task blocks compared with rest blocks. For example, in a comparison of activation against rest, the null hypothesis would be that there are no differences between the scans in the activation condition, and the scans in the rest condition. The advantage of blocked designs is that they are efficient in detecting differences between two conditions however they offer less flexibility in the experimental design required for studying complex cognitive functions, such as memory (see section 1.6.3). Improvements in sensitivity and temporal resolution of fMRI have allowed the possibility of event-related fMRI.

1.4.2.4.2 Event-related fMRI

Event-related fMRI is defined as the detection of transient haemodynamic responses to brief stimuli or tasks. This technique, derived from those used by electrophysiologists to study event-related potentials, enables trial-based rather than block-based experiments to be carried out. Trial-based designs have a number of methodological advantages (139), in particular that the trial order can be randomised, thus avoiding some of the confounds of blocked designs, and that trials can be categorised post-hoc according to a subject's performance on a subsequent test (see section 1.6.3). Event-related experiments may be more vulnerable to alterations in the HRF (e.g. due to pathology). When analysing event-related data, the explanatory variables are created by convolving a set of delta functions, indicating the onset times of a particular event with a set of basis functions that model the

haemodynamic responses to those events (139). The approach adopted in our studies was to employ the canonical HRF.

1.4.2.5 Group analyses

Statistical inferences about groups of subjects may be of two types; fixed or random-effects analyses. A fixed effects analysis gives results specific to the particular subjects at the time of scanning and is drawn from the effect size relative to the within subject variability. The effect size is averaged across subjects to provide a representative mean across subjects. However, the limitation of this type of analysis is that an effect size may be primarily driven by a few subjects.

A random effects analysis allows inferences to be made about the population from which the sample of subjects was drawn. One observation per subject per condition is entered into a random effects analysis (usually a contrast of parameter estimates from a 1st level analysis). Hence the effect size is compared against the between subject variability in these contrasts. This type of analysis is, therefore, not at risk of being biased by strong effects in a subset of subjects.

Random effects analyses were used for all the second level analyses performed in this thesis. At the second level of the random effects analysis, a single contrast image for each subject is entered into a one-sample t-test to examine effects across the whole group, testing whether the estimated effect size is significantly greater than zero across all subjects. Two-sample t-tests can be used to compare two groups, allowing the detection of brain regions demonstrating greater or less activation in one group compared with another. Finally regression analyses can be performed between a particular contrast and a covariate of interest (e.g. memory performance) to look for brain regions where activation correlates with that covariate.

1.4.3 Diffusion imaging

Diffusion is a random process whereby molecules mix through thermal agitation with each molecule behaving independently from the others. Collisions between the molecules cause a random displacement and each one follows a path known as the random walk. It is possible to calculate a measure of diffusion distance over a given time, averaged over a number of molecules, the so-called

root mean square (r.m.s.) distance. If diffusion is unhindered, this displacement increases with time, with a constant of proportionality equal to D, the diffusion constant of that fluid. If diffusion is restricted or hindered (as in the brain) we cannot talk about a single diffusion constant and therefore refer to the Apparent Diffusion Coefficient (ADC). Where barriers or restrictions exist, diffusion is characterized by different ADCs in different directions.

1.4.3.1 Diffusion weighted imaging

As already described the signal in an MR image arises from the behaviour of proton spins in a magnetic field. RF pulses are used to excite the sample and the magnetization is then typically refocused using another 180 degree RF pulse. In the absence of motion or diffusion any dephasing of the spins is refocused, however for moving spins this refocusing is only partial. This imperfect refocusing leads to reduced signal amplitude. Gradients may be applied in a particular direction to deliberately sensitise the sequence to this effect. These gradients have no effect on stationary spins, but cause loss of signal from moving spins, thus creating diffusion weighted (DW) images.

In 1965, Stejkal and Tanner proposed the pulsed field gradient diffusion weighted spin echo scheme for introducing diffusion weighting into an MRI acquisition. A pulsed gradient, g, is introduced into the sequence, either side of the 180 degree refocusing pulse. The amplitude, duration and separation of the diffusion gradients are varied to obtain different amounts of diffusion weighting, or *b*-values. This method can be included in most MRI sequences to introduce diffusion weighting along a specific direction (given by the direction along which the diffusion gradient is applied). This gives reduced signal in areas of the sample where the diffusion coefficient in that direction is greater.

When diffusion is the same in all directions, as in cerebrospinal fluid (CSF), it is said to be isotropic. These areas will appear dark on DW images, independent of the direction of application of the diffusion gradient. In other areas tissue structure causes restricted diffusion. When this restriction is arranged in a highly directional manner, such as in white matter fibres, the diffusion is said to be anisotropic. In these anisotropic regions, such as the corpus callosum, the signal attenuation is most evident when the diffusion gradients are applied along the direction of highest diffusivity.

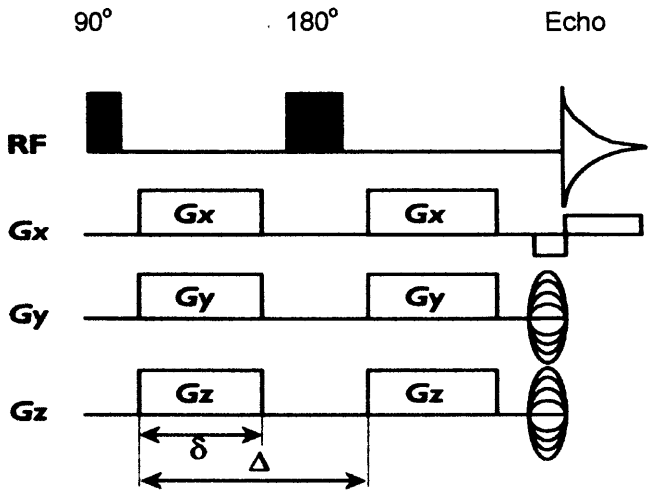

Figure 1.4 Stejskal-Tanner pulsed field gradient diffusion weighted spin echo scheme
The degree of diffusion sensitization (b value) is determined by duration (δ) and strength (height) of sensitizing pulsed-gradients (*G*), and time interval between two pulsed gradients (Δ).

1.4.3.2 Quantitative analysis of DWI

DWI offers ways of introducing different contrasts in MRI, which can help the visual interpretation of images but is only a qualitative type of study. In order to measure the diffusion coefficient, a minimum of two acquisitions with different diffusion weightings are necessary. These different diffusion weightings are given by different *b*-values; the lowest, b_{min} or *b*0, signifying little or no diffusion weighting and the highest, b_{max} signifying heavy diffusion weighting. From this ADC maps can be calculated where the value at each voxel represents the average diffusion coefficient of the tissue contained in that voxel. The intensity scale of the ADC map is inverted relative to the DWI with areas of high diffusivity, such as CSF, that appear dark on DWIs, appearing bright on the ADC maps.

1.4.3.3 Diffusion tensor imaging

ADC measurements depend on the subject's orientation relative to the magnet and gradient coils, thus potentially confounding cross sectional and serial studies. A fuller description of diffusion is given by the diffusion tensor, D, which has the advantage of more fully modelling the underlying properties of the

sample. In addition, measures of diffusion can be calculated from the tensor which are independent of the orientation of the subject with respect to the direction of measurements, including the mean diffusivity (MD) and the fractional anisotropy (FA). This rotational invariance makes diffusion tensor imaging (DTI) a robust quantitative technique.

The diffusion tensor can be calculated from a non diffusion-weighted image plus six or more diffusion-weighted measurements along non-collinear directions (140). The tensor can be diagonalised to give three eigenvectors, $\varepsilon_1, \varepsilon_2, \varepsilon_3$ representing the principal directions of diffusion, and three eigenvalues $\lambda_1, \lambda_2, \lambda_3$, representing the magnitude of diffusion (or the corresponding ADC values) along these directions. The eigenvectors are ordered with decreasing values of their eigenvalues so that ε_1 represents the principal direction of diffusivity, and λ_1 will be the ADC value along ε_1. This corresponds to the maximum diffusion in each voxel regardless of the orientation of the subject's head. MD is used to summarise the diffusion properties of a voxel and is given by the average of eigenvalues of the tensor. The FA is an estimate of what proportion of the magnitude of D is due to anisotropic diffusion and is proportional to the square root of the variance of the eigenvalues divided by the square root of the sum of the squares of the eigenvalues (141).

$$D = \begin{pmatrix} D_{xx} & D_{xy} & D_{xz} \\ D_{yx} & D_{yy} & D_{yz} \\ D_{zx} & D_{zy} & D_{zz} \end{pmatrix}$$

Figure 1.5 The diffusion tensor

1.4.3.4 Acquisition of DT images

Because of the large gradients used to sensitise the sequence to diffusion of water all DW techniques are particularly prone to artefacts caused by head motion. This can be partially overcome by using fast acquisition methods (e.g. single shot EPI) or by using motion correction 'navigation' techniques to minimise the effects. A further problem is that of pulsation of the brain, caused by CSF motion and

synchronized to the heartbeat. This pulsation of the brain and CSF can cause artefacts affecting the diffusion tensor (D). Synchronising the acquisition and the cardiac cycle can reduce errors in the calculation of D. This is done by cardiac gating, whereby the acquisition of the data happens during the 'flat' part of the electrocardiogram (ECG), when the heart muscle is relaxed. This reduces the efficiency of the sequence as the delay between acquisitions of groups of slices means that fewer slices can be collected within a TR period. Cardiac gating can be either triggered every QRS complex of the ECG or every n^{th} QRS complex. Triggering every QRS has the advantage of ensuring that the data acquisition stays in phase with the cardiac cycle, even during large variations of the heartbeat (142).

The acquisition protocol used depends upon the question being asked, the scanning time available and the scanner hardware being used. Although it is possible to calculate the diffusion tensor from a minimum of six encoding directions, sampling more directions reduces directional bias and improves SNR. As a whole volume is required for each diffusion-weighting direction and a large number of slices are required for whole brain coverage very large datasets are acquired. It has been recommended that for optimum results, the number of images with higher DW, b_{max} should be approximately nine times the number with lower DW, b_{min} (143). To obtain full brain coverage in a single scan using this protocol it is necessary to select a very long TR. This has a number of advantages, including SNR benefits from the very low T1 weighting but causes problems if cardiac gating occurs every n^{th} QRS complex. Normally n equals the number of RR intervals in a TR so that some slices are collected as much as 20-25s after the initial cardiac trigger. If all slices are timed relative to the initial trigger then synchronization with the cardiac cycle is likely to be lost for the later slices, leaving them effectively ungated. This can be overcome by having cardiac gating triggered every QRS complex (142).

1.4.3.5 Resolving crossing fibres

The modelling of diffusion as a single tensor fails to take into account the existence of complex intravoxel structures, and in voxels where fibres cross, diverge or experience high curvature the single tensor model is a poor approximation for the behaviour of the water molecules. One method used to overcome this looks at the shape of the ADC profile, which is the estimate of the diffusion coefficient along a predefined range of diffusion directions. When diffusion is Gaussian the ADC profile is fully

described by the diffusion tensor, however when diffusion is non-Gaussian (e.g. when there are crossing fibres present) a single tensor is insufficient to explain the shape of the ADC profile.

Areas where the single tensor fits the data poorly can be detected using the spherical-harmonic voxel-classification algorithm whereby spherical harmonics of 0^{th}, 2^{nd} and 4^{th} order are used to model the measured ADC profile (144). In these voxels a mixture of two Gaussian probability densities is then fitted and the principal diffusion directions of the two diffusion tensors provide estimates of the orientations of the crossing fibres. In all other voxels a single tensor model is fitted. Using this method, crossing fibres have been identified in brain regions where the corona radiata and superior longitudinal fasciculus cross, and in the pons (145). Other methods have also been developed that allow the estimation of crossing fibres within voxels (146-149).

1.4.3.6 Fibre tractography

The ability of DTI to reflect underlying tissue structure provides the basis for MR tractography, a method by which it is possible to measure brain connectivity non-invasively and rapidly. The principal eigenvalue and eigenvector can be used to make inferences regarding the orientation of white matter fibres in vivo (150) and this can be used to evaluate connectivity between voxels and determine pathways of anatomical CNS connections in vivo. Streamline tractography techniques use the orientation of maximum diffusion at each voxel and are performed by following these orientation estimates to reconstruct pathways that, within a coherent bundle, correspond to the underlying fibre pathway (151). Numerous mathematical algorithms have been used for this (143;151-156).

The fast marching tractography (FMT) technique (155) detects possible connection pathways from a seed point in the brain, providing 3D connectivity maps representing an informal probability of connectivity between a seed point and each voxel in the brain. FMT is based on level set theory and the fast-marching algorithm and models the evolution of a front over time from a seed point using the principal eigenvector (ε_1) of the diffusion tensor (157). The ε_1 field provides a variable rate of propagation for the front, causing every voxel in a volume data to be crossed by the front at different times. FMT uses the maps of time of arrival from the seed point to generate a 3D connectivity map. This map represents a metric of connectivity that can be considered as an informal likelihood of connectivity

between the seed point and every other voxel. This metric (or connectivity value) allows all possible routes of connection to be ranked by how well they correspond to the information provided by the DTI data.

FMT's advantages are its capability to provide an informal estimate of the likelihood of connection between different points in the brain using a connectivity metric, the lack of any curvature constraints, and its ability to demonstrate branching tracts. It has been partly validated by comparison with animal data and standard human brain atlases (156) and its reliability has been assessed in a reproducibility study (158). FMT is the tractography technique used in chapter 3 of this thesis.

1.4.3.7 Probabilistic tractography

The majority of tractography algorithms used adopt linear or streamlined approaches, using the principal eigenvector (ε_1) of the diffusion tensor to provide a propagation direction for each voxel along the path, as it is generally accepted that ε_1 is colinear with the principal orientation of fibre bundles (140). These types of streamlined approaches are generally susceptible to errors in the orientation of ε_1 due both to noise and to instances where the direction of the underlying tract anatomy is ambiguous or reflects the presence of multiple non-colinear fibre pathways. They assume absolute knowledge in fibre direction at every point and therefore have no concept of the uncertainty present in the recovered pathway. An erroneous pathway, due to noise or partial volume effects, is therefore assigned as much significance as 'true' pathways (159). An allowance for the assignment of the confidence in any connections seen would clearly improve the technique.

Probabilistic tractography approaches exploit this inherent uncertainty in the orientation of ε_1 for each voxel to generate maps of connection probability. Parker et al adapted the commonly used streamline approach to exploit the uncertainty in the orientation of the principal direction of diffusion in each image voxel (159). Orders of uncertainty based upon the anisotropy of the tensor and the relative magnitudes of the eigenvalues are used to generate probability density functions (PDFs) of the result of the diffusion tensor mixture model. These are a means of describing the local uncertainty in fibre orientation.

Each PDF is intended to interpret the information from a diffusion imaging acquisition in terms of the likely underlying fibre structure at each point within the brain. The end result is that for every voxel, a

distribution of directions rather than a single principal eigenvector is obtained. Any of these points can then be selected as a starting place for running a streamline propagation process. This can be repeated a large number of times (N), and the number of times that any voxel in the brain is encountered over N repetitions provides an index of connectivity for that voxel to the start point, eventually giving a map of probability of connection, or a Probabalistic Index of Connectivity (PICo) to the chosen seed point. The probability of connection in any experiment generally decreases with distance from the start point due to the cumulative effect of the uncertainties in propagation at each step in the streamline process.

The effects of noise on this model are also explicitly simulated and used to analyse the uncertainty associated with the principal diffusion direction of each diffusion tensor. It is observed that this uncertainty, and therefore the distribution of the principal diffusion direction, decreases as the fractional anisotropy increases. These PICo maps also benefit from the increased information provided by the multi-tensor decomposition described previously, allowing more accurate definition of pathways (145). PICo is the tractography technique used in chapters 4, 8 and 9 of this thesis.

Other probabilistic tractography algorithms have also attempted to characterise the uncertainty in the orientation of the principal direction of diffusion defined for each voxel to generate maps of probability of connection to chosen start points (160;161). One alternative method for determining and visualising uncertainty in estimates of fibre orientation is the bootstrap method. This works by randomly selecting individual measurements from a set of repeated measurements, thus generating many samples. By generating a sufficient number of bootstrap samples it is possible to obtain a measure of uncertainty of the given statistic. This information can then be used construct maps of 'cones of uncertainty', enabling both fibre orientation and uncertainty to be visualized concurrently. This approach has been used to demonstrate high uncertainty in fibre orientation where fibres cross or merge and anisotropy is low (162). Again the information about uncertainties in fibre orientation obtained using this method could be used to generate probabilistic tractography maps.

1.4.3.8 Limitations of tractography

When assessing the validity of connections identified by tractography, there is no perfect way of establishing whether they are genuine or whether they represent false positives or negatives.

Comparison with known human anatomy and known connectivity in primate brains are methods of validation, although precise knowledge of fibre pathways in humans is limited and the exact degree of similarity between monkey and human connectivity is unknown. Several factors contribute to the limitations of DTI tractography as a non-invasive tool for determining CNS connectivity.

Firstly, the poor resolution of DTI data (mm) in comparison to the size of the fibre tracts (μm) can lead to the false definition of a tract direction in a voxel, especially in the presence of fibres crossing within individual voxels. This limited spatial resolution can lead to false positives. In addition, this limited spatial resolution may lead to false negatives by ignoring small fibre tracts that may be functionally important. The ability of histological techniques to pick up connections at a cellular and synaptic level is an obvious advantage over the more macroscopic picture of brain connections generated by tractography.

Secondly, the relatively low SNR of DTI data introduces errors in the information obtained using DTI. SNR is inversely proportional to spatial resolution, in that increasing spatial resolution (i.e. decreasing voxel size) leads to a reduction in SNR. Using a higher magnetic field or longer acquisition times can compensate for this loss of SNR but may limit its use as a clinical application. Thirdly, tractography methods are blind to whether the fibres shown represent feed-forward or feed-backward projections and are therefore unable to distinguish between afferent and efferent fibre tracts (163). It therefore follows that when making comparisons between tractography findings and known human anatomy expert knowledge and interpretation is required.

1.5 FUNCTIONAL MRI AND LANGUAGE

1.5.1 The neuroanatomy of language function

The basic neurological model of language function dates back to the work of Broca and Wernicke in the nineteenth century. In 1861, Broca reported a post-mortem study of a patient with impaired speech production, finding an area of damage in the third frontal convolution of the left hemisphere (164). Subsequently Wernicke reported a post-mortem study of a patient with an impairment of speech comprehension with damage to the posterior superior temporal cortex (165). These areas became known as Broca's and Wernicke's areas respectively. Wernicke also predicted that damage to the white matter tracts connecting these two areas (the arcuate fasiculus) would lead to a particular aphasia with intact speech comprehension, intact speech production but a specific deficit in repetition. Alternatives to this simple anatomical model were proposed by cognitive psychologists in the twentieth century. They emphasised the complexity of language function without being constrained by the relevant anatomical structures involved and produced highly sophisticated models describing the many different components involved in linguistic function (166).

Over the past ten years, functional neuroimaging has provided a new means for mapping the functional anatomy of language. Whereas lesional studies identify which brain regions are necessary for a particular task functional imaging studies identify a whole network of regions that are used for a specific task, thereby providing complimentary information. Many functional studies have provided support for the original lesional data and the areas known as Broca's and Wenicke's have been localised more precisely to the anterior insula and the posterior superior temporal sulcus (166). Additional regions involved in semantic processing have been demonstrated in the left angular gyrus and the left inferior and middle temporal gyri, and a region in the left posterior inferior temporal cortex has been shown to be activated by a range of word retrieval tasks (166).

1.5.2 Paradigm design

The most widely used tasks in language fMRI experiments are verbal fluency tasks including word generation and verb generation, and semantic decision tasks. These are generally strongly lateralizing and reliably identify 'expressive language functions' in the dominant inferior frontal gyrus (IFG)

(Brodmann Areas (BA) 44, 45). It is always important to scan patients with tasks they can perform and although these tasks are usually covert they have been reliably replicated in numerous studies in both normal and patient populations. In addition their within-subject reproducibility has been demonstrated, although frontal activations have been shown to be more reliable than temporoparietal ones (167). While tasks of verbal fluency do show language-related activations they are not pure language tasks, containing substantial components of executive processing and of working and verbal memory. These activations are typically seen in the middle frontal gyrus (MFG) (BA 46, 49).

They are also less reliable at identifying 'receptive' language areas located in the dominant temporal lobe. These processing areas are best assessed by tasks that probe language comprehension such as reading sentences or stories, which tend to activate superior temporal cortex extending to supramarginal gyrus (BA 20,21,39) (168;169), but are less strongly lateralizing than verbal fluency tasks. A study demonstrated that using a panel of fMRI tasks (verbal fluency, reading comprehension and auditory comprehension) was helpful in reducing inter-rater variability and helped in the evaluation of language laterality in patients with focal epilepsy (170).

Decisions regarding laterality are usually based on an asymmetry index (AI), reflecting the difference between activated voxel counts on the left and right, and calculated using the formula;

$$AI = (L - R) / L + R)$$

This can be done for the whole hemisphere or using regions of interest (ROIs) targeted to known language areas and AI thresholds of 0.20 or 0.25 tend to be used, with an AI threshold above 0.20 reflecting left hemisphere dominance; below –0.20 right dominance; and between –0.20 and 0.20 bilateral dominance (171).

This type of AI calculation has some problems, in particular the fact that the AI can differ according to the significance threshold chosen for the activation map from which it is calculated (172). Alternative approaches to quantifying brain activity in order to calculate an AI include measuring the mean signal intensity change induced by the task within a brain volume of interest (172), and performing a statistical

comparison of the magnitude of task-induced activation in homotopic regions of the two hemispheres (173). Other studies have suggested that visual rating appears to work as well as calculating AI (174).

The simplest forms of study designs (including those described above) employ cognitive subtraction designs. These involve selecting a task that activates the cognitive process of interest and a baseline task that controls for all but the process of interest. One problem of this type of design is that it depends on an assumption known as pure insertion, which supposes that a new cognitive component can be inserted without affecting those processes that are also engaged by the baseline task (175). Another problem with cognitive subtraction is in finding baseline tasks that activates all but the process of interest. These problems can be overcome by using more complex experimental designs, such as factorial designs and cognitive conjunctions.

Factorial designs use two or more variables (e.g. sentence vs. word presentation and auditory vs. visual presentation) and allow the effect one variable has on the other to be measured explicitly. The analysis of this type of design involves calculating the main effects of each variable and the interaction between them (175). Cognitive conjunctions are an extension of cognitive subtraction paradigms. While cognitive subtraction looks for activation differences between a single pair of tasks, cognitive conjunction looks at two or more task pairs which share a common processing difference (176). The advantages of this approach are that it allows greater freedom in selecting the baseline task as it is not necessary to control for all but the component of interest, and that it does not depend on the assumption of pure insertion.

1.5.3 Language lateralisation

For a number of years the IAT has been widely regarded as the 'gold standard' for language lateralisation. Focal epilepsy may be associated with disrupted lateralisation and localisation of language regions therefore one would expect a higher probability of abnormal language lateralisation in these groups. Nevertheless significant differences have been reported between centres in the relative proportions of right and left hemisphere dominant patients, some of which may be due to the different criteria used for assessing dominance. The percentage of left hemisphere dominant right handed

patients has ranged from 63% to 96% (177) while for left handers a similar variation has been reported between 38% (178) to 70% (179).

Functional MRI has been used to study language lateralisation in normal subjects as well as epilepsy patients. Pujol et al used silent word generation to define the occurrence of atypical language lateralisation in 50 left handed subjects and 50 right handed subjects. 96% of right-handed subjects showed fMRI changes lateralised to the left hemisphere, whereas 4% showed a bilateral activation pattern. In contrast, left-hemisphere lateralisation occurred in 76% of left handers, bilateral activation in 14% and right-hemisphere lateralisation in the remaining 10%. Exclusive right hemisphere lateralisation only occurred in a single left-handed subject (180). These results showing greater atypical language dominance in left handers were in keeping with the data from IAT literature.

Springer et al performed a comparison between 100 right-handed healthy subjects and 50 right-handed epilepsy patients to investigate the factors influencing language dominance. 94% of the normal subjects were considered left hemisphere dominant and 6% had bilateral representation, findings in keeping with those of Pujol et al. The epilepsy group showed greater variability of language dominance, with 78% showing left hemisphere dominance, 16% symmetric activation and 6% showing right hemisphere dominance. Atypical language dominance was associated with an earlier age of brain injury and with weaker right hand dominance (181).

The localisation of the epileptogenic lesion and epileptic activity (182) has also been shown to influence language organisation. In a retrospective study of 183 patients with HS who had undergone presurgical evaluation, Jansky et al found that atypical speech dominance occurred in 24% of those with left sided HS whereas all those with right-sided HS had left sided speech dominance. In addition they found that atypical speech representation was associated with higher spiking frequency and in those with sensory auras suggesting ictal involvement of the lateral temporal structures. No association was demonstrated between either age at epilepsy onset or age at initial precipitating injury and atypical speech representation (183).

Thivard et al looked at reorganisation of both frontal (using a fluency task) and temporal lobe (using a story listening task) language functions in patients with unilateral TLE (184). Controls and right TLE patients had a significantly more left lateralised pattern of language activation compared to left TLE

patients, and in patients with atypical language representation the degree of reorganisation towards the right hemisphere was greater in the temporal lobes than in the frontal lobes. In a study of 50 patients with focal epilepsy, greater atypical language dominance was seen in those with left hemisphere seizure focus (185). Left TLE patients who did not have atypical language also had lower asymmetry indices in both frontal and temporal ROIs, mainly due to greater activation in homologous right hemisphere regions.

The degree of language lateralisation has also been related to the nature of the epileptogenic lesion with early acquired lesions, such as HS, considered to be associated with greater incidence of atypical language lateralization compared with developmental lesions originating in utero, such as MCDs. One recent study has demonstrated a higher degree of atypical language dominance, in both frontal and temporal language areas, in patients with left HS compared to patients with left frontal and lateral temporal lesions (186), suggesting that the hippocampus itself may play an important role in the establishment of language dominance. A further study however demonstrated no difference in the frequency of atypical language lateralisation between left TLE patients with HS and those with developmental tumours (187).

It is interesting to speculate on how TLE affects language lateralisation, and it is possible that strong connectivity between inferior frontal and temporal areas make frontal lobe functions particularly sensitive to temporal pathology. The increased incidence of atypical language dominance in epilepsy illustrates the importance of establishing language dominance prior to performing surgical resection and as a consequence much of the work on fMRI in epilepsy has been directed towards trying to replace the IAT as a means of doing this.

1.5.4 Comparison of fMRI, IAT and ECS findings

Early studies performing comparisons between fMRI and the IAT occurred in the mid 1990s and since then a number of series have been published. These are summarised in Table 1.3. Just as IAT protocols differ between centres, a number of fMRI paradigms to determine language dominance have been employed but overall a concordance of approximately 90% is seen between the two techniques.

The remaining cases generally exhibit partial disparity where one method shows bilateral language representation and the other lateralised language dominance.

These results in part reflect the explicit aim of the studies with tasks being selected specifically to provide strong lateralizing data. For example, Benson et al examined the lateralizing qualities of three language tasks in controls, including object naming, single word reading and verb generation. The latter was chosen for the patient experiments after being found to be the strongest predictor of laterality (188).

Although overt disagreement between fMRI and IAT is rare, concordance is not perfect, with one of the studies suggesting that fMRI may be less reliable in left-sided neocortical epilepsy (25% disparity) in comparison with left-sided medial TLE (3% disparity) (174). An interesting case of false lateralisation of language function in a post-ictal patient with left hippocampal sclerosis also illustrates the need for caution in the interpretation of results in individual patients. No activation was seen in the left temporal lobe during multiple language tasks after a cluster of left temporal lobe seizures but in a repeat fMRI experiment two weeks later activation was seen predominantly over the left temporal region (189).

A combination of four different language tasks has shown more reliable and robust lateralisation in normal subjects (190) by targeting brain regions common to different tasks, thereby focusing on areas critical to language function. This approach was subsequently used on patients with typical and atypical language dominance according to the IAT. Concordance was seen in 10/11 patients with left language dominance, 3/4 with mixed dominance and 2/3 with right hemisphere dominance on IAT, again suggesting higher concordance rates in patients with typical language dominance (191).

It is worth bearing in mind however that the IAT, although widely considered as the 'gold standard' investigation, has a number of limitations. As well as being invasive and expensive, it cannot be easily repeated, does not provide localising data, and data from normal subjects is unavailable. It is even debatable whether fMRI and IAT are directly comparable as they probe different aspects of language.

Comparisons have also been performed between fMRI activation maps and regions showing disruption of function during intraoperative electrocortical stimulation (ECS). In order for fMRI to be used instead of ECS it must demonstrate a high predictive power for the presence as well as the absence of critical language function in regions of the brain. As with IAT, these studies show strong, but incomplete agreement with fMRI: while the sensitivity of fMRI is over 90% the specificity is only 67% (192-194).

Although false positive activation (fMRI activation but no ECS disruption) is relatively common this is not surprising given that fMRI activates whole networks of regions, not all of which are essential for the task in question. False negative findings (regions showing disruption by ECS but no fMRI activation) are more critical when planning a surgical resection and these were identified in two patients out of 21 reported in two series. Activation and disruption was typically within 5mm in frontal regions and 10mm in temporal areas.

Rutten and colleagues demonstrated that a combination of four different fMRI language tasks corresponded well with ECS findings in the temoroparietal region. Sensitivity was 100% in all but one patient. This high negative predictive value suggested that areas where no significant fMRI activity was present could be safely resected without using ECS. fMRI activity however was not always absent at noncritical language areas (specificity 61%) limiting its positive predictive value for the presence of critical language areas to 51%. They concluded that although this precluded replacing ECS with fMRI it could be used to speed up intracranial mapping procedures and to guide the extent of the craniotomy (191).

Table 1.3 Concordance between fMRI language lateralisation and the IAT

Authors	Sample*	fMRI language lateralisation tasks	Concordance
Desmond et al (1995) (195)	*n* = 7	Semantic decision task	100%
Binder et al (1996) (196)	*n* = 22	Semantic decision task	r = 0.96
Hertz-Pannier et al (1997) (197)	n = *6***	Verbal fluency paradigm	100%
Yetkin et al (1998) (198)	*n* = 13	Word generation task	r = 0.93
Benson et al (1999) (188)	*n* = 12	Verb generation task	100%
Lehericy et al (2000) (169)	*n* = 10	Semantic fluency Sentence repetition Story listening	Semantic fluency > story listening > sentence repetition. Greater concordance between IAT results and activation asymmetry in frontal than temporal lobes.
Carpentier et al (2001) (199)	*n* = 10	Identification of syntactic /semantic errors in target sentences	80%
Gaillard et al (2002) (171)	*n* = 21	Reading paradigm	85%
Woermann et al (2003) (174	*n* = 100	Word generation	91%
Sabbah et al (2003) (200)	*n* = 20 ***	Word generation Semantic decision	95%

* Some of these studies report fMRI data on larger samples. However only the patients with fMRI and IAT data are included here.
** (Age range 8 – 18)
*** Patients with suspected atypical language lateralisation were selected

1.5.5 Prediction of postoperative language deficits

In addition to the well recognised decline in verbal memory, some studies have also reported selective language deficits following ATLR. Davies et al (201) found that 39% of their patients demonstrated a significant decline on the Boston Naming Test following dominant ATLR, and Saykin et al (202) also reported a decline in naming abilities following the same procedure. It has also been suggested that the

risk for postoperative decline in naming abilities increases with age of seizure onset and the extent of lateral temporal neocortex resected (203).

Preoperative cortical stimulation via subdural grid electrodes has been used to further localise language function. Devinsky et al (204) found that that early onset of dominant temporal lobe seizure foci leads to a more widespread or atypical distribution of language areas, particularly naming and reading areas. A subsequent study also reported that markers of early left hemisphere damage (such as early seizure onset, poor verbal IQ, left handedness and right hemisphere memory dominance) increase the chances of essential language areas being located in more anterior temporal regions. Again these areas were identified using naming and reading tasks (205).

These findings suggest that naming and reading abilities are the language skills most at risk following dominant temporal lobe surgery. While the IAT may provide a useful index of language laterality, it does not provide detailed information on the localisation of these specific language skills. As these may also vary in location between individuals, the role IAT can play in the prediction of postoperative deficits in individual patients is therefore limited. Designing fMRI paradigms that specifically probe naming and reading skills would provide a useful clinical tool for mapping relevant language skills that could be used in the prediction of postoperative deficits.

One study has used preoperative functional neuroimaging to predict language deficits following left ATLR. fMRI AIs for a semantic decision task were calculated in homologous regions of interest in 24 patients undergoing left ATLR . The fMRI AI in the temporal lobe was found to be predictive of deficits seen on a postoperative naming test with a greater degree of language lateralisation toward the left hemisphere related to poorer naming outcome and language lateralisation toward the right hemisphere associated with less or no decline. Interestingly the correlation between temporal lobe fMRI AI and naming deficits was stronger than that seen in the frontal lobes and also stronger than that between IAT and naming deficits. Single subject data showed that 13 of the 16 patients with clearly left lateralised temporal lobe language function declined on naming tasks >2SD below the mean for a right ATLR group, whereas none of the 8 patients with symmetric or right-lateralised language functions declined to that degree (206).

Interestingly, many patients do not suffer any language deficits following ATLR, suggesting that multiple degenerate sets of neural systems exist that are capable of performing the same cognitive function, and that some of these may be engaged following focal brain injuries. Noppeney et al showed that in normal subjects, sentence comprehension activated a primarily left lateralised fronto-temporal system extending into the left temporal pole. They then looked at patients who had undergone left ATLR but did not have deficits in sentence comprehension and found that they had decreased activation in undamaged areas of the normal left hemisphere system but increased activation in several right frontal and temporal regions not usually engaged by normal subjects (207). This suggests that there is more than one neural system capable of sustaining sentence comprehension.

This study was unable to tell whether this functional reorganisation to the right IFG occurred pre- or post-operatively. One recent study has looked at the role of the right IFG by comparing its functional activation on a verbal fluency task in controls with 12 left TLE patients (208). The patients were shown to activate a more posterior right IFG region compared to controls although left IFG activation did not differ significantly between the two groups. Further, verbal fluency-related activation in the right IFG was not anatomically homologous to left IFG activation in either patients or controls. This extended the findings of Noppeney et al by demonstrating that the reorganisation took place pre-operatively in patients with chronic left TLE, and suggested the possibility that the prediction of language outcome following left ATLR may depend not only on the extent of preoperative right hemisphere activation, but also its location.

1.5.6 Conclusion

fMRI allows the non-invasive assessment of language function to be performed and offers a valid alternative to the IAT for establishing language dominance. By tailoring paradigms towards the localisation of the specific language skills most at risk following ATLR it will be possible to map relevant language functions in the epilepsy surgery population. This in turn will allow better assessment of the risks posed by surgery in each individual patient, enabling better preoperative patient counselling and modification of surgical technique to minimise such risks.

1.6 FUNCTIONAL MRI AND MEMORY

1.6.1 Introduction

Long- term episodic memory function in humans is dependant on MTL function. The MTL consists of the hippocampus, amygdala and parahippocampal regions. Bilateral injury to these areas leads to a characteristic amnesic syndrome (103) (43), while unilateral lesions lead to material-specific deficits (see section 1.3.6.2) (44) (45) (109) (110). fMRI has the potential to offer more precise localisation of cognitive processes than lesion studies, however there are important caveats when considering the role of fMRI. Firstly, areas activated by a particular fMRI paradigm are not necessarily crucial for the performance of that task. Secondly, it does not necessarily follow that all areas involved in a task will be activated by a particular fMRI paradigm. Thirdly, the extent of activation seen in a task, in terms of both the area activated and the magnitude of the peak, may bear no relation to the competence with which that task is performed. Caution will also be needed in the interpretation of results bearing in mind that fMRI techniques, while useful for the localisation of cognitive function, may not reliably indicate the capacity of unilateral temporal lobe structures.

1.6.2 Problems with clinical memory fMRI

The extensive use of fMRI in cognitive neurosciences, along with the wide availability of the technology and data analysis techniques, made it tempting to speculate that existing paradigms could be readily applied to patient populations and used as clinical tests. This has not been the case for a number of reasons. fMRI is based upon the observation that increased neuronal activity is associated with a regionally specific but disproportionate increase in cerebral blood flow. The resulting increase in the oxyhaemoglobin to deoxyhaemoglobin ratio leads to a change in MR signal in activated regions that can be detected by rapid imaging techniques and forms the basis of the BOLD effect. The relationship between neuronal activity and the BOLD signal is believed to reflect mainly synaptic activity (135). It is not yet clear however whether this neurovascular coupling occurs in the same manner in pathological brains. fMRI is also extremely sensitive to motion although generally epilepsy patients are familiar with MRI scanners and may move less than control subjects (171).

A further problem is that some of the brain regions of most interest in epilepsy, such as the inferior frontal and MTL are subject to geometric distortions and signal loss during fMRI acquisition (see section 1.4.1.6) (128). This can result in reduced sensitivity and anatomical uncertainties when interpreting the images. Most epilepsy studies have been performed on 1.5 Tesla clinical MRI scanners. Scanning at higher field strength improves SNR but increases distortions and dropout. The use of high-performance gradients and thin slice acquisitions ameliorate these problems and improve fMRI quality. It has been demonstrated that signal loss due to susceptibility artefact is most prominent in the inferior frontal and inferolateral temporal regions (209) and as the hippocampus rises from anterior to posterior one would expect greater susceptibility-induced signal loss in the anterior (inferior) relative to posterior (superior) hippocampus. This may have been one reason for the relative lack of anterior hippocampal activation in early fMRI studies of memory (210).

One study has directly examined the effects of susceptibility artefact on hippocampal activation by demonstrating its differential effect on the anterior versus the posterior hippocampus. The averaged resting voxel intensity in an anterior hippocampal ROI was significantly less than in a posterior hippocampal ROI and intensity decreases were substantial enough to leave many voxels below the threshold at which BOLD effects could be detected (210). On top of this, it has been shown that the sensitivity to BOLD changes is proportional to signal intensity at rest so that voxels with a lower baseline signal (such as those in anterior hippocampal regions) would be more difficult to activate than those with higher baseline signals (211).

An important issue when designing paradigms for patients with neurological deficits is to use tasks that they are able to perform. A differential pattern of activation between patients and normal subjects is only interpretable if patients are performing the task adequately (212). Finally the different questions being asked by cognitive neuroscientists and clinicians lead to different approaches to data analysis. The approach of neuroscientists is to look at groups of matched controls performing the same task and determine which brain regions are commonly activated across the group. The emphasis is on avoiding false positive results (Type I errors) and conservative statistical thresholds need to be used, which may lead to an under-representation of brain areas truly involved. Conversely, clinicians are considering individual patients where the priority is to identify all brain regions involved in a task, i.e. avoiding false

negatives (Type II errors). As a result, less stringent statistical thresholds are required and indeed thresholds used may need to vary on an individual basis.

The assessment of ability to sustain memory is critical for planning ATLR. The use of fMRI in the prediction of postoperative memory deficits is more challenging than for language. This is partly due to the different components involved in memory processing, such as encoding and retrieval, and the fact that the nature of the material being encoded or retrieved influences which brain areas are activated. A further difficulty is how to separate brain activity related specifically to memory from that related to other cognitive processes. In consequence more complex paradigms are required when studying memory than for examining language function.

1.6.3 Memory paradigm design

Standard fMRI experiments initially used block design paradigms looking for regions of the brain showing greater activation during task blocks (e.g. hand tapping or word generation) compared with rest blocks. A problem when designing memory fMRI experiments was how to separate brain activity due specifically to memory from that due to other cognitive processes being used in the task. Early fMRI studies of memory encoding employed blocked experimental designs to contrast tasks promoting differing memory performance, using the 'depth of encoding' principle (213). This states that if you manipulate material in a 'deep' way (e.g. make a semantic decision about a word) then it is more likely to be recalled successfully than material manipulated in a 'shallow' way (e.g. make a decision of whether the first letter of a word is alphabetically before the last letter). The results of these studies, e.g. intentional learning versus reading (214) and semantic versus non-semantic classification (215;216), tended to show consistent activation in left prefrontal cortical regions (217) along with less reliable MTL activation. Similar assumptions underlie the use of 'novelty' paradigms in probing memory encoding. During these experiments, alternating blocks of novel and repeated stimuli are presented, with the hypothesis being that more memory encoding takes place while viewing a block of novel stimuli than when viewing the same repeated stimulus (218). One study has directly compared two fMRI paradigms in a group of control subjects, both using complex visual scenes as stimuli (219). One emphasised the novelty of stimuli, comparing activation between blocks of novel versus repeated stimuli, while the other

emphasised 'relational processing' (the formation of associations), by comparing blocks of novel stimuli with scrambled images. They found that both caused hippocampal activation but that relational processing resulted in a larger volume of hippocampal activation and more anterior hippocampal activation.

The advantage of blocked designs is that they are efficient in detecting differences between two conditions. The main problem in their interpretation however lies in the inference that the effects shown by these contrasts reflect differences in memory encoding, rather than any other differences between the two conditions (e.g. response to novelty, semantic processing) that are independent from differences in memory encoding.

Attempts were made to overcome this problem using parametric block designs. In this type of experimental design, the magnitude of the fMRI signal during a block is correlated with the number of items remembered from that block on a subsequent memory test. This type of study, first applied to fMRI by Fernandez et al (220), could claim to examine successful memory encoding but was soon superseded by the advent of event-related studies (see section 1.4.2.4.2).

Event-related fMRI is defined as the detection of transient haemodynamic responses to brief stimuli or tasks (221) (222) (223) (224). It has a number of methodological advantages (139), one of which is that trials can be categorised according to a subject's performance on a subsequent test in order to obtain fMRI data at the individual item level. Therefore when studying memory encoding, activations for individual items presented can be contrasted according to whether they are remembered or forgotten in a subsequent memory test. This type of analysis allows the identification of brain regions showing greater activation during the encoding of items that are subsequently remembered compared with items subsequently forgotten (subsequent memory effects), which are then taken as candidate neural correlates of memory encoding (225).

In spite of these problems, a number of fMRI studies have now demonstrated hippocampal activation in the context of episodic memory. A wide range of stimuli have been used, including words, faces, line drawings, patterns, objects, scenes and routes, and both memory encoding and retrieval have been studied. The data so far has given us important insights into the way memory processing in the human brain occurs. The distribution of MTL activation seen varies both in lateralisation and localisation

depending on the type of material being used, i.e. verbal or non-verbal, and the stage of memory processing, i.e. encoding or retrieval.

1.6.4 Material specific lateralisation of memory function

Patients with unilateral MTL lesions have provided evidence of dissociation in function between the dominant (usually the left) hippocampus, mediating verbal memory (44) and non-dominant (usually the right) hippocampus mediating non-verbal or visual memory (45). A study of patients following unilateral ATLR showed deficits in topographical memory following right ATLR and episodic memory deficits following left ATLR suggesting a material specific lateralisation of function in MTL structures (110). These observations have led many researchers to use functional imaging studies to look for lateralisation of cerebral activation patterns during episodic memory processes. Several early PET and fMRI studies revealed greater activation in left prefrontal cortex (PFC) during verbal encoding (215) (226;227). Other studies have shown material-specific lateralisation in prefrontal regions, with right inferior prefrontal activation during encoding for non-verbal information, such as abstract visual patterns (228) and left prefrontal activation for word encoding and right sided activation for non-verbal encoding using word and checkerboard encoding (229).

Using a blocked experimental design comparing intentional and incidental encoding Kelley and colleagues investigated memory encoding for three stimulus types: written words, nameable line drawn objects and unfamiliar faces. Word encoding versus fixation on a cross-hair produced left-lateralised activation, face encoding produced right–lateralised activation and object encoding produced bilateral activation. These results were observed in both dorsal frontal cortex and MTL. They indicated regions in both hemispheres that could be differentially engaged depending on the nature of the material being encoded, although in this study only five normal subjects were tested, and subsequent memory effects were not specifically investigated (214).

Golby and colleagues compared activations for the encoding of four kinds of materials – words, faces, scenes and abstract patterns – using a novelty paradigm (218). Verbal encoding resulted in left-lateralised activation of the inferior PFC and MTL. Pattern encoding activated the right inferior PFC and

right MTL. Scenes and faces resulted in approximately symmetrical activation in both regions. These results suggested that the lateralisation of encoding is determined by the verbalisability of the stimuli, however the disadvantages of this type of paradigm were discussed in the previous section.

Not all the studies linking MTL activation with episodic encoding have shown such clear lateralisation of function. Fernandez et al found significant positive correlation between the number of recalled words and activation in posterior hippocampal regions, although no difference between left and right was revealed (220). Bilateral parahippocampal activation has also been demonstrated for the encoding of pictures, spatial environments and colour photographs of everyday scenes, all of which involve both verbal and non-verbal memory processes (230) (231).

Two early studies used event-related fMRI to show subsequent memory effects in the MTL. Brewer et al showed in six normal subjects that the magnitude of activation in bilateral parahippocampal and right frontal areas during the study of complex, colour photographs predicted which photographs were later remembered or forgotten. In addition there was greater parahippocampal activity during encoding for pictures that were 'remembered' specifically than for pictures that just seemed familiar, and also greater parahippocampal activity for familiar pictures compared to forgotten pictures, although there was no clear lateralisation of activation (216).

In a paper published simultaneously, Wagner and colleagues reported two experiments, one using a blocked design and one using an event-related design to examine verbal encoding processes. In the blocked-design experiment, twelve subjects performed alternating task blocks consisting of semantic processing, non-semantic processing and visual fixation. As expected, subsequent memory performance was significantly higher for semantic than for non-semantic blocks and greater fMRI activation was seen during semantic processing in left PFC, left parahippocampal and left fusiform gyri. In the second experiment thirteen subjects performed a word encoding trial that was categorised according to whether a word was subsequently remembered or forgotten. Event-related activity in left prefrontal, left parahippocampal and left fusiform gyri correlated with subsequent memory (216).

1.6.5 Process specific lateralisation of memory function

A further hemispheric asymmetry emerged from early PET studies showing lateralisation due to the separate components involved in memory processing, a finding seemingly at odds with lesion-deficit models. Data showed that during encoding left PFC tended to show greater activation than right PFC, whereas during retrieval right PFC tended to show greater activation than left. This pattern of results was dubbed the Hemispheric Encoding/Retrieval Asymmetry (HERA) model (232) (233). These findings have been demonstrated for both verbal (234) and non-verbal materials (235). Similar findings have since been demonstrated in some fMRI studies (236). Others have argued that this asymmetry of PFC activations may reflect the material used rather than the memory processes. In addition the HERA effect has not been demonstrated in the MTL.

1.6.6 Process specific localisation of memory function

In addition to the functional division between left and right there is also evidence for further dissociation of function within each MTL. The amygdala, lying anterior to the hippocampus is a structure that has been linked to emotional memory (237), and patients with isolated amygdala damage show a specific impairment of recall of emotional stimuli (238). Functional imaging has demonstrated amygdala activity correlating with subsequent memory for emotional material (239). Lateralised amygdala activation was seen in TLE patients using a fearful face paradigm known to cause bilateral amygdala activation in controls, leading the authors to speculate that this type of fMRI paradigm may have clinical value in the presurgical assessment of TLE (240).

Other evidence points to a functional localisation within each hippocampus dependant on the stage of memory processing. A meta-analysis of 54 published PET studies of memory by Lepage et al demonstrated this functional dissociation with activations associated with memory encoding located in anterior hippocampal regions and activations associated with retrieval located more posteriorly. They referred to this pattern of encoding and retrieval activations as the HIPER (Hippocampal Encoding/Retrieval) model (241). Evidence from fMRI experiments has proved contradictory with many

early studies refuting the HIPER model (242) (243). More recent event-related studies however have supported the PET model of anterior hippocampal activation during memory encoding (244).

Further functional segregation within the hippocampus has been suggested, with differential anteroposterior activation in relation to stimulus familiarity (245) and dissociable perirhinal, hippocampal and parahippocampal activations during free recall of words presented during scanning (246). Using high resolution structural and functional MRI, Zeineh and colleagues "unfolded" the hippocampal cortex, revealing the entirety of each hippocampal region and adjacent neocortical regions in a single "flat map" and were able to demonstrate differential activation of hippocampal subregions during memory encoding (247). This unfolding technique was then used to demonstrate a dissociation in function between memory encoding (associated with activation in dentate gyrus and CA fields 2 and 3), and memory retrieval (associated with activation in the subiculum) (248). Although these results would suggest that different subdivisions within the hippocampus make distinct contributions to new memory formation, the combination of fMRI's limited spatial resolution and the anatomical distortions seen in the MTL would suggest that such conclusions should be treated cautiously.

In summary, it is clear that many factors may affect the anatomical correlates of memory as seen with functional neuroimaging in normal subjects. These include material type, the nature of the encoding strategy adopted by the subject, the type of subsequent memory test used (recognition, free recall, cued recall) and other item-specific qualities such as distinctiveness (both semantically and physically). All these sources of variability may affect both the magnitude and also, possibly, the distribution of the subsequent memory effect seen. Nevertheless it would appear that an important functional relationship between prefrontal and medial temporal structures lies at the heart of both memory encoding and retrieval.

1.6.7 The effect of TLE on memory processes

There has been much speculation regarding the possible role of fMRI of memory in epilepsy, in particular with regard to the presurgical evaluation of TLE patients. It has potential both in replacing the IAT and in providing additional data regarding memory lateralisation, currently assessed primarily by

baseline neuropsychological assessment. In contrast with the IAT, fMRI is cheaper, non-invasive and repeatable.

Caution will be needed in the interpretation of results bearing in mind that fMRI techniques, while useful for the localisation of cognitive function, cannot be used to assess the capacity of unilateral temporal lobe structures (98). This is in contrast to the IAT which is useful in safeguarding against a severe postoperative amnesic syndrome, but less relevant in predicting the types of material specific memory impairments seen following surgery, i.e. impaired verbal memory following left ATLR, and impaired non-verbal, or visuospatial memory following right ATLR. Indeed, with the improvements in structural MRI, the risk of a postoperative amnesic syndrome has dramatically reduced, and of all the postoperative unilateral temporal lobe amnesic patients written up in the literature, none would have had an entirely normal contralateral hippocampus in terms of size and structure on modern MRI scans (102).

A number of studies have used fMRI to look at the lateralisation of memory in patients with TLE compared to that seen in normal subjects, and also compared the findings with the results of the IAT, however a number of these have employed blocked design studies, and therefore cannot claim that subsequent memory effects have been specifically examined.

Detre et al used an encoding task during which subjects were shown alternating blocks of complex visual scenes and abstract patterns. Although subjects were told to memorise the scenes for subsequent testing, subsequent memory effects were not looked at and an assumption of incidental memory encoding was made. The symmetry of the fMRI activations in 9 patients with TLE were compared with the results of IAT performed as part of their pre-operative evaluation. Task activation, which was located posteriorly in the hippocampal formation, was near symmetric in normal subjects, whereas in patients with TLE significant asymmetries were observed. Furthermore, in all 9 patients the asymmetry of the activation concurred with the assessment of hemispheric memory skills from the IAT, including 2 patients with paradoxical IAT memory lateralisation ipsilateral to seizure focus. Task correlated activity was seen to be higher in controls and patients with good performance, although successful lateralisation was seen even in patients who complained that the task was too difficult.

Correlating the results of a single fMRI memory paradigm with those from an IAT in which multiple memory tests were performed may however be problematic (249).

Dupont et al found that patients with left HS produced different functional activations on a verbal episodic memory task compared with normal subjects. The experimental design for memory encoding and retrieval consisted of blocks of word learning and silent free recall respectively, compared to visual fixation on the letter A. Again an assumption was made that the contrast seen was due to memory encoding but subsequent memory effects were not looked at. While controls demonstrated bilateral activation of the PHG amongst other areas during memory retrieval, the patients demonstrated slightly less parahippocampal activation but significantly increased left prefrontal activations during the encoding and retrieval phases of the task. No hippocampal activation was detected. Memory test performance was significantly worse in patients, with a mean recall of 3.1 out of 17 words, than in normal subjects whose mean recall was 10.7. This result was interpreted as a dysfunctional response due to the epilepsy and left HS (250). They subsequently examined activation patterns during a 24 hour-delayed retrieval of the word list in the same group of controls and left TLE patients. Controls showed a similar left occipitotemporofrontal network activated during both immediate and delayed retrieval conditions but additional right hippocampal activation during the delayed retrieval. Memory test performances for this group were broadly similar over 24 hours. In the patients with left TLE this distributed neocortical and MTL network was very poorly activated during delayed retrieval. The authors suggested this reflected an inability to reactivate areas important for retrieving stored information although it is worth noting that memory test performance was not significantly worse for delayed versus immediate retrieval and that both were significantly worse for patients compared with the control group (251).

A complementary study was performed using the same paradigm in patients with right TLE. Surprisingly, verbal memory performances were also significantly impaired for these patients compared with controls and their activation patterns showed a global reduction of left hemisphere activations compared with controls. This suggested bilateral functional consequences of unilateral HS upon memory processing (252).

Other experiments have utilised memory tasks that produce unilateral temporal lobe activations in normal subjects. Bellgowan and colleagues used a block design paradigm comparing deep and shallow encoding known to cause extensive left prefrontal and temporal activation in normal right-handed subjects to investigate activation during verbal encoding in 28 patients with TLE. They found that patients with right TLE showed much stronger activation in the left MTL, including hippocampus, PHG and collateral sulcus, than patients with left TLE, who showed little significant activation in these regions. Activation of language areas in the frontal and parietal lobes was similar in both groups. Neither group showed activation of any of these regions in the right hemisphere. Its success in discriminating left TLE from right TLE would suggest a possible role for fMRI techniques in contributing to the prediction of the side of seizure focus in patients with MRI negative TLE (253).

Jokeit and colleagues also investigated the hemispheric asymmetries of MTL activation in 30 patients with TLE using a task employing mental navigation and recall of landmarks based on retrieval of individually familiar visuospatial knowledge (Roland's Hometown Walking Test (254)). This task was shown to reliably activate MTL structures even in a child of 7 and a patient with an IQ of 51. Asymmetry ratios of activation were calculated from significantly activated voxels. This activation was bilateral and symmetric in both parahippocamapal gyri in normal subjects but in 90% of patients with unilateral TLE the activation was reduced on the side of seizure onset as judged by absolute numbers of activated voxels and asymmetry ratios. No inferences were made about whether the MTL activation seen was related to memory or memory-independent visuospatial abilities, however it can be seen how such lateralising and localising data may provide complementary information for presurgical evaluation, in particular when results of other investigations have been contradictory (255). This paradigm was subsequently combined with a fearful face paradigm that caused bilateral amygdala activation in control subjects but lateralised amygdala activation in patients with MTLE. The combination of results from both fMRI paradigms was shown to improve the lateralisation of the side of seizure onset in these patients (240).

Using the paradigm described earlier (see section 1.6.4) for normal subjects, Golby et al studied memory lateralisation in 9 patients with TLE undergoing presurgical evaluation. Lateralisation was calculated using an AI for significantly activated voxels within the MTL region of interest. In 8 of these,

lateralisation was concordant with that obtained from the IAT. At a group level, greater activation was also demonstrated in the MTL contralateral to the seizure focus such that in the left TLE group, verbal encoding engaged the right MTL and in the right TLE group, nonverbal encoding engaged the left MTL (256).

Impairment of memory encoding following ATLRs suggests that anterior MTL regions are critical for successful memory encoding. A number of the studies discussed above have however proved contradictory with many showing encoding related activations in posterior hippocampal and parahippocampal regions which would be left intact following ATLRs. One possible explanation for this apparent conflict is that anterior temporal regions are subject to signal loss during fMRI sequences. Alternatively, as the above studies employed blocked rather than event-related designs, the areas of activation seen may have been due to other cognitive processes, separate from memory encoding.
An event-related fMRI study looked at verbal memory encoding in non-amnesic right-handed patients with left HS. Verbal memory encoding involved activation of the left hippocampus in normal subjects, but was associated with reorganisation to the right hippocampus and PHG in the patient group when compared to the normal group. These areas of activation were all located in anterior MTL structures expected to be disrupted by ATLRs. In addition, the presence of left amygdala sclerosis resulted in the reorganisation of encoding of emotional verbal material to the right amygdala (244). In the same patient group, the severity of left hippocampal pathology predicted memory performance for both neutral and emotional words, whereas the severity of amygdala pathology predicted memory performance for emotional words only (257).

1.6.8 The prediction of postoperative memory changes

Prediction of post-operative memory decline is necessary to make an informed decision regarding surgical treatment and some of the prognostic indicators for this have are discussed in section 1.3.6.2. To date three groups have used fMRI to predict the effect of left or right ATLR on verbal and non-verbal memory. Richardson et al used an event-related verbal memory encoding paradigm pre-operatively in patients with left HS, demonstrating that greater verbal memory encoding activity in the left

hippocampus compared to the right hippocampus predicted the extent of verbal memory decline following left ATLR (258). In a further analysis of the same patients, they found that visual inspection of individual patient activation maps was difficult due to the number of false positive activations. A regression analysis however demonstrated that greater activation within a left hippocampal ROI predicted a greater postoperative decline in verbal memory. Surprisingly right hippocampal activation correlated with activation in the left hippocampus and therefore also predicted postoperative verbal memory outcome (259).

Rabin and colleagues used a complex visual scene-encoding task that causes symmetrical MTL activation in controls (260) to demonstrate a correlation between MTL activation asymmetry ratios and post-surgical memory outcome in patients with both left and right TLE, with increased activation ipsilateral to the seizure focus correlating with greater memory decline. The sole memory outcome variable used however was a change in recognition performance for the visual scenes used in their fMRI task and there was no discussion of relationship to change on measures of verbal and non-verbal memory that are the standard measures of post-operative change. Finally, Janszky et al found a correlation between the preoperative asymmetry index of fMRI activation on Roland's Hometown Walking Task and the change between a pre and postoperative measure of non-verbal memory (261).

As discussed in section 1.3.6.2, two different models of hippocampal function have been proposed to explain memory deficits following unilateral ATLR; hippocampal reserve and functional adequacy (111). Studies using AIs are unable to address this important issue however the findings of Richardson et al support the functional adequacy theory (259). Rabin et al also found that increased activation in the left MTL to be inversely correlated with memory outcome while no correlation was seen in the contralateral hippocampus, providing support for the functional adequacy model (260).

One study has looked at memory encoding before and after ATLR (262). Preoperatively a verbal encoding task demonstrated left lateralised frontal lobe activation in both controls and right TLE patients but more bilateral frontal activation in left TLE patients. Following surgery, the left TLE patients' verbal encoding-related activation became more left lateralised, with a reduction in right frontal activation. The authors speculated that the right frontal activation seen preoperatively was a compensatory functional response to left sided pathology and that its reduction following (contralateral) surgery was due to an

indirect effect of reduced seizure activity, or improved baseline cognitive function. This experiment employed a blocked design with subsequent memory effects not specifically tested and no MTL effects were reported.

1.6.9 Summary

fMRI is a non-invasive and widely available tool which has had a dramatic impact in cognitive neurosciences. Considerable effort is being made in the development of memory paradigms that can lateralise MTL functions and provide meaningful data at the single subject level.This information, in combination with structural MRI to evaluate hippocampal pathology and baseline neuropsychology, will enable pre-operative prediction of likely material specific memory impairments seen following unilateral ATLR to be made with greater accuracy. In consequence it will be possible to modify surgical approaches in those patients most at risk and to improve pre-operative patient counseling. Investigating how the brain sustains memory postoperatively also requires further investigation. Longitudinal studies are required to look at functional reorganisation following surgical resection of dominant and non-dominant hemispheres and these will offer valuable insights into brain plasticity. As experience grows in the interpretation of patterns of pre-operative language and memory fMRI results associated with good and bad postoperative outcomes, there will be a reduction in need for invasive procedures such as the IAT.

1.7 BRAIN CONNECTIVITY AND THE ROLE OF MR-TRACTOGRAPHY

1.7.1 Human brain connectivity

Complex behaviours such as language and memory rely upon networks of neurons which integrate the functions of spatially remote brain regions. Understanding the relationship between brain structure and behaviour would be made easier by a detailed knowledge of the anatomical connections of the white matter fibres linking these regions. Histological techniques have been developed that employ microscopy to visualise the active transport of exogenous tracer materials. Tracers used include proteins, such as horseradish peroxide, attenuated viruses and fluorescent dyes. These techniques use both anterograde and retrograde axonal transport and take advantage of the fact that some of the tracers are transported across synapses. Analysis of connectivity data from experiments using these techniques has provided insights into the organisation of functional systems in the primate brain (263;264).

While histological visualization of fibre pathways has provided insights into primate brain connectivity, little is still known about anatomical connectivity in the human brain. All of the tract-tracing techniques described above are necessarily invasive and cannot be extended to humans and the human connectivity data available so far comes mainly from dissection (138) and histological staining of post mortem tissue (265). The study of degenerating axons using silver-staining (the Nauta method) has also been used but requires the use of patients with brain lesions (266). In addition none of these techniques have provided detailed information on any but the more major pathways. However these types of invasive tract-tracing procedures remain the gold standard against which any new anatomical technique should be judged (163).

1.7.2 MTL connectivity

The MTL consists of the hippocampus, amygdala and parahippocampal regions and is known to play an important role in long term episodic memory. As the name implies, the PHG lies adjacent to the hippocampal formation and is structurally and functionally closely associated with this structure. It includes the entorhinal cortex anteriorly, an area known to have direct and extensive connections with the hippocampus and dentate gyrus. A popular theme in theories of hippocampal function in memory is

the translation of temporary hippocampal information storage to a more permanent storage in cortical association areas (267) and the anatomical framework for this is that the PHG mediates this transfer of information. At the centre of this is a loop involving the entorhinal cortex and hippocampus with afferent projections to the dentate gyrus and efferent projections from the CA1 and the subiculum to the entorhinal cortex (268).

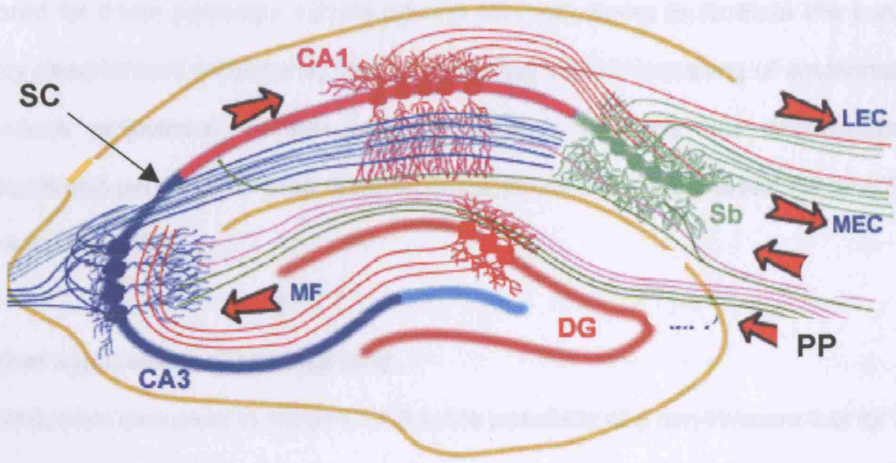

Figure 1.6 Schematic diagram of the intrahippocampal connections
Diagram of the human hippocampus showing the anatomical subregions and excitatory pathways. Input from the entorhinal cortex forms connections with the dentate gyrus (DG) via the perforant path (PP). CA3 neurons receive input from the DG via the mossy fibre pathway (MF). CA3 pyramidal cells then excite CA1 via the Schaeffer collateral pathway. CA1 send axons to the subiculum (SB) and these in turn send the main hippocampal output back to the entorhinal cortex (EC).

Neuroanatomical tracing methods in primates have provided information on cortical input to the MTL, demonstrating widespread connections from sensory-specific and multimodal association cortices converging on the PHG. In their work on Rhesus monkeys, Van Hoesen and Pandya used silver impregnation techniques to demonstrate three cortical areas that were sources of afferent projections to the entorhinal cortex (an area known to have direct and extensive connections with the hippocampus and dentate gyrus). One of these, area TH, was located in the posterior PHG, a second, in the prepiriform cortex in the anterior temporal lobe, and the third was located in the orbitofrontal area (269). Similar results have since been shown using horseradish peroxidase injected into the entorhinal cortex

as a retrograde tracer (270). These anterior temporal and orbitofrontal areas in turn have been shown to receive projections from visual, auditory and somatic sensory association areas (271).

Connections between occipital lobe visual association cortices and MTL structures have been central to theories of higher visual processing. Tract-tracing studies in monkeys have shown projections from visual area V4 to the PHG (272) and back projections from the amygdala to V2 and V4 (273). Possible roles suggested for these pathways include priming MTL structures to facilitate the consolidation of visual memory (feed-forward projections), and in enhancing visual processing of emotionally significant stimuli (feed-back projections). Further work in macaque monkeys has demonstrated that the parahippocampal and perirhinal cortices receive cortical inputs from visual areas TE and TEO, and the posterior parietal lobe (274).

1.7.3 Clinical applications of tractography

Despite the limitations discussed in section 1.4.3.8, the possibility of a non-invasive tool for investigating brain connectivity has important clinical implications and may increase our understanding of many neurological and psychiatric disorders. The confidence with which MR tract tracing methods may be applied in a clinical context depends firstly on validating the results obtained using them. This may be done in two ways, by comparison firstly with knowledge of anatomical connections in primate brains from histological studies, and secondly with known anatomy and functional connectivity from classical neuroanatomical studies on post-mortem human brains (275).

Catani et al used a tractography algorithm to elucidate the major white matter pathways in a single human brain (276). Among the tracts visualized were the superior longitudinal fasiculus (SLF), the inferior longitudinal fasiculus, the superior fronto-occipital fasiculus, the corpus callosum and the internal capsule, and the pathways seen were faithful to the classical descriptions found in neuroanatomy studies. They used a two ROI approach, such that only those pathways passing through two regions defined by the investigators (and based on known neuroanatomy) were retained for analysis. Such an approach naturally places a priori constraints on the results and avoids picking up false positive pathways to other areas of the brain.

In a further evaluation of tractography methods, Parker et al determined the connectivity of the corticospinal tracts and optic radiations in the macaque monkey, showing that the pathways demonstrated were consistent with known anatomy. The anatomical resolution of the macaque DTI study was limited however, restricting the level of detail of connectivity that could be determined, and improved acquisition protocols will be needed to enable anatomical resolution in monkey DTI which allows a true validation by comparison with results from tract-tracing experiments (156).

Understanding normal brain function requires not only the description of activated cortical areas, as provided by fMRI but also a description of the underlying connectivity. The combination of fMRI and tractography offers an opportunity to study the relationship between brain structure and function by providing a selective tracing of connectivity within a behaviourally characterized network (277). In addition, the use of fMRI activations for seed point selection offers the possibility of operator-independent placement, potentially reducing one source of variability in tractography results. The combination of fMRI (using a hand tapping paradigm) and tractography was used to demonstrate the connectivity of the human primary motor cortex in 8 controls and one patient with a left frontal tumour. Seed points were selected in the white matter adjacent to the location of the maximum fMRI activation and demonstrated strong connections to the pyramidal tracts, premotor areas, thalamus and cerebellum. These connections were more extensive in the dominant hemisphere and altered connectivity was seen in the patient with the tumour (278). Another study studied structure-function relationships in the visual system (279). It used photic stimulation to induce visual cortex activity and probabilistic tractography to track the optic radiations from a seed point near the lateral geniculate body (LGB) of the thalamus. The mean FA of the optic radiations correlated significantly with a measure of fMRI activation, although no correlation was demonstrated for tract volumes.

1.7.4 Tractography in epilepsy

1.7.4.1 Presurgical evaluation

Knowledge of MTL connectivity would be useful in the presurgical assessment of patients with temporal lobe epilepsy. The structural connections of an epileptic focus may underlie epileptogenic networks and spread of epileptiform activity within these networks. Furthermore, the integrity of connections of cortical

areas subserving cognitive functions such as language and memory are necessary for normal function. Identification of the major connections of these abnormally and normally functioning areas will be important in planning surgical resections to maximise the chance of seizure remission and to minimise the risks of cognitive impairment. We would hypothesize that the connections of cerebral areas involved in language and memory will be demonstrable pre-operatively, and will show disruption post-operatively in those patients that have impairment of language and memory function following anterior temporal lobe resection.

Selective language deficits may occur in up to 40% of patients following language dominant ATLR (201). Two recent studies have used tractography to study the connections of Broca's and Wernicke's areas (280;281) using anatomical guidelines to define starting points for fibre-tracking. One investigated the lateralisation of language pathways, demonstrating stronger connections in the left hemisphere than in the right (280). They used anatomical guidelines to define Broca's and Wernicke's areas as ROIs for initiating fibre tracking and constrained their analysis to only identify pathways passing through both regions. The ROIs used were significantly larger in size in the left hemisphere due to the known hemispheric anatomical differences in the frontal and temporal lobes (282-286). This asymmetry could possibly affect the volumes and extent of the connections obtained, although there was no correlation between the ROI volumes and the resulting volumes of connecting tracts.

Catani et al used tractography to study perisylvian language networks in the left hemisphere (281). In addition to the direct pathway connecting Broca and Wernicke's areas they used a two-ROI approach to demonstrate a second, indirect pathway passing through the inferior parietal cortex. This ran laterally to the direct pathway and was composed of an anterior segment connecting Broca's area with the inferior parietal lobe and a posterior segment connecting the inferior parietal lobe to Wernicke's area. The authors argued that the existence of this second pathway helped to explain the diverse clinical spectrum of aphasic disconnection syndromes. While both provide interesting new insights into the course of the SLF, both used a two ROI approach, whereby the analysis is constrained to only include pathways passing through both regions. In addition, manual definition of starting regions may be prone to observer bias.

Visual field defects (VFDs) are a well recognised complication of ATLRs and occur due to disruption of Meyer's loop, the anterior part of the optic radiation. The fibres of the optic radiation pass from the LGB to the calcarine cortex in two separate bundles. The dorsal bundle passes posteriorly to the superior bank of the calcarine cortex while the ventral bundle passes anteriorly before making a sharp turn, known as Meyer's loop, and coursing posteriorly, terminating in the inferior bank of the calcarine cortex (287). Typically VFDs occur in the superior homonymous field contralateral to the resection and are due to disruption to Meyer's loop. The anterior extent of Meyer's loop is not well localised on conventional imaging and varies from person to person (288), and as a result the occurrence and extent of a postoperative VFD cannot be accurately predicted by conventional MRI or from the extent of the resection performed. Using tractography to delineate the course and anterior extent of the optic radiation preoperatively may help to reduce the risk of visual field defects following ATLR.

1.7.4.2 Detection of subtle abnormalities

Evidence from a number of imaging modalities including quantitative MRI and MR volumetry (289-291), MR-spectroscopy (292), voxel based morphometry (VBM) (293) and PET (83) suggests the existence of more widespread abnormalities in TLE associated with HS than demonstrated by conventional MRI. One study has performed tractography in TLE and unilateral HS, showing bilateral symmetrical abnormalities and FA reduction of the fornix and cingulum, suggesting that HS is associated with bilateral limbic system pathology not revealed on conventional neuroimaging (294). Given the existence of direct connections between the hippocampus and these structures, the authors speculated that this may reflect downstream axonal Wallerian degeneration.

1.7.5 Summary

A detailed knowledge of the anatomical connections of the white matter fibres linking functional regions would add to our understanding of the relationship between brain structure and function. MR-tractography offers a non-invasive technique of mapping white matter pathways in the human brain, offering the opportunity to study their course in detail as well as being a potentially useful tool in the presurgical assessment of patients undergoing ATLR.

CHAPTER II COMMON METHODOLOGY

This chapter describes the methods which were common to a number of the studies described in subsequent chapters. Information is provided on subject recruitment, MR data acquisition, the psychological tasks used for the fMRI and the tractography algorithms used. Subsequent chapters refer back to this section, although where a particular analysis was used only in one study it is included in the relevant chapter, along with any further information on the subjects scanned in that study.

2.1 SUBJECT RECRUITMENT

Patients were recruited from the epilepsy clinics at the National Hospital for Neurology and Neurosurgery, London, UK, and the National Society for Epilepsy, Chalfont St Peter, UK. All had medically refractory TLE and were undergoing pre-surgical evaluation at the National Hospital for Neurology and Neurosurgery. Further details on patient demographics, neurological and neuropsychological test results, and surgical outcome data where relevant, are included in each chapter. Control subjects were all English-speaking healthy volunteers with no history of neurological or psychiatric disease. All studies were approved by the National Hospital for Neurology and Neurosurgery and the Institute of Neurology Joint Research Ethics Committee and informed written consent was obtained from all subjects.

2.2 ACQUISITION OF CLINICAL DATA

All patients had undergone structural MRI (62) and hippocampal volumetry had been carried out according to a previously published protocol (295). Electro-clinical assessment had been carried out with video-EEG at the National Hospital. All patients were on anti-epileptic medication and all were fluent English speakers. Handedness was determined using the Edinburgh Hand Preference Inventory (296).

All patients had a baseline standardised neuropsychological assessment and in those undergoing surgery, this was repeated postoperatively (297). We used verbal recall and verbal learning as measures of verbal memory, and figure recall and design learning as measures of non-verbal memory (298). These measures of memory are routinely used in our surgical programme. In the verbal recall

task the subject is read a short story and recall is tested immediately and at a 30 minute delay. The percentage of the story retained at 30 minutes was used as an indicator of verbal memory competence. In the verbal learning task the subject is read a list of 15 words five times and on each presentation has to attempt to recall as many of the words as possible. The percentage of correct responses was used as a second measure of verbal memory efficiency. In the figure recall task the subject firstly copies a complex design and reproduces it from memory immediately and at a 30 minute delay. The percentage of the figure remembered following the delay was employed as a measure of non-verbal memory competence. In the design learning task the subject is presented with a design on five occasions with recall being tested after each presentation. The percentage of correct responses over the five trials was used as a second measure of non-verbal memory efficiency.

2.3 FUNCTIONAL MRI

2.3.1 MR data acquisition

All MRI studies were performed on a 1.5T General Electric Signa Horizon scanner. Standard imaging gradients with a maximum strength of 22mTm^{-1} and slew rate 120Tm^{-1} s^{-1} were used. All data were acquired using a standard quadrature birdcage head coil for both RF transmission and reception. For each subject we acquired a whole brain high resolution EPI image comprising 60 contiguous 2.3mm slices with a 22cm field of view, 256x256 matrix and in plane resolution of 0.9x0.9mm. This had matching distortions to the images acquired during the fMRI tasks but a longer TR (299). It allowed whole-brain coverage and was used as an anatomical reference and to aid spatial normalisation. A group mean EPI image was calculated on which results were displayed. For both the memory encoding task and the three language tasks, gradient-echo echo-planar T2*-weighted images were acquired, providing BOLD contrast.

2.3.1.1 Memory fMRI

Each volume comprised 12 contiguous 2.3mm oblique axial slices through the temporal lobes, with a 22cm field of view, 96 x 96 acquisition matrix, reconstructed as a 128 x 128 matrix giving an in-plane resolution of 1.72mm x 1.72mm. TE was 40ms and TR 4.5s. The field of view was positioned to cover

the temporal lobes with the antero-posterior axis aligned with the long axis of the hippocampus on sagittal views with the body of the hippocampus in the centre.

2.3.1.2 Language fMRI

Each volume comprised 17 contiguous 4.6mm axial slices, with a 22cm field of view and 96 x 96 acquisition matrix, reconstructed as a 128 x 128 matrix giving an in-plane voxel size of 1.72mm x 1.72mm. TE was 40ms and TR 4.5s. The field of view was positioned to maximise coverage of the frontal and temporal lobes.

2.3.2 Paradigms used

2.3.2.1 Memory task

We designed a novel fMRI memory encoding paradigm. Stimuli of three different material types (Pictures (P), Words (W) and Faces (F)) were visually presented to the subjects during a single scanning session. Stimuli were presented on a black background using Cogent 2000 (www.fil.ion.ucl.ac.uk/cogent2000). The pictures were black and white nameable line drawn objects from the Snodgrass and Vanderwart set (300), the words were single concrete nouns, and the faces were black and white photographs unfamiliar to the subjects. A total of 210 stimuli were presented, one every 4s, in 7 cycles. Each cycle consisted of a block of 10 pictures, a block of 10 words and a block of 10 faces (each lasting 40 seconds) followed by 20s of crosshair fixation. Subjects performed a deep encoding task which involved making a judgement on whether each stimulus was pleasant or unpleasant (213). Sixty minutes after scanning, subjects performed a recognition test which was not scanned; this comprised three blocks, one for each of the three material types. During each recognition block the 70 stimuli of each type presented during scanning were randomly mixed with 35 foils and presented in a manner identical to that used during scanning. Subjects were instructed to indicate whether they could remember seeing each stimulus during scanning (R response) or whether it was new (N response).

The 210 encoding stimuli that had been presented during scanning were then classified according to the responses made during the recognition test. Two conditions were possible: correct R response ('hit')

indicated the stimulus had been remembered, while an incorrect N response ('miss') indicated the stimulus had been forgotten. For each of the three stimulus types (P, W, and F), R and N responses were identified, giving a total of six event types: PR, PN, WR, WN, FR and FN. These were then entered as regressors in the design matrix. To calculate recognition accuracy, stimuli seen in the recognition test were classified as 'hits' (stimuli correctly remembered) and 'false alarms' (foils incorrectly tagged as remembered). Recognition accuracy was calculated for each stimulus type as hit rate minus false alarm rate.

2.3.2.2 Language tasks

Subjects performed three language fMRI experiments; verbal fluency, verb generation and reading comprehension. These paradigms consisted of a blocked experimental design with 30s task blocks alternating with 30s of rest over 5½ minutes. During the verbal fluency task block subjects were asked to silently generate different words starting with a particular letter presented visually. The rest block consisted of visual fixation on a crosshair. During the verb generation task concrete nouns were visually presented every 3s in blocks of 10 nouns. Subjects were instructed to covertly generate verbs from the nouns during the task block and to silently repeat the nouns during the rest block. These paradigms were used to identify anterior language regions in the inferior and middle frontal gyri (173;174).

During the reading comprehension activation condition, subjects silently read 9-word sentences covering a range of different syntactic structures and semantic content. No explicit task was required during scanning in order to avoid inducing additional executive processes. In the baseline condition, subjects attentively viewed 9-word sentences after all the letters were transformed into false fonts. This baseline controlled for visual input but not lexical, semantic or syntactic content. The paradigm therefore maximised our chances of seeing reading related activation at any level of the reading system. Blocks of six sentences were interleaved with blocks of six false font sentences. Sentences and false fonts were presented one word at a time at a fixed rate (word duration 500ms, sentence duration 5000ms; block length: 30s). This serial presentation mode was used to control for visual input, eye movements and to be matched for the subjects' reading pace. This paradigm was designed to identify posterior language regions in the superior and middle temporal gyri (207;301).

2.3.3 Data analysis

The images were transferred to a Sun workstation and converted to ANALYZE format for analysis. All imaging data were analysed using Statistical Parametric Mapping (SPM2) (using SPM2 software from the Wellcome Department of Imaging Neuroscience, London; http//www.fil.ion.ucl.ac.uk/spm) (137). Language and memory scans from each subject were realigned using the first as a reference, spatially normalised (using the whole brain EPI) into standard anatomical space, and smoothed with a Gaussian kernel of 10 mm full width half maximum. In order to remove low frequency noise (e.g. due to scanner drift) the time-series in each voxel was highpass filtered with a cutoff of 1/128 Hz.

2.3.3.1 Memory

2.3.3.1.1 Event-related analysis

To test for subsequent memory effects, an event-related design was used to compare encoding-related responses to individual stimuli that were subsequently remembered versus stimuli that were forgotten (302). A two-level random-effects analysis was employed. At the first level, trial-specific responses were modelled for each subject by convolving a delta function that indicated each event onset with the canonical HRF to create regressors of interest, one regressor for each of the six event types described above. Each subject's movement parameters were included as confounds. Parameter estimates pertaining to the height of the HRF for each regressor of interest were calculated for each voxel. Contrasts of parameter estimates were calculated in a voxel-wise manner to produce, for each subject, one contrast image corresponding to the subsequent memory effect for each material type (PR-minus-PN, WR-minus-WN, FR-minus-FN) and an overall memory effect for each subject (R-minus-N, collapsed across all three stimulus types). All these images were used for the second-level analysis.

Second level analyses were performed to examine group effects for both the controls and the left and right TLE groups. Each subject's contrast image was entered into a one-sample *T* test to examine effects across each group separately. This was performed for the main effect of subsequent memory for each material type and for the subsequent memory effect collapsed across all stimulus types. In addition, two-sample *T* tests were performed to compare each patient group in turn with controls. This

allowed us to identify brain regions demonstrating greater or less activation in patients compared with controls.

Unless specified otherwise we report all MTL activations at a threshold of $P<0.005$, uncorrected for multiple comparisons. This uncorrected threshold was adopted because of the low SNR in the anterior temporal lobe (209;246) and as we were testing a specific hypothesis regarding MTL activation. In all studies MTL regions of activation were labelled with reference to Duvernoy's *The Human Hippocampus* (303).

2.3.3.1.2 Blocked analysis

In addition we performed a blocked analysis of the data. Regressors of interest were formed by creating four boxcar functions (one for pictures, one for words, one for faces and one for crosshair fixation) convolved with the canonical HRF. Each subject's movement parameters were included as confounds and parameter estimates for the regressors were calculated for each voxel. Contrast images for each material type against fixation were created to produce, for each subject, one contrast image corresponding to the main effect of each material type. Performance in the recognition test was not taken into account in this model, which therefore only assumes encoding without testing for subsequent memory effect. All these images were used for the second-level analysis.

At the second level of the random effects analysis, each subject's contrast image was entered into a one-sample *T* test to examine effects across each group. This was performed for each material type. Two-sample *T* tests were also performed to compare activation between patient groups and controls. We report all MTL activations at a threshold of $P<0.005$, uncorrected for multiple comparisons. We also report activations within the fusiform gyrus in the immediate vicinity of those previously reported by Grill-Spector et al. for faces (304) and Stern et al. (231) for pictures.

2.3.3.2 Language

A two-level random effects analysis was employed. At the first level, condition-specific effects for each subject were estimated according to the general linear model (137). Regressors of interest were formed for each task by creating boxcar functions of task against rest. Parameter estimates for these regressors

were then calculated for each voxel. Three contrast images were produced for each subject, corresponding to the main effects of verbal fluency, verb generation and reading comprehension against the control conditions. All these images were used for the second-level analysis.

At the second level of the random effects analysis, each subject's contrast image was entered into a one-sample *T* test to examine effects across the whole group. This was performed for the main effects of verbal fluency, verb generation and reading comprehension. Unless specified otherwise the group activation maps were thresholded at $p<0.001$ (uncorrected). For each task, we derived asymmetry indices for each subject's mean fMRI activation, (AI = L – R), over spherical regions of interest (10mm radius) centred on each group's peak frontal and temporal activations.

2.4 MR TRACTOGRAPHY

2.4.1 MR data acquisition

MRI studies were performed on a 1.5T General Electric Signa Horizon scanner. Standard imaging gradients with a maximum strength of 22 mTm^{-1} and slew rate $120Tm^{-1}\ s^{-1}$ were used. All data were acquired using a standard quadrature birdcage head coil for both RF transmission and RF reception. The DTI acquisition sequence was a single-shot spin-echo EPI, cardiac gated (triggering occurring every QRS complex) (142), with TE = 95ms, 96x 96 acquisition (128 x 128 reconstructed) matrix, 22cm x 22cm field of view. Acquisitions of 60 contiguous 2.3mm-thickness axial slices were obtained, covering the whole brain, with diffusion sensitizing gradients applied in each of 54 non-colinear directions (maximum b value of $1148mm^2\ s^{-1}$ (δ=34ms, Δ=40ms, using full gradient strength of $22mTm^{-1}$)) along with 6 non-diffusion weighted (b=0) scans. The reconstructed voxel size was 1.72 x 1.72 x $2.3mm^3$. The DTI acquisition time for a total of 3600 images was approximately 25 minutes (depending on the heart rate).

2.4.2 Diffusion tensor analysis

The diffusion tensor eigenvalues λ_1, λ_2, λ_3 and eigenvectors ε_1, ε_2, ε_3 were calculated from the DTI data, and FA maps were generated (141;305), using locally written software. For the studies using PICo, we used the method of Parker and Alexander (145) to reduce fibre orientation ambiguities in voxels

containing fibre crossings. Voxels in which the single tensor fits the data poorly were identified using the spherical-harmonic voxel-classification algorithm of Alexander et al (144). In these voxels a mixture of two Gaussian probability densities was fitted and the principal diffusion directions of the two diffusion tensors provided estimates of the orientations of the crossing fibres. In all other voxels a single tensor model was fitted.

2.4.3 Tractography algorithms

2.4.3.1 Fast marching tractography (FMT)

FMT was used to generate the fibre tracts connecting the parahippocampal gyrus, described in chapter 3. This method is based on level set theory and the fast-marching algorithm which model the evolution of a front over time from a seed point using the principal eigenvector (ε_1) of the diffusion tensor (157). The ε_1 field provides a variable rate of propagation for the front, causing every voxel in a volume data to be crossed by the front at different times. FMT uses the maps of time of arrival from the seed point to generate a 3D connectivity map. This map represents a metric of connectivity that can be considered as an informal likelihood of connectivity between the seed point and every other voxel. This is related to the confidence that we have that a fibre bundle exists between two points; this confidence being modulated by anatomical and experimental conditions. It is reproducible across subjects and allows all possible routes of connection to be ranked by how well they correspond to the information provided by the DTI data. We applied an anisotropy threshold of 0.1, thus excluding all voxels with FA values lower than this and avoiding false positive paths passing through CSF.

2.4.3.2 Probabilistic index of connectivity (PICo)

We used the PICo algorithm extended to cope with crossing fibers (145;159) to track the optic radiations (chapter 4) and the language-related pathways (chapters 9 and 10). This adapts the commonly used streamline approach to exploit the uncertainty due to noise in one or more fibre orientations defined for each voxel. This uncertainty is defined using PDFs constructed using simulations of the effect of realistic data noise on fibre directions obtained from the mixture model (145). The streamline process is

repeated using Monte Carlo methods to generate maps of connection probability or confidence of connection to chosen start points (159) .

CHAPTER III CONNECTIONS OF THE MEDIAL TEMPORAL LOBE

This chapter describes a study using MR-tractography to study the connections of the MTL in a group of normal subjects. The material in this chapter has been published in; Powell HWR et al. *Noninvasive in vivo demonstration of the connections of the human parahippocampal gyrus.* **Neuroimage** 2004;22:740-7.

3.1 OBJECTIVE

The aim of this study was to delineate the main connections of the anterior parahippocampal gyrus (PHG), a white matter pathway closely related, structurally and functionally, to the hippocampus. These connections are likely to play an important role both in normal memory function and seizure propagation and may be disrupted during ATLR.

3.2 INTRODUCTION

Little is known about the anatomical connections of regions involved in behaviours such as memory, emotion and perception. Hippocampal and parahippocampal regions have been closely linked to these higher order behaviours. The PHG includes the entorhinal cortex anteriorly, an area known to have direct and extensive connections with the hippocampus and dentate gyrus. The PHG is thought to be involved in the translation of temporary hippocampal information storage to a more permanent trace in cortical association areas (267).

Neuroanatomical tracing methods have provided information on cortical input to the MTL, demonstrating widespread connections from sensory-specific and multimodal association cortices converging on the PHG (271). These types of invasive tract-tracing procedures, such as the histological staining of post-mortem tissue (265;271) and the study of degenerating axons using silver staining (266) have significant limitations when used on the human brain (163). In addition none of these techniques have provided detailed information on any but the more major pathways.

We used the FMT technique (refer to methods section 2.4.3.1) to detect possible connection pathways from a seed point in the anterior PHG. FMT provides 3D connectivity maps representing an informal probability of connectivity between this seed point and each voxel in the brain. Our aim was to use FMT

to study the connectivity of the human anterior PHG in vivo. This is an area of particular interest in the presurgical assessment of patients with TLE. The structural white matter connections of an epileptic focus may underlie epileptogenic networks and spread of epileptiform activity within these networks. Furthermore, the integrity of connections of cortical areas subserving cognitive functions such as memory are necessary for normal function. Identification of the major connections of these abnormally and normally functioning areas will be important in planning surgical resections to maximise the chance of seizure remission and to minimise the risks of cognitive impairment.

3.3 METHODS

3.3.1 Subjects

Ten healthy volunteers (6 males) without any history of neurological or psychiatric disorders were included in this study. The age range of the subjects was 30-54 years with a median of 35. Eight subjects were right handed, and two were left handed.

3.3.2 MR data acquisition

MRI acquisition was performed according to our common protocol (refer to section 2.4.1). Diffusion tensor imaging and analysis was performed according to the previously described protocol (refer to section 2.4.2).

3.3.3 Tractography method

FMT was the tractography algorithm used in this study and is described in the common methodology section 2.4.3.1.

3.3.4 Seed point selection

Seed points were selected in the anterior PHG based on the following anatomical rules.

- From a sagittal reformat of the data, we selected the slice in which the long axis of the PHG was most clearly visible.

- We then selected a voxel in the most anterior part of the white matter with the principal eigenvector, when projected on the axial plane, orientated anterior-posterior.

We selected 3 adjacent seed points in each hemisphere. This was based on the observation that connectivity maps from neighbouring voxels can result in markedly different patterns of connectivity by subsampling different sets of cortical connections (278). We chose 3 adjacent voxels in the left right axis and each seed point was processed separately using the FMT algorithm. Selection along the left-right axis was chosen in order to sample a larger cross-section of the PHG and provide more robust connectivity maps.

3.3.5 Individual connectivity maps

For each subject, we generated a single 'union' connectivity map for each hemisphere from the connectivity maps of each of the 3 seed points. This was done using SPM99, by selecting in any given voxel the maximum value from the three maps. This technique has been shown to be preferable to averaging the three maps as it avoided the effects of overlaps between each map (278). The resulting 3D maps of connectivity were displayed in all subjects as colour-scaled connectivity maps. The colour scale represented the range of connectivity values without threshold (extending from 0 to a theoretical maximum of 1). We normalised these 3D connectivity maps by normalising the non-diffusion-weighted data from the DTI acquisition against the EPI template provided by SPM99 and then applying the transformation parameters to the connectivity maps.

Labelling of connectivity maps was done using software called 'mni2tal' (http://www.mrc-cbu.cam.ac.uk/Imaging/mnispace.html) to derive Talairach coordinates from the Montreal Neurological Institute (MNI) coordinates. The resulting connectivity maps of the whole brain were displayed without applying any threshold.

3.3.6 Group mapping

Group maps were generated using SPM99 by averaging the connectivity maps for each subject, with the left and right sides considered separately. The group connectivity maps demonstrate the areas of

highest connectivity over the whole group whereas single subject connectivity maps were used to examine tract origin and termination points as well as other smaller branches in more detail.

3.4 RESULTS

3.4.1 Group maps

The unthresholded maps showed connections from the seed points selected in the anterior PHG in all subjects on the left and right side. These were evaluated based on the colour-coded connectivity values of the tracts in the figures and different connections are described here based on these connectivity values. The connectivity values reported below are related to the confidence that we have that a fibre bundle exists between regions, and suggest a hierarchy in the 'likelihood' of connection (Figures 3.1-3).

- ***Connectivity values >0.3***

The main connections followed the course of the PHG anteriorly to the entorhinal area and posteriorly as far as the hippocampal tail and were seen in all 10 subjects.

- ***Connectivity values between 0.2 and 0.3***

One group of connections extended anteriorly to the temporal pole and to the inferior frontal lobe. Two groups extended posteriorly to the extrastriate occipital lobe. One followed the PHG posteriorly and joined the lingual gyrus, following its occipital lobe course. The other followed the fusiform gyrus posteriorly. One group followed the course of the pyramidal tracts, along the internal capsule and corona radiata to the ipsilateral motor cortex. This pathway was seen showing high connectivity in 3 of the 10 subjects only and it is likely that this represents a false positive tract. One group involves the ipsilateral middle cerebellar peduncle and cerebellar hemisphere.

- ***Connectivity values <0.2***

These connections were widespread all over the brain and were totally non-specific.

When comparing left and right group maps the pattern of connections were similar although the false positive pyramidal tracts were more prominent on the right. No significant differences in connectivity were seen between left and right hemispheres or between left and right handers.

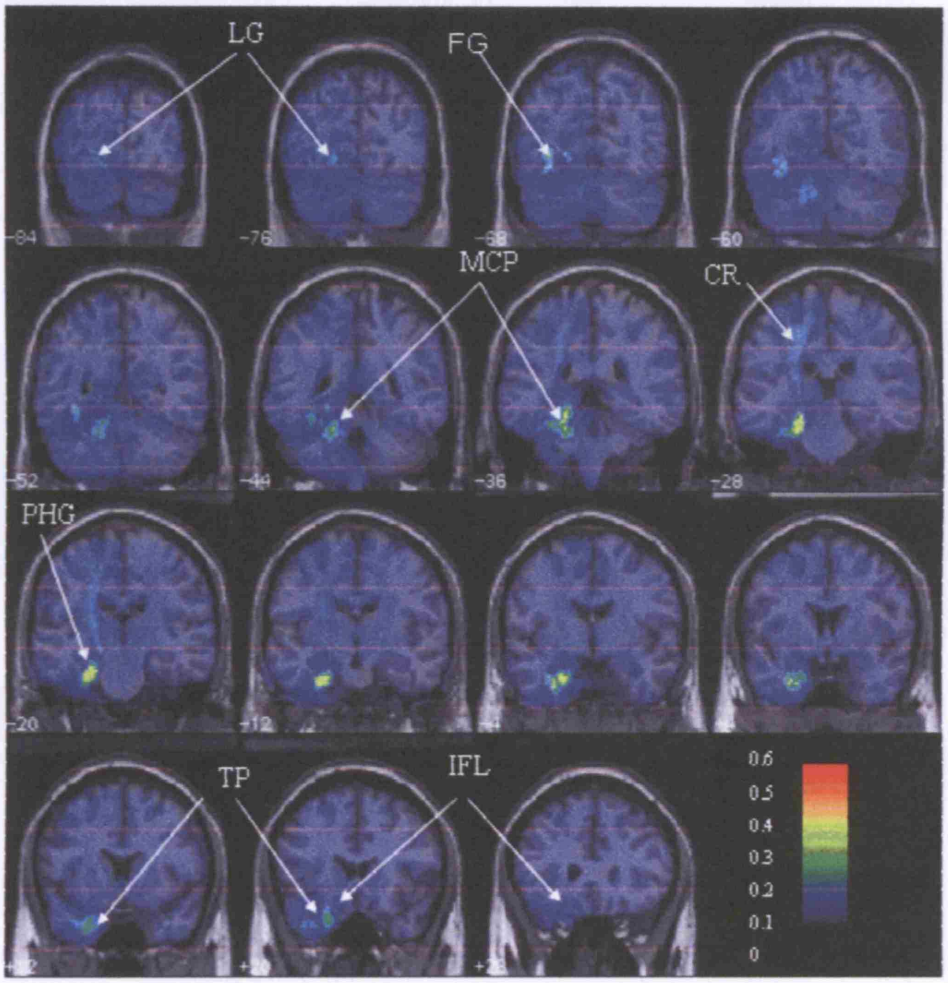

Figure 3.1 Parahippocampal gyrus group connectivity map – coronal views
Averaged connectivity maps from the left PHG in 10 controls, superimposed on the normalised single-T1 images from the MNI provided by SPM99 (coronal views). The left of the brain is on the left of the images.These maps are displayed without applying any threshold to the connectivity values. LG, lingual gyrus; FG, fusiform gyrus; MCP, middle cerebellar peduncle, CR, corona radiata, PHG parahippocampal gyrus; TP, temporal pole; IFL, inferior frontal lobe.

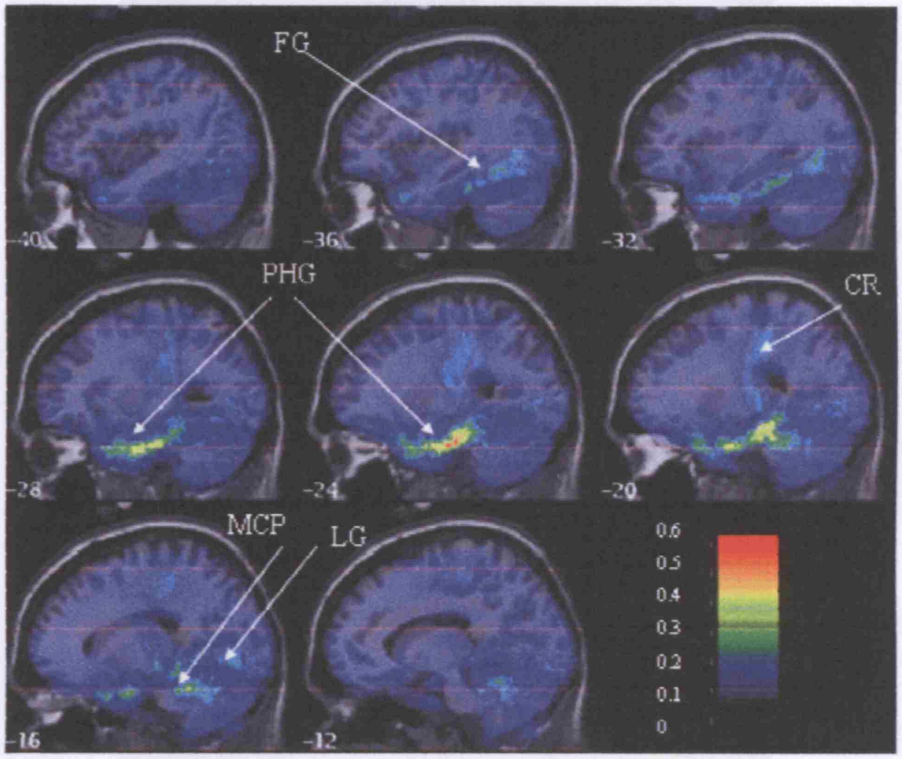

Figure 3.2 Parahippocampal gyrus group connectivity map – sagittal views
Averaged connectivity maps from the left PHG in ten control subjects, unthresholded and superimposed on the normalised T1 images from the MNI preovided by SPM99 (sagittal views). FG, fusiform gyrus; PHG, parahippocampal gyrus; CR, corona radiata; MCP, middle cerebellar peduncle; LG, lingual gyrus.

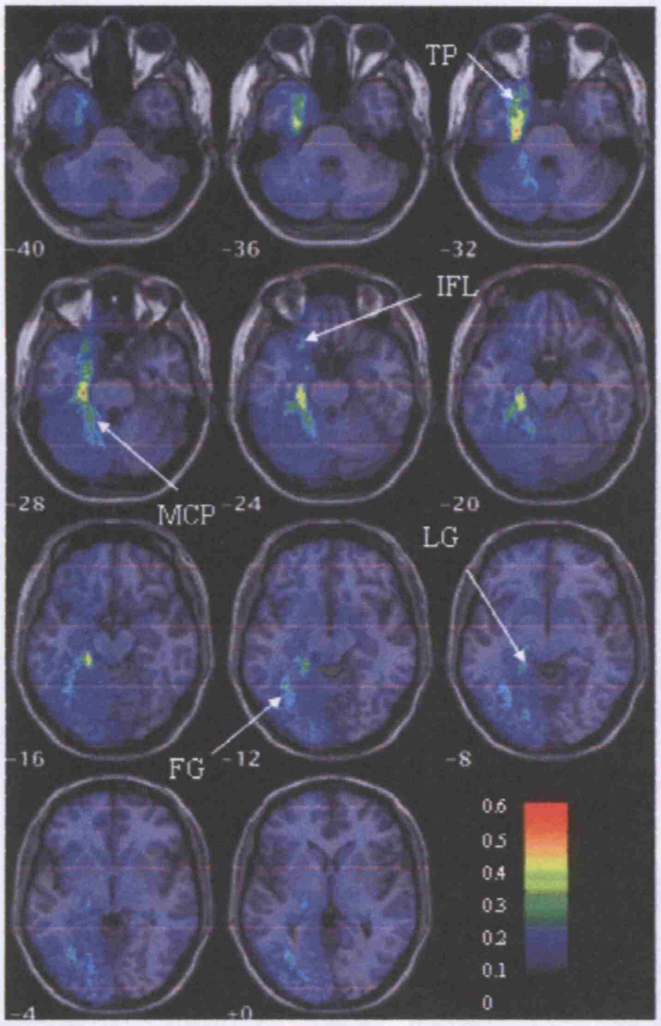

Figure 3.3 Parahippocampal gyrus group connectivity map – axial views
Averaged connectivity maps from the left PHG in 10 control subjects, unthresholded and superimposed on the normalised T1 images from the MNI provided by spm99 (axial views). FG, fusiform gyrus; TP, temporal pole; IFL, inferior frontal lobe; MCP, middle cerebellar peduncle; LG, lingual gyrus.

3.4.2 Individual subjects

Direct connections were detected between the PHG and the hippocampus itself in 3 subjects (Figure 3.4). In the case shown two sets of communications were seen, one anteriorly at the level of the amygdala and another posteriorly connecting to the body of the hippocampus. Both of these connections had high connectivity values (>0.3). In other subjects more extensive connections with the inferior frontal and the occipital lobe were observed. In the example shown fibres were clearly seen to track into the grey matter of the occipital and temporal cortices, a level of detail not seen on the group maps. Additionally, the connection between anterior temporal and inferior frontal regions was seen to occur via the uncinate fasiculus (Figure 3.5).

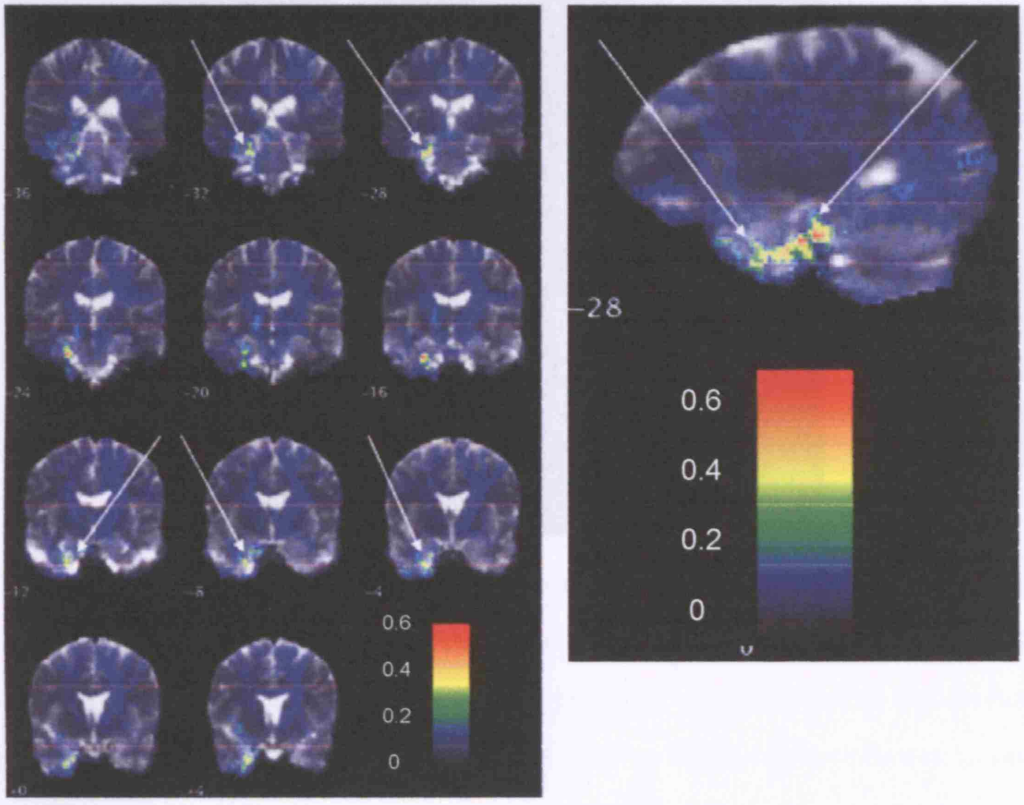

Figure 3.4 Parahippocampal gyrus individual connectivity map – hippocampal connections
Single subject connectivity map from the left PHG (coronal and sagittal views) unthresholded and superimposed on the normalised b0 image. Direct connections between the hippocampus and parahippocampal gyrus are seen anteriorly at the level of the amygdala and posteriorly to the body of the hippocampus (arrowed).

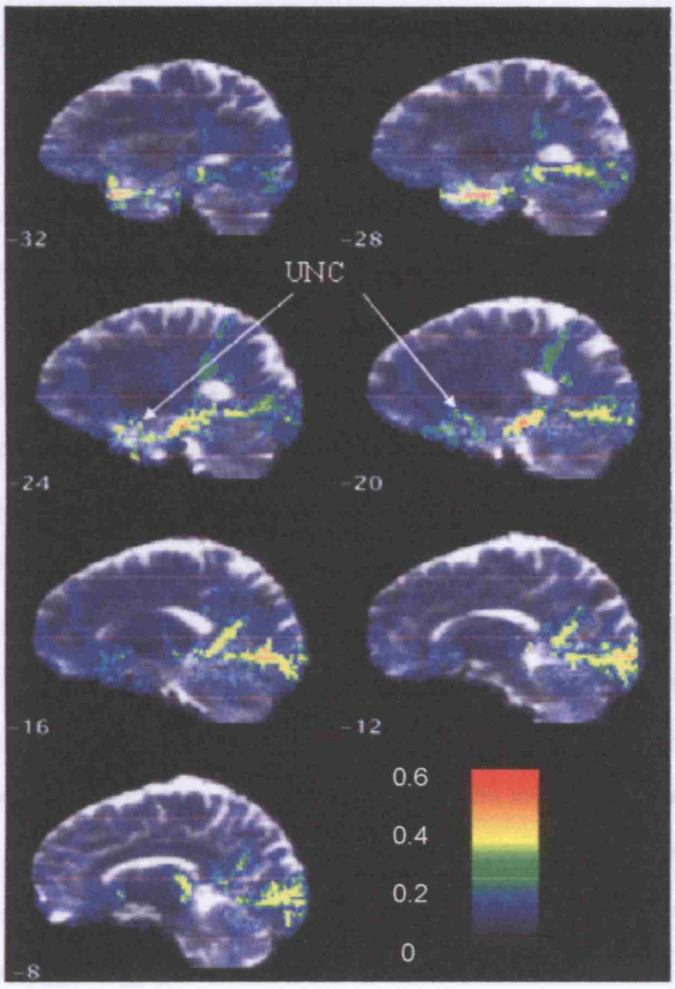

Figure 3.5 Parahippocampal gyrus individual connectivity map – frontal and occipital connections
Single subject connectivity map from the left PHG unthresholded and superimposed on the normalised b0 image. Extensive connections to extrastriate occipital lobe and inferior frontal lobe are demonstrated. UNC, uncinate fasiculus.

3.5 DISCUSSION

This study provides an in vivo demonstration of the connectivity between the PHG and anterior temporal lobe, orbitofrontal areas and posterior temporal and extrastriate occipital areas via the lingual and fusiform gyri. We also demonstrated direct hippocampal-parahippocampal connectivity for the first time non-invasively. These multisynaptic connections between neocortical areas and the hippocampus via the PHG may provide the structural basis for memory processing and integration of the internal and external environments.

3.5.1 Comparison with previous findings

Our results corroborate a study using tractography to visualize human occipito-temporal connections, in particular looking at the inferior longitudinal fasiculus (276). Catani et al demonstrated a fibre bundle arising in the extrastriate visual areas including the lingual and fusiform gyri and running forward to the anterior temporal lobe to the superior, middle and inferior temporal gyri laterally, and the PHG medially. They concluded that this was a direct connection between the occipital and anterior temporal regions and was distinct from the optic radiations. Previous studies had questioned the existence of this direct connection and suggested that it was actually the temporal loop of the optic radiation that had been mislabelled (306), a finding at odds with existing neuropsychological and neurophysiological evidence. It is encouraging that our approach, using FMT to rank connectivity of all brain areas to our chosen seed point without any a priori hypothesis, revealed a similar result to Catani et al. Our results also reveal other areas of likely connectivity in the inferior frontal lobe as well as a probable false positive connection to the pyramidal tracts. In contrast, Catani et al used a two ROI approach, such that only those pathways passing through both regions, in this case the white matter of the anterior temporal and occipital lobes were retained for analysis. Although justified as the primary aim was to establish the presence or absence of direct connections between the two regions, such an approach naturally places a priori constraints on the results. The two ROI approach avoids picking up false positive pathways to other areas of the brain, but has the potential disadvantage of giving clear prominence to apparent connections between two sites.

Tract-tracing studies in monkeys have shown projections from V4 to the PHG (272) and back projections from the amygdala to V2 and V4 (273). Given that functional imaging studies have shown human V4 to lie on the fusiform gyrus (307) and human V2 located on the lingual gyrus (308) these would be consistent with the connections demonstrated in our study although we are unable to determine whether these are feed-forward or feed-back projections. Possible roles suggested for these pathways include priming MTL structures to facilitate the consolidation of visual memory (feed-forward projections), and in enhancing visual processing of emotionally significant stimuli (feed-back projections). Further work in macaque monkeys has demonstrated that the parahippocampal and perirhinal cortices receive cortical inputs from visual areas TE and TEO, and the posterior parietal lobe (274).

Our findings are also in concordance with other previous work in rhesus monkeys which, using silver impregnation techniques, demonstrated three cortical areas that were sources of afferent projections to the anterior PHG: one area (TH) was located in the posterior PHG, a second in the prepiriform cortex (anterior temporal lobe), and the third was located in the orbitofrontal area (269). Similar results have since been shown using horseradish peroxidase injected into the entorhinal cortex as a retrograde tracer (270). These anterior temporal and orbitofrontal areas in turn have been shown to receive projections from visual, auditory and somatic sensory association areas (271).

The PHG is classically separated anatomically and functionally into an anterior part (consisting of the entorhinal and perirhinal cortices) and a posterior part. The entorhinal cortex is the major source of projections to the hippocampus and also the target of hippocampal efferent projections. It receives the majority of its input from adjacent perirhinal and posterior parahippocampal cortices, which in turn have been shown in monkeys to receive projections from unimodal and polymodal areas in the frontal, temporal and parietal lobes (43). Although the precise location of the seed points is difficult to assess on the anisotropy maps, we hypothesise that they are located in the white matter underlying the perirhinal and entorhinal cortices (309).

3.5.2 Methodological considerations

When assessing the validity of connections identified by tractography there is no perfect way of establishing whether they are genuine or whether they represent false positives or negatives. Comparison with known human anatomy and known connectivity in primate brains are methods of validation, although precise knowledge of fibre pathways in humans is limited and the exact degree of similarity between monkey and human connectivity is unknown. Histological visualization of fibre pathways remains the gold standard against which any new anatomical techniques should be judged.

The validity and limitations of the FMT method have been discussed previously in a study comparing connectivity maps of corticospinal tracts and optic radiations in macaque and human brain with known anatomy (156). FMT's advantages are its capability to provide an informal estimate of the likelihood of connection between different points in the brain using a connectivity metric and ability to demonstrate branching tracts. Several factors contribute to the limitations of DTI tractography as a non-invasive tool for determining CNS connectivity and have been discussed in section 1.4.3.8.

Firstly, the poor resolution of DTI data (mm) in comparison to the size of the fibre tracts (μm) can lead to the false definition of a tract direction in a voxel, especially in the presence of fibres crossing within individual voxels. This limited spatial resolution can lead to false positives such as that seen in this study by the demonstration of the motor pathways as a likely connection, a finding at odds with existing anatomical knowledge. It seems likely that the close proximity of the cerebral peduncles medial to the parahippocampal gyrus has caused FMT to pick up a false positive connection which follows the course of the pyramidal tracts, via the internal capsule and corona radiata to the ipsilateral motor cortex. In addition, this limited spatial resolution may lead to false negatives by ignoring small fibre tracts that may be functionally important. The ability of histological techniques to pick up connections at a cellular and synaptic level is an obvious advantage over the more macroscopic picture of brain connections generated by tractography.

Secondly, the relatively low SNR of DTI data introduces errors in the information obtained using DTI. SNR is inversely proportional to spatial resolution, in that increasing spatial resolution (i.e. decreasing voxel size) leads to a reduction in SNR. Using a higher magnetic field or longer acquisition times can compensate for this loss of SNR. Thirdly, tractography methods are blind to whether the fibres shown

represent feed-forward or feed-backward projections and are therefore unable to distinguish between afferent and efferent fibre tracts (163).

Tractography techniques are generally susceptible to errors in the orientation of ε_1 due both to noise and to instances where the direction of the underlying tract anatomy is ambiguous or reflects the presence of multiple crossing fibre pathways. They assume absolute knowledge in fibre direction at every point and therefore have no concept of the uncertainty present in the recovered pathway. An erroneous pathway, due to noise or partial volume effects, is therefore assigned as much significance as 'true' pathways (159). An allowance for the assignment of the confidence in any connections seen would clearly improve the technique. New types of 'probabilistic' tractography approaches exploit this inherent uncertainty in the orientation of ε_1 for each voxel to generate connectivity maps. These types of approaches will have the advantage of giving probability values for connections and also be expected to deal with areas of high curvature and crossing fibres more effectively.

A further problem associated with FMT is that it is based on the single tensor model of diffusion in the brain. Areas where crossing or branching pathways exist violate this assumption and will therefore have falsely low anisotropy, preventing correct tract propagation. This may explain why the connections between the MTL and the rest of the limbic system are not shown. Theoretically one would anticipate visualising a group of tracts running superiorly and following the course of the cingulate gyrus but it is likely that the curvature and low anisotropy value due to numerous crossing fibres in this region prevented these from being picked up. The close proximity of the cingulate to CSF in the lateral ventricles also makes it vulnerable to partial volume effects.

3.5.3 Seed point selection

A further source of error in tractography techniques is in seed point selection. Previous studies have shown significantly different connectivity maps generated from neighbouring voxels and the selection of three adjacent seed points and generating a 'union' connectivity map has been shown to reduce the possibility of missing important pathways of connection due to small errors and variations in seed point placement (278). A recent reproducibility study used measurements of anisotropy and volume for quantification of FMT derived white matter tracts, and showed that the level of reproducibility between

subjects depended upon fibre organisation and length of the pathway (158). In addition, comparing FMT experiments by the same observer at different times and by different observers has shown that, with clear anatomical guidelines, the placement of the seed point is fairly consistent with a mean distance between trials of less than a voxel (158). The development of accurate guidelines to define seed point selection and the use of higher magnetic fields to improve spatial resolution will allow more precise definition of seed points to be made. An alternative and novel approach is to use fMRI to generate seed points for tractography by selecting the most significantly activated voxel during a particular task. This has recently been used with good effect to demonstrate the connectivity of the human primary motor cortex (278) and further examples of this will be demonstrated in chapters 8 and 9.

3.5.4 Clinical applications

Potential clinical applications of DTI tractography include the demonstration of subtle white matter abnormalities in a variety of diseases including stroke, multiple sclerosis and schizophrenia (150). Another potential use would be in the presurgical assessment of patients with TLE. A decline in verbal memory following resection of the language-dominant anterior temporal lobe has been consistently reported and studied (109), and could be due to disruption of important connections as well as loss of grey matter centres. It is desirable to be able to identify those who are at greatest risk of impairment, in order to modify surgical approaches to minimize these risks. Tractography will add another dimension to functional imaging studies that investigate cognitive tasks involving the MTL and frontal lobes and demonstrate the structural basis of functional connectivity.

In addition, the structural white matter connections of an epileptic focus may underlie epileptogenic networks and spread of epileptiform activity within these networks. The demonstration of the connections of the MTL provides us with possible explanations for some of the seizure semiology of patients with TLE: ipsilateral motor automatisms are seen frequently in CPSs of temporal lobe origin and may be due to seizure spread from a MTL focus to the ipsilateral cerebellum via the pathways seen here; frontal and occipital lobe connections may explain rapid seizure spread as seen in some patients with known temporal lobe pathology giving rise to semiology more in keeping with frontal or occipital lobe seizures. Data from functional studies also provides support for the connections shown in this

study. Van Paesschen et al used SPECT to study cerebral perfusion changes during CPSs in patients with TLE (87). Perfusion changes were seen in the ispsilateral frontal lobe, occipital lobes and the cerebellum. Previous studies have also shown ipsilateral or contralateral ictal cerebellar hyperperfusion during temporal lobe CPSs (310;311).

3.6 CONCLUSION

In conclusion, our findings provide in vivo evidence of human MTL connectivity that is in keeping with existing histological evidence from animal studies. The fact that the findings of a tractography study are consistent with known data from monkey studies is an encouraging development and supports the validity of the technique. The connections demonstrated, to frontal and occipital lobes and to the cerebellum, along with direct hippocampal-parahippocampal connections, may play an important role, both in normal memory function and in seizure propagation in patients with MTLE.

CHAPTER IV DISRUPTION OF THE OPTIC RADIATION FOLLOWING ANTERIOR TEMPORAL LOBE RESECTION

In this chapter we describe a potential role for tractography as a clinical tool in the prediction of visual field defects (VFDs) following ATLR. The material in this chapter has been published in; Powell HWR et al. *MR tractography predicts visual field defects following temporal lobe resection.* **Neurology** 2005;65:596-9.

4.1 OBJECTIVE

VFDs due to disruption of the optic radiation (OR) are a well recognized complication of ATLR. In this study we performed DTI both before and after ATLR in a patient who developed a quadrantanopia. A second patient without this complication was scanned for comparison. Our aim was to relate Meyer's loop as assessed using preoperative tractography to the extent of surgery, to determine changes in its course due to surgical disruption and demonstrate the potential of the method to predict the risk of VFD.

4.2 INTRODUCTION

A VFD occurs in approximately 10% of patients following ATLR and in 5% is severe enough to render the patient ineligible for a driving license, despite being seizure free (312). A superior homonymous quadrantanopia is the most well recognised VFD and occurs due to disruption of Meyer's loop of the OR.

The fibres of the OR pass from the lateral geniculate body (LGB) to the calcarine cortex in two separate bundles. The dorsal bundle passes posteriorly to the superior bank of the calcarine cortex while the ventral bundle passes anteriorly and laterally adjacent to the temporal horn before making a sharp turn, known as Meyer's loop, and coursing posteriorly, terminating in the inferior bank of the calcarine cortex (287). Typically VFDs occur in the superior homonymous field contralateral to the resection and are due to disruption to Meyer's loop. The anterior extent of Meyer's loop and its relationship to the temporal pole and the tip of the temporal horn vary from person to person (288), and as a result the occurrence

and extent of a postoperative VFD cannot be accurately predicted by conventional MRI or from the extent of the resection performed.

4.3 METHODS

4.3.1 Subjects

Two men (aged 37 and 47 years) underwent pre-surgical DTI at the National Hospital for Neurology and Neurosurgery for medically refractory TLE due to unilateral HS. This was repeated 2 months following ATLR. Surgery was uncomplicated, and further neurological examination was normal, except for a superior homonymous quadrantanopia in one patient.

4.3.2 MR data acquisition

MRI acquisition was performed according to our common protocol (refer to section 2.4.1). Diffusion tensor imaging and analysis was performed according to the previously described protocol (refer to section 2.4.2).

4.3.3 Tractography method

PICo was the tractography algorithm used in this study and is described in the common methodology section 2.4.3.2.

4.3.4 Seed point selection

For each tract, we chose a single voxel as a seed point based on the following anatomical guidelines.

- We identified the LGB by selecting the axial slice at the level of the transition from the posterior limb of the internal capsule to the cerebral peduncle.
- At this level the LGB is visible posterolateral to the peduncles.
- We then selected a voxel immediately anterior to the LGB with the main eigenvector in an anterior-medial to posterior-lateral orientation in the axial plane.

4.3.5 Connectivity maps

For each start voxel, 10,000 Monte Carlo tracking iterations were performed. The results were displayed using MRIcro (http://www.psychology.nottingham.ac.uk).

4.4 RESULTS

Post-operative perimetry revealed a contralateral superior quadrantanopia in patient 1 but no VFD in patient 2 (Figures 4.1a and 4.2a). The course of the OR was identified in full from the seed point in the LGB, with the dorsal and ventral loops visible. The extent of the resections in both patients was comparable.

In patient 1, post-operative tractography revealed loss of the anterior edge of Meyer's loop (Figure 4.1c). Overlay of the preoperative OR tractography on the postoperative image demonstrates how the resection causes disruption of Meyer's loop (Figure 4.1d). By contrast, in patient 2 the full course of the left OR was visible on the pre- and post-operative images (Figures 4.2b and c). The anterior extent of Meyer's loop did not overlie the resected area of the anterior temporal lobe (Figure 4.2d). On comparison of the two patients' pre-operative tractography, the anterior boundary of Meyer's loop extended further anteriorly and inferiorly in patient 1, who developed a quadrantanopia (Figures 4.1d and 4.2d).

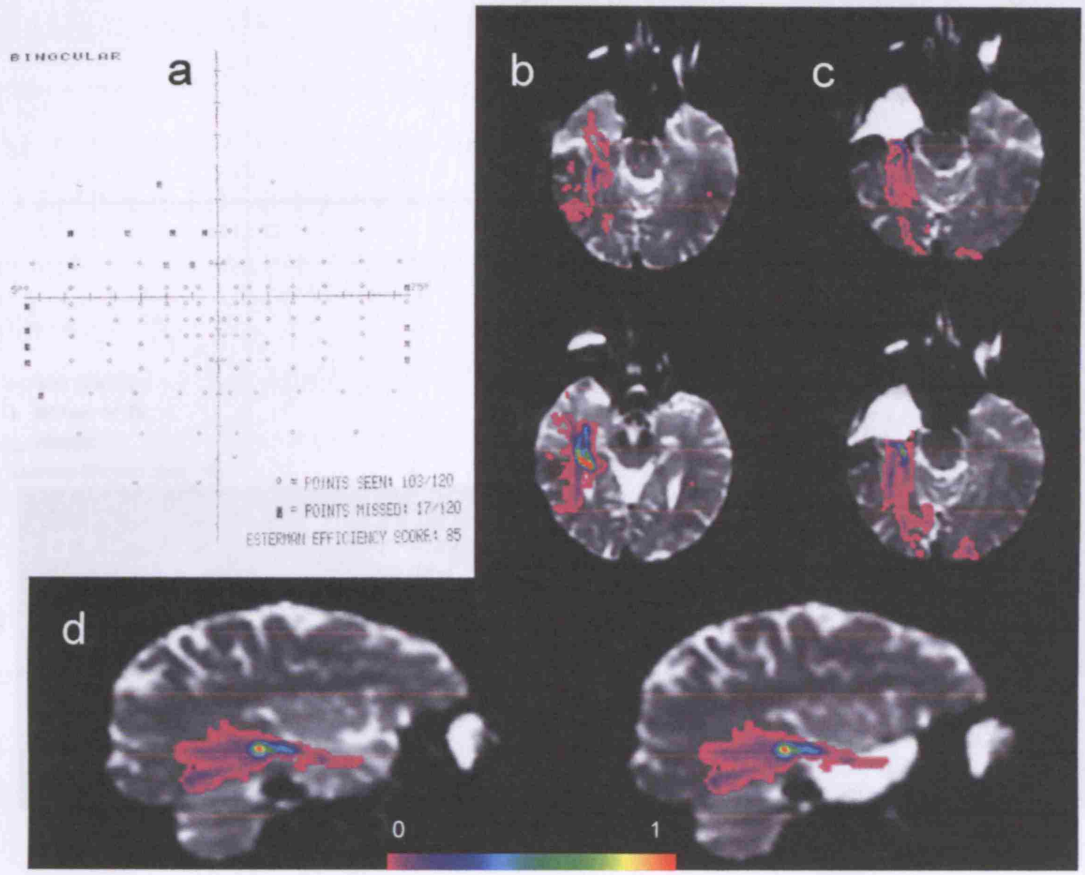

Figure 4.1 Patient 1: Pre and postoperative optic radiation

a) Postoperative visual fields demonstrating a superior homonymous quadrantanopia

b) Preoperative right OR overlaid on preoperative axial MR images.

c) Postoperative right OR overlaid on postoperative axial images showing disruption of the anterior segment of Meyer's loop.

d) Preoperative OR tractography overlaid on preoperative (left) and postoperative (right) sagittal images. The preoperative tracts overlie the resected anterior temporal lobe and the anterior border of Meyer's loop extends more anteriorly and inferiorly compared with patient 2.

The tracts are overlaid on the subject's non-diffusion-weighted b=0 image. Note that right on images is patients' left.

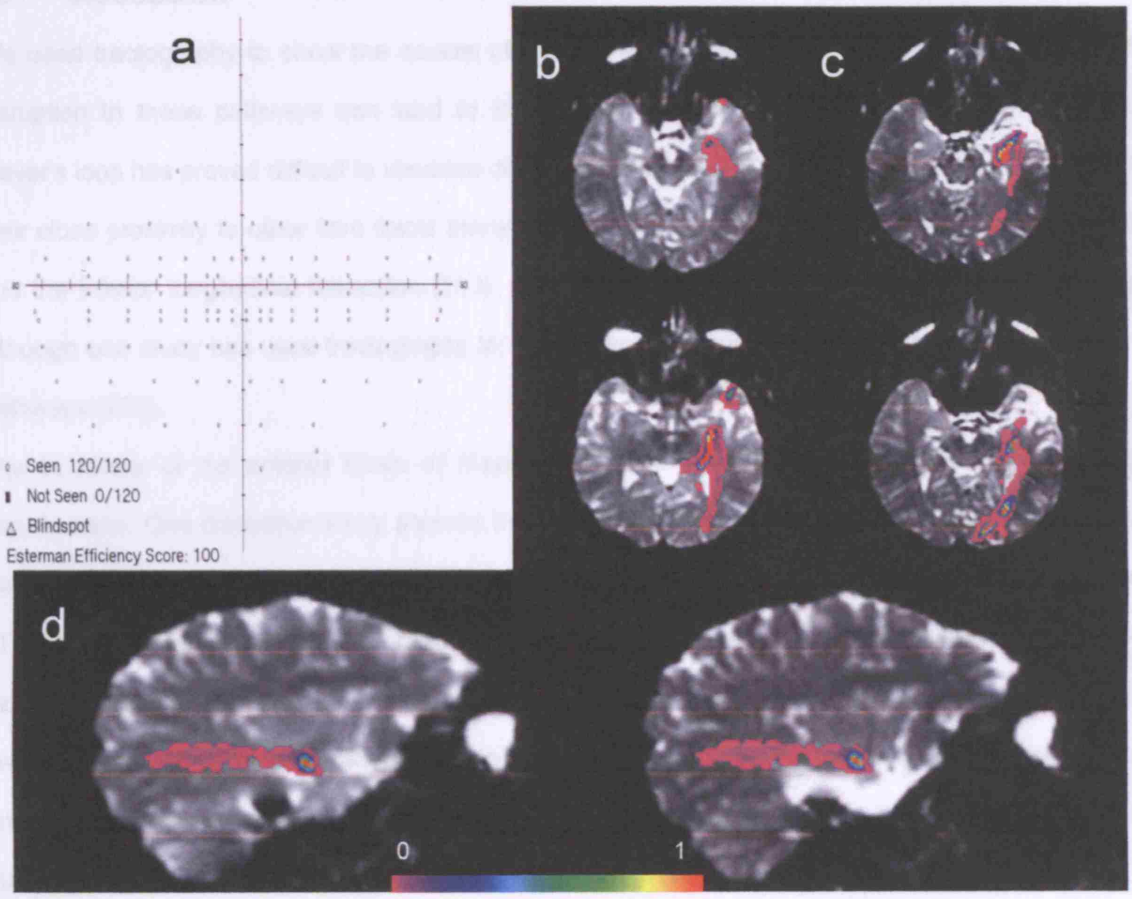

Figure 4.2 Patient 2: Pre and postoperative optic radiation

a) Postoperative visual fields showing no visual field defect

b) Preoperative left OR overlaid on preoperative axial images.

c) Postoperative left OR overlaid on postoperative axial images showing that the anterior border of Meyer's loop remains intact.

d) Preoperative OR tractography overlaid on preoperative (left) and post-operative (right) sagittal images showing that the tracts do not overlie the resected anterior temporal lobe.

The tracts are overlaid on the subject's non-diffusion-weighted b=0 image. Note that right on images is patients' left.

4.5 DISCUSSION

We used tractography to show the course of the OR and demonstrated non-invasively how surgical disruption to these pathways can lead to the superior temporal quadrantanopia seen after ATLR. Meyer's loop has proved difficult to visualize directly by dissection due to the small size of the fibres and their close proximity to other fibre tracts traversing the temporal stem, such as the uncinate fasciculus and the inferior longitudinal fasciculus (313). Meyer's loop is not seen on conventional neuroimaging although one study has used tractography to good effect to delineate the trajectories of these different pathways (276).

The boundary of the anterior fibres of Meyer's loop and their relationship to the temporal pole is controversial. One dissection study showed that the anterior edge of Meyer's loop varied from 10mm in front to 5mm behind the tip of the temporal horn (288). Other studies based on clinical observations of VFDs following temporal lobe surgery have suggested that the anterior limit of Meyer's loop is located more rostrally than previously believed and that the occurrence of VFDs correlated with the extent of the resection (314;315). More recently, using a new technique whereby MR imaging was used to guide anatomic dissection, the anterior extent of Meyer's loop was shown to be at the level of the amygdala but did not reach the level of the tip of the temporal horn (316).

VFDs are among the commonest complications seen following ATLR. There is as yet no pre-operative investigation to assess the individual patient's risk of a VFD. There has been much speculation regarding possible clinical applications of tractography, in particular in demonstrating motor pathways prior to brain tumour resection (317). We anticipate that the use of tractography pre-operatively to image the anterior boundary of Meyer's Loop will enable us to identify those patients at greatest risk of VFDs. Knowing this information pre-operatively would guide surgical technique to minimize such risks, and also allow improved pre-operative patient counseling.

4.6 CONCLUSION

In conclusion, we used tractography to demonstrate disruption of the OR following ATLR in a patient with a VFD. This report provides an example of how a novel advanced neuroimaging technique may be incorporated into routine preoperative evaluation. We suggest that this technique has the potential to

reduce the risk of postoperative VFDs and to inform patients of the risk more accurately. Further paired studies in larger populations are necessary to provide estimates of inter-subject variations of Meyer's loop and of the postoperative risk of VFDs.

CHAPTER V MEMORY FUNCTION IN HEALTHY SUBJECTS: MATERIAL-SPECIFIC MEMORY ENCODING IN THE MEDIAL TEMPORAL LOBE

This chapter describes the use of a new fMRI paradigm to study the lateralisation and localisation of memory encoding in the medial temporal lobe in a group of normal subjects. The material in this chapter has been published in; Powell HWR et al. *Material-specific lateralization of memory encoding in the medial temporal lobe: blocked versus event-related design.* **Neuroimage** 2005;27:231-9.

5.1 OBJECTIVE

Lesion-deficit studies have provided evidence for a functional dissociation between the left and right MTL. While a small number of fMRI studies have demonstrated similar findings none have looked specifically for material-specific lateralisation using subsequent memory effects. In addition, in many fMRI studies, encoding activity has been located in posterior MTL structures, at odds with evidence from lesion-deficit studies. In this study we used an experimental design which permits data analysis either as a blocked design, or as an event-related design of successful encoding of each material type. We test the hypothesis that the successful encoding of verbal and non-verbal material shows different lateralisation in the MTL. We also determined whether analysis as a blocked design reveals activity in the posterior MTL regions, whereas an event-related design shows anterior hippocampal activity.

5.2 INTRODUCTION (refer to sections 1.6.3 and 1.6.4 for more details)

Evidence from studies of amnesic patients and targeted lesions in animals led to the hypothesis that the hippocampus and related MTL structures are critical for the encoding of information for subsequent long term storage (43). Such studies have provided evidence for a dissociation in function between the dominant (usually the left) MTL, mediating verbal memory (44) and non-dominant (usually the right) MTL mediating non-verbal or visual memory (45). Further evidence for this material-specific lateralisation in function comes from patients undergoing unilateral ATLR for refractory TLE. Typically these patients show a decline in verbal memory following surgery involving the language-dominant hemisphere (109) and deficits in topographical memory following non-dominant temporal lobe resection (110).

Memory encoding involves a network of regions including prefrontal cortices in addition to the MTL. While a number of PET and fMRI studies have provided strong evidence for a functional dissociation in the prefrontal cortices (215;216;227;229;236;318), this has been less well documented in the MTL. Few studies have attempted to demonstrate functional dissociation of encoding of different stimulus types in the same subjects and in the same experimental session; however, it is only through such studies that functional dissociation can be demonstrated. One study by Kelley and colleagues used three different material types; words, line-drawings of objects and unfamiliar faces, to demonstrate a clear lateralisation of activation in both dorsal frontal cortex and MTL in five healthy control subjects. They concluded that encoding of words was left-lateralised, faces right lateralised and objects bilateral in both brain regions (214). Similar findings from Golby et al. suggested that the lateralisation of encoding processes is determined by the verbalisability of the stimuli being encoded (218).

Both these studies employed blocked experimental designs and therefore could not specifically look for successful encoding, as determined by subsequent memory effect. By using an event-related experimental design it is possible to compare activation for those items subsequently remembered with those forgotten, allowing successful memory encoding to be directly studied. One study employed an event-related design to show encoding for words in the left hippocampus in normal subjects but did not examine non-verbal memory (244) while other studies linking MTL activation with episodic encoding have not shown such clear lateralisation of function (220;231).

A further area of debate concerns the localisation of memory encoding within the MTL. The clinical description of patients with impaired memory encoding following ATLR suggests that anterior MTL regions are critical for successful memory encoding. Functional imaging studies however have proved contradictory with many showing encoding related activations located in posterior hippocampal and parahippocampal regions (214;218;231;242;249;250;318). One possible explanation for this apparent conflict is that anterior temporal regions are subject to susceptibility artefacts and signal loss leading to reduced SNR. Another possibility is that, as all the above studies employed blocked rather than event-related designs, the areas of activation seen were due to other cognitive processes, separate from memory encoding.

5.3 METHODS

5.3.1 Subjects

We studied 10 right-handed native English-speaking healthy volunteers with no history of neurological or psychiatric disease. The age range was 23-37 years (median 30).

5.3.2 MR data acquisition

MRI acquisition was performed according to our common protocol (refer to section 2.3.1).

5.3.3 Memory task

The memory task and subsequent recognition test used in this study are described in the common methodology section 2.3.2.1.

5.3.4 Data analysis

The basic fMRI data analysis is described in the common methodology chapter. The pre-processing steps are described in section 2.3.3, the event-related analysis in section 2.3.3.1.1 and the blocked analysis in section 2.3.3.1.2.

5.3.4.1 Interactions between memory and material

We also produced contrast images of interactions between subsequent memory and material type for each subject, giving a further three contrast images for each subject; subsequent memory x picture/word ((PR-minus-PN)-(WR-minus-WN)), subsequent memory x word/face ((WR-minus-WN)-(FR-minus-FN)) and subsequent memory x picture/face ((PR-minus-PN)-(FR-minus-FN)). These demonstrated regions more active for the subsequent memory of one material type compared to another. At the second level of the random effects analysis, each of these images was entered into a one-sample *T* test to examine effects across the whole group. This was performed for and to examine each of the three interactions between subsequent memory and material type.

5.3.4.2 Small volume correction

We carried out a small volume correction (SVC) to the *P* values of the reported hippocampal and parahippocampal maxima. For this purpose we created anatomically-defined ROIs. In the hippocampus this region was centered on coordinates previously reported by Richardson et al (244) for word encoding, along with the contralateral homotopic region. In the PHG this region was centered on coordinates previously reported for picture encoding (319), along with the contralateral homotopic region. All significant regions reported as uncorrected *P* values survived the SVC at $P<0.05$ unless stated otherwise.

5.3.4.3 Interactions between side and material

In order to test for hemispheric lateralisation we defined spherical ROIs (10mm radius) around the peak hippocampal voxels for effects of interest. We used these ROIs to test two and three-way interactions involving hemispheric lateralisation and intra-hemispheric localisation, using SPSS for Windows, release 11.

5.4 RESULTS

5.4.1 Behavioural performance

Recognition accuracy for the stimuli seen during scanning was calculated for each stimulus type. A one-way ANOVA revealed significantly better performance on memory for pictures (median 0.69, range 0.38-0.94) and words (median 0.64, range 0.3–0.9) compared to memory for faces (median 0.06, range 0.01-0.23) ($F=39.44$, $P<0.001$). A subsequent memory effect was shown with recognition accuracy being significantly different from zero for all three material types (words $T=9.823$, $P<0.001$, pictures $T=11.115$, $P<0.001$ and faces $T=3.241$, $P=0.01$).

5.4.2 Event-related design

We first examined the main effect of subsequent memory (R-minus-N, collapsed across stimulus types, summarised in table 5.1), revealing an area of activation in the left hippocampus ($P<0.001$, Figure 5.1a). We then looked at the main effect of subsequent memory for each stimulus type. Word encoding (WR-

minus-WN) was associated with activation in the left hippocampus (P=0.002, Figure 5.1b). For picture encoding (PR-minus-PN) there were bilateral areas of MTL activation in the left (P=0.001) and right parahippocampal regions (P<0.001), both in the depths of the collateral sulcus (Figure 5.1c). Two MTL areas were associated with face encoding (FR-minus-FN); right hippocampus (P=0.001) and right amygdala (P=0.002, Figure 5.1d).

Table 5.1 **Activation peaks in the medial temporal lobe.**

For each effect, the MNI coordinate, Z score, anatomical location and relevant figure are given.

Contrast	Figure	MNI coordinates	Z-score	Region
Main effect of memory	Figure 5.1a	-30 -16 -14	4.16	Left hippocampus
Word encoding	Figure 5.1b	-34 -14 -20	2.82	Left hippocampus
Picture encoding	Figure 5.1c	-32 -10 -26	3.03	Left parahippocampal region
		38 -10 -36	3.46	Right parahippocampal region
Face encoding	Figure 5.1d	24 -14 -26	3.02	Right hippocampus
		28 -2 -18	2.82	Right amygdala
2-way interactions between stimulus type and memory				
Pictures greater than	Figure 5.2a	-24 -10 -30	3.33	Left parahippocampal gyrus
words		40 -10 -36	3.37	Right parahippocampal gyrus
Faces greater than words	Figure 5.2b	32 -38 -16	3.20	Right fusiform gyrus
		-38 -46 -18	4.29	Left fusiform gyrus
Pictures greater than faces	Figure 5.2c	-26 -12 -32	2.57	Left parahippocampal gyrus
Blocked analysis				
Words	Figure 5.4	-26 -30 -18	4.07	Left parahippocampal gyrus
Pictures	Figure 5.4	-26 -30 -18	4.31	Left parahippocampal gyrus
		36 -38 -20	3.46	Right fusiform gyrus
		-32 -52 -18	3.31	Left fusiform gyrus
Faces		-44 -36 -22	4.00	Left fusiform gyrus
		42 -32 -26	2.89	Right fusiform gyrus

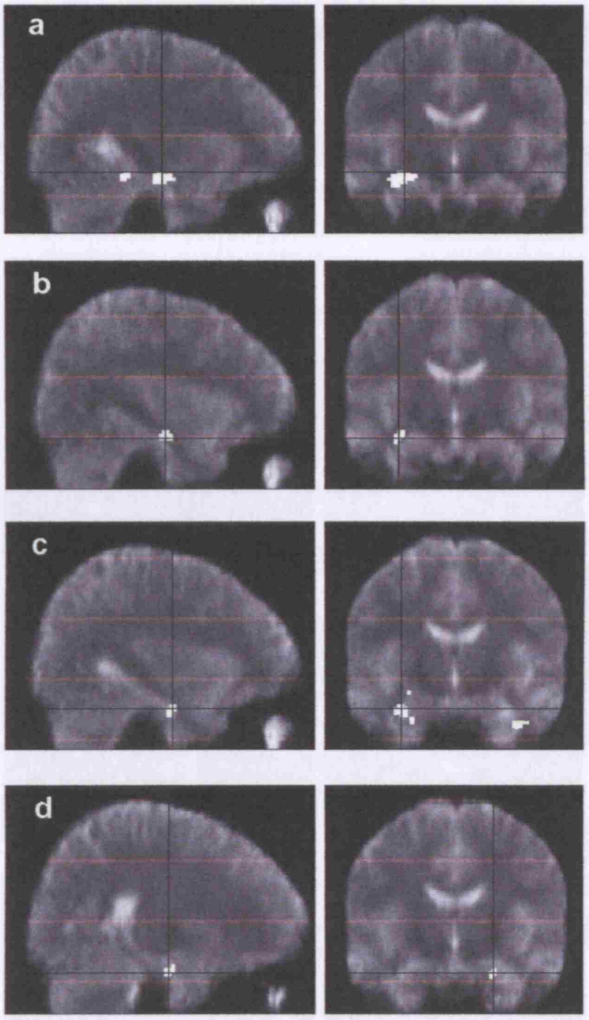

Figure 5.1 Event-related design: Main effects of subsequent memory
Significant regions (threshold here and all subsequent figures $p<0.01$) are superimposed onto the normalized mean EPI image from all 10 subjects.

a) Main effect of memory collapsed across all three material types, left hippocampal activity.
b) Subsequent memory effect for words, left hippocampal activity.
c) Subsequent memory effect for pictures, activity in bilateral parahippocampal regions in the depths of the collateral sulci.
d) Subsequent memory effect for faces, right hippocampal activity.

Two-way interactions between material type and subsequent memory revealed greater activity in bilateral parahippocampal regions, in the depths of the collateral sulcus, for pictures compared to words (P<0.001, Figure 5.2a), and in bilateral fusiform gyri for faces compared to words (P<0.001, Figure 5.2b). There was also greater activity for pictures than faces in the left parahippocampal region adjacent to the collateral sulcus (P=0.005, Figure 5.2c).

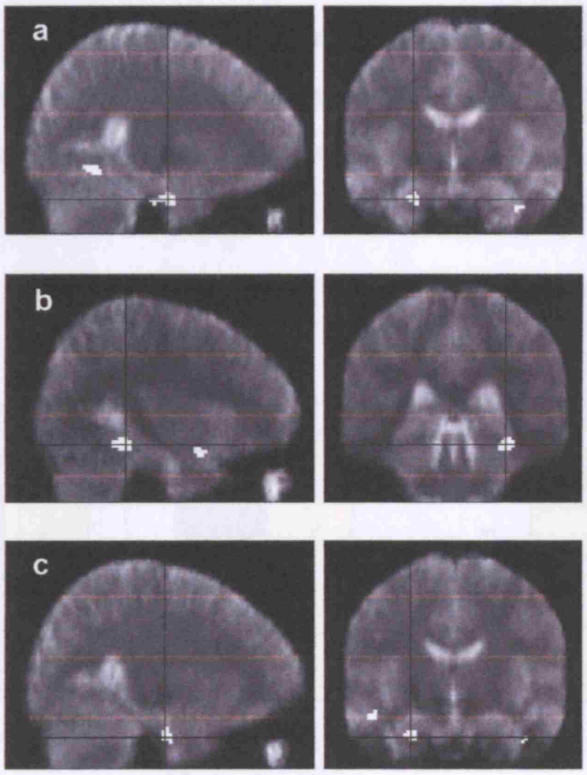

Figure 5.2 Event-related design: Two-way interactions between stimulus type and memory

a) Regions more active for pictures remembered than words remembered - bilateral parahippocampal activity in the depths of the collateral sulci.
b) Regions more active for faces remembered than words remembered - bilateral fusiform gyri.
c) Regions more active for pictures remembered than faces remembered - left parahippocampal activity adjacent to the collateral sulcus.

5.4.2.1 Region of interest analysis

Two-way interactions were tested using ROIs centred on the peak MTL voxels for word, picture and face encoding and their homotopic opposite hippocampal voxels. The two-way interaction between subsequent memory and hemisphere was significant for words (T=2.317, P=0.046, Figure 5.3) and faces (T=3.387, P=0.008, Figure 5.3). This was characterised by greater activation in the left hippocampus than the right for subsequently remembered words and greater activation in the right hippocampus than the left for subsequently remembered faces. The two-way interaction between subsequent memory and hemisphere was not significant for pictures (T=0.048, P=0.963, Figure 5.3). Finally, using data from the two ROIs centred on the peak hippocampal voxels for words and faces we demonstrated a significant three-way interaction between subsequent memory, material type (words or faces) and laterality ($F_{[1,9]}$=6.044, P=0.036, Figure 5.3).

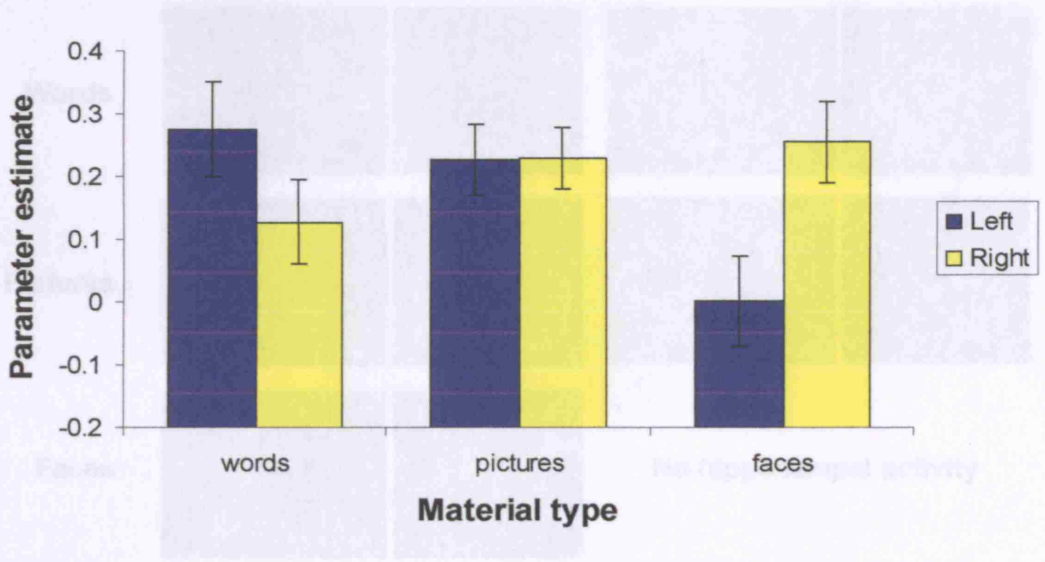

Figure 5.3 Interactions between memory, material type and hemisphere
Event-related design: Parameter estimates (+/-SEM) for left and right regions of interest (ROIs) across all subjects. ROIs were centred on the peak left and right MTL voxels for word, picture and face encoding. A significant interaction between subsequent memory, material type and hemisphere is demonstrated, characterised by greater activation in the left hippocampus than the right for subsequently remembered words and greater activation in the right hippocampus than the left for subsequently remembered faces.

5.4.3 Blocked design

We then analysed the results using a blocked design. Viewing words (irrespective of performance on subsequent memory test) was associated with an area of activation in the left PHG (P<0.001), posterior to the hippocampal region implicated in the event-related design (Figure 5.4). Viewing pictures was also associated with a peak of activation in the left PHG (P<0.001), the location of which was again more posterior than that activated by successful picture encoding (Figure 5.4). Additional areas of activation were seen in bilateral fusiform gyri (all P<0.001). Viewing faces was associated with activation in bilateral fusiform gyri (left P<0.001, right P=0.002) but no hippocampal activation.

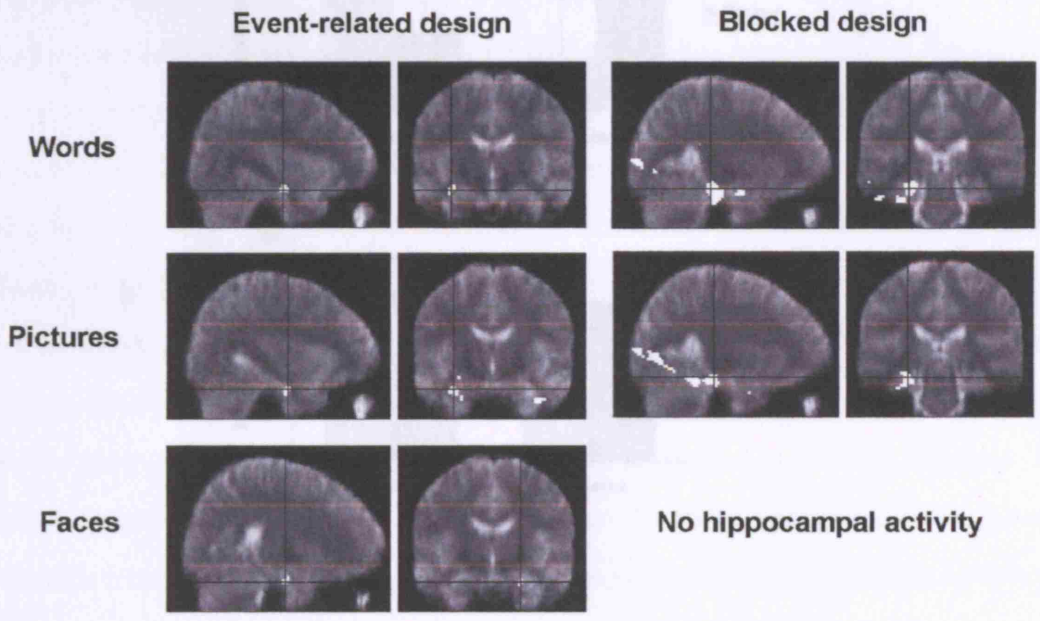

Figure 5.4 Comparison of event-related and blocked experimental design
For pictures and words, the effects of subsequent memory in the MTL, as revealed by the event-related analysis, are located more anteriorly than those revealed by the blocked analysis.

Significant interactions were seen between MTL localisation (anterior or posterior) and analysis method (event-related or blocked design) for both words ($F_{[1,9]}$=26.264, P=0.001, Figure 5.5) and pictures ($F_{[1,9]}$=5.368, P=0.046, Figure 5.5). This was characterised by greater anterior MTL activation for the event-related analysis and greater posterior activation for the blocked analysis.

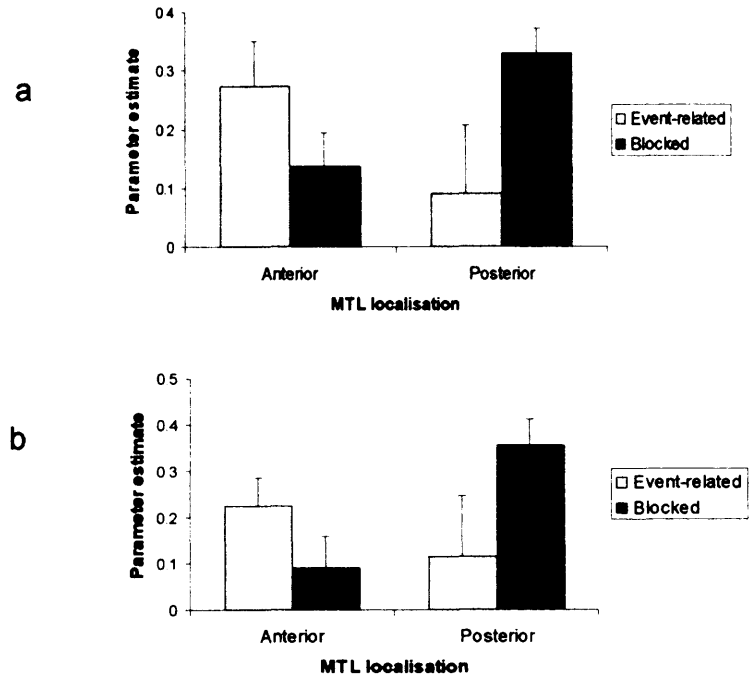

Figure 5.5 Interactions between MTL localisation and analysis method
Parameter estimates (+/-SEM) for anterior and posterior MTL regions of interest (ROIs) across all subjects for words (a) and pictures (b). ROIs were centred on the peak anterior hippocampal voxels demonstrated by the event-related analysis and the posterior hippocampal voxels demonstrated by the blocked analysis. A significant interaction between MTL localisation and analysis method is seen for both words and pictures characterised by greater anterior activation for the event-related analysis and greater posterior activation for the blocked analysis.

5.5 DISCUSSION

Using an event-related fMRI paradigm we demonstrated material-specific lateralisation of memory encoding in the anterior MTL in healthy control subjects. Activation was left-lateralised for word encoding, bilateral for picture encoding, and right-lateralised for face encoding. For the blocked design the main effects for words and pictures was left lateralised, while bilateral fusiform gyrus activation was seen for faces.

5.5.1 Material-specific memory encoding - comparison with previous findings

Patients with unilateral MTL lesions have provided evidence of dissociation in function between the dominant (usually the left) hippocampus, mediating verbal memory (44) and non-dominant (usually the right) hippocampus mediating non-verbal or visual memory (45). Both neuropsychological and technical factors have made this dissociation difficult to demonstrate using functional neuroimaging. A problem faced when designing fMRI memory experiments lies in how to separate brain activity due specifically to memory from that due to other cognitive processes used in the task.

One study by Kelley and colleagues employed a blocked design comparing blocks of intentional encoding for words, line-drawings and unfamiliar faces versus a low-level baseline in five control subjects, demonstrating a lateralisation of activation in both dorsal frontal cortex and MTL. During the encoding task the subjects were instructed to pay careful attention to each item for a later memory test whereas during the baseline blocks they were instructed to fixate on a crosshair. The disadvantage of this type of blocked design is that it is not possible to differentiate whether the effects shown reflect differences in memory encoding or any other differences between the two conditions, such as response to novelty, or semantic and sensory processing, that may be independent of differences in memory encoding (214).

Our event-related study allows memory encoding to be directly examined by classifying individual stimuli according to subsequent memory effects. Only event-related studies allow the identification of brain regions showing greater activation during the encoding of items that are subsequently remembered compared with items that are forgotten, which are then taken as candidate neural correlates of memory

encoding. These advantages, however, have to be weighed up against the greater efficiency of blocked designs (320).

Kirchhoff and colleagues used a paradigm alternating novel and repeated stimuli to study the encoding of pictures and words (318). A recognition test was performed after scanning, enabling stimuli to be classified as remembered or forgotten. Both pictures and words demonstrated novelty responses in posterior hippocampal and parahippocampal regions, with words showing a greater novelty effect on the left and pictures being more bilateral. Furthermore, these regions were demonstrated to be more active during the encoding of subsequently remembered than subsequently forgotten pictures although this effect was less clear for words.

5.5.2 MTL localisation of memory encoding

The localisation of activation within the MTL has been the subject of much debate. A meta-analysis of PET studies of memory demonstrated a functional dissociation within each hippocampus dependent on the stage of memory processing, with activations associated with memory encoding located in anterior hippocampal regions and activations associated with retrieval located more posteriorly (241). The idea that anterior MTL structures are essential for memory encoding is in keeping with the observation that memory encoding is affected following ATLR. In addition, in the patient HM, who was rendered amnesic following bilateral temporal lobe resections, more posterior MTL structures remained intact (321). Intracranial electrophysiological recordings during a verbal encoding task in humans have also shown greater responses in anterior hippocampal and parahippocampal regions for words remembered than those forgotten, although recordings from the posterior hippocampus were not performed (322).

Evidence from a number of fMRI memory studies looking at MTL activation has been contradictory, with many showing encoding related activations located in posterior hippocampal and parahippocampal regions (214;218;231;242;249;250), a finding often attributed to signal drop out in anterior temporal regions. All of these however used blocked experimental designs which may not be optimal for detecting encoding related activations in the anterior MTL.

Conceptually, the results of event-related and blocked designs reflect different things. The subsequent memory effect represents the difference between remembered and forgotten events while the blocked

effect is very similar to the average of remembered and forgotten events. It is therefore not surprising that they yield different patterns of activation. The fact that blocked designs are contaminated with trials in which other processes (e.g. visual processing) occur means that activations specifically reflecting subsequent memory may not be revealed.

Our finding that anterior MTL activations were greater for the event-related than for the blocked analysis (and posterior activations greater for blocked than event-related) suggests that this is the case, and it provides further support for the hypothesis that memory encoding is localised in anterior hippocampal regions. Some event-related fMRI studies have supported the original PET model of anterior hippocampal activation during memory encoding (216;244;246), while others have revealed both anterior and posterior MTL activations in response to remembered rather than forgotten words (323-326). In those event-related designs that failed to demonstrate anterior MTL activations (216) scanning parameters may not have been optimized for MTL sensitivity, with higher field strength and thicker slices leading to greater susceptibility effects in the anterior and medial temporal lobe. Overall we do not feel that these studies contradict our findings, namely that in order to reliably detect anterior MTL subsequent memory effects, an event-related design is required. Event-related designs may also reveal additional activation located more posteriorly.

The relative lack of anterior hippocampal activation for the blocked design is nevertheless surprising. The small posterior hippocampal activation during the event-related design is understandable as any activity unrelated to memory encoding is controlled for by comparing remembered versus forgotten events. We would, however, expect to see both anterior and posterior activation during the blocked analysis. The likeliest explanation is that there was a relative increase in BOLD signal in the anterior hippocampus during the baseline condition. If the anterior hippocampal BOLD signal was higher during baseline than during forgotten events then a contrast between all pictures (remembered and forgotten) and baseline may not reveal significant activation in this region. One study has compared various different baseline conditions in a 'memory encoding' task and found that MTL activation was higher during rest than during a number of other simple tasks (e.g. deciding whether a presented number was odd or even) (327). Such activation during 'rest' presumably represents ongoing mental processing of some sort and may reduce, eliminate or even reverse the sign of activation during a cognitive task.

5.5.3 Behavioural performance

One problem we encountered was the poor behavioural performance of the subjects for faces. Although the recognition accuracy was significantly worse than that for pictures and words it was significantly different from zero over the group as a whole and therefore does represent a subsequent memory effect, albeit a weak one. Although this represents a weakness in our study we do not feel it is critical when discussing the differences between event-related and blocked analyses as the anterior-posterior dissociation was seen for pictures and words, and not for faces. The recognition accuracy was significantly better for these two stimuli, representing a stronger subsequent memory effect. We attempted to address this further by splitting the subjects into two groups according to their behavioral performance for faces. Group membership was not a predictor of MTL activation and no significant difference was seen in the parameter estimates (over a 10mm radius sphere centered on the peak voxel in the right hippocampus) between those with good memory for faces and those with poor memory.

5.5.4 Fusiform gyrus activation

Viewing of both faces and pictures was associated with bilateral fusiform activation. Evidence from multiple modalities supports the role of the fusiform gyrus in the processing of faces, from single cell recordings in monkeys (328), lesional studies (329) and functional neuroimaging (304;330-332). Bilateral fusiform gyrus activation has also been seen using fMRI for novel picture encoding (231;318) and corresponds to the inferotemporal cortex in non-human primates, which has been shown to play a role in object discrimination and recognition (333).

5.5.5 Technical considerations

We optimised the image acquisition parameters to medial temporal responses by selecting thin slices and choosing a field of view covering only the temporal lobes and centred on the body of the hippocampus. It has been shown that smaller voxels often do produce more activation in MTL fMRI studies, possibly due to partial volume effects (334), and that oblique axial is the most suitable orientation for acquiring EPI in the MTL (335). It is clear from the functional imaging literature that other brain regions, in particular the prefrontal cortices play a role in episodic memory encoding (214;216-

218;226;227;229;236). In our study however we were testing specific hypotheses about MTL function and therefore restricted our coverage to focus on these brain regions.

fMRI studies of MTL regions has been hampered by susceptibility artefact . Ideally in the absence of an applied gradient, the magnetic field would be homogenous throughout the bore of an MRI scanner. Unfortunately the different magnetic properties of bone, tissue and air introduce inhomogeneities in the field when a head is introduced into the bore. Brain regions closest to boundaries between paranasal sinuses and brain or bone and brain are most affected and therefore especially likely to suffer geometric distortions or loss of BOLD signal (128). This effect is greater in the MTL, particularly its anterior extent (209) and may explain the relative lack of anterior hippocampal activation in many early fMRI memory experiments. By acquiring thin slices and only focusing on the area of interest within the temporal lobes we have reduced the effect of susceptibility artefact and signal loss. We anticipate that by scanning at higher field strength with high-performance gradients to ameliorate the increased susceptibility artefact, we will achieve wider coverage with a better SNR.

Geometric distortions of the EPI data make it difficult to directly overlay fMRI activations directly on co-registered high-resolution scans. They can be unwarped using techniques that map the local field in the head (129), though it has been shown that approaches of this kind can introduce extra noise into the corrected EPI data (130). In our study, we acquired whole brain high resolution EPI images with matching distortions to our functional images. Using these as structural images upon which to overlay our activations we reduced the problem of geometric distortions confounding the interpretation of fMRI results overlaid on data with very different geometric properties.

5.5.6 Methodological considerations

We defined ROIs to test for interactions between subsequent memory, material type and hemisphere. It is only by testing in this way that true functional segregation can be demonstrated, as opposed to merely describing suprathreshold activations. We acknowledge however that our interactions were biased because we chose ROIs based upon where the subsequent memory effect was seen. Although an alternative would have been to define regions by orthogonal contrasts, only subsequent memory effects were seen in the anterior hippocampus (i.e. we did not see 'blocked effects' in this region).

5.6 CONCLUSION

In conclusion we have used an event-related paradigm and optimal acquisition sequence to demonstrate material-specific lateralisation of memory encoding in the anterior MTL of normal subjects on a 1.5T clinical MRI scanner. We have also examined the methodological basis of the difference between event-related approaches, identifying encoding in anterior regions, versus blocked designs, which show apparent encoding effects in posterior regions. The ability to use event-related designs to look specifically for encoding related activation means that the role of MTL structures in memory in health and disease can now be characterised more satisfactorily.

CHAPTER VI MEMORY FUNCTION IN TEMPORAL LOBE EPILEPSY: REORGANISATION OF VERBAL AND NON-VERBAL MEMORY

The previous chapter studied memory encoding in the MTL in normal subjects. In this chapter we apply the same paradigm to a group of patients with TLE and unilateral HS to study the effects of hippocampal pathology on memory function. The material in this chapter has been accepted for publication in; Powell HWR et al. *Reorganisation of verbal and non-verbal memory in temporal lobe epilepsy.* **Epilepsia** 2007.

6.1 OBJECTIVE

Patients with TLE due to HS often suffer from material specific memory impairments. The purpose of this study was to use fMRI to study the organization of specific memory functions in these patients. Previous studies have shown reduced functional activation within the damaged MTL but few have demonstrated reorganisation of function in comparison with normal subjects. Functional reorganisation has been demonstrated following other brain injuries but it is not clear whether this is associated with better performance. We performed fMRI in patients with left or right HS, and compared the results with those from the control group, to study reorganisation of function due to HS. We hypothesised that pathology in the left MTL would result in reorganisation of verbal encoding to the right MTL and that pathology in the right MTL would lead to reorganisation of non-verbal encoding to the left MTL. We also looked for brain regions where functional activation correlated with performance on standard neuropsychological measures to determine whether ipsi- or contralateral MTL structures are responsible for retaining memory function in the presence of unilateral MTL pathology.

6.2 INTRODUCTION (refer to section 1.6.7 for more details)

Patients with TLE due to unilateral HS typically have medically refractory seizures but a good outcome following ATLR. Patients undergoing unilateral ATLR for refractory TLE typically show a decline in verbal memory following surgery involving the language-dominant hemisphere (109) and deficits in topographical memory following non-dominant temporal lobe resection (110). Prediction of memory change may reflect both the functional integrity of the to-be-resected temporal lobe as well as the capacity of the contralateral temporal lobe to maintain memory function. The known risk factors suggest

that it is the functional adequacy of the resected MTL rather than the functional reserve of the contralateral MTL that determines the extent of post-operative memory decline. It therefore appears that patients with residual memory function in the pathological hippocampus are at greater risk of memory impairment postoperatively.

Functional imaging studies have demonstrated how reorganisation of function occurs in response to brain injuries but recruitment of contralateral structures does not necessarily effectively maintain performance (336). While inter-hemispheric reorganisation of language function has been shown to be associated with recovery from post-stroke aphasia (337;338) other studies have shown recovery related to activation within unaffected ipsilateral brain regions (339), and reorganisation to the opposite hemisphere to be associated with poor recovery (336;340). Reorganisation of function also occurs in TLE due to unilateral HS with a higher incidence of atypical language dominance being demonstrated in patients with left TLE (172;181), and earlier age of onset of epilepsy being associated with more bilateral language activation (341). So far, reorganisation of function to the contralateral hippocampus has only been reported in patients with left HS, showing reorganisation of function to the right hippocampus and PHG in patients compared to controls (244).

6.3 METHODS

6.3.1 Subjects

We studied 14 patients (median age 33.5; range 25-47 years; 7 female) with medically refractory TLE undergoing pre-surgical evaluation at the National Hospital for Neurology and Neurosurgery, London, UK. Structural MRI at 1.5T showed left HS in 7 patients and right HS in 7. Video-EEG had confirmed seizures arising from the ipsilateral medial temporal lobe in all 14. All patients had a normal contralateral hippocampus on structural imaging. Language dominance was assessed using a range of fMRI tasks (301). All patients had undergone standardised neuropsychological assessment preoperatively (297). Patient demographics, neurological and neuropsychological test results, and surgical outcome data are detailed in table 6.1.

6.3.2 MR data acquisition

MRI acquisition was performed according to our common protocol (refer to section 2.3.1).

6.3.3 Memory task

The memory task and subsequent recognition test used in this study are described in the common methodology section 2.3.2.1.

6.3.4 Data analysis

The basic fMRI data analysis is described in the common methodology chapter. The pre-processing steps are described in section 2.3.3, the event-related analysis in section 2.3.3.1.1 and the blocked analysis in section 2.3.3.1.2.

6.3.5 Correlations between structure and function

In order to test for correlations between areas of fMRI activation and severity of pathology, regression analyses were performed between encoding-related activation and hippocampal volume. We used left hippocampal volume as the covariate for the left HS group and right hippocampal volume as the covariate for the right HS group. To account for the variability in hippocampal volumes due to the different brain sizes of the subjects we used total intracranial volume as a second covariate of no interest in our regression analyses (257).

6.3.6 Correlations between fMRI and memory performance

We also tested for a relationship between patients' fMRI activation and their performance on routine pre-operative memory assessment. For patients with left HS we used verbal recall and verbal leaning scores as measures of verbal memory and for patients with right HS we used figure recall and design learning scores as measures of non-verbal memory (298). These measures of memory are routinely used in our surgical programme and are described in the common methodology section 2.2. In order to test for correlations with fMRI activation we defined spherical ROIs (10mm radius) in the anterior hippocampus. On the left this was centred on the coordinates of peak word encoding-related activation

reported in controls in the previous chapter. A homotopic ROI was defined on the right. We tested for correlations between patients' fMRI activation within these ROIs and their performance on the memory tests using SPSS for Windows, release 11.

6.4 RESULTS

6.4.1 Hippocampal volumes

Left and right hippocampal volumes were significantly different in both left and right TLE patients; left TLE group mean (SD) right hippocampal volume 2.78 (0.38) cm^3, mean left hippocampal volume 1.71 (0.26) cm^3 (paired *T*-test P=0.001, 2-tailed); right TLE group mean right hippocampal volume 1.98 (0.63) cm^3, mean left hippocampal volume 2.61 (0.24) cm^3, (paired *T*-test P=0.044, 2-tailed). There was a significant interaction between group and hippocampal volume ($F_{[1,12]}$=29.8, P<0.001).

6.4.2 Behavioural results

Recognition accuracy for the stimuli seen during scanning was calculated for each stimulus type in all three groups and results were compared with a 3 x 3 within-subjects ANOVA. This revealed a significant main effect of stimulus ($F_{[2,21]}$=106.5, P<0.001), with better recognition accuracy for words (controls 0.64, left TLE 0.37, right TLE 0.55) and pictures (controls median 0.69, left TLE 0.60, right TLE 0.61) compared to faces (controls 0.06, left TLE 0.10, right TLE 0.05). There were no significant differences between groups ($F_{[2,21]}$=1.9, P=0.17). The group by stimulus interaction across all 3 groups and stimulus types was not significant ($F_{[4,42]}$=1.9, P=0.12) however looking only at the performance for words and faces revealed a significant interaction between left and right TLE groups and stimulus type characterised by lower recognition accuracy for words in left TLE patients and lower recognition accuracy for faces in right TLE patients ($F_{[1,12]}$= 20.95, P=0.004). A subsequent memory effect was shown with recognition accuracy being significantly different from zero for all three material types (words *T*=11.429, P<0.0001, pictures *T*=16.441, P<0.0001 and faces *T*=4.340, P<0.0001).

6.4.3 Imaging results

6.4.3.1 Left TLE

We examined the main effects of subsequent memory for each stimulus type (Table 6.2). No significant MTL activation was seen for word or picture encoding. Face encoding was associated with areas of activation in the right hippocampus (P=0.001, Figure 6.1a) and entorhinal cortex (P=0.001, Figure 6.1b). The blocked analysis demonstrated that viewing words and pictures was associated with activation in the right parahippocampal gyrus (P<0.001, Figures 6.1c and d). Viewing faces was associated with activation in the right fusiform and parahippocampal gyri (P<0.001, Figures 6.1e and f).

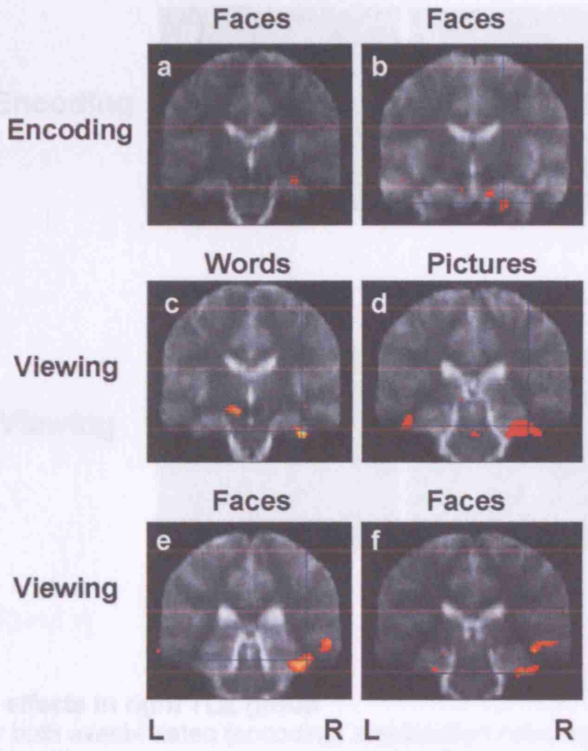

Figure 6.1 Main effects in left TLE group
Results are shown for both event-related (encoding) and blocked (viewing) designs. Significant regions are superimposed onto the normalized mean EPI image from 10 healthy control subjects. Left (L) and right (R) side of the brain are indicated.

a) Main effect of face encoding, right hippocampal activity.
b) Main effect of face encoding, right entorhinal cortex activity.
c) Main effect of viewing words, right PHG activity.
d) Main effect of viewing pictures, right PHG activity.
e) Main effect of viewing faces, right fusiform gyrus activity.
f) Main effect of viewing faces, right PHG gyrus activity.

6.4.3.2 Right TLE

Word encoding was associated with activation in the left hippocampus (P<0.001, Figure 6.2a) and picture encoding was associated with activation in the left PHG (P=0.005, Figure 6.2b). No significant MTL activation was seen for face encoding.

There was no significant MTL activation for viewing words. Viewing pictures was associated with activation in the left hippocampus (P<0.001, Figure 6.2c) and viewing faces was associated with activation in the right hippocampus (P<0.001, Figure 6.2d).

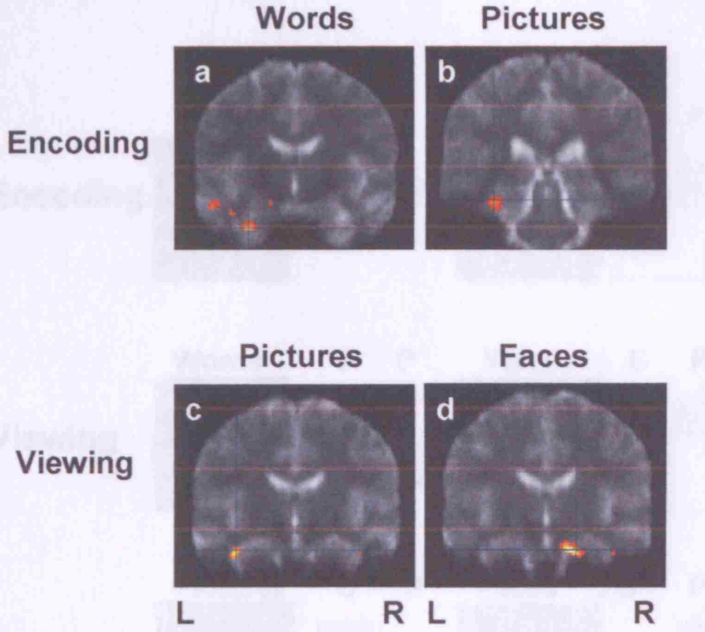

Figure 6.2 Main effects in right TLE group
Results are shown for both event-related (encoding) and blocked (viewing) designs.
a) Main effect of word encoding, left hippocampal activity.
b) Main effect of picture encoding, left PHG activity.
c) Main effect of viewing pictures, left hippocampal activity.
d) Main effect of viewing faces, right hippocampal activity.

6.4.3.3 Group comparisons with controls

We performed two-sample T tests to highlight brain regions demonstrating more or less activation in patient groups compared to normal controls. This was done for the results of both the event-related and blocked analysis (Table 6.3).

6.4.3.3.1 Left TLE

For both word encoding (P<0.005, Figure 6.3a) and face encoding (P=0.001, Figure 6.3b) left TLE patients showed greater activation in the right PHG than controls. No significant differences were seen in the MTL between controls and the left TLE group for picture encoding.

For viewing words, left TLE patients showed less activation in the left hippocampus (P<0.001, Figure 6.3c) and greater activation in the right PHG (P=0.001, Figure 6.3d) compared with controls. Left TLE patients showed less activation in the left hippocampus for viewing pictures (P<0.001, Figure 6.3e), and greater activation in the right fusiform gyrus for viewing faces (P<0.001, Figure 6.3f), compared with controls.

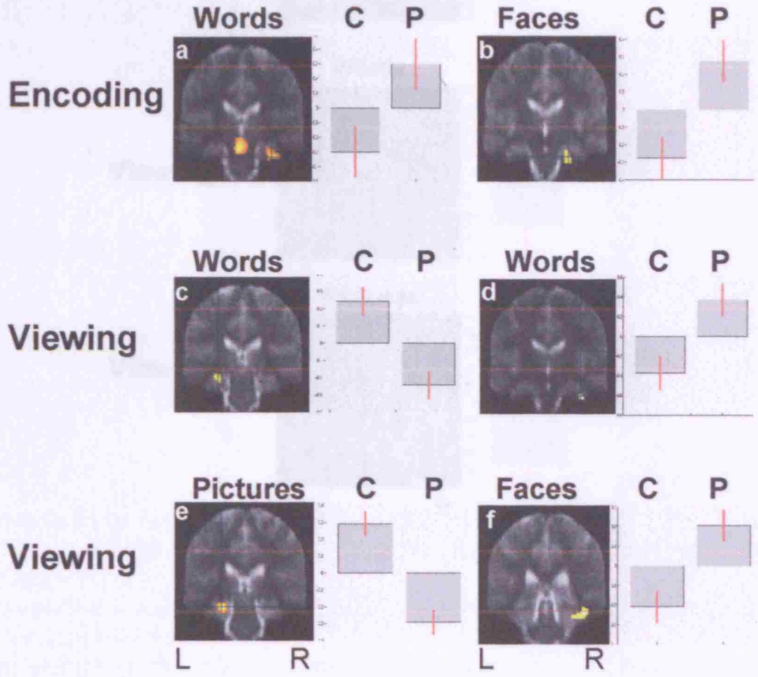

Figure 6.3 Group comparisons: left TLE and controls
Regions showing significant differences between left TLE patients and controls are highlighted. Contrast estimates are shown on the right of the SPMs. For all graphs, controls (C) are on the left and patients (P) on the right.

a) Word encoding; greater activity in left TLE than in controls in the right PHG.
b) Face encoding: greater activity in left TLE than in controls in the right entorhinal cortex.
c) Viewing words: less activity in left TLE than in controls, left hippocampus.
d) Viewing words: greater activity in left TLE than in controls, right PHG.
e) Viewing pictures: less activity in left TLE than in controls, left hippocampus.
f) Viewing faces: greater activity in left TLE than in controls, right fusiform gyrus.

6.4.3.3.2 Right TLE

For word encoding right TLE patients showed greater activation than controls in both the left hippocampus (P=0.001, Figure 6.4a) and left amygdala (P=0.001). No significant differences were seen in the MTL between right TLE patients and controls for picture or face encoding. Right TLE patients showed greater activation in the left hippocampus for viewing words (P=0.001, Figure 6.4b) and pictures (P<0.001, Figure 6.4c), compared with controls.

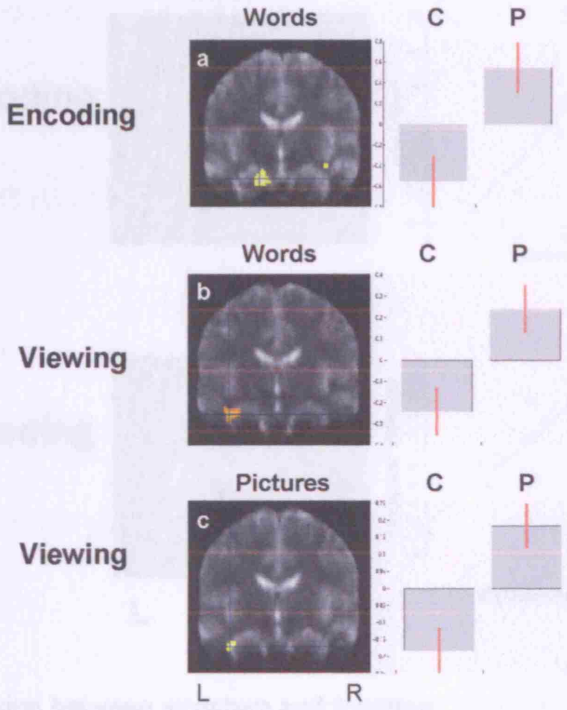

Figure 6.4 Group comparisons: right TLE and controls.
Regions showing significant differences between right TLE patients and controls are highlighted. Contrast estimates are shown on the right of the SPMs. For all graphs, controls (C) are on the left and patients (P) on the right.

a) Word encoding: greater activity in right TLE than in controls, left hippocampus.
b) Viewing words: greater activity in right TLE than in controls, left hippocampus.
c) Viewing pictures: greater activity in right TLE than in controls, left hippocampus

6.4.3.4 Correlations between structure and function

We found a positive correlation between left hippocampal volume and encoding-related activation for words with less activation in the left hippocampus if left hippocampal atrophy was more severe (r=0.885;

P=0.001, Figure 6.5a, Table 6.4). A positive correlation was also seen between right hippocampal volume and encoding-related fMRI activation for pictures with more severe pathology leading to reduced activation in the right hippocampus (*r*=0.865; *P*=0.001, Figure 6.5b, Table 6.4). The inverse correlations were not seen in the contralateral hippocampi and no correlations were observed between face encoding and hippocampal volume.

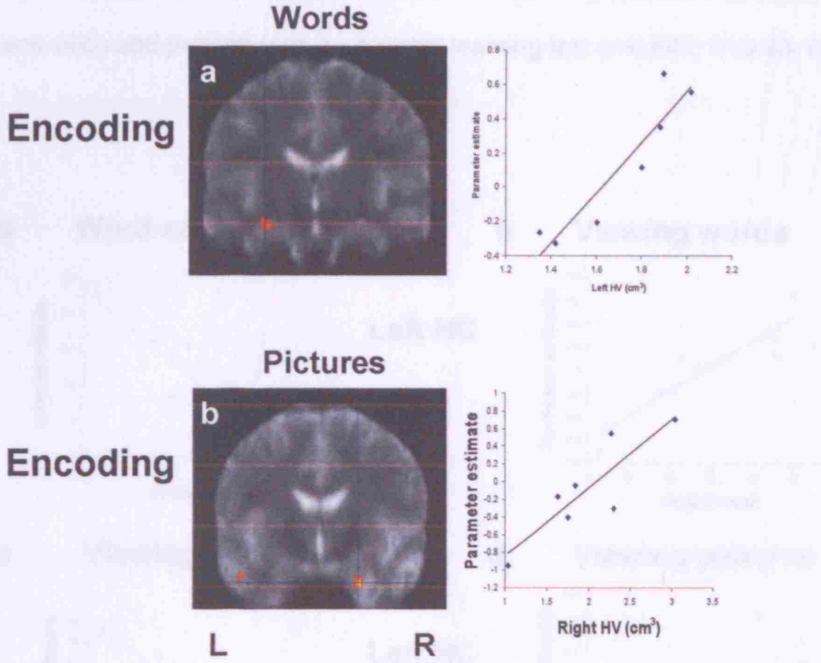

Figure 6.5 Correlations between structure and function
Graphs on the right of the SPMs demonstrate the correlation between hippocampal volume (cm^3) and fMRI activation (arbitrary units).

a) Positive correlation in the left hippocampus between left hippocampal volume and word encoding-related fMRI activation.
b) Positive correlation in the right hippocampus between right hippocampal volume and picture encoding-related fMRI activation.

6.4.3.5 Correlations between fMRI and memory performance

Regression analyses were performed to examine the relationship between left and right hippocampal fMRI activation and performance on pre-operative memory tests.

6.4.3.5.1 Left TLE

For word encoding a negative correlation was seen between right hippocampal fMRI activation and both verbal recall (*r*=-0.948; *P*=0.001, Figure 6.6a) and verbal learning performance (r^2=0.716; *P*=0.016).

There was a trend for increased left hippocampal activation to correlate with better verbal recall but this was not significant (r=0.68; P=0.09).

For viewing words there was a positive correlation between left hippocampal fMRI activation and both verbal recall (r=0.898; P=0.006, Figure 6.6b) and verbal learning performance (r=0.768; P=0.01), and a negative correlation was demonstrated between right hippocampal activation and verbal recall (r=-0.914; P=0.004, Figure 6.6c). For viewing pictures there was a positive correlation between left hippocampal fMRI activation and performance on a verbal learning test (r=0.647; P=0.03, Figure 6.6d).

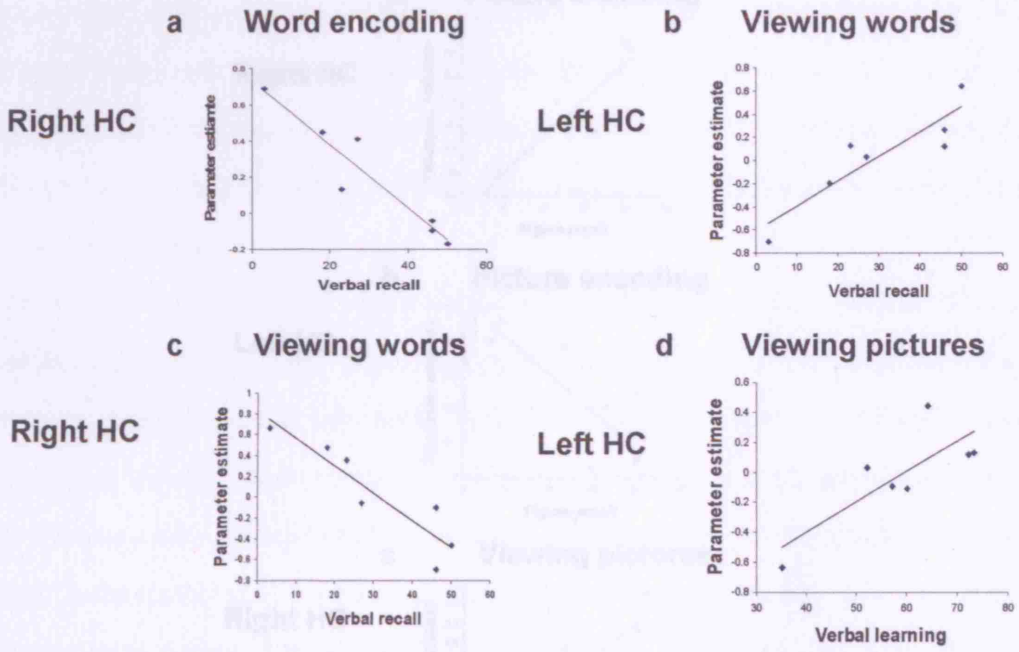

Figure 6.6 Correlations between fMRI and memory performance: left TLE

The graphs demonstrate the correlation between performance on standard memory tests and fMRI activation (arbitrary units). HC = hippocampus.

a) Negative correlation in the right hippocampus between verbal recall score and word encoding-related fMRI activation.
b) Positive correlation in the left hippocampus between verbal recall score and fMRI activation for viewing words.
c) Negative correlation in the right hippocampus between verbal recall score and fMRI activation for viewing words.
d) Positive correlation in the left hippocampus between verbal learning score and picture encoding-related fMRI activation.

6.4.3.5.2 Right TLE

For picture encoding, there was a positive correlation between right hippocampal fMRI activation and figure recall performance (r=0.916; P=0.004, Figure 6.7a) and a negative correlation was demonstrated between left hippocampal activation and figure recall (r=-0.849; P=0.016, Figure 6.7b). No significant correlations were seen for face encoding. A positive correlation was seen between right hippocampal fMRI activation for viewing pictures and figure recall performance (r=0.891; P=0.007, Figure 6.7c). No significant correlations were seen for viewing faces. No correlations were seen between hippocampal fMRI activation and performance on the design learning test.

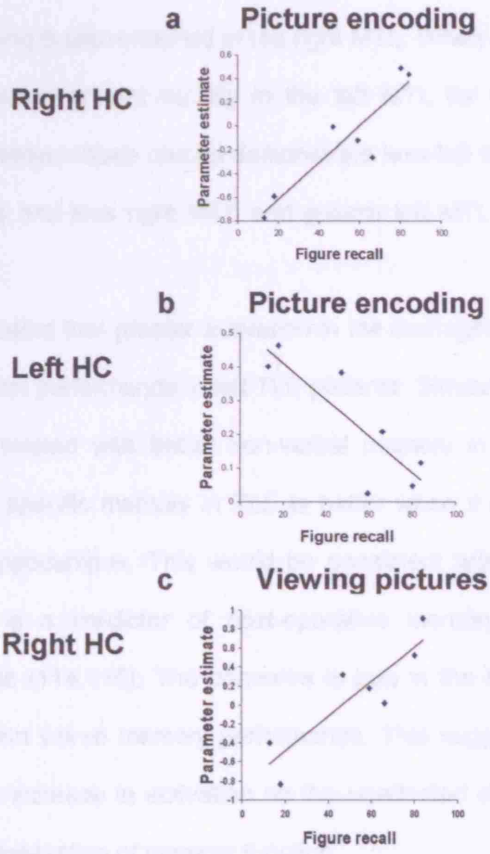

Figure 6.7 Correlations between fMRI and memory performance: right TLE

a) Positive correlation in the right hippocampus between figure recall score and picture encoding-related fMRI activation.

b) Negative correlation in the left hippocampus between figure recall score and picture encoding related fMRI activation.

c) Positive correlation in the right hippocampus between figure recall score and fMRI activation for viewing pictures.

6.5 DISCUSSION

6.5.1 Summary of results

In patients with unilateral TLE due to HS we found a reorganisation of material-specific memory encoding (Table 6.5). In contrast to the left sided MTL activation associated with word and picture encoding in normal control subjects, in patients with left TLE the main effect of viewing words and pictures was seen in the right MTL. For face encoding and viewing faces MTL activation remained right-sided. When compared directly with controls, left TLE patients had less left MTL activation for viewing words and pictures and greater right MTL activation for both word and face encoding. In patients with right TLE the right sided MTL activation seen for picture and face encoding in controls was not seen. The main effect of viewing faces remained in the right MTL. When compared directly with controls, right TLE patients demonstrated greater activity in the left MTL for word encoding, viewing words and viewing pictures. In summary these results demonstrate less left MTL and greater right MTL activation in the left TLE patients and less right MTL and greater left MTL activation in the right TLE patients compared with controls.

Secondly, we demonstrated that greater activation in the damaged left hippocampus is correlated with better verbal memory test performance in left TLE patients. Similarly, greater activation in the damaged right hippocampus correlated with better non-verbal memory in right TLE patients (Table 5). This suggests that material specific memory in TLE is better when it is sustained by functional activation within the damaged hippocampus. This would be consistent with the observation that pre-operative memory performance is a predictor of post-operative memory decline, with better performance predicting worse decline (114;115). The converse is true in the contralateral MTL, with greater fMRI activation correlating with worse memory performance. This suggests that although there is to some extent a compensatory increase in activation on the unaffected side this is an inefficient process and does not lead to the preservation of memory function.

Finally we demonstrated correlations between hippocampal volume and fMRI activation. This relationship between structure and function has previously been demonstrated with left hippocampal pathology predicting the magnitude of fMRI activation for word encoding, with less severe left hippocampal pathology being associated with more left hippocampal activation (257). Our findings

replicate and extend this to show a similar correlation between right hippocampal volume and right hippocampal activation for picture encoding. In summary it appears that more severe hippocampal pathology is associated with worse memory and with less ipsilateral and greater contralateral activation. The extent of the functional reorganisation that takes place therefore appears to be proportional to the degree of damage to the hippocampus.

6.5.2 Limitations of the study

Partial volume effects may contribute to the findings. A sclerotic hippocampus will contain fewer voxels that may demonstrate a BOLD effect. Our study focused on reorganisation within MTL structures and our choice of imaging parameters and statistical thresholds were based on this pre-existing hypothesis (342). It is possible that reorganisation may take place to other neocortical regions both within and outside the temporal lobes; however we were unable to assess the degree of extra-temporal reorganisation that may have occurred in these patients. Our findings also refer to a relatively small sample of patients and the findings will require confirmation in larger groups. However our results replicate and extend previous fMRI findings in an independent patient sample (244;257), and are consistent with clinical findings from patients undergoing ATLR.

6.5.3 Comparison with previous findings

Several studies have used fMRI in the assessment of memory function in patients with unilateral TLE. A blocked design experiment comparing presentation of complex visual scenes with randomly 'scrambled' pictures demonstrated symmetrical MTL activation in controls and asymmetric MTL activation concordant with results from intracarotid amytal testing (IAT) in patients with unilateral TLE (249). Greater left MTL activation was observed in patients with right TLE than left TLE using a semantic decision task, where an assumption of incidental encoding was made (253). Dupont et al demonstrated different patterns of activation in patients with left TLE compared to controls during memory encoding and retrieval of word lists (250). An area of activation in the posterior parahippocampal gyrus was identified to be greater in controls than in patients; however there was a highly significant difference in task performance between the two groups, with patients performing the task poorly, which limits the

interpretation. Mental navigation of a familiar spatial environment has been shown to result in bilateral symmetric pattern of MTL activation in controls but an asymmetric pattern of activation in patients with unilateral TLE with reduced activation ipsilateral to the affected MTL (255). Finally, Golby et al used a blocked design experiment comparing novel versus repeated stimuli, finding that the side of the epileptic focus influenced the lateralisation of fMRI activation within the MTL, with greater activation contralateral to the affected side (256).

Some of these studies only revealed areas of activation in posterior MTL, used blocked experimental designs which involved an assumption of memory encoding, did not perform direct comparisons with normal subjects and (while showing regions of reduced activation) did not demonstrate any reorganisation of function to other brain regions. Using an event-related design, Richardson et al demonstrated a reorganisation of verbal memory encoding from left to right MTL in left TLE patients however non-verbal memory was not assessed in this study (244). Our study extends these findings by assessing both verbal and non-verbal memory in patients with left and right TLE and by looking at correlations between functional activation and memory performance.

6.5.4 Neurobiological implications

6.5.4.1 Hippocampal functional adequacy versus functional reserve

Two different models of hippocampal function have been proposed to explain memory deficits following ATLR; hippocampal reserve and functional adequacy (111). According to the hippocampal reserve theory, postoperative memory decline depends on the capacity or reserve of the contralateral hippocampus to support memory following surgery, while the functional adequacy model suggests that it is the capacity of the hippocampus that is to be resected that determines whether changes in memory function will be observed. Evidence from baseline neuropsychology (112), the IAT (113), histological studies of hippocampal cell density (96) and MRI volumetry (70) has suggested that of the two, it is the functional adequacy of the ipsilateral MTL, rather than the functional reserve of the contralateral MTL that is most closely related to the typical material specific memory deficits seen following ATLR.

By correlating performance on standard neuropsychological tests with memory-related fMRI activation we demonstrated that MTL activation ipsilateral to the pathology is correlated with better performance

while contralateral, compensatory activation correlates with poorer performance. This suggests that reorganisation to contralateral MTL structures is not an effective way of maintaining memory function. The conclusion that memory function in unilateral TLE is better when sustained by the activation within the damaged hippocampus adds further support to the functional adequacy model of hippocampal function.

6.5.4.2 Functional reorganisation

Functional imaging studies have demonstrated reorganisation of function in the presence of other neurological disease, including stroke (337;340;343), multiple sclerosis (344) and peripheral motor denervation (345). A number of these suggest that functional reorganisation to the contralateral hemisphere takes place but it is not clear whether this necessarily provides an effective mechanism of maintaining performance. Contradictory evidence has emerged from studies of stroke patients with inter-hemispheric reorganisation of language function associated with recovery from post-stroke aphasia in some studies (337;338), while others have shown clinical recovery related to activation within unaffected ipsilateral brain regions (339), and reorganisation to the opposite hemisphere to be associated with poor recovery (336;340;343). It is only by correlating fMRI with behavioural measures that it is possible to demonstrate brain regions where functional activation correlates with better performance. In a study of patients with intact reading skills following left ATLR, Noppeney et al used reading scores in patients who had had left ATLR as covariates in order to identify brain regions where activation increased with reading ability (207). The patients' reading skills relied upon integration of regions from the normal (bilateral) reading system along with recruitment of other right hemisphere regions. In a study of patients with Alzheimer's disease Golby et al also found correlations between behavioural measures of memory function and activation in posterior MTL, lingual and fusiform areas (346).

Our findings suggest that reorganisation to contralateral MTL structures is not an effective way of maintaining memory function and are analogous to those of Ward et al in patients recovering motor function following stroke. Patients with more complete recovery were more likely to have 'normal' motor

activation whereas activation in other motor-related brain regions correlated negatively with outcome (336).

6.5.5 Clinical implications

The ability to predict the effect of left or right ATLR on verbal and non-verbal memory in an individual patient is an important part of the presurgical evaluation. Current predictors of post-operative memory outcome include the severity of hippocampal sclerosis on pre-operative structural imaging with larger hippocampal volume being correlated with a decline in verbal memory following resection (70). Preoperative memory performance on neuropsychological testing has been related to degree of postoperative memory impairment, with better performance increasing the risk of clinically significant memory decline (112;114;115). Our findings demonstrate that both hippocampal volume and memory performance are correlated with functional activation within the to-be-resected hippocampus, hence explaining why these are risk factors for memory decline following ATLR.

6.6 CONCLUSION

In conclusion, using a paradigm that allows the assessment of verbal and non-verbal memory in a single scanning session, we have demonstrated a partial reorganisation of verbal and non-verbal memory in patients with both left and right TLE due to HS, with the extent of reorganisation being proportional to the degree of hippocampal damage. We also demonstrate that good memory performance is sustained by activation within the pathological MTL, explaining why patients with better pre-operative memory functioning are most at risk of post-operative memory impairment.

Age/ gender	Handed ness	AO	Seizure types and frequency (per month)	Post-op outcome (Engel class.)	MRI and pathological diagnosis	Clinical and EEG	VIQ	PIQ	Verbal recall	Figure recall	Right HV (cm3)	Left HV (cm3)	Total intracranial volume (cm3)	Hippocampal volume ratio (%)	AEDs (mg/day)	LD
25/F	Right	17	CPS 8 SGTC 0.5	IA	Left HS	Left TLE	82	80	46	60	2.729	1.351	168.53	50	TPR 150 LTG 200	Left
37/M	Left	1	SPS 12 CPS 4	IB	Left HS	Left TLE	94	93	23	49	3.3	1.88	175	57	VPA 800 CBZ 800 LVT 2000	Left
33/M	Right	1	SPS 4 CPS 4	IA	Left HS	Left TLE	86	88	46	91	2.83	2.02	NM	71	PMD 500 CBZ 1200 CLB 10 TPR 175 LVT 4000	Left
32/F	Right	22	SPS 30 CPS 5 SGTC 0.25	NA	Left HS	Left TLE	88	111	27	40	2.359	1.789	152.9	76	OXC 1050 TPR 200	Left
37/F	Right	18	CPS 10	IA	Left HS	Left TLE	105	110	50	66	2.912	1.602	143.5	55	CBZ 1200 GBP 2700	Left
28/M	Right	3	CPS 1	IA	Left HS	Left TLE	76	81	18	10	3.077	1.417	171.24	46	LVT 3000 LTG 600	Left
34/M	Right	21	CPS 5	NA	Left HS	Left TLE	67	76	3	8	2.235	1.896	172.2	85	LVT 2000 VPA 2000	Left
25/M	Right	5	CPS 3	NA	Right HS	Right TLE	101	90	50	59	1.84	2.35	NM	78	PHT 200 LVT 3000	Left
47/M	Right	13	CPS 1	IB	Right HS	Right TLE	73	86	36	18	1.038	2.769	145.92	37	LVT 500 PHT 300 CBZ 800	Left
44/F	Right	14	CPS 4	IA	Right HS	Right TLE	95	104	64	80	2.606	3.034	154.9	86	LVT 750 PHT 400 CLB 10	Left
46/F	Right	8	CPS 5	IA	Right HS	Right TLE	88	84	60	13	1.756	2.695	147	65	TPR 600 PMD 1000 OXC 2400	Left
32/F	Right	19	CPS 2	IIIA	Right HS	Right TLE	87	110	80	66	2.299	2.562	139.55	90	CBZ 1600 LVT 1000	Left
29/M	Right	9	CPS 30 SGTC 4	NA	Right HS	Right TLE	93	114	88	84	2.273	2.978	162.86	76	VPA 2400	Left
41/F	Right	14	CPS 4	IA	Right HS	Right TLE	90	88	75	47	1.628	2.302	150.8	71	TGB 15	Left

Table 6.1 Patient clinical and demographic data

M = male; F = female; AO = age of onset; CPS = complex partial seizure; SGTC = secondary generalised tonic-clonic seizure; NA = not applicable; HS = hippocampal sclerosis; EEG = electroencephalogram; TLE = temporal lobe epilepsy; VIQ = verbal intelligence quotient; PIQ = performance intelligence quotient; HV = hippocampal volume; AED = antiepileptic drug; TPR = topiramate; LTG = lamotrigine; VPA = sodium valproate; CBZ = carbamazepine; LVT = levetiracetam; PMD = primidone; CLB = clobazam; OXC = oxcarbazepine; GBP = gabapentin; PHT = phenytoin; TGB = tiagabine; LD = language dominance.

Table 6.2 Activation peaks in the medial temporal lobe for left and right TLE groups

For each effect, the MNI coordinate, Z score, anatomical location and relevant figure are given.

Group	Material	Contrast	Figure	MNI coordinates	Z-score	Region
Left TLE	Faces	Remembered > forgotten	Figure 6.1a	34 -24 -16	2.99	Right hippocampus
	Faces	Remembered > forgotten	Figure 6.1b	22 -14 -32	2.98	Right entorhinal cortex
	Words	Viewing > fixate	Figure 6.1c	40 -20 -30	4.07	Right parahippocampal gyrus
	Pictures	Viewing > fixate	Figure 6.1d	40 -32 -24	3.72	Right parahippocampal gyrus
	Faces	Viewing > fixate	Figure 6.1e	38 -36 -24	3.33	Right fusiform gyrus
	Faces	Viewing > fixate	Figure 6.1f	38 -30 -30	3.10	Right parahippocampal gyrus
Right TLE	Words	Remembered > forgotten	Figure 6.2a	-30 -10 -36	3.33	Left hippocampus
	Pictures	Remembered > forgotten	Figure 6.2b	-34 -34 -18	2.6	Left parahippocampal gyrus
	Pictures	Viewing > fixate	Figure 6.2c	-40 -20 -26	4.19	Left hippocampus
	Faces	Viewing > fixate	Figure 6.2d	16 -18 -26	4.07	Right hippocampus

Table 6.3 Activation peaks in the medial temporal lobe for group comparisons
For each effect, the MNI coordinate, Z score, anatomical location and relevant figure are given.

Group comparison	Material	Contrast	Figure	MNI coordinates	Z-score	Region
Left TLE > Controls	Words	Remembered > forgotten	Figure 6.3a	34 -26 -28	2.60	Right parahippocampal gyrus
Left TLE > Controls	Faces	Remembered > forgotten	Figure 6.3b	26 -22 -30	3.15	Right entorhinal cortex
Left TLE < Controls	Words	Viewing > fixate	Figure 6.3c	-28 -28 -16	3.78	Left hippocampus
Left TLE > Controls	Words	Viewing > fixate	Figure 6.3d	38 -20 -30	3.04	Right parahippocampal gyrus
Left TLE < Controls	Pictures	Viewing > fixate	Figure 6.3e	-26 -30 -18	4.44	Left hippocampus
Left TLE > Controls	Faces	Viewing > fixate	Figure 6.3f	44 -36 -18	3.40	Right fusiform gyrus
Right TLE > Controls	Words	Remembered > forgotten	Figure 6.4a	-18 -14 -28	3.07	Left hippocampus
Right TLE > Controls	Words	Remembered > forgotten		-28 -6 -30	3.28	Left amygdala
Right TLE > Controls	Words	Viewing > fixate	Figure 6.4b	-40 -18 -26	2.99	Left hippocampus
Right TLE > Controls	Pictures	Viewing > fixate	Figure 6.4c	-40 -16 -30	3.60	Left hippocampus

Table 6.4 Activation peaks in the medial temporal lobe for structure-function correlations
For each effect, the MNI coordinate, Z score, anatomical location and relevant figure are given.

Group	Correlation	Figure	MNI coordinates	Z-score	Region
Structure-function correlations	Word encoding v left HV	Figure 6.5a	-30 -18 -18	3.04	Left hippocampus
	Picture encoding v right HV	Figure 6.5b	24 -8 -32	3.18	Right hippocampus

Table 6.5(over) Results summary
Summary of all the results including main effect of encoding and viewing each stimulus type for each group, comparison between patient and controls, and correlations with memory performance. HC = hippocampus, PHG = parahippocampal gyrus, A = amygdala, FG = fusiform gyrus, ERC = entorhinal cortex.

Group	Material	Contrast	Region of main effect	Comparison with controls (increased/decreased, location)	Correlation with memory performance (location, correlating measure)
Controls	Words	Remembered > forgotten	Left HC		
	Pictures		Bilateral PHG		
	Faces		Right HC, A		
	Words	Viewing > fixate	Left PHG		
	Pictures		Left PHG		
	Faces		Bilateral FG		
Left TLE	Words	Remembered > forgotten	-	Increased, Right PHG	Right HC, 1/verbal recall
	Pictures		-	-	-
	Faces		Right HC, ERC	Increased, Right ERC	-
	Words	Viewing > fixate	Right PHG	Reduced, Left HC Increased, Right PHG	Left HC, verbal recall Right HC, 1/verbal recall
	Pictures		Right PHG	Reduced, Left HC	-
	Faces		Right PHG, FG	Increased, Right FG	
Right TLE	Words	Remembered > forgotten	Left HC	Increased, Left HC	-
	Pictures		Left PHG	-	Right HC, figure recall Left HC, 1/figure recall
	Faces		-	-	-
	Words	Viewing > fixate	-	Increased, Left HC	-
	Pictures		Left HC	Increased, Left HC	Right HC, figure recall
	Faces		Right HC	-	-

CHAPTER VII PREDICTION OF POSTOPERATIVE MEMORY DECLINE

In this chapter we use the memory fMRI paradigm described in the previous two chapters and evaluate its role in the prediction of memory change following ATLR. The material in this chapter has been submitted to the JNNP.

7.1 OBJECTIVE

ATLR benefits many patients with refractory TLE but may be complicated by material specific memory impairments, typically of verbal memory following left ATLR and non-verbal memory following right ATLR. Preoperative memory fMRI may help in the prediction of these deficits. In this study we report results of preoperative fMRI and pre- and post-operative neuropsychological assessment in individual left and right TLE patients undergoing ATLR. We hypothesised that, in keeping with the functional adequacy hypothesis of hippocampal function, greater ipsilateral fMRI activation would be associated with greater verbal memory decline following ATLR resection on the language-dominant side and greater non verbal memory decline following non-dominant ATLR.

7.2 INTRODUCTION (refer to section 1.6.8 for more details)

ATLR may lead to seizure freedom in at least 60% of patients with medically refractory TLE and is now being carried out earlier and in those with less severe epilepsy (99). The hippocampus and medial temporal structures play an important role in memory encoding (43) and ATLR carries a risk of memory impairment. With improved patient selection cases of dense amnesia are fortunately rare (108), nevertheless more subtle, but clinically important memory deficits remain common. Patients undergoing unilateral ATLR are at risk of a decline in verbal memory following surgery involving the language-dominant hemisphere (109) and a decline in topographical memory following non-dominant temporal lobe resection (110).

Prognostic indicators for material specific memory decline following ATLR include the severity of HS on MRI, with less severe left HS increasing the risk of verbal memory decline (70), and preoperative memory performance, with better performance increasing the risk of memory decline

(112;114;115;347). Memory decline has also been found to correlate inversely with the severity of HS in the resected hippocampus, with patients with more severe HS having less memory decline (116;117).

The IAT has been advocated for the prediction of post-operative memory deficits. The IAT was introduced into surgical programmes to establish language dominance and to identify the risk of post-operative amnesia (98). During the IAT the affected temporal lobe is temporarily anaesthetized allowing language and mnestic capacity of the contralateral hemisphere to be assessed. The IAT has a number of disadvantages, notably the fact that it is an expensive, invasive procedure and significant variations exist between centres in many aspects of its methodology (98). Prediction of post-operative verbal memory decline is likely to be overestimated as deactivation of the language dominant hemisphere will cause increased errors on verbal memory testing.

fMRI has potential for replacing the IAT and for providing additional data to that provided by baseline neuropsychological assessment. Recent studies have suggested that fMRI may help to predict memory decline following ATLR. Richardson et al showed that greater verbal memory encoding activity in the left hippocampus compared to the right hippocampus predicted the extent of verbal memory decline following left ATLR (258). Rabin and colleagues used a complex visual scene-encoding task that causes symmetrical MTL activation in controls (260) to demonstrate a correlation between MTL activation asymmetry ratios and post-surgical memory outcome, with increased activation ipsilateral to the seizure focus correlating with greater memory decline. Janszky et al used Roland's Hometown Walking test in right TLE patients, and demonstrated a correlation between preoperative fMRI asymmetry index during this task and postoperative change in non-verbal memory following right ATLR (261).

The previous two chapters demonstrated a material-specific lateralisation of function in the MTL in controls and evidence of some reorganisation of function to the contralateral MTL in TLE patients. Contralateral re-organisation of function was not as effective as ipsilateral hippocampal function as correlations between fMRI activation and baseline memory performance showed that patients using their ipsilateral, to-be-resected hippocampus had better memory performance than those with encoding reorganised to the opposite side.

7.3 METHODS

7.3.1 Subjects

We studied 15 patients (median age 36; range 22-47 years; 7 female) with medically refractory TLE undergoing ATLR at the National Hospital for Neurology and Neurosurgery, London, UK. All patients had undergone structural MRI at 1.5T (62). Of the 7 left TLE patients, 6 had HS (one of whom additionally had a ganglioglioma in the left fusiform gyrus) and one had a MTL dysembryoblastic neuroepithelial tumour (DNET). Of the 8 right TLE patients 6 had HS, one had a MTL DNET and one a MTL glioma. Video-EEG had confirmed seizures arising from the ipsilateral medial temporal lobe in all 15. All patients had a normal contralateral hippocampus on structural imaging. Hippocampal volumetry was carried out according to a previously published protocol (295). All patients were on anti-epileptic medication and all were fluent English speakers. Handedness was determined using a standardised questionnaire (296). Language dominance was assessed using a range of fMRI tasks (301), revealing left hemisphere dominance in all but one patient. This patient (patient 10) was left handed and confirmed to be right hemisphere dominant for language on both fMRI and IAT. His pattern of neuropsychological test results, with a decline in verbal memory score and little change in non-verbal memory, were also in keeping with a resection of the language-dominant hemisphere. All patients underwent standardised neuropsychological assessment pre- and postoperatively (297).

Patient demographics, neurological test results and surgical outcome data are detailed in table 7.1. The ILAE classification of post-operative seizure outcome following epilepsy surgery was used (100). Pre- and postoperative neuropsychological test results are detailed in table 7.2. The study was approved by the National Hospital for Neurology and Neurosurgery and the Institute of Neurology Joint Research Ethics Committee and informed written consent was obtained from all subjects.

7.3.2 Neuropsychological tests

The measures of memory employed in this study are standard in our surgical programme (298) and are described in the common methodology section 2.2. We used verbal learning and design learning, rather than verbal recall and figure recall, as reliable change indices (RCIs) (348) were available for these scores, allowing us to identify which subjects underwent clinically significant memory change. In

addition, verbal learning has less semantic content than verbal recall and is therefore a better test of hippocampal function.

Each memory test was repeated 3 months after surgery in each patient, and measures of memory change following surgery were calculated as preoperative verbal learning minus postoperative verbal learning, and preoperative design learning minus postoperative design learning. These measures of memory change were then used to test for correlations between preoperative fMRI activation and memory change following ATLR. Patients with a clinically significant postoperative decline were identified using RCIs. The RCI (80% confidence interval) was 16 for verbal learning and 28 for design learning.

We also tested for correlations between pre-operative hippocampal volume and memory change following surgery. For this, and all subsequent group analyses, the patients were split according to whether they underwent dominant or non-dominant hemisphere ATLR and analyses were performed using SPSS for Windows, release 11. The patient with right TLE and right language dominance was therefore included in the dominant group along with all the left TLE patients. We calculated the Pearson's correlation coefficient between left (dominant) hippocampal volume and change in verbal memory following dominant ATLR, and between right (non-dominant) hippocampal volume and change in non-verbal memory following non-dominant ATLR. Finally we tested for correlations between pre-operative memory performance and memory change following surgery. We calculated the Pearson's correlation coefficient between pre-operative verbal learning and change in verbal learning following dominant ATLR, and between pre-operative design learning and change in design learning following non-dominant ATLR

7.3.3 MR data acquisition

MRI acquisition was performed according to our common protocol (refer to section 2.3.1).

7.3.4 Memory task

The memory task and subsequent recognition test used in this study are described in the common methodology section 2.3.2.1.

7.3.5 Data analysis

The basic fMRI data analysis is described in the common methodology chapter. The pre-processing steps are described in section 2.3.3, and the event-related analysis in section 2.3.3.1.1. In this study we only considered the event-related results demonstrating subsequent memory effects and the blocked analysis was not used.

7.3.6 'Difference image' analysis

For each subject we created 'difference images' by rotating the contrast images by 180 degrees in the x-axis and subtracting this 'flipped' image from the original contrast image (258). This created images of encoding asymmetry for each stimulus type showing left minus right activation in the left hemisphere and right minus left activation on the right.

At the second level of the random effects analysis, simple regression was used within each group to look for brain regions showing correlations between preoperative encoding asymmetry and both verbal and non-verbal memory change following surgery. We report all MTL activations at a threshold of $P<0.001$, uncorrected for multiple comparisons. This uncorrected threshold was adopted because of the low signal-to-noise ratio in the anterior temporal lobe (209;246) (342) and as we were testing a specific hypothesis regarding MTL activation. MTL regions of activation were labelled with reference to Duvernoy's The Human Hippocampus (303).

7.3.7 Region of interest analysis

We defined spherical (10mm radius) ROIs for the left and right hippocampus. The left sided ROI was centred on hippocampal coordinates previously reported to show a correlation between encoding asymmetry and change in verbal memory following left ATLR (258). A homotopic ROI was created on the right. We used the fMRI parameter estimates within the left and right ROIs, and calculated the Pearson's correlation coefficient between hippocampal fMRI and change in memory following dominant and non-dominant ATLR.

7.4 RESULTS

7.4.1 Memory change following surgery

7.4.1.1 Resection in language-dominant hemisphere (n=8)

The memory test data is summarized in table 7.2 with patients showing a clinically significant memory decline highlighted. Seven of the eight patients undergoing dominant ATLR had a post-operative decline in verbal learning score, four of which were clinically significant. The remaining patient had no change. The mean change between pre and post-operative verbal learning score was -14, ranging from 0 to -22 (P=0.001). One patient also had a clinically significant decline in design learning score. The mean change between pre and post-operative design learning score was 5, ranging from an increase of 27 to a decline of 31 (P=0.46).

7.4.1.2 Resection in non-dominant hemisphere (n=7)

Only one patient undergoing non-dominant ATLR had a clinically significant post-operative decline in design learning score, and in one there was a clinically significant increase. The mean change between pre and post-operative design learning score was -3, ranging from an increase of 31 to a decline of 39 (P=0.76). One patient also had a clinically significant decline in verbal learning score. The mean change between pre and post-operative verbal learning score was -5, ranging from an increase of 7 to a decline of 24 (P=0.3).

7.4.2 Recognition accuracy

For the patients undergoing dominant ATLR, there was no significant correlation between the recognition accuracy score for words derived from the pre-operative fMRI and pre-operative verbal learning (Pearson's correlation coefficient=0.54; P=0.21). For the patients undergoing non-dominant ATLR there was a correlation between the recognition accuracy score for faces derived from the pre-operative fMRI and pre-operative design learning (Pearson's correlation coefficient=0.74; P=0.035).

7.4.3 Correlations between hippocampal volume and postoperative memory change

There were no significant correlations between hippocampal volume and verbal memory decline in the dominant ATLR patients or between hippocampal volume and non-verbal memory decline in the non-dominant ATLR patients.

7.4.4 Correlations between pre-operative memory performance and postoperative memory change

There were no significant correlations between pre-operative verbal learning and verbal memory decline in the dominant ATLR patients. In the non-dominant ATLR patients a significant correlation was seen between pre-operative design learning and non-verbal memory decline (Pearson's correlation coefficient=-0.751; P=0.032), characterised by greater decline in patients with better pre-operative memory function.

7.4.5 Correlations between pre-operative fMRI and postoperative memory change

7.4.5.1 Difference images

In patients undergoing dominant ATLR correlations were seen between left-right difference in hippocampal encoding activation for words (r^2=0.92; P<0.001, Figure 7.1a) and for overall memory encoding (r^2=0.93; P<0.001, Figure 7.1b), and decline in verbal learning score. No correlations were seen between fMRI activation in these regions and change in verbal learning score in patients undergoing non-dominant ATLR (Figures 7.1a-b).

In the patients undergoing non-dominant ATLR a correlation was observed between right-left difference in amygdala encoding activation for faces and change in design learning score (r^2=0.98 P<0.001, Figure 7.1c). In the patients undergoing dominant ATLR, no correlations were seen between fMRI activation in this region and change in memory (Figure 7.1c).

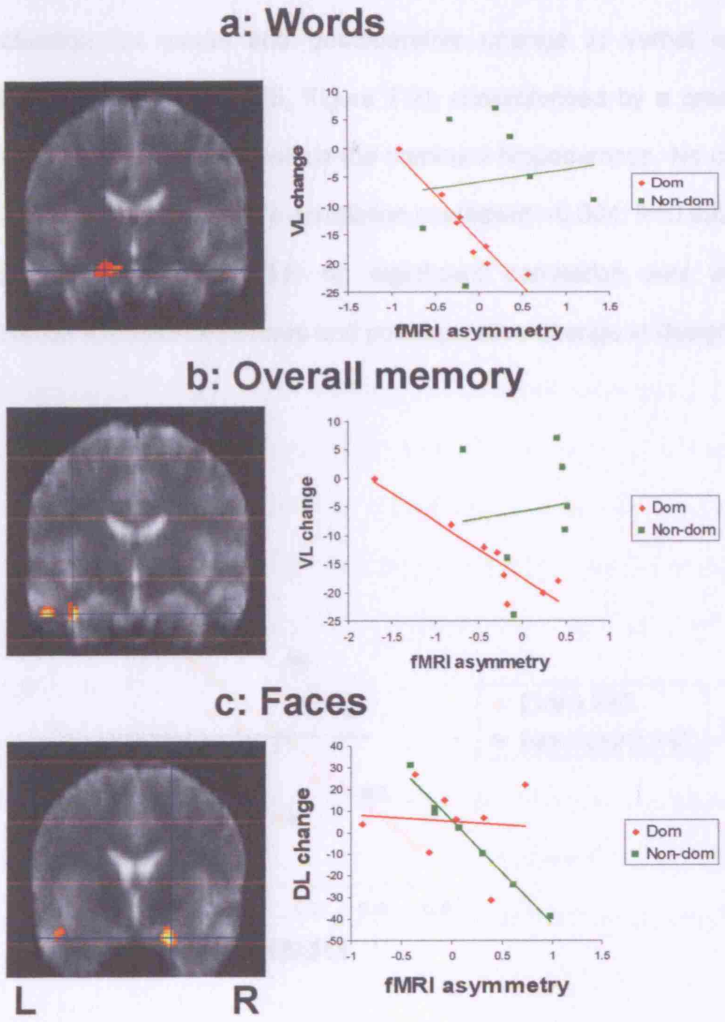

Figure 7.1 Correlations between pre-operative fMRI and post-operative memory change
Regions showing a significant correlation between fMRI activation asymmetry and post-operative change in verbal learning (VL) are superimposed onto the normalized mean EPI image from 10 healthy control subjects. Left (L) and right (R) side of the brain are indicated. The correlation at the peak voxel is illustrated graphically on the right for both the dominant ATLR group (red line) and the non-dominant ATLR group (green line). For patients undergoing dominant ATLR, significant correlations are seen between hippocampal fMRI activation asymmetry for words (a; MNI coordinates -14 -14 -16, Z score 3.9) and overall memory (b; MNI coordinates -38 -14 -28, Z score 3.69), and post-operative change in verbal learning. For patients undergoing non-dominant ATLR, a significant correlation was seen between amygdala fMRI activation asymmetry for faces (c; MNI coordinates 22 -2 -26, Z score 3.95), and post-operative change in design learning.

7.4.5.2 Region of interest analysis

In the patients undergoing dominant ATLR there was a significant correlation between dominant hippocampal encoding activation for words and postoperative change in verbal learning score (Pearson's correlation coefficient=-0.811; P=0.015, Figure 7.2), characterised by a greater decline in verbal memory in patients with greater activation within the dominant hippocampus. No correlation was seen in the non-dominant hippocampus (Pearson's correlation coefficient=-0.004; P=0.992, Figure 7.2). In the patients undergoing non-dominant ATLR no significant correlation was seen between hippocampal encoding activation for faces or pictures and post-operative change in design learning.

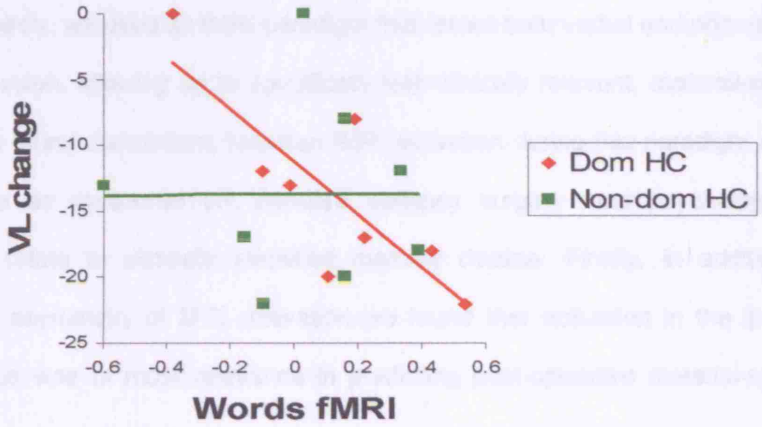

Figure 7.2 Correlations between pre-operative fMRI and post-operative memory change
Relationship between pre-operative fMRI activation and post-operative memory change within dominant and non-dominant hippocampal ROIs. For patients undergoing dominant ATLR, a significant correlation was seen between dominant hippocampal encoding-related fMRI activation for words and post-operative decline in verbal learning (VL) (red line). No significant correlation was seen in the non-dominant hippocampus (green line).

7.5 DISCUSSION

7.5.1 Summary of results

In patients with unilateral TLE performing an fMRI test of memory encoding, relatively greater ipsilateral compared to contralateral MTL activation predicted declines in both verbal and non-verbal memory following dominant and non-dominant hemisphere ATLR. Furthermore, for dominant hemisphere resections, activation within the ipsilateral hippocampus was predictive of postoperative memory change with greater hippocampal activation for word encoding being correlated with greater verbal memory decline following surgery. No such correlation was observed in the contralateral hippocampus.

This study has a number of strengths. Firstly, it was performed on a consecutive group of patients with both left and right TLE, typical of an epilepsy surgery programme. Secondly, the event-related analysis allowed us to specifically test for subsequent memory effects rather than make an assumption of memory encoding. Thirdly, we used an fMRI paradigm that tested both verbal and non-verbal memory in a single scanning session, allowing us to specifically test clinically relevant, material-specific memory function. Fourthly, we found correlations between fMRI activation during this paradigm and changes in memory performance as measured on standard epilepsy surgery neuropsychological tests and accordingly findings relate to clinically identified memory decline. Finally, in addition to showing correlations between asymmetry of MTL activation we found that activation in the ipsilateral, to-be-resected hippocampus was of most relevance in predicting post-operative material-specific memory deficits.

7.5.2 Comparison with previous findings

Our findings corroborate and extend findings from previous studies. In a group of patients with left HS, relatively greater activation for word encoding in the left hippocampus compared with right hippocampus predicted the extent of verbal memory decline following left ATLR (258). A regression analysis demonstrated that greater activation within a left hippocampal ROI predicted a greater postoperative decline in verbal memory, a similar finding to this study. Right hippocampal activation however also predicted postoperative verbal memory outcome (259), a finding not supported in our current study.

In a study of right TLE patients, a correlation was found between an asymmetry index of MTL fMRI activation and decline in non-verbal memory following right ATLR, characterised by increased right compared to left sided activity being associated with greater memory decline (261). In a group of left and right TLE patients, asymmetry ratios of MTL activation during a visual scene encoding task were correlated with memory outcome (260). Increased ipsilateral activation was inversely correlated with memory outcome and no correlation was seen in the contralateral hippocampus. The measure of memory outcome used was the change between pre- and post-surgical scene recognition performance, likely to be more sensitive to right MTL pathology, rather than a more standard neuropsychological measure of memory.

In chapter V, we demonstrated a material-specific lateralisation of memory encoding in the medial temporal lobes in healthy controls; with word encoding seen in the left MTL, picture encoding relatively bilateral and face encoding being mainly on the right. As a number of other memory fMRI studies had only observed activation in posterior hippocampal and parahippocampal structures, separate from the areas normally resected during ATLR (214;218;242;249;250), we optimised our fMRI acquisition and paradigm to visualise activation in anterior hippocampal and MTL, regions that would be resected during ATLR. In chapter VI we demonstrated, at a group level, increased encoding activation in the contralateral MTL in patients with unilateral HS indicating a reorganisation of function. Correlating preoperative fMRI with baseline memory function demonstrated that increased activation in the damaged hippocampus correlated with better memory performance, while increased activation in the contralateral hippocampus correlated with worse performance. This suggested that while there was evidence for functional reorganisation to the opposite hippocampus, this was a less efficient process, incapable of preserving good memory function, and supported the functional adequacy theory of hippocampal function.

Activation asymmetry measures do not distinguish between whether it is retained ipsilateral or lack of contralateral activation that is the principal risk factor for memory decline following ATLR, i.e. whether the functional adequacy or hippocampal reserve model holds true. Our finding that greater activation in the damaged hippocampus correlates with greater postoperative memory decline, with no significant correlation demonstrated contralaterally, along with our previous finding that increased activation in the

damaged hippocampus correlated with better baseline memory performance (349) supports the functional adequacy model of hippocampal function.

7.5.3 Clinical implications

The study confirmed previous research findings of a significant decline in verbal memory following left ATLR (109;347). There was no significant change in non-verbal memory for the left TLE group and no significant change in either non-verbal or verbal memory for the right TLE group as a whole. This may reflect the small sample sizes however significant changes in memory following right ATLR have been reported and more recent studies exploring individual in addition to group changes have highlighted considerable variability in memory outcome for this group (350).

Clinically it is what happens to individual patients that is important and it is noteworthy that one of our non-dominant ATLR cases showed a larger post-operative decline in verbal memory than the dominant ATLR cases, and a second patient had a verbal memory decline of 14 points. From figure 7.1a it can be seen that both these patients had greater hippocampal activation on the right than on the left (left minus right activation is negative) for the verbal memory encoding task. It is not easy to explain why these two right TLE patients should be primarily using the right hippocampus for verbal memory. Declines in verbal memory have been reported by other investigators following right ATLR and this serves to highlight that the two hippocampal systems may not work as independently as has been suggested by the material specific hypothesis (350). For example visual strategies such as imagery may be used to enhance verbal memory competence and it may be that the verbal memories of individuals making use of such strategies pre-operatively may be disproportionately affected by right ATLR. Alternatively the presence of additional pathology in the left MTL, not seen on neuroimaging, may lead to patients using their right hippocampus for verbal memory function preoperatively. Of the cases showing significant decline in verbal memory following right ATLR in this study, all were rendered seizure free by surgery and there were no electroclinical features to suggest left MTL pathology. Whatever the reason, our finding suggests that fMRI is able to provide important predictive information, above and beyond that provided by baseline neuropsychology; namely that removing the functional area, regardless of its site, leads to a decline in function.

When assessing the clinical utility of any new predictor of memory change it is important to consider whether a change in score is significant, or meaningful, to the individual patient. RCIs have been reported as one way of identifying patients with a clinically significant postoperative decline (348). The RCI (80% confidence interval) is 16 for verbal learning and 28 for design learning, therefore all patients with a postoperative score of 16 (verbal learning) or 28 (design learning) lower than their preoperative score may be classified as having a clinically significant decline. The numbers of patients in this study do not permit conclusions as to whether patients with a clinically significant memory decline differed from others. Assessment of this issue is complicated further by studies showing that subjective memory complaints bear little relation to formal neuropsychological test scores and may be more closely related to levels of anxiety and depression (351). It does not appear that newer definitions of memory change such as RCIs are any more closely allied with the subjective experience of postoperative change than traditional measures.

Relatively greater right compared to left amygdala activation for face encoding predicted non-verbal memory decline following non-dominant ATLR but no correlation was observed with right amygdala activation alone. The amygdala has been implicated in the processing of fearful expressions (352-355). Impaired recognition of fearful facial expressions has been shown in patients with bilateral amygdala damage (238). Some of the faces included in this study had fearful expressions and we previously demonstrated that face encoding in normal controls was associated with right amygdala activation (342). Given that the amygdala has been shown to be involved in face encoding and is resected during ATLR it is not surprising that activation within this structure correlates with postoperative memory change.

7.5.4 Comparison with other predictors of memory change

The ability to predict postoperative verbal and non-verbal memory deficits for individual patients following left and right ATLR is an important part of the presurgical evaluation. Current predictors of post-operative memory outcome include the severity of hippocampal sclerosis on pre-operative structural imaging with larger hippocampal volume being correlated with a decline in verbal memory following resection (70) and preoperative memory performance on neuropsychological testing, with

better performance increasing the risk of clinically significant memory decline (112;114;115;347). Given the small number of subjects in this study it is not a surprise that we did not see any correlations between hippocampal volume and memory outcome. Nevertheless fMRI predicted memory changes in this sample and indicates that fMRI activation is not merely an indirect marker of hippocampal atrophy. While there was no correlation between preoperative verbal memory and post-operative decline we did observe a correlation between preoperative non-verbal memory performance and post-operative decline.

7.6 CONCLUSION

In conclusion, individual patients with relatively greater ipsilateral compared to contralateral MTL activation had greater memory decline following ATLR. This was the case for both verbal memory decline following dominant ATLR and for non-verbal memory decline following non-dominant ATLR. For verbal memory decline, activation within the dominant hippocampus alone was predictive of postoperative memory change whereas activation in the non-dominant hippocampus was not. The post-operative memory changes observed in this study are in keeping with the view that decline in verbal memory following dominant ATLR is clinically more important than decline in non-verbal memory following non-dominant ATLR. It is therefore encouraging that it was in these patients that fMRI was of greatest predictive value.

These findings suggest that preoperative memory fMRI, in combination with baseline neuropsychology and structural MRI will enable pre-operative prediction of material specific memory impairments seen following unilateral ATLR to be made with greater accuracy, and provide support for the functional adequacy theory of hippocampal function. They also suggest that fMRI may provide additional information, over that provided by neuropsychology, for use in the prediction of postoperative memory decline.

Table 7.1 Patient clinical and demographic data

M = male; F = female; CPS = complex partial seizure; SGTC = secondary generalised tonic-clonic seizure; NA = not applicable; HS = hippocampal sclerosis; MTL = medial temporal lobe; DNET = dysembryoplastic neuroepithelial tumour; EEG = electroencephalogram; TLE = temporal lobe epilepsy; RHV = right hippocampal volume; LHV = left hippocampal volume; TIV = total intracranial volume; HVR = hippocampal volume ratio; AED = antiepileptic drug; TPR = topiramate; LTG = lamotrigine; VPA = sodium valproate; CBZ = carbamazepine; LVT = levetiracetam; PMD = primidone; CLB = clobazam; GBP = gabapentin; CLN = clonazepam; PHT = phenytoin; TGB = tiagabine.

#	Age/ gender	Handedness	Epilepsy onset (years)	Seizure types and frequency (per month)	Post-op outcome (ILAE class.)	MRI and pathological diagnosis	Clinical and EEG	RHV (cm3)	LHV (cm3)	TIV (cm3)	HVR (%)	AEDs (mg/day)	Language dominance
1	25/F	Right	17	CPS 8 SGTC 0.5	1	Left HS	Left TLE	2.729	1.351	168.5	50	TPR 150 LTG 200	Left
2	37/M	Left	1	SPS 12 CPS 4	2	Left HS	Left TLE	3.3	1.88	175	57	VPA 800 CBZ 800 LVT 2000	Left
3	33/M	Right	1	SPS 4 CPS 4	1	Left HS	Left TLE	2.83	2.02	NM	71	PMD 500 CBZ 1200 CLB 10 TPR 175 LVT 4000	Left
4	37/F	Right	18	CPS 10	1	Left HS	Left TLE	2.912	1.602	143.5	55	CBZ 1200 GBP 2700	Left
5	28/M	Right	3	CPS 1	1	Left HS	Left TLE	3.077	1.417	171.2	46	LVT 3000 LTG 600	Left
6	31/M	Right	10	CPS 50 SGTC 3	1	Left MTL DNET	Left TLE	3.731	3.797	187.2	98	CBZ 1200 CLN 1.5 LTG 100	Left
7	37/F	Right	1	SPS 12 CPS 8 SGTC 1	3	Left HS, left fusiform gyrus ganglioglioma	Left TLE	2.8	2.385	134.8	85	CBZ 1000 CLB 10	Left
8	47/M	Right	13	CPS 1	2	Right HS	Right TLE	1.038	2.769	145.9	37	LVT 500 PHT 300 CBZ 800	Left
9	44/F	Right	14	CPS 4	1	Right HS	Right TLE	2.606	3.034	154.9	86	LVT 750 PHT 400 CLB 10	Left
10	36/M	Left	15	SPS 6 CPS 6 SGTC 3	1	Right MTL glioma	Right TLE	3.118	2.774	152.3	89	CBZ 1600 CLB 20 LTG 400	Right
11	46/F	Right	8	CPS 5	1	Right HS	Right TLE	1.756	2.695	147	65	TPR 600 PMD 1000 OXC 2400	Left
12	32/F	Right	19	CPS 2	4	Right HS	Right TLE	2.299	2.562	139.5	90	CBZ 1600 LVT 1000	Left
13	29/M	Right	9	CPS 30 SGTC 4	3	Right HS	Right TLE	2.273	2.978	162.9	76	VPA 2400	Left
14	22/M	Left	18	CPS 3 SGTC 0.33	1	Right MTL DNET	Right TLE	2.493	2.554	168.4	98	VPA 2000 GBP 600	Left
15	41/F	Right	14	CPS 4	1	Right HS	Right TLE	1.628	2.302	150.8	71	TGB 15	Left

Table 7.2 Patient neuropsychological data
VIQ = verbal intelligence quotient; PIQ = performance intelligence quotient.
* Subjects with a significant memory change as identified using RCIs.

#	Resection side	VIQ	PIQ	Pre-op verbal learning	Post-op verbal learning	Verbal learning change	Pre-op design learning	Post-op design learning	Design learning change
1	Left	82	80	73	53	-20*	87	56	-31*
2	Left	94	93	57	39	-18*	51	42	-9
3	Left	86	88	60	47	-13	80	95	+15
4	Left	105	110	72	64	-8	76	82	+6
5	Left	76	81	52	40	-12	58	62	+4
6	Left	91	99	48	48	0	55	82	+27
7	Left	70	94	80	63	-17*	53	75	+22
8	Right	73	86	51	56	+5	27	29	+2
9	Right	95	104	79	65	-14	80	56	-24
10	Right	82	99	63	41	-22*	57	64	+7
11	Right	88	84	66	57	-9	36	67	+31*
12	Right	87	110	56	51	-5	80	41	-39*
13	Right	93	114	68	73	+5	64	73	+9
14	Right	93	92	52	59	+7	76	66	-10
15	Right	90	88	69	45	-24*	31	42	+11

CHAPTER VIII LANGUAGE FUNCTION IN HEALTHY VOLUNTEERS: A COMBINED fMRI AND TRACTOGRAPHY STUDY

This chapter describes the use of fMRI paradigms to study the localisation of language function in a group of normal subjects. The functional regions are then used as seed points for tractography to study the structural connections underlying these language regions. The material in this chapter has been published in; Powell HWR et al. *Hemispheric asymmetries in language-related pathways: a combined functional MRI and tractography study.* **Neuroimage** 2006;32:388-99.

8.1 OBJECTIVE

In this study we use these two imaging techniques to examine connectivity between functionally-defined language areas in frontal and temporal lobes and test the hypothesis that in the functionally dominant left hemisphere, there would be stronger connections between language areas than between equivalent areas in the right hemisphere. We also looked for a correlation between subjects' degree of functional asymmetry and the lateralisation of the structural connections seen. If the pattern of structural connections truly reflected the underlying function then we would expect those subjects with more lateralised language function to have more lateralised structural connections.

8.2 INTRODUCTION

The 19th century lesion-deficit model proposed by Broca and Wernicke recognised that language function depends upon both frontal and temporal cortical regions and the white matter tracts connecting them. In 1861, Broca reported a post-mortem study of a patient with impaired speech production, finding an area of damage in the third frontal convolution of the left hemisphere (164). Subsequently Wernicke reported a post-mortem study of a patient who had an impairment of speech comprehension with damage to the left posterior superior temporal cortex (165). Wernicke's theory that damage to the connecting tracts would result in a specific language deficit, with intact speech comprehension and production but a deficit in repetition, was confirmed by the first reporting of a case of 'conduction aphasia' (356).

Around the same time the dissections of Dejerine (275) identified the trajectories of major white matter fibre bundles, and these pathways were subsequently visualised in three dimensions (357). The superior

longitudinal or arcuate fasciculus (SLF), a long association tract connecting frontal, parietal and temporal cortex, was seen to originate in the inferior and middle frontal gyri, projecting posteriorly before arching around the insula into the temporal lobe. Lesions causing conduction aphasias typically lie in the inferior parietal cortex and therefore cause an interruption of these fibres as they pass between Broca's and Wernicke's area.

The lateralisation of language function is a striking feature of human brain function and one that was recognised by both Broca and Wernicke. Two recent fMRI studies have demonstrated 94% (181) and 96% (180) of right-handed subjects to be left hemisphere dominant for language function. These findings are in keeping with studies of previously normal patients with aphasias secondary to stroke (358) and epilepsy patients who did not have early brain injuries (179). Greater atypical (bilateral and right-hemisphere) dominance is seen in left-handed subjects (180) and in those with early left-hemisphere lesions (172;179;181).

An important question is the extent to which structural differences between left and right hemispheres underlie the lateralisation of function, and whether this structural lateralisation reflects the degree of functional lateralisation from subject to subject. One brain region where asymmetry is evident is the upper surface of the temporal lobe adjacent to the sylvian fissure. In his original description of the anterior transverse gyrus (Heschl's gyrus), Heschl noted asymmetries in cortical folding (359), and the area of superior temporal cortex posterior to this, the planum temporale, has also been demonstrated to be larger on the left than the right (360;361). This macroscopic asymmetry was reflected at the cellular level in the greater extent of the cytoarchitectonic area Tpt (temporoparietal cortex) on the left side (362) More recently, volumetric MRI studies (285;363) and voxel-based morphometry (284) have revealed white matter asymmetries in temporal and frontal lobes.

Two recent studies have used tractography to study the connections of Broca's and Wernicke's areas (280;281), using anatomical guidelines to define starting points for fibre-tracking. While both provide interesting new insights into the course of the SLF, both used a two volume-of-interest approach, whereby the analysis is constrained to only include pathways passing through both regions. In addition, manual definition of starting regions may be prone to observer bias.

The combination of fMRI to identify cortical regions involved in specific functions and MR-tractography to visualise pathways connecting these regions offers an opportunity to study the relationship between brain structure and function by providing a selective tracing of connectivity within a behaviourally characterized network (277). The use of fMRI-derived starting points also minimises observer bias. This combination has previously been used to investigate the motor (278;364) and visual (279) systems.

8.3 METHODS

8.3.1 Subjects

We studied 10 right-handed native English-speaking healthy volunteers with no history of neurological or psychiatric disease. Handedness was determined using the Edinburgh Hand Preference Inventory (296). The age range was 23-50 years (median 29.5).

8.3.2 MR data acquisition

MRI acquisition for both fMRI and tractography was performed according to our common protocol (refer to sections 2.3.1 and 2.4.1). Diffusion tensor imaging and analysis was performed according to the previously described protocol (refer to section 2.4.2).

8.3.3 Language fMRI tasks

The language tasks used in this study are described in the common methodology section 2.3.2.2.

8.3.4 Data analysis and seed point ROI definition

The fMRI data analysis is described in the common methodology chapter. The pre-processing steps are described in section 2.3.3, and the blocked analysis in section 2.3.3.2. The group activation maps were thresholded at $p<0.001$ (uncorrected) and reverse normalised into each individual's native space. These reverse normalised (native space) group fMRI activation maps were used to define ROIs for initiating probabilistic fibre tracking. A total of four ROIs were defined for each subject based on the fMRI activation maps; one each in the left and right inferior frontal gyri and left and right superior temporal gyri. These were created by drawing over selected areas of fMRI activation (see results for details) on consecutive

brain slices, using MRIcro (http://www.psychology.nottingham.ac.uk). As tract volume is likely to be affected by seed volume, we specified that each ROI was of identical volume, comprising of 125 voxels.

8.3.5 Tracography method

We used the PICo tractography algorithm as described in the common methodology section 2.4.3.2. This was extended to cope with the presence of crossing fibres using the technique of Parker and Alexander (145), of particular importance when studying the SLF where it crosses the corona radiata. Each subject's output connectivity map was normalised to standard space and then thresholded at probability values ranging from 0.002 to 0.2 to construct binary masks. The masks were averaged across the group, to produce variability (or commonality) maps. These indicated the degree of spatial variability and overlap of the identified connections (158;280). A voxel commonality value C of 1.0 indicates that each individual had a connection identified in this voxel while C of 0.0 indicates that none of them did (280).

8.3.6 Calculating tract volumes

For the commonality maps shown, we calculated connecting volumes V(C) at different values of C to show the volume in standard space occupied by voxels above the commonality threshold C. Finally, an asymmetry index AI was calculated to assess lateralisation of the connected volumes between hemispheres;

$$AI\,(C) = (V(C)_{left} - V(C)_{right}) / (V(C)_{left} + V(C)_{right})$$

Where $V(C)_{left}$ and $V(C)_{right}$ are the tract volumes in cm^3 above a threshold value of C in the left and right hemispheres, respectively (280). No specific consideration was made for interhemispheric tracts.

The normalised tract volumes were also calculated for the left and right tracts of every subject at each probability threshold (279). From these a mean volume of left and right tracts was obtained for each threshold and a paired T-test was used to compare the volumes.

8.3.7 Calculating mean FA

For each probability threshold the mean FA of the connected volume in native space was calculated for the left and right tracts. These were calculated by multiplying the binary masks with that subject's fractional anisotropy images and calculating the mean intensity value of the voxels isolated at each threshold. From these a mean FA value of left and right tracts was obtained for each threshold and a paired T-test was used to compare these.

8.3.8 Correlations between structure and function

In order to investigate structure-function relationships in this group, we tested for correlations between the lateralisation of fMRI activation and of the lateralisation of the derived connections. For the fMRI we defined 10mm radius spheres based on the peak activations in the left frontal and bilateral temporal lobe, along with a homotopic volume in the right frontal lobe, and calculated left minus right activation for each subject. For the tractography we calculated lateralisation indices as before to assess lateralisation of both mean FA and connecting volumes between left and right sided tracts. We calculated the Pearson's correlation coefficient to test our hypothesis that there would be a correlation between the two values, with subjects with greater functional lateralisation also having more left-lateralised connections.

8.3.9 SPM regression analysis

Each subject's fMRI contrast image was entered into a SPM2 simple regression model with the mean FA of the left sided tracts as a covariate. This allowed us to look at a voxelwise level for regions showing correlation between fMRI activation and the mean FA of the connections of language-related areas (279). The resulting SPM maps were thresholded at $p<0.001$.

8.4 RESULTS

8.4.1 fMRI results

Verbal fluency and verb generation were associated with areas of activation in the left IFG, left middle frontal gyrus and left insula (Table 8.1, Figures 8.1a and b). Reading comprehension was associated with areas of activation bilaterally in the superior temporal gyri, adjacent to the superior temporal sulci (Figure

8.1c) as well as a further area in the left posterior superior temporal gyrus (Figure 8.1d). From these areas of activation we created four ROIs for initiating fibre tracking (Figure 8.1e). One was placed in the left IFG and corresponded to an area of fMRI activation seen for both the verbal fluency and verb generation paradigms. As no significant activation was seen in this region on the right, a homotopic ROI of identical size was manually defined using MRIcro. A further two functionally-defined ROIs of identical size were placed bilaterally in the superior temporal gyri adjacent to the superior temporal sulci. These corresponded to the areas of bilateral activation seen during the reading comprehension task.

Table 8.1 Activation peaks for all fMRI effects of interest
For each effect, the MNI coordinate, Z score, anatomical location and relevant figure are given.

Contrast	Figure	MNI coordinates	Z-score	Region
Verbal fluency	Figure 8.1a	-44 2 24	4.28	Left inferior frontal gyrus
		-32 26 -4	4.49	Left inferior frontal gyrus
		-38 18 10	4.31	Left insula
Verb generation	Figure 8.1b	-44 2 24	5.56*	Left inferior frontal gyrus
		-44 30 22	5.32*	Left middle frontal gyrus
		-38 22 2	5.52*	Left insula
Reading	Figure 8.1c	-44 -56 12	4.99*	Left posterior superior temporal gyrus
comprehension		-52 -26 -6	4.63	Left superior temporal gyrus
		48 -26 -4	3.53	Right superior temporal gyrus
Regression analysis: word generation and mean FA	Figure 8.6a	-56 -40 22	4.26	Left supramarginal gyrus
Regression analysis:reading and mean FA	Figure 8.6b	-36 12 20	3.08	Left inferior frontal gyrus

* P<0.05 corrected for multiple comparisons

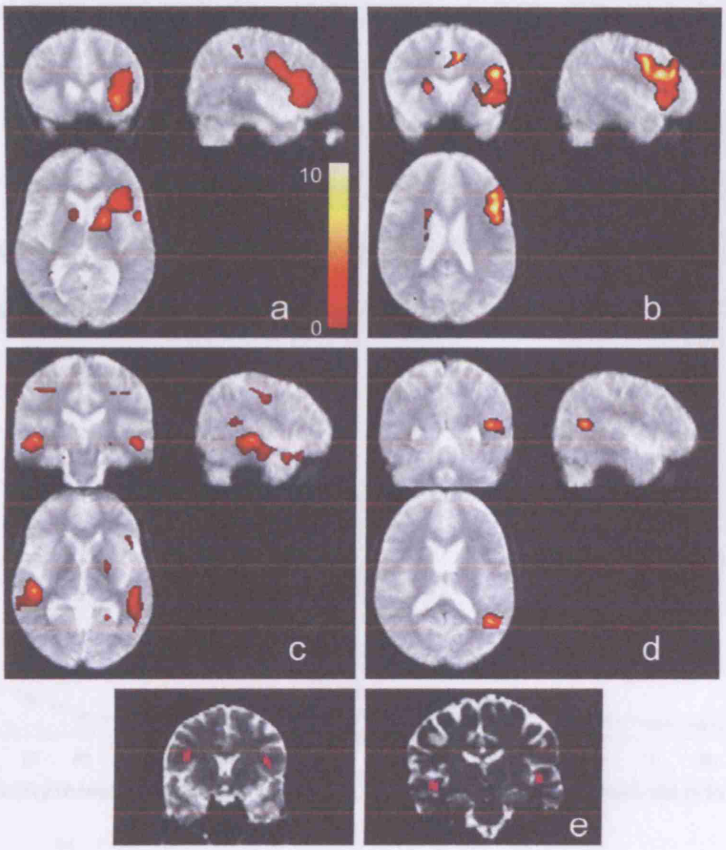

Figure 8.1 fMRI results: main effects of the three language paradigms

Significant regions (threshold here and all subsequent figures $p<0.001$) are superimposed onto the normalized mean EPI image from all 10 subjects. The left of the brain is displayed on the right of the image. Radiological viewing convention is used and the colour bar indicates T scores.

a) Verbal fluency, left inferior frontal gyrus activation.
b) Verb generation, left inferior frontal gyrus activation.
c) Reading comprehension, activation bilaterally in the superior temporal gyri, adjacent to the superior temporal sulci.
d) Reading comprehension left posterior superior temporal gyrus activation.
e) Examples from a single subject of the four ROIs defined for initiation of fibre tracking (coronal views). The ROIs are located in bilateral inferior frontal gyri (left) and bilateral superior temporal gyri (right). ROIs are overlaid on that subject's non-diffusion weighted b=0 image in native space.

8.4.2 Tract volumes and mean FA

As the PICo connection probability threshold increased the tract volumes and the variability decreased, as the core tracts were increasingly identified. Tract volume was significantly greater on the left than the right for both pairs of ROIs across all different thresholds ($p<0.05$) (Figures 8.2a and b). Increasing the PICo connection probability threshold had no significant effect on the overall mean FA of the combined left and right tracts. For the frontal ROIs the mean FA was significantly greater on the left than the right ($p<0.05$) across all different thresholds (Figure 8.2c). For the temporal ROIs there was no significant overall difference between left and right ($p=0.06$) (Figure 8.2d). For both ROIs it can be seen however that the degree of left lateralisation in mean FA value was greater at higher PICo thresholds (Figures 8.2c and d).

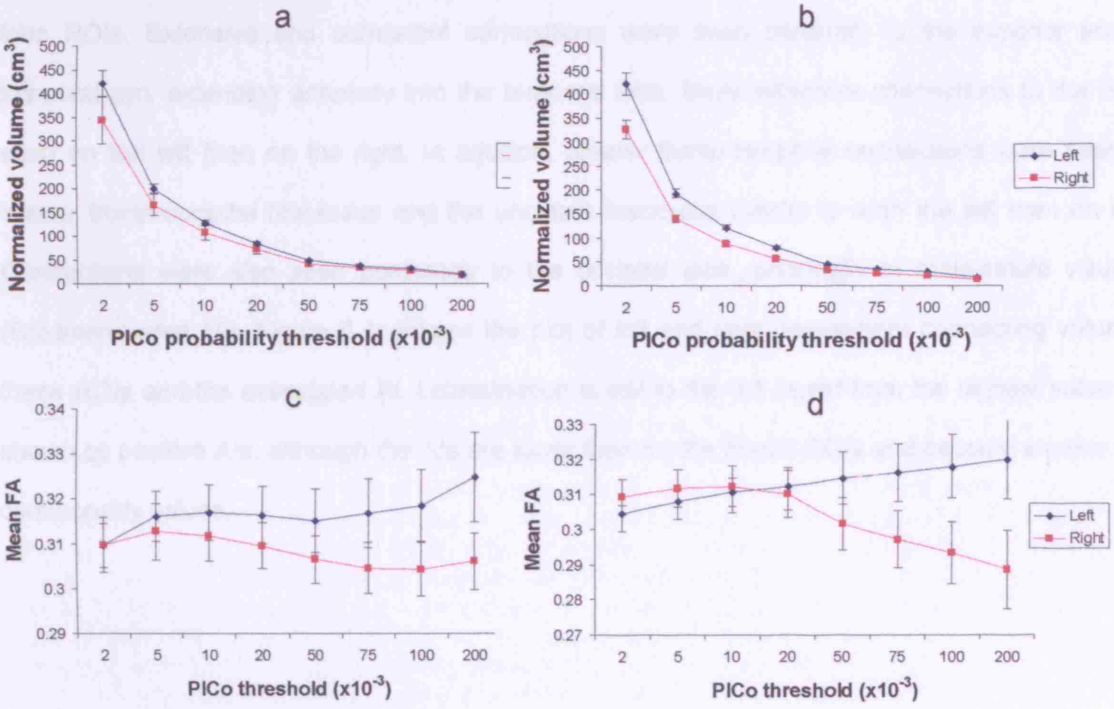

Figure 8.2 Tract volumes and mean FA
Tract volumes and mean FA as a function of PICo threshold (threshold range 0.002 to 0.2) for connections from frontal (a,c) and temporal (b,d) ROIs (+/- SE). Tract volumes were greater on the left than the right over all thresholds for both sets of connections, and difference in mean FA was more marked at higher thresholds with higher values on the left than the right.

8.4.3 Tractography results

The group variability maps (at a probability threshold of 0.05) for the volumes of connection from both pairs of ROIs are shown below. For the frontal connections consistent bilateral connections were demonstrated extending posteriorly from Broca's to Wernicke's area via the SLF (Figure 8.3). A clear qualitative difference was seen between the left and right maps with respect to the temporal lobe connections, with greater connectivity to the left superior and middle temporal gyri than the right. Connections to the supramarginal gyrus (Brodmann area 40) area were seen bilaterally and again this was greater on the left. Figure 8.3c shows a plot of left and right hemisphere connecting volumes and AI as a function of commonality value C. The left had a larger connected volume at all values of C and this lateralisation was greater in regions of high commonality.

Figure 8.4 shows the group variability maps for the volumes of connection obtained from the temporal lobe ROIs. Extensive and consistent connections were seen bilaterally to the superior and middle temporal gyri, extending anteriorly into the temporal lobe. More extensive connections to the SLF were seen on the left than on the right. In addition, greater fronto-temporal connections were seen via the inferior fronto-occipital fasciculus and the uncinate fasciculus inferior to it on the left than on the right. Connections were also seen posteriorly to the occipital lobe, principally to extra-striate visual cortex (Brodmann area 19). Figure 8.4c shows the plot of left and right hemisphere connecting volumes from these ROIs and the associated AI. Lateralisation is still to the left (apart from the highest value of C) as shown by positive AIs, although the AIs are lower than for the frontal ROIs and become smaller at higher commonality values.

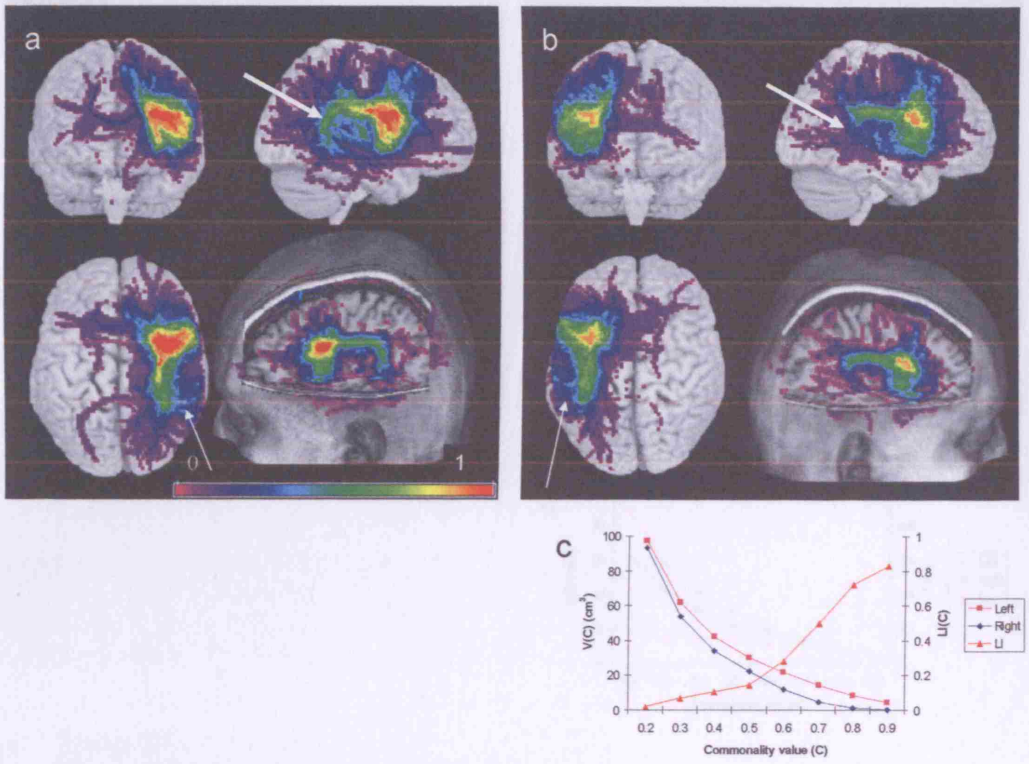

Figure 8.3 Frontal lobe connections

Group variability maps of the connecting paths tracked from the left (a) and right (b) frontal ROIs. The first three images in each show brain surface rendering with embedded spatial distribution of connections in the coronal, sagittal and axial planes. The fourth images show homotopic sagittal slices. The colour scale indicates the degree of overlap among subjects (expressed as commonality value (C)); for example, a value of 1 (pure red) represents 100% subject overlap (i.e. every subject's identified tract contains the voxel in question). These images show the maximum intensity of the connection patterns in each plane of view as a brain surface rendering. Connections to the temporal lobe are greater on the left than the right (thick arrows) as were connections to the supramarginal gyrus (thin arrows). Figure 8.3c shows connecting volume V(C) and asymmetry index AI(C) as a function of commonality value C. The left has a larger connected volume at all values of C and the lateralisation is greater in regions of high commonality.

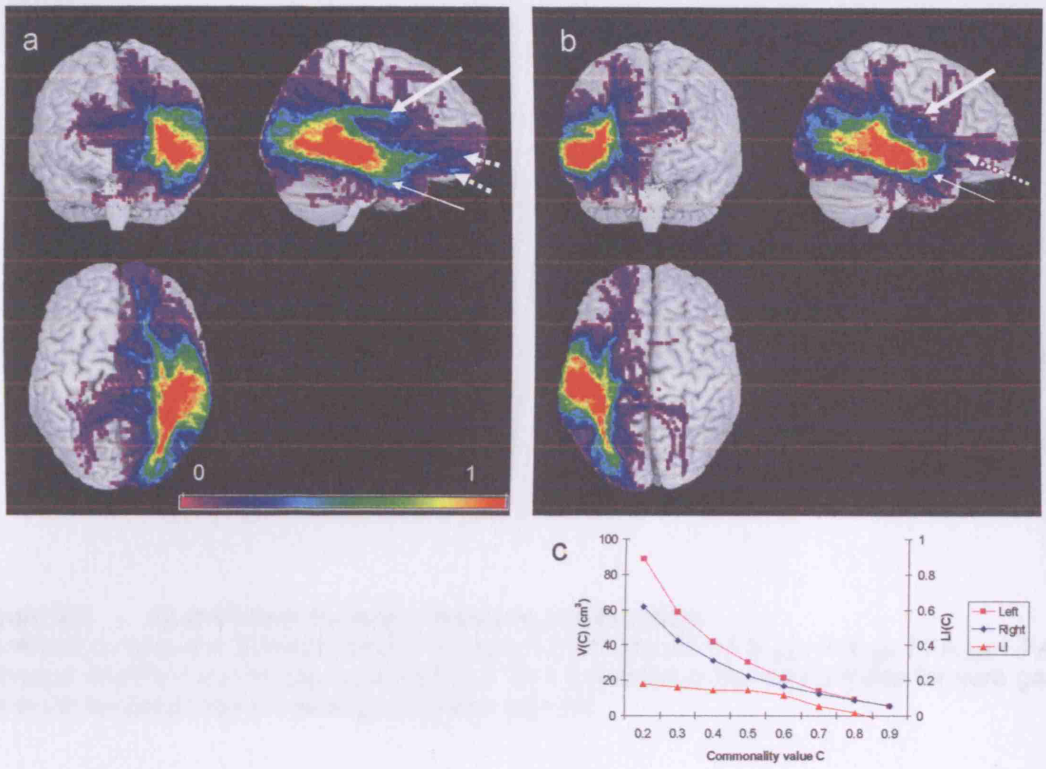

Figure 8.4 Temporal lobe connections
Group variability maps of the connections from the left (a) and right (b) superior temporal ROIs. Consistent bilateral connections were seen to the superior and middle temporal gyri, extending anteriorly into the temporal lobe (thin arrows). Greater fronto-temporal connections were seen on the left than on the right, both via the superior longitudinal fasciculus (thick arrows) and via the inferior fronto-occipital and uncinate fasciculi (dotted arrows). Posterior connections to the extra-striate visual cortex were relatively symmetrical. Figure 8.4c shows connecting volume V(C) and asymmetry index AI(C) as a function of commonality value C.

8.4.4 Correlations between structure and function

There was a significant correlation between the degree of lateralisation of mean FA and lateralisation of fMRI activation for verb generation in the frontal lobes (Pearson's correlation coefficient=0.782; *P*=0.008, Figure 8.5a) and for reading comprehension in the temporal lobes (Pearson's correlation coefficient=0.651; *P*=0.042, Figure 8.5b), characterised by greater structural lateralisation in subjects with greater functional lateralisation. No significant correlation was seen between tract volumes and functional activation.

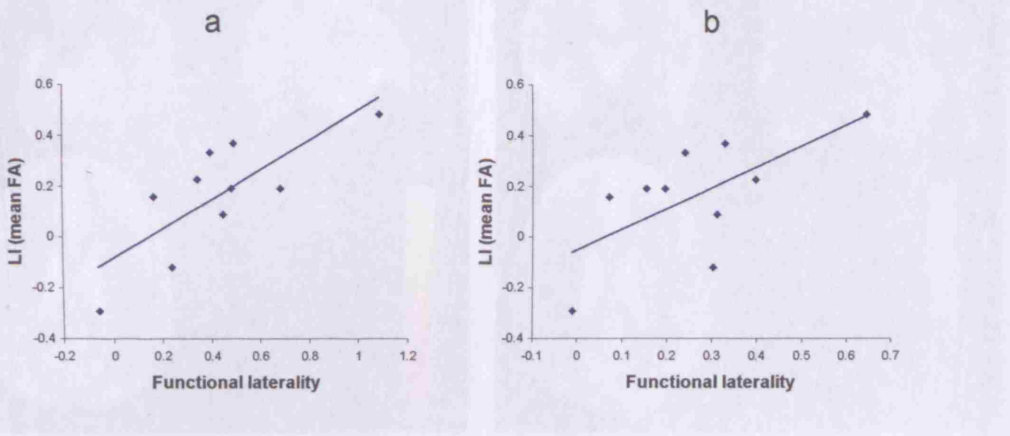

Figure 8.5 Correlations between structure and function
Significant correlations between mean FA asymmetry index ($AI = FA_{left} - FA_{right} / FA_{left} + FA_{right}$) of the pathways identified and functional laterality of fMRI activation in the frontal lobes for verb generation (a) and in the temporal lobe for reading comprehension (b).

8.4.5 Regression analysis

Correlations between the mean FA of the left frontal connections and voxelwise fMRI activity for verbal fluency were most significant in the left supramarginal gyrus (Figure 8.6a). For reading comprehension activation within a region in the left IFG was significantly correlated with mean FA of the left temporal connections (Figure 8.6b).

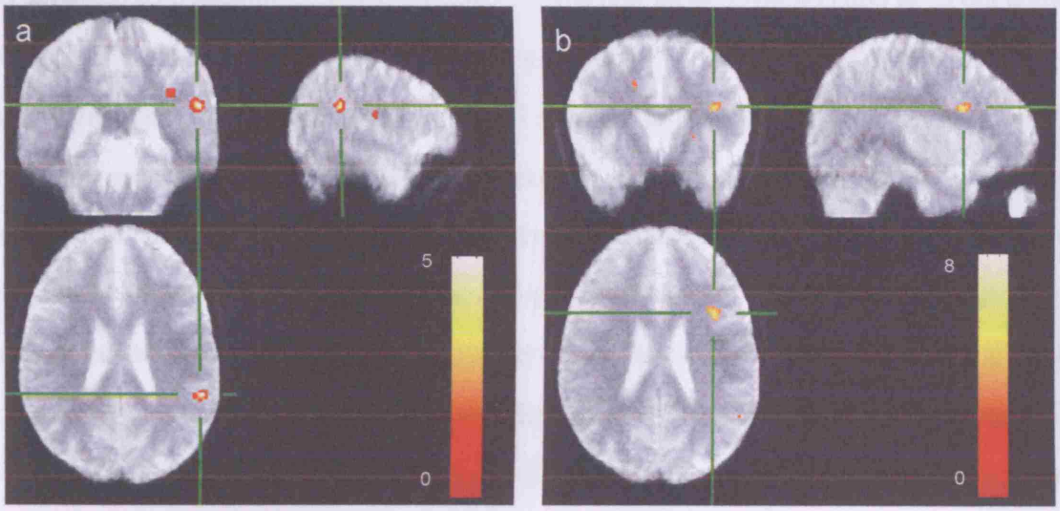

Figure 8.6 Regression analyses
Regression analysis between fMRI contrasts for verbal fluency (a) and reading comprehension (b) and the mean FA of the left frontal ROI connections. For verbal fluency, a significant correlation was seen in the left supramarginal gyrus and for reading in the left IFG.

8.5 DISCUSSION

In this chapter, we used MR-tractography to demonstrate the structural connections of the cortical regions activated by expressive and receptive language tasks. A direct connection, corresponding to the SLF, was traced bilaterally between the inferior frontal and posterior temporal lobes but visual inspection showed there was a clear structural asymmetry with greater connectivity in the left hemisphere than the right. This asymmetry was most striking in the pattern of connectivity from the inferior frontal ROIs with more extensive connections to the temporal lobe on the left. Similarly, when tracking was initiated in the temporal lobes, greater connectivity to frontal regions was seen on the left. This structural asymmetry, namely greater fronto-temporal connectivity on the left, reflects the left-sided lateralisation of language function in the human brain.

We also demonstrated a significant correlation between the structural lateralisation of the identified pathways and the left-right difference in functional activation in both frontal and temporal lobes, with subjects with more highly lateralised language function having a more lateralised pattern of connections.

This suggests a possible relationship between brain structure and function and is, to our knowledge, the first such demonstration in the human language system.

Tracking the connectivity of white matter regions adjacent to Broca and Wernicke's areas, and their right hemisphere homologues, also revealed connections not considered specifically related to language function. In addition to the asymmetry seen in the language-specific pathways, stronger fronto-temporal connections via the inferior fronto-occipital and uncinate fasciculi were seen on the left. Experimental studies in monkeys have shown a monosynaptic route of connection between frontal and temporal lobes via the uncinate fasciculus (316) therefore this increased connectivity may also reflect the greater functional role played by the left inferior frontal lobe. Connections were also seen to the supramarginal gyrus, again being more prominent on the left.

More symmetrical connections were seen extending from the temporal lobe ROIs to the anterior temporal lobe and posteriorly to the occipital lobe. Studies have suggested that the superior temporal sulcus is a multisensory area important for integrating auditory and visual information (365-367) and electrophysiological studies have shown individual neurons in monkey STS that respond to both auditory and to visual stimuli (368). It is therefore interesting that seed points in this region demonstrate extensive connections to visual and auditory cortex, along with other connections to frontal and parietal language areas. These connections may represent a structural framework for multimodal convergence of sensory information at a multisensory region.

A feature of human language processing is the ability of written and spoken words to access the same semantic meaning. The connections demonstrated here provide an anatomical substrate upon which this may occur, and correspond to the ventral processing streams from primary sensory areas converging in anterior temporal and inferior frontal regions, as described by Marinkovic et al (369).

We also found quantitative differences between left and right hemispheres, with the overall tract volumes being significantly higher on the left than the right. Examination of tract volumes as a function of commonality showed that the degree of left-lateralisation was higher for the tracts derived from the frontal lobe ROIs than for the tracts derived from the temporal lobe ROIs and that this was higher in areas of higher commonality. Further, the mean FA of the estimated tracts derived from the frontal ROIs was also

significantly higher on the left than the right. These results corresponded to the pattern of functional activation which was highly lateralised in the frontal lobes but more bilateral in the temporal lobes.

As the PICo probability threshold is increased the volume of the connections decreases and the mean FA increases. This occurs as the core pathways are increasingly identified. Low voxel anisotropy implies higher uncertainty in fibre orientation within that voxel therefore probabilistic tracking through such regions may become dispersed, implying a larger apparent connected volume. Importantly however at any chosen probability threshold the tract volume will be lower for the tract with lower anisotropy, explaining the differences seen between left and right hemispheres, with both volumes and mean FA being greater on the left.

8.5.1 Defining starting regions

One other recent study has used tractography to investigate the lateralisation of language pathways, also demonstrating stronger connections in the left hemisphere (280). They used anatomical guidelines to define Broca's and Wernicke's areas as ROIs for initiating fibre tracking and constrained their analysis to only identify pathways passing through both regions. The ROIs used were significantly larger in size in the left hemisphere due to the known hemispheric anatomical differences in the frontal and temporal lobes (282-286). This difference in size of starting ROIs could possibly affect the volumes and extent of the connections obtained, although there was no correlation between the ROI volumes and the resulting volumes of connecting tracts.

Our approach provides a number of benefits over the two-ROI method for identifying regions involved in language function. Firstly the observer bias inherent in manual ROI definition is reduced by using fMRI-derived tracking start ROIs. Secondly, by using mirror image ROIs of identical volume in the non-dominant hemisphere the possibility of ROI-induced tract volume errors is reduced, although it could be argued that erroneous placement of the mirror image ROIs (for example in an inappropriate gyrus) could lead to incomplete tract localisation. Thirdly, the use of probabilistic tracking from single ROIs for each functional localisation in each individual allows the possibility of identification of patterns of connectivity without imposing strong prior user knowledge. Lastly, the use of specific functional paradigms allows the

identification of pathways associated with cortical regions involved in mediating specific tasks, rather than those associated with classically-identified language-related regions.

In order to minimise operator bias in seed point selection and to ensure consistency in our method we used the group activation peak, rather than each individual subject's own activation peak. We realise that this may reduce our sensitivity in identifying subtle differences in connection patterns between individuals but concluded that it was the most robust and reliable method for detecting group level differences between the left and right hemispheres.

By using functionally-defined ROIs we aimed to make our method as operator-independent as possible, however the use of fMRI to define starting points for tractography is not without problems, in particular with regard to the precise co-registration of fMRI and DTI. The steps of normalisation to standard space (to obtain the group activation maps) and subsequent reverse normalisation to native space, along with the differences in susceptibility and other artefacts between fMRI and DTI images are potential sources of error when co-registering the two modalities. By defining relatively large ROIs (each consisted of 125 voxels) we tried to limit the effect of small registration errors. Spatial smoothing of the fMRI scans (performed to improve signal-to-noise, and better meet the assumptions of Gaussian field theory) leads to blurring of activations across neighbouring voxels, leading to activations which include both grey and white matter. While this may initially appear problematic, one consequence is that it provided a relatively unbiased choice of white matter voxels for tractography seeding, avoiding both the complexity of trying to track deep within grey matter (where most tractography algorithms fail) and the necessity to manually define the white matter voxels expected to subserve a particular grey matter area.

The lateralisation of language function inevitably leads to problems in the identification of the right hemisphere homologues to Broca's and Wernicke's areas. Our solution was to manually define right hemisphere ROIs of identical size in areas homotopic to the functionally defined regions. The aim again was to minimise operator bias, although we recognise the limitations of this approach given that structurally homotopic regions do not necessarily correspond functionally. One recent study has indeed demonstrated that right frontal activation on tasks of verbal fluency was not homologous to that seen in the left frontal lobe and that in a group of patients with left TLE the right frontal activation shifted in location (208). For the superior temporal gyrus however we had areas of fMRI activation from the reading

comprehension paradigm in both left and right hemispheres which we used for defining left and right sided ROIs. Tracking from these regions was therefore free from operator bias, and using these bilateral functionally-defined regions we still demonstrated a left-right asymmetry in the fronto-temporal connections seen. We therefore feel that this strengthens our findings for the frontal lobe connections.

Another difference between our method and that described in the previous study (280) was the use of a single starting region and a more sensitive probabilistic tractography technique. Using a single ROI for each tracking experiment imposed fewer *a priori* constraints on the results. It may be the case that some pathways which play a role in certain aspects of language processing do not directly connect Broca and Wernicke's areas (for example the connections between Wernicke's area and visual and auditory cortex) and therefore would not be seen when the results are constrained by using two ROIs. The two region approach reduced the likelihood of false positive pathways but had the disadvantage of potential bias due to the *a priori* assumption that connections between the two sites do actually exist. As a result, clear prominence is given to apparent connections between these sites, thus ignoring other potentially interesting connections. The probabilistic algorithm adapts the commonly used streamline approach to exploit the uncertainty in one or more fibre orientations defined for each voxel. The use of a probabilistic method provides a measure of confidence, in terms of the model of diffusion employed, to the connections seen. The use of the multi-tensor model allows tracking through regions exhibiting fibre crossings such as those affecting the SLF (145). To the best of our knowledge this is the first application of probabilistic fibre tracking using crossing fibre information.

Despite numerous differences in the methods used for establishing start points for tractography and those used for fibre tracking our results are broadly similar to those of Parker et al who also demonstrated larger volume of connections, particularly to the temporal lobe, on the left than the right (280). This reinforces the conclusion that this does represent a genuine biological difference between left and right hemispheres. In addition we investigated anatomical connectivity to language-related regions defined in the superior temporal gyrus and observed a lesser degree of lateralisation (Figure 8.4). This suggests that the lateralisation observed in the connections of Broca's and Wernicke's areas is not just an artefact of general left-sided tract dominance (284).

8.5.2 Structural asymmetries in the human brain

Left-right asymmetries have been previously demonstrated, both anatomically and using neuroimaging. Asymmetries have been noted both in Heschl's gyrus (359) and the planum temporale (360;361). Differences in white matter tract volumes have been demonstrated in histological studies of the optic radiations (265) and pyramidal tracts (370) with larger volumes in the left hemisphere seen in right handed subjects.

A volumetric MRI study has demonstrated white matter asymmetry with increased white matter volumes in left frontal and temporal lobes (285) and post-mortem volume measurements have shown greater white matter content in the left posterior superior temporal lobe (371). Voxel-based morphometry has demonstrated grey matter asymmetries in posterior language regions, but not in anterior language regions (372) and a leftward asymmetry in white matter volume adjacent to Heschl's gyrus and the planum temporale (284). One recent study used voxel-based statistics on fractional anisotropy (FA) maps derived from DTI to show an asymmetry in the SLF, with greater FA values on the left (373).

At a microscopic level asymmetries have been demonstrated in the extent of the cytoarchitectonic area Tpt (temporoparietal cortex) (362) and in the columnar and connectional structure of neuronal networks in language cortex (374). Taken together, these studies suggest that asymmetries in cerebral structure may reflect asymmetries in brain function. These asymmetries have been shown to be present in white matter and also in regions known to be important for language function. Our study, however, is the first to demonstrate specific asymmetries in particular tracts connecting functionally active regions.

8.5.3 Functional networks of language regions

Catani et al used tractography to study perisylvian language networks in the left hemisphere (281). In addition to the direct pathway connecting Broca and Wernicke's areas they used a two-ROI approach to demonstrate a second, indirect pathway passing through the inferior parietal cortex. This ran laterally to the direct pathway and was composed of an anterior segment connecting Broca's area with the inferior parietal lobe and a posterior segment connecting the inferior parietal lobe to Wernicke's area and the authors argued that the existence of this second pathway helped to explain the diverse clinical spectrum of aphasic disconnection syndromes. This was an area that had also been shown to have connections to

both Broca's and Wernicke's areas by Parker et al (280). Our findings are in keeping with these as we demonstrate a connection to the supramarginal gyrus (Brodmann area 40) in the inferior parietal lobe, a region implicated in a number of language-related tasks (375;376). The single ROI approach does not allow us to distinguish whether this is a separate and discrete pathway from the other fronto-temporal connections demonstrated.

Electrophysiological evidence also supports our current findings. In patients undergoing invasive monitoring with subdural electrodes for epilepsy surgery, stimulation of the anterior language area elicited 'cortico-cortical evoked potentials' (CCEPs) in the middle and posterior parts of the superior and middle temporal gyri as well as the supramarginal gyrus (377). Stimulation of the posterior temporal area produced CCEPs in the anterior language area, suggesting a bidirectional connection between Broca's and Wernicke's areas. The pattern of connections revealed in this study provides an anatomical substrate for this functional connectivity.

8.5.4 Structure-function relationships

We demonstrated a significant correlation between the lateralisation of mean FA of the identified pathways and the left-right difference in functional activation. This correlation was seen for both frontal lobe activation during verb generation, and for temporal lobe activation during reading comprehension. This suggests a difference in pathways between subjects that reflects their degree of functional asymmetry and demonstrates an interesting relationship between structure and function.

A previous study has combined functional MRI and DTI with tractography to study structure-function relationships in the visual system (279). It used photic stimulation to induce visual cortex activity and PICo to track the optic radiations from a seed point near the lateral geniculate body of the thalamus. The mean FA of the optic radiations correlated significantly with fMRI parameter estimates (a measure of functional activity), although, as in our study, no correlation was demonstrated for tract volumes.

The regression analysis identified regions where the mean FA of the tracts correlated with voxelwise fMRI activity. The correlation in the left frontal lobe was demonstrated during the reading paradigm and that in the supramarginal gyrus during the verbal fluency paradigm. These were distant to the main areas of

activation although still in language related regions, supporting the existence of widespread networks involved in language function.

8.6 CONCLUSION

In conclusion, we have combined functional MRI language tasks and probabilistic tractography to study the pattern of language related pathways in right-handed healthy control subjects. We demonstrated an asymmetry in the pattern of connectivity with greater connections between frontal and temporal lobes on the left, reflecting the lateralisation of language function. The findings described here are from a group of strongly right-handed subjects and it will be important to compare these results with those from left-handed subjects including some with atypical language dominance. Further developments including improved methods of co-registering fMRI and DTI images and quantification of tractography output will improve the delineation of language related pathways, and comparison with studies of functional connectivity will enable a better understanding of language networks and the effect of diseases upon them.

CHAPTER IX LANGUAGE FUNCTION IN PATIENTS: DIFFUSE ABNORMALITIES OF LANGUAGE NETWORKS IN TEMPORAL LOBE EPILEPSY

The previous chapter used a combination of fMRI and tractography to demonstrate the structure of the white matter tracts connecting functionally-defined language regions in healthy controls. In this chapter we use the same technique in a group of patients with TLE and unilateral HS to study the effects of hippocampal pathology on language structure and function. The material in this chapter has been published in; Powell HWR et al. *Abnormalities of language networks in temporal lobe epilepsy.* **Neuroimage** 2007;36:209-21.

9.1 OBJECTIVE

fMRI in patients with TLE has demonstrated re-organisation of language functions with greater involvement of the non-dominant hemisphere. The structural brain connections supporting this atypical language dominance have not previously been identified. The previous chapter demonstrated a structural asymmetry in control subjects with more extensive connections from language regions in the language-dominant hemisphere. In this study we extend this to look for evidence of changes in language pathways in patients with TLE and unilateral HS and test the hypothesis that in left TLE patients the language connections would reflect the pattern of functional activation, with reduced ipsilateral and increased contralateral connections.

9.2 INTRODUCTION

TLE may be associated with disrupted lateralisation and localisation of language. fMRI studies have demonstrated a higher incidence of atypical language dominance in preoperative left TLE patients (172;184), suggesting that dominant hemisphere lesions can lead to functional reorganisation of language to contralateral cortical regions. The recruitment of right hemisphere regions not activated in control subjects was involved in maintaining reading skills in patients following left ATLR (207). Verbal fluency fMRI tasks show relative shifts in activation to the right hemisphere in patients with left temporal lobe seizures (169;172;174;208), probably due to epileptic activity affecting normal left hemisphere language

organization (183). Greater right hemisphere reorganisation has been demonstrated for receptive, temporal lobe language functions than for productive, frontal lobe language functions (184).

A number of factors may influence this atypical language activation. Language function may be affected by subtle abnormalities remote from the hippocampus. Evidence from a number of imaging modalities including quantitative MRI and MR volumetry (289;290), MR-spectroscopy (292), voxel based morphometry (293) and positron emission tomography (83) suggests the existence of more widespread abnormalities in TLE associated with HS than demonstrated by conventional MRI. The strong connectivity between the inferior frontal and medial temporal lobes may make frontal lobe functions particularly sensitive to MTL pathology (378), while electrophysiological disruption of extratemporal regions may lead to cognitive impairments, in particular on tests of executive function (379). Knowing whether any structural changes existed within the white matter pathways involved in language function in TLE patients would be clinically useful as well as providing important insights into the mechanisms underlying functional plasticity within cerebral networks.

9.3 METHODS

9.3.1 Subjects

We studied 14 patients (median age 35.5; range 25-47 years; 7 female) with medically refractory TLE undergoing pre-surgical evaluation at the National Hospital for Neurology and Neurosurgery, London, UK. Structural MRI at 1.5T showed unilateral left HS in 7 patients and right HS in 7 on qualitative and quantitative criteria (72). Video-EEG had confirmed seizures arising from the ipsilateral medial temporal lobe in all 14. Post-operative histology confirmed HS in all cases. All patients were on anti-epileptic medication and all were fluent English speakers. Patients' details are given in table 9.1.

9.3.2 MR data acquisition

MRI acquisition for both fMRI and tractography was performed according to our common protocol (refer to sections 2.3.1 and 2.4.1). Diffusion tensor imaging and analysis was performed according to the previously described protocol (refer to section 2.4.2).

9.3.3 Language fMRI tasks

Verb generation and reading comprehension tasks were used in this study as described in the common methodology section 2.3.2.2.

9.3.4 Data analysis and seed point ROI definition

The fMRI data analysis is described in the common methodology chapter. The pre-processing steps are described in section 2.3.3, and the blocked analysis in section 2.3.3.2. Maps of the main effect of each task across all subjects (controls and patients combined) were generated, thresholded at $p<0.001$ (uncorrected) and transformed into each individual's native space. These reverse-normalised group maps were then used to define ROIs for initiating probabilistic fibre tracking. A total of four ROIs were defined for each subject, one each in the left and right IFG and left and right superior temporal gyri (STG), by drawing over selected areas of fMRI activation (see results for details) on consecutive brain slices, using MRIcro (http://www.psychology.nottingham.ac.uk). Each ROI was of identical volume, comprising 125 voxels.

9.3.5 Tractography method

We used the PICo tractography algorithm, extended to cope with the presence of crossing fibres, as described in the common methodology section 2.4.3.2. Each output connectivity map was spatially normalised and based on the previous chapter's results, binary masks at a threshold connection probability of 0.05 were constructed. These were averaged across the group, to produce variability (or commonality) maps indicating the degree of spatial variability and overlap of the identified connections (280). Normalised tract volumes were calculated for the left and right tracts of every subject (279) and paired *T*-tests were used to compare these within groups. Unpaired *T*-tests were used to compare the patient and control groups and repeated measures ANOVA was used to test for interactions between group and hemisphere. The mean FA of the connected volume in native space was calculated as described in section 8.3.7. We used a paired *T*-test to compare left and right-sided mean FA within each group. Unpaired *T*-tests were used to compare the patient and control groups and repeated measures ANOVA was used to test for interactions between group and hemisphere.

9.3.5 Correlations between structure and function

We tested for correlations between the lateralisation of fMRI activation and of the lateralisation of the derived connections. For the fMRI we defined 10mm radius spheres based on the peak activations in the left frontal and bilateral temporal lobes, along with a homotopic volume in the right frontal lobe, and calculated left minus right activation for each subject. For the tractography we calculated AIs to assess lateralisation of mean FA between hemispheres;

$$AI = (\text{Mean FA}_{left} - \text{Mean FA}_{right}) / (\text{Mean FA}_{left} + \text{Mean FA}_{right})$$

We calculated the Spearman correlation coefficient to test for correlations between the two values.

9.4 RESULTS

9.4.1 fMRI results

Verb generation was associated with activation in the left IFG in all three groups, with activation in the right IFG in the left TLE group only (Table 9.2). Reading comprehension was associated with activation in bilateral STG, adjacent to the superior temporal sulci, in both controls and right TLE patients but left TLE patients showed only an area of subthreshold activation in the posterior left temporal lobe. Frontal lobe AIs for verb generation were significantly more left lateralised in controls and right TLE patients than left TLE patients (F=9.530, P=0.001) (Figure 9.1). There was no significant difference in temporal lobe AIs between the three groups for reading comprehension (F=1.092, P=0.35) (Figure 9.1). Four ROIs were defined for initiating fibre tracking. One was placed in the left IFG and corresponded to the peak IFG activation seen for verb generation. As no significant activation was seen in this region on the right, a homotopic ROI of identical size was manually defined using MRIcro. Two further ROIs corresponded to the areas of bilateral STG activation seen (Figure 9.1) during the reading comprehension task.

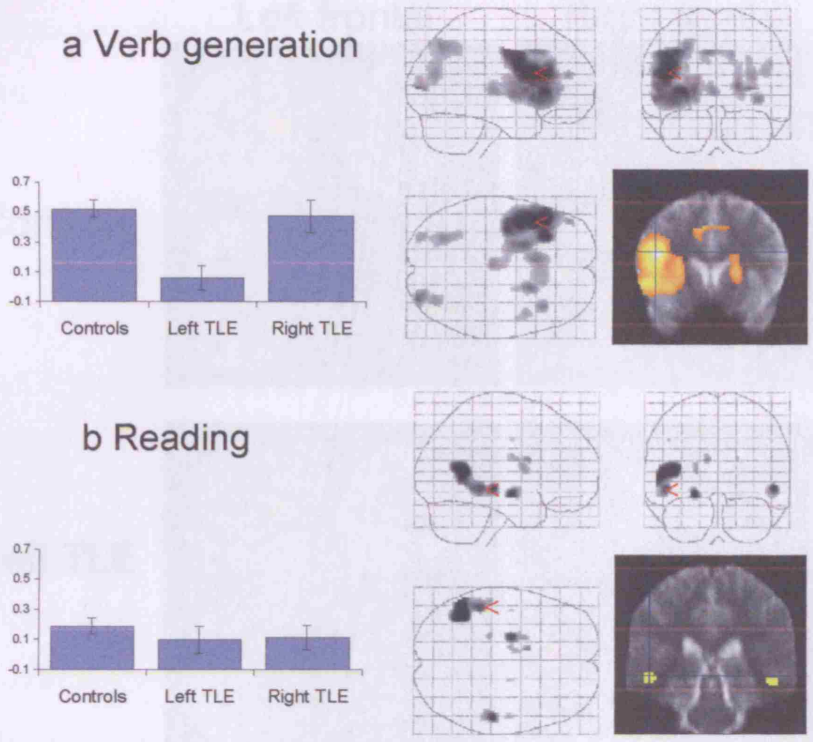

Figure 9.1 fMRI results
Glass brain representation of the main fMRI effects in the three groups combined for verb generation (a) and reading comprehension (b). The regions of activation shown in the coronal slices were used to define ROIs for initiating fibre tracking. The bar graphs demonstrate the AIs (+/- SE) for each group separately for frontal lobe (a) and temporal lobe (b) activation. An AI of 1 would indicate a fully left lateralised pattern of activation while an AI of -1 would indicate a fully right lateralised pattern of activation. The AIs for verb generation were significantly more left lateralised in controls and right TLE patients than left TLE patients (P=0.001).

9.4.2 Tractography results

9.4.2.1 IFG connections

The group variability maps for the volumes of connection from the frontal lobe ROIs are shown in figure 9.2. As reported previously in the control group greater connections (particularly fronto-temporal connections via the SLF) were seen in the left hemisphere than the right. Both connection volumes (left 48.5cm^3, right 41cm^3; P<0.05) and mean FA (left 0.317, right 0.308; P<0.05) were greater on the left than the right.

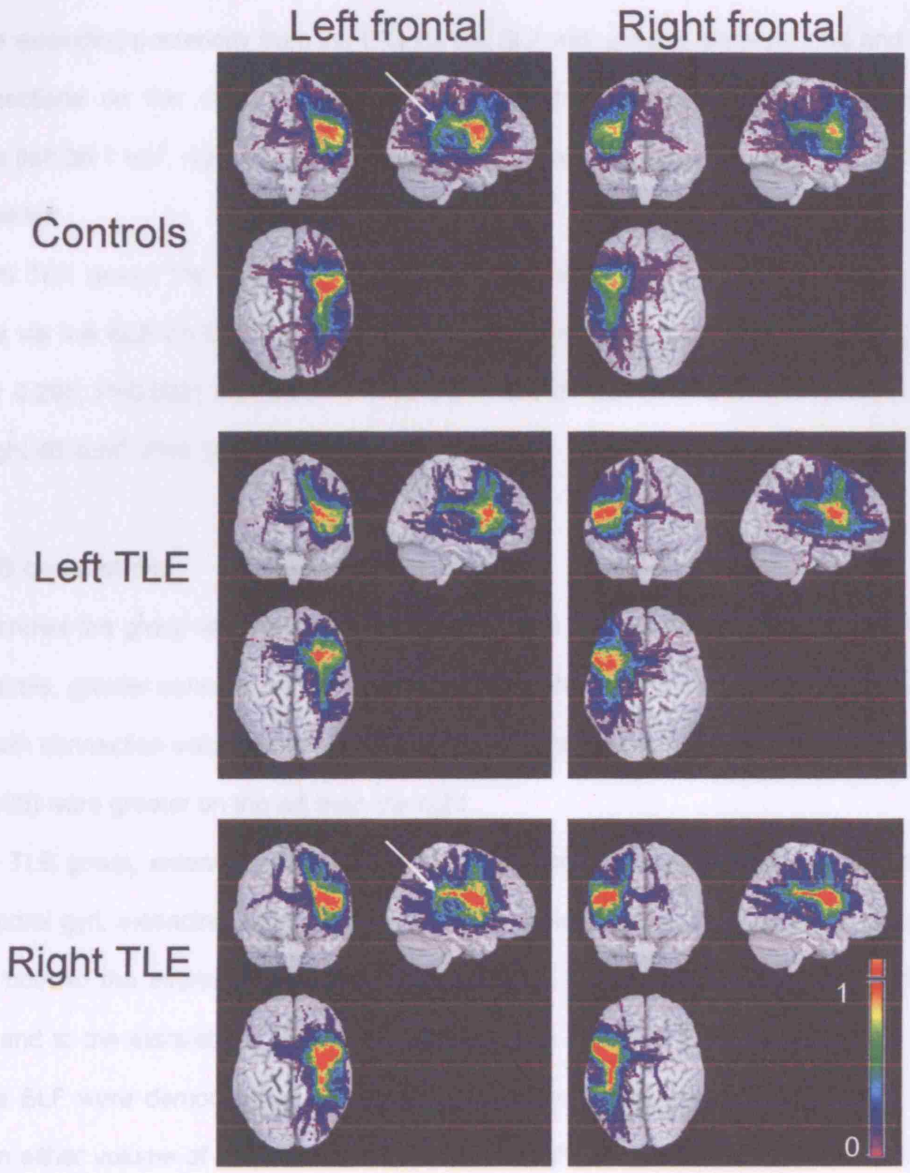

Figure 9.2 Frontal lobe connections
Group variability maps (at a probability threshold of 0.05) of the connecting paths tracked from the left and right frontal ROIs for each of the 3 groups. Each image shows the maximum intensity of the commonality maps in each plane of view as a brain surface rendering. The colour scale indicates the degree of overlap among subjects (expressed as commonality value); for example, a value of 1 (pure red) represents 100% subject overlap (i.e. every subject's identified tract contains the voxel in question). Controls and right TLE patients show a similar pattern of connections with greater SLF connections to the temporal lobe on the left (arrowed) than the right. In the left TLE group the opposite pattern is seen with greater temporal lobe connections on the right.

For the left TLE group, visual assessment of the pattern of connections demonstrated consistent bilateral connections extending posteriorly from the IFG via the SLF with greater temporal lobe and supramarginal gyrus connections on the right than on the left. Paired *T*-tests revealed both greater volume of connections (left 36.1 cm^3, right 44.9cm^3; *P*=0.018) and mean FA (left 0.301, right 0.316; *P*=0.05) on the right than the left.

For the right TLE group, the pattern of connections is similar to controls, with greater fronto-temporal connections via the SLF on the left than the right. Mean FA was greater on the left than the right (left 0.307, right 0.295; *P*=0.032) but there was no significant difference in the volume of connections (left 46.6cm^3, right 40.4cm^3; *P*=0.15).

9.4.2.2 STG connections

Figure 9.3 shows the group variability maps for the volumes of connection from the temporal lobe ROIs. For the controls, greater connections were seen in the left hemisphere than the right, in particular along the SLF. Both connection volumes (left 44.8cm^3, right 32.3cm^3; *P*<0.001) and mean FA (left 0.313, right 0.303; *P*=0.05) were greater on the left than the right.

For the left TLE group, extensive and consistent connections were seen bilaterally to the superior and middle temporal gyri, extending anteriorly into the temporal lobe. More extensive right-sided connections were seen both to the inferior frontal lobe via the inferior fronto-occipital fasciculus and the uncinate fasciculus, and to the extra-striate visual cortex (Brodmann area 19). Connections to the inferior frontal lobe via the SLF were demonstrated on the left but not on the right. Overall there was no significant difference in either volume of connections (left 41.8cm^3, right 40.2cm^3; *P*=0.77) or mean FA (left 0.290, right 0.297; *P*=0.48) between left and right hemispheres.

For the right TLE group most connections were relatively symmetrical, although greater connections along the SLF were demonstrated on the left. The volume of connections was greater on the left than the right (left 57.4cm^3, right 43.6cm^3; *P*=0.006) but there was no significant difference in mean FA (left 0.305, right 0.294; *P*=0.12).

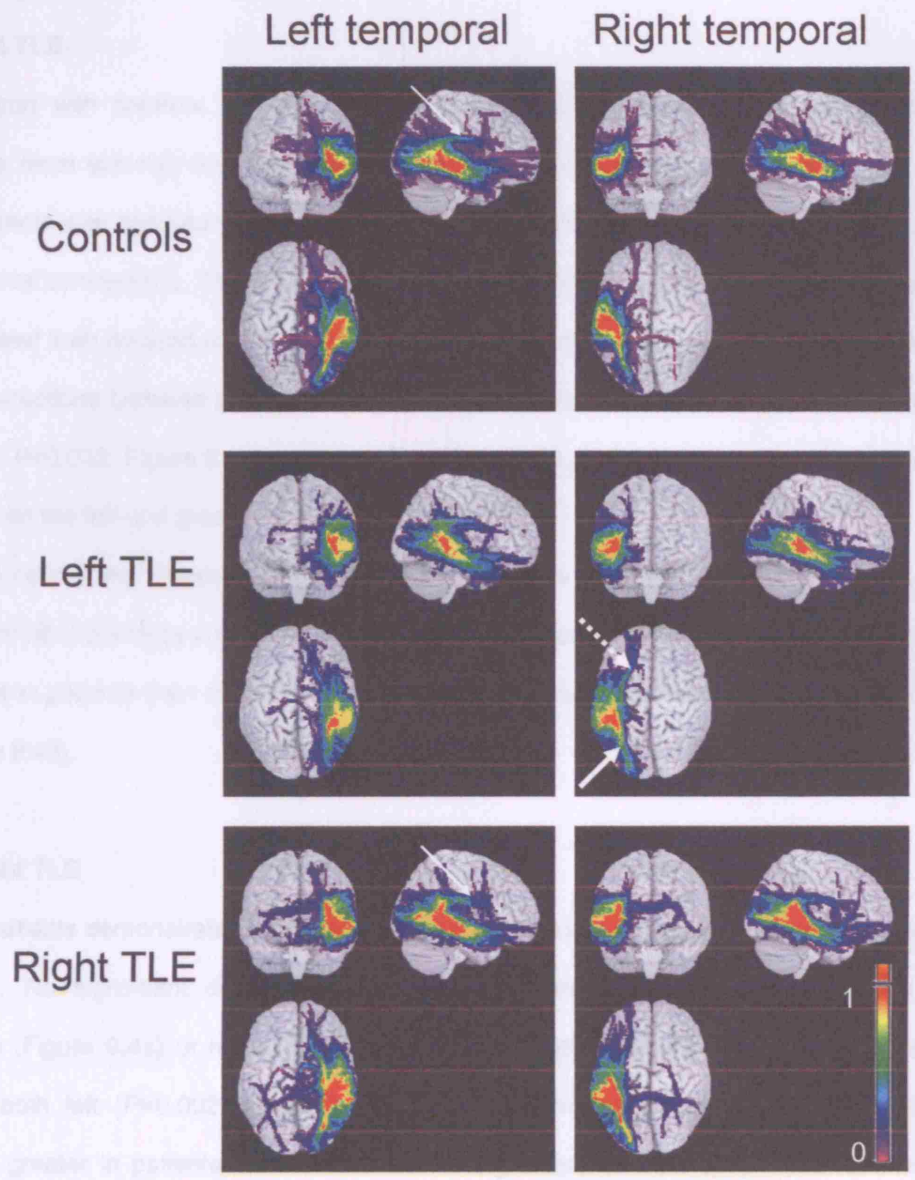

Figure 9.3 Temporal lobe connections
Group variability maps of the connecting paths tracked from the left and right temporal ROIs for each of the 3 groups. Controls and right TLE patients show a similar pattern of connections with more substantial SLF connections to the frontal lobe on the left (arrowed) than the right, and relatively symmetrical occipital lobe connections. In the left TLE group more extensive right-sided connections to the inferior frontal lobe via the inferior fronto-occipital fasciculus and the uncinate fasciculus (dotted arrow), and to the extra-striate visual cortex (thick arrow). Consistent bilateral connections were seen to the superior and middle temporal gyri, extending anteriorly into the temporal lobe, in all three groups.

9.4.3 Comparison with controls

9.4.3.1 Left TLE

In comparison with controls, left TLE patients demonstrated less left-sided and greater right-sided connections, most strikingly from the frontal lobe ROIs (Figure 9.2). The overall connecting volume of the left frontal tracts was significantly less than controls (P=0.006) but there was no significant difference in the right frontal connections. There was a trend for the patients' mean FA to be lower than controls on the left and greater than controls on the right although neither of these differences was significant. Significant two-way interactions between group and hemisphere were demonstrated for both volume of connections ($F_{[1,6]}$= 7.76, P=0.032; Figure 9.4a) and mean FA ($F_{[1,6]}$= 14.6, P=0.009; Figure 9.4b) with left TLE patients being lower on the left and greater on the right than controls.

The overall connecting volume of the right temporal tracts was significantly greater in patients than controls (P=0.031) but there was no significant difference in left temporal connections (Figure 9.4c). Mean FA was less in patients than controls on the left (P=0.036) but there was no significant difference on the right (Figure 9.4d).

9.4.3.2 Right TLE

Right TLE patients demonstrated a similar pattern of results to controls with greater connections in the left hemisphere. No significant differences from controls were observed in either frontal volumes or connections (Figure 9.4a) or mean FA (Figure 9.4b). For temporal connections the overall connecting volume of both left (P=0.002; Figure 9.4c) and right (P=0.033; Figure 9.4c) temporal tracts were significantly greater in patients than in controls No significant differences in mean FA were observed between patients and controls (Figure 9.4d).

9.4.3.3 Comparison of Left and Right TLE groups

For the frontal lobe connections right TLE patients demonstrated a significantly lower mean FA on the right than left TLE patients (P=0.042). There were significant two-way interactions between group and hemisphere for both volume of connections ($F_{[1,6]}$= 16.23, P=0.007; Figure 9.4a) and mean FA ($F_{[1,6]}$= 21.79, P=0.003; Figure 9.4b) with left TLE patients being lower on the left and greater on the right. The

overall connecting volume of the left temporal tracts was significantly less in left than right TLE patients (P=0.018) but there was no significant difference for the right temporal connections (Figure 9.4c). No significant differences were observed between the two patient groups in mean FA (Figure 9.4d).

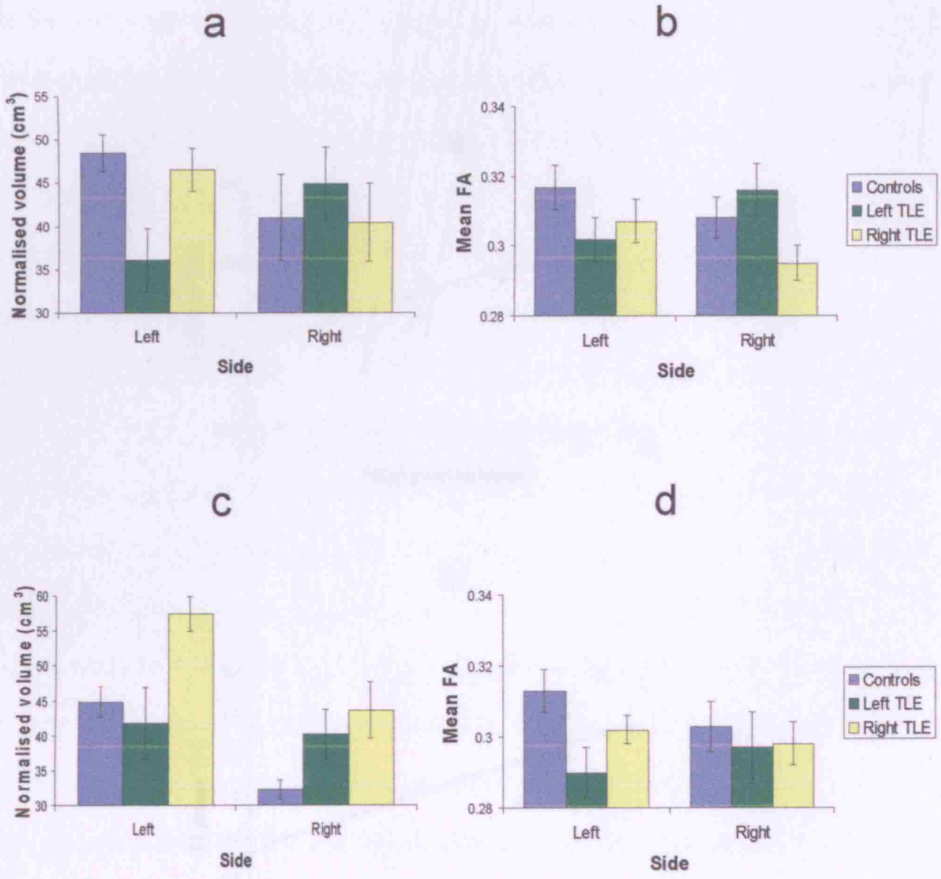

Figure 9.4 Comparison of patients and controls
a) Comparison of normalized tract volumes (NV) (+/- SE) between controls, left and right TLE patients for frontal lobe connections.
b) Comparison of mean FA (+/- SE) between controls, right TLE and left TLE patients for frontal lobe connections.
c) Comparison of NV between controls, left and right TLE patients for temporal lobe connections.
d) Comparison of mean FA between controls, left and right TLE patients for temporal lobe connections.
For the frontal lobe connections, significant two-way interactions between group and hemisphere are seen for both NV and FA characterised by left TLE patients having lower values on the left and greater values on the right, compared with both controls and right TLE patients.

9.4.4 Correlations between structure and function

Significant correlations were seen between lateralisation of mean FA, and functional lateralisation in the frontal lobes in left TLE patients (Spearman coefficient=0.857; *P*=0.014, Figure 9.5a), and in the temporal lobes in right TLE patients (Spearman coefficient=0.786; *P*=0.036, Figure 9.5b). These were characterised by greater structural lateralisation in subjects with greater functional lateralisation.

a

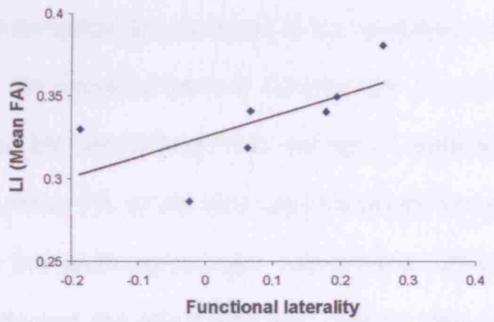

b

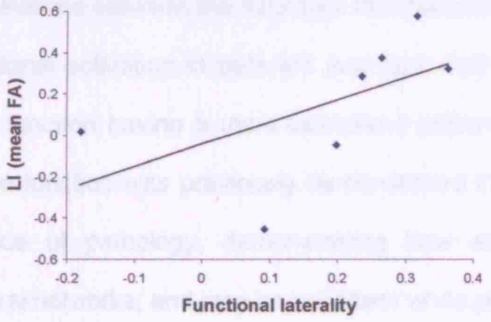

Figure 9.5 Correlations between structure and function
Significant correlations between mean FA asymmetry index (AI = $FA_{left} - FA_{right} / FA_{left} + FA_{right}$) of the pathways identified and functional laterality of fMRI activation in the frontal lobes for verb generation in left TLE patients (a), and in the temporal lobe for reading comprehension in right TLE patients (b).

9.5 DISCUSSION

9.5.1 Summary of results

We found evidence for structural re-organisation of white matter tracts underlying altered language lateralisation in patients with unilateral TLE. In patients with left TLE there were reduced left hemisphere language connections compared to both controls and right TLE patients. This was evident both on visual inspection of the pathways delineated, and quantitatively by comparing the volume and mean FA of the tracts. In contrast, in the right hemisphere there were greater connections in left TLE patients than both controls and right TLE patients. This suggests a reduction in structural connections in the pathological left hemisphere and a possible compensatory increase in the unaffected right hemisphere.

For the right TLE patients the overall pattern of connectivity was similar to controls with greater fronto-temporal connections in the left hemisphere than the right. Quantitatively the only significant difference from controls was greater mean FA of the left sided temporal connections. This suggests a degree of reorganisation away from the pathological right hemisphere, although given that the non-language-dominant hemisphere is affected, the effect was less marked than in left TLE patients. In summary left TLE had less left sided and greater right sided connections than controls and right TLE patients had greater left sided connections than controls.

We also demonstrated correlations between the structural lateralisation of the identified pathways and the left-right difference in functional activation in both left and right TLE patients, with subjects with more highly lateralised language function having a more lateralised pattern of connections. This relationship between brain structure and function was previously demonstrated in controls. It is interesting that it is maintained in the presence of pathology, demonstrating how structural reorganisation underpins functional plasticity in cerebral networks, and may be important when planning ATLR.

The pattern of reorganisation reflects the fMRI results. Although all subjects were right handed functional activation for the expressive language task was more left lateralised in controls and right TLE than left TLE patients in whom overall activation was more bilateral. A number of studies have shown that left TLE patients have a more symmetrical, less lateralised pattern of language activation than controls and right TLE patients (172;183;184;208). The degree of reorganisation of white matter tracts demonstrated in this

study is more pronounced than the fMRI and provides hard evidence for altered structural connectivity associated with functional reorganisation.

9.5.2 Comparison with previous findings

A few studies have used tractography to look at the white matter pathways underlying language function in control subjects, demonstrating a left lateralised pattern of connections, reflecting the functional dominance of the left hemisphere (280;380). Our study reports these connections in a patient population and differs from work of other groups in that we use fMRI to define functionally active regions to use as start points for fibre tracking, specifically probing the neuronal networks connecting cortical regions subserving particular functions.

One previous tractography study in TLE and unilateral HS, showed bilateral symmetrical abnormalities and FA reduction of the fornix and cingulum, suggesting that HS is associated with bilateral limbic system pathology not revealed on conventional neuroimaging (294). Given the direct connections between the hippocampus and these structures, the authors speculated that this may reflect downstream axonal Wallerian degeneration (381). A more likely explanation for our findings is that structural reorganisation occurs along with functional plasticity secondary to a pathological process affecting the temporal lobe early in life. In patients with left HS this functional reorganisation could lead to reduced left hemisphere activation and an increased role for the right hemisphere in language function which in turn could affect the neuronal architecture underlying language functions. The effect is similar to that observed in people with early blindness, in whom tractography of the optic radiations has revealed reduced thalamocortical connections compared to normal controls (382), and suggests that the status of the structural components of cerebral networks may be critical in understanding the overall changes in function.

9.5.3 Limitations of the study

The lateralisation of language function inevitably leads to problems in the identification of the right hemisphere homologues to Broca's and Wernicke's areas. Our solution in the frontal lobes was to manually define right hemisphere ROIs of identical size in areas homotopic to the functionally defined regions. The aim was to minimise operator bias, although we recognise the limitations of this approach

given that structurally homotopic regions do not necessarily correspond functionally. One recent study has indeed demonstrated that right frontal activation on tasks of verbal fluency was not homologous to that seen in the left frontal lobe and that in a group of patients with left temporal lobe epilepsy the right frontal activation shifted in location (208). For the superior temporal gyrus however we had areas of fMRI activation from the reading comprehension paradigm in both left and right hemispheres which we used for defining left and right sided ROIs.

9.5.4 Clinical implications

Both the quantitative measures used, namely tract volume and mean FA, reflect the underlying structural organisation of the pathways in question. FA is a measure of intravoxel fibre coherence and has been shown to be reduced in a number of diseases including multiple sclerosis (383) and epilepsy (384), reflecting axonal degeneration (294) or loss of myelination. The lower values of tract volume and FA seen in the non-dominant hemisphere of healthy subjects, and in the patients' pathological hemisphere, are consistent with a reduction in the number and the coherence of axons within the white matter pathways, indicating a reduction in structural organisation relative to the dominant and undamaged hemispheres.

Selective language deficits have been reported following language dominant ATLR in patients with medically refractory TLE. In one study, nearly 40% of patients demonstrated a significant postoperative decline on a standard neuropsychological naming test (201). Our results suggest that tractography, in combination with fMRI, may be able to predict and minimise such post-operative language deficits.

9.6 CONCLUSION

In summary, we provide in-vivo evidence for structural reorganisation of white matter tracts that reflects the altered functional language lateralisation in patients with left TLE. Structural connections of language areas were right-lateralised, whilst the pattern of functional activation was more symmetrical. The combination of fMRI and tractography offers a promising tool for studying the reorganisation of language functions in many neurological conditions and may prove useful in predicting language deficits following temporal lobe surgery. Tractography also has broader applications to delineate the structural basis of cerebral connectivity and how it is affected by disease.

Table 9.1 Patient clinical and demographic data

M = male; F = female; CPS = complex partial seizure; SGTC = secondary generalised tonic-clonic seizure; HS = hippocampal sclerosis; MTL = medial temporal lobe; EEG = electroencephalogram; TLE = temporal lobe epilepsy; VIQ = verbal intelligence quotient; PIQ = performance intelligence quotient; HV = hippocampal volume; AED = antiepileptic drug; TPR = topiramate; LTG = lamotrigine; VPA = sodium valproate; CBZ = carbamazepine; LVT = levetiracetam; PMD = primidone; CLB = clobazam; OXC = oxcarbazepine; GBP = gabapentin; PHT = phenytoin; TGB = tiagabine.

Age /gender	Handedness	Epilepsy onset (years)	Seizure types and frequency (per month)	MRI and pathological diagnosis	Clinical and EEG	VIQ	PIQ	Verbal recall	Figure recall	Right HV (cm3)	Left HV (cm3)	Hippocamp volume rat (%)
25/F	Right	17	CPS 8 SGTC 0.5	Left HS	Left TLE	82	80	46	60	2.729	1.351	
37/M	Left	1	SPS 12 CPS 4	Left HS	Left TLE	94	93	23	49	3.3	1.88	
33/M	Right	1	SPS 4 CPS 4	Left HS	Left TLE	86	88	46	91	2.83	2.02	
32/F	Right	22	SPS 30 CPS 5 SGTC 0.25	Left HS	Left TLE	88	111	27	40	2.359	1.789	
28/M	Right	3	CPS 1	Left HS	Left TLE	76	81	18	10	3.077	1.417	
34/M	Right	21	CPS 5	Left HS	Left TLE	67	76	3	8	2.235	1.896	
37/F	Right	1	SPS 12 CPS 8 SGTC 1	Left HS, left fusiform gyrus ganglioglioma	Left TLE	70	94	16	69	2.8	2.385	
47/M	Right	13	CPS 1	Right HS	Right TLE	73	86	36	18	1.038	2.769	
44/F	Right	14	CPS 4	Right HS	Right TLE	95	104	64	80	2.606	3.034	
44/M	Right	10	CPS 4	Right HS	Right TLE	117	118	63	58	2.775	3.047	
46/F	Right	8	CPS 5	Right HS	Right TLE	88	84	60	13	1.756	2.695	
32/F	Right	19	CPS 2	Right HS	Right TLE	87	110	80	66	2.299	2.562	
29/M	Right	9	CPS 30 SGTC 4	Right HS	Right TLE	93	114	88	84	2.273	2.978	
41/F	Right	14	CPS 4	Right HS	Right TLE	90	88	75	47	1.628	2.302	

Table 9.2 Activation peaks for all fMRI effects of interest
For each effect, the MNI coordinate, Z score and anatomical location are given.

Group	Contrast	MNI coordinates	Z-score	Region
Controls	Verb generation	-44 2 24	5.56*	Left inferior frontal gyrus
		-40 20 0	5.52*	Left inferior frontal gyrus
	Reading comprehension	-44 -56 12	4.99*	Left posterior superior temporal gyrus
		-52 -26 -6	4.63	Left superior temporal gyrus
		48 -26 -4	3.53	Right superior temporal gyrus
Right TLE	Verb generation	-42 14 22	5.09*	Left inferior frontal gyrus
	Reading comprehension	-46 28 -2	5.04*	Left inferior frontal gyrus
		-52 -52 6	4.90	Left superior temporal gyrus
		-56 -30 -12	4.04	Left superior temporal gyrus
		54 -28 -12	3.60	Right superior temporal gyrus
Left TLE	Verb generation	-40 10 12	4.60	Left inferior frontal gyrus
		38 6 18	3.18	Right inferior frontal gyrus
	Reading comprehension	-62 -46 -2	2.78**	Left superior temporal gyrus

* P<0.05 corrected for multiple comparisons ** Sub-threshold activation only

CHAPTER X OVERALL CONCLUSIONS

10.1 INTRODUCTION

This thesis aimed to apply the imaging techniques of functional MRI and MR-tractography to study brain structure and function of language, memory and vision in patients with TLE. Tractography was used to identify the connections of the MTL in healthy control subjects, and in the presurgical mapping of the optic radiation. We developed a paradigm for studying the normal pattern of memory encoding function in control subjects, which could be applied to TLE patients in order to study the effects of a localised lesion, and ultimately surgical resection on memory. Finally we combined both these techniques to study the relationship between brain structure and function in the language system. Tractography was used to delineate the white matter pathways underlying functional language regions in control subjects, and to investigate the effects of pathology upon these connections.

10.2 SUMMARY OF THE MAIN FINDINGS

- In control subjects, white matter connections were demonstrated between the anterior PHG and anterior temporal lobe, orbitofrontal cortex, posterior temporal and extrastriate occipital areas. Direct connections between hippocampus and parahippocampal gyrus were also visualised.

- The disruption of the anterior extent of Meyer's Loop of the optic radiation was demonstrated in a patient who suffered a VFD following ATLR and who had a Meyer's loop that projected far anteriorly and inferiorly. A more anterior and inferior extent of Meyer's Loop appears to be associated with a greater risk of VFD following ATLR.

- In controls, memory encoding in the MTL was lateralised according to the material being encoded, with word encoding taking place on the left, face encoding on the right and picture encoding bilaterally.

- A further functional dissociation was demonstrated in controls between anterior and posterior hippocampus. The main effects of memory encoding, demonstrated specifically using an event-related analysis, were seen in the anterior hippocampus, with the main effects of viewing stimuli, demonstrated using a blocked analysis, being located in more posterior regions.

- In patients with unilateral HS, a reorganisation of memory function was seen, with less left MTL and greater right MTL activation in the left TLE patients and less right MTL and greater left MTL activation in the right TLE patients compared with controls.

- In both left and right TLE patients, memory function was better when it was sustained by activation within the damaged hippocampus. Conversely, greater activation in the contralateral hippocampus was associated with worse memory performance suggesting that reorganisation to the opposite side was an inefficient process, incapable of preserving memory function at the same level.

- In both left and right TLE patients a positive correlation was demonstrated between hippocampal volume and hippocampal fMRI activation.

- Individual patients with relatively greater ipsilateral compared to contralateral MTL activation had greater memory decline following ATLR. This was the case for both verbal memory decline following dominant ATLR and for non-verbal memory decline following non-dominant ATLR. For dominant hemisphere resections, activation within the ipsilateral hippocampus alone was predictive of postoperative memory change with greater hippocampal activation for word encoding being correlated with greater verbal memory decline following surgery. Hippocampal fMRI activation was of greater value in predicting postoperative memory decline than either baseline memory test performance or hippocampal volume.

- In control subjects, asymmetries (both qualitative and quantitative) of the structural connections of cortical regions involved in language functions were demonstrated, with greater fronto-temporal connections in the left hemisphere than the right, reflecting the lateralisation of language function.

- In TLE patients, a structural re-organisation (both qualitative and quantitative) of white matter tracts underlying language function was demonstrated, with reduced left hemisphere and greater right hemisphere connections in patients with left TLE compared to both controls and right TLE patients. Right TLE patients had a similar pattern of results to controls. This structural reorganisation reflected the altered functional lateralisation seen in left TLE patients.

- Significant correlations were demonstrated between structure and function in controls and patients, with subjects with more highly lateralised language function having a more lateralised pattern of connections.

10.3 NEUROBIOLOGICAL AND CLINICAL IMPLICATIONS

The role of surgery for patients with medically refractory TLE is increasingly important with ATLR leading to seizure freedom in at least 60% of patients. As a result, surgery is now being carried out earlier, in a larger number of centers, and in those with less severe epilepsy (99). The presurgical evaluation of these patients aims to maximise the chances of achieving seizure freedom while minimising any unwanted post-operative complications. Among the more common complications of ATLR are deficits in material-specific memory and language, along with visual field defects. Baseline neuropsychometry is used to assess preoperative language and memory function and plays a role in the prediction of post-operative outcome; however its value in predicting specific deficits in individual patients is limited. The IAT is used in some centers to establish language dominance and to identify the risk of post-operative amnesia but is an expensive, invasive procedure. The establishment of non-invasive imaging techniques that provide additional information for predicting postoperative deficits in individual patients would therefore be welcome.

Mapping the connections of the MTL provided results in keeping with evidence from invasive studies in animals, currently the gold standard method of studying brain connectivity. The connections demonstrated, to frontal and occipital lobes and to the cerebellum, along with direct hippocampal-parahippocampal connections, may play an important role, both in normal memory function, and in seizure propagation in patients with medial temporal lobe epilepsy. We anticipate that knowing the extent of these connections in patients undergoing ATLR may be useful for predicting both seizure outcome and memory change following surgery, with patients with stronger connections at greater risk of memory decline.

Currently there is no accurate method of predicting which patients are most at risk of VFDs following ATLR, due to the variability in the anterior extent of the optic radiation from person to person and the lack of any techniques for visualising this structure. Our case reports suggest that using tractography preoperatively to map the anterior and inferior extent of Meyer's Loop will allow a more accurate prediction of which patients will suffer VFD.

An important issue when designing paradigms for patients with neurological deficits is to use tasks that they are able to perform. A differential pattern of activation between patients and normal subjects is only interpretable if patients are performing the task adequately (212). We developed an event-related memory encoding paradigm capable of testing verbal and non-verbal memory in both controls and TLE patients in a single scanning session. Our image acquisition parameters were optimised to medial temporal responses by selecting thin slices and choosing a field of view covering only the temporal lobes and centred on the body of the hippocampus. We were therefore able to demonstrate encoding-related activation in the anterior hippocampus, something a number of previous fMRI memory studies had failed to do. This anterior localisation of memory encoding, along with the material-specific lateralisation, were in keeping with evidence from lesion-deficit models, and help explain the memory changes typically observed following ATLR.

Current predictors of greater verbal memory decline following dominant ATLR are preoperative memory performance and hippocampal volume, with better performance and larger volume predicting worse decline. Our findings in patients with unilateral TLE, that memory function in unilateral TLE is better when it is sustained by activation within the damaged (to-be-resected) hippocampus, along with the

correlation between hippocampal volume and hippocampal fMRI activation are consistent with, and help to explain these observations. Our findings in a small group of patients that fMRI activation using our paradigm had predictive value above and beyond that provided by baseline neuropsychometry and hippocampal volume suggests a role in the future preoperative assessment of these patients.

Finally we combined both techniques to study the white matter pathways underlying functional language regions. We observed a structural asymmetry in control subjects that reflected the normal pattern of language lateralisation in right-handed subjects. Patients with right HS had a similar, left-lateralised, pattern of functional activation and structural connections to controls and patients with left HS had a more symmetrical pattern of activation and structural connections. The pattern of structural connections therefore reflected the functional activation both across the three groups and at an individual subject level, with subjects with more highly lateralised language function having a more lateralised pattern of connections.

This provides an insight into possible mechanisms underlying neuronal plasticity following a known neurological insult early in life (i.e. the development of hippocampal sclerosis). One possibility is that a functional reorganisation takes place that in turn leads to a structural reorganisation, or an alteration of development; alternatively more widespread structural changes occur following the occurrence of HS, some of which may involve language regions, and that these serve as an anatomical substrate upon which the atypical language function develops. Tracking pathways involved in language pathways may also play an additional role in the prediction of language deficits following ATLR, with subjects with stronger temporal lobe connections being at higher risk of postoperative decline.

10.4 LIMITATIONS OF THE STUDIES

All studies in this thesis contain relatively small numbers of patients. This was primarily due to the decommissioning of the 1.5T GE scanner and installation of a new 3T-MRI scanner half-way through the duration of the PhD. Much of the work involved development and implementation of new techniques and for the memory fMRI studies our findings extend previous work in the group (244;257) in an independent sample group, increasing our confidence in the findings. Nevertheless our groups were too small to study the influence of other factors, such as age of onset and duration of epilepsy, effects of

AEDs and seizure frequency, on patterns of brain structure and function. It is likely that some or all of these contribute to the degree of lateralisation of both the functional activation and of the connections seen, and larger sized groups will be necessary to test this.

A criticism of MTL fMRI is that partial volume effects may contribute to the findings. A sclerotic hippocampus will contain fewer voxels capable of demonstrating a BOLD effect. Given the small number of subjects in this study it is maybe no surprise that we did not see any correlations between hippocampal volume and memory change following ATLR. Nevertheless fMRI was of greater predictive value than hippocampal volume in this sample and indicates that fMRI activation is not merely an indirect marker of hippocampal atrophy.

For the memory fMRI studies we focused on reorganisation within MTL structures. It is however possible that reorganisation may take place to other neocortical regions both within and outside the temporal lobes, with plasticity leading to new networks capable of sustaining memory encoding. In order to obtain optimal imaging of the temporal lobes we confined our coverage to this region of the brain and so were unable to assess the degree of extra-temporal reorganisation that may have occurred in these patients.

Most of the studies in this thesis involved relatively homogenous groups of patients, usually those with unilateral HS. While homogenous samples of patients are necessary to draw conclusions about group-level changes, if these techniques are to be adopted as routine presurgical investigations their value over existing investigations will need to be proven in patients with the other pathologies encountered in an epilepsy surgical programme.

10.5 FUTURE WORK

Clinically it is what happens to individual patients that is important and the next step in the validation of these techniques will involve similar studies with larger numbers of patients. These should include more heterogeneous samples, including both left and right TLE undergoing ATLR. As well as showing group level correlations either at the voxel-level or within a predefined ROI, it will be important to establish methods for using this data to predict language and memory changes in individual cases. Functional changes occurring after surgery are of great interest and longitudinal fMRI studies with pre- and post-

operative imaging, including correlations with neuropsychological measures of language and memory, will be required to study these. Work is in progress to address these issues.

Similarly for tractography, larger prospective studies are required to map the course of the OR in patients undergoing ATLR. If our preliminary results are substantiated, it is hoped that this information may be used preoperatively to inform the neurosurgeon of the anterior extent of the OR, allowing more accurate prediction of which patients will suffer VFDs. This in turn will allow better preoperative counselling and possibly modification of the surgical procedure to minimise the risk.

Both fMRI and tractography are fast-moving fields of research. Methodological developments occur continuously with improvements in both hardware and software. In particular, it is hoped that the combination of imaging at higher magnetic fields and the use of parallel imaging techniques will lead to improved signal-to-noise with reduced signal dropout and distortion in the MTL. This should make it easier to demonstrate meaningful hippocampal activation at an individual level during memory encoding fMRI experiments. A number of technical developments will increase the sensitivity of fibre-tracking techniques, including different methods of resolving areas of crossing fibres, and improved quantification of results, including the use of probabilistic tracking techniques. Improved methods of co-registering fMRI and tractography will allow these techniques to be combined more easily and accurately, improving the study of the structural connections of functional regions. Finally, further work is required to improve the registration of fMRI EPI data with T1-weighted anatomical data to enable accurate alignment of the two modalities and improve the anatomical localisation of functional regions.

Our study of language structure and function provided some insights about neuronal plasticity following brain injury. Longitudinal studies of fMRI and tractography, correlating structural and functional changes with behavioural and neuropsychological measures will be of great interest in studying changes in networks involved in language and memory function following surgery. It would also be highly informative to study early changes in structure and function following the initial occurrence of hippocampal sclerosis, in order to establish the age these changes take place and the order in which they occur. These types of studies however will be complicated by the age of the participants.

BIBLIOGRAPHY

1. MacDonald BK, Cockerell OC, Sander JW, Shorvon SD. The incidence and lifetime prevalence of neurological disorders in a prospective community-based study in the UK. Brain 2000;123 (Pt 4):665-76.

2. Sander JW, Shorvon SD. Epidemiology of the epilepsies. J.Neurol.Neurosurg.Psychiatry 1996;61(5):433-43.

3. Sander J.W. The incidence and prevalence of epilepsy. In: Sander J.W., Walker M.C., Smalls J.E., editors. Epilepsy 2005. From neuron to NICE - A Practical Guide. 2005. p. 1-7.

4. Proposal for revised clinical and electroencephalographic classification of epileptic seizures. From the Commission on Classification and Terminology of the International League Against Epilepsy. Epilepsia 1981;22(4):489-501.

5. World Health Organisation: Dictionary of Epilepsy. Geneva: WHO; 1973.

6. Proposal for revised classification of epilepsies and epileptic syndromes. Commission on Classification and Terminology of the International League Against Epilepsy. Epilepsia 1989;30(4):389-99.

7. Engel J, Jr. A proposed diagnostic scheme for people with epileptic seizures and with epilepsy: report of the ILAE Task Force on Classification and Terminology. Epilepsia 2001;42(6):796-803.

8. Sotelo J, Guerrero V, Rubio F. Neurocysticercosis: a new classification based on active and inactive forms. A study of 753 cases. Arch.Intern.Med. 1985;145(3):442-5.

9. Sander JW, Hart YM, Johnson AL, Shorvon SD. National General Practice Study of Epilepsy: newly diagnosed epileptic seizures in a general population. Lancet 1990;336(8726):1267-71.

10. Robinson RA, Gardiner RM. Molecular genetics of the epilepsies. In: Sander J.W., Walker M.C., Smalls J.E., editors. Epilepsy 2005: From Neuron to NICE - A Practical Guide. 2005. p. 55-72.

11. Kullmann DM. The neuronal channelopathies. Brain 2002;125(Pt 6):1177-95.

12. Ottman R, Annegers JF, Risch N, Hauser WA, Susser M. Relations of genetic and environmental factors in the etiology of epilepsy. Ann.Neurol. 1996;39(4):442-9.

13. Berkovic SF, Howell RA, Hay DA, Hopper JL. Epilepsies in twins: genetics of the major epilepsy syndromes. Ann.Neurol. 1998;43(4):435-45.

14. Duvernoy HM. Structure, Functions and Connections. The Human Hippocampus. Second Edition ed. Springer; 1998. p. 5-39.

15. Engel J, Jr. Surgery for seizures. N.Engl.J.Med. 1996;334(10):647-52.

16. Quigg M, Bertram EH, Jackson T. Longitudinal distribution of hippocampal atrophy in mesial temporal lobe epilepsy. Epilepsy Res. 1997;27(2):101-10.

17. Briellmann RS, Jackson GD, Mitchell LA, Fitt GJ, Kim SE, Berkovic SF. Occurrence of hippocampal sclerosis: is one hemisphere or gender more vulnerable? Epilepsia 1999;40(12):1816-20.

18. Mathern GW, Babb TL, Leite JP, Pretorius K, Yeoman KM, Kuhlman PA. The pathogenic and progressive features of chronic human hippocampal epilepsy. Epilepsy Res. 1996;26(1):151-61.

19. Wieser HG. ILAE Commission Report. Mesial temporal lobe epilepsy with hippocampal sclerosis. Epilepsia 2004;45(6):695-714.

20. Thom M. Neuopathology of epilepsy. In: Sander J.W., Walker M.C., Smalls J.E., editors. Epilepsy 2005: From Neuron to NICE - A Practical Guide. 2005. p. 21-54.

21. Armstrong DD. The neuropathology of temporal lobe epilepsy. J.Neuropathol.Exp.Neurol. 1993;52(5):433-43.

22. Houser CR. Granule cell dispersion in the dentate gyrus of humans with temporal lobe epilepsy. Brain Res. 1990;535(2):195-204.

23. Houser CR, Swartz BE, Walsh GO, Delgado-Escueta AV. Granule cell disorganization in the dentate gyrus: possible alterations of neuronal migration in human temporal lobe epilepsy. Epilepsy Res.Suppl 1992;9:41-8.

24. Harding B, Thom M. Bilateral hippocampal granule cell dispersion: autopsy study of 3 infants. Neuropathol.Appl.Neurobiol. 2001;27(3):245-51.

25. Lurton D, el Bahh B, Sundstrom L, Rougier A. Granule cell dispersion is correlated with early epileptic events in human temporal lobe epilepsy. J.Neurol.Sci. 1998;154(2):133-6.

26. Thom M, Sisodiya SM, Beckett A, Martinian L, Lin WR, Harkness W et al. Cytoarchitectural abnormalities in hippocampal sclerosis. J.Neuropathol.Exp.Neurol. 2002;61(6):510-9.

27. Parent JM, Tada E, Fike JR, Lowenstein DH. Inhibition of dentate granule cell neurogenesis with brain irradiation does not prevent seizure-induced mossy fiber synaptic reorganization in the rat. J.Neurosci. 1999;19(11):4508-19.

28. Eriksson PS, Perfilieva E, Bjork-Eriksson T, Alborn AM, Nordborg C, Peterson DA et al. Neurogenesis in the adult human hippocampus. Nat.Med. 1998;4(11):1313-7.

29. Roy NS, Wang S, Jiang L, Kang J, Benraiss A, Harrison-Restelli C et al. In vitro neurogenesis by progenitor cells isolated from the adult human hippocampus. Nat.Med. 2000;6(3):271-7.

30. Sutula T, Cascino G, Cavazos J, Parada I, Ramirez L. Mossy fiber synaptic reorganization in the epileptic human temporal lobe. Ann.Neurol. 1989;26(3):321-30.

31. Longo BM, Mello LE. Effect of long-term spontaneous recurrent seizures or reinduction of status epilepticus on the development of supragranular mossy fiber sprouting. Epilepsy Res. 1999;36(2-3):233-41.

32. Falconer Ma, Serafetinides Ea, Corsellis Ja. Etiology And Pathogenesis Of Temporal Lobe Epilepsy. Arch.Neurol. 1964;10:233-48.

33. Mathern GW, Babb TL, Vickrey BG, Melendez M, Pretorius JK. The clinical-pathogenic mechanisms of hippocampal neuron loss and surgical outcomes in temporal lobe epilepsy. Brain 1995;118 (Pt 1):105-18.

34. Davies KG, Hermann BP, Dohan FC, Jr., Foley KT, Bush AJ, Wyler AR. Relationship of hippocampal sclerosis to duration and age of onset of epilepsy, and childhood febrile seizures in temporal lobectomy patients. Epilepsy Res. 1996;24(2):119-26.

35. Fernandez G, Effenberger O, Vinz B, Steinlein O, Elger CE, Dohring W et al. Hippocampal malformation as a cause of familial febrile convulsions and subsequent hippocampal sclerosis. Neurology 1998;50(4):909-17.

36. Baulac M, De Grissac N, Hasboun D, Oppenheim C, Adam C, Arzimanoglou A et al. Hippocampal developmental changes in patients with partial epilepsy: magnetic resonance imaging and clinical aspects. Ann.Neurol. 1998;44(2):223-33.

37. Hardiman O, Burke T, Phillips J, Murphy S, O'Moore B, Staunton H et al. Microdysgenesis in resected temporal neocortex: incidence and clinical significance in focal epilepsy. Neurology 1988;38(7):1041-7.

38. Li LM, Fish DR, Sisodiya SM, Shorvon SD, Alsanjari N, Stevens JM. High resolution magnetic resonance imaging in adults with partial or secondary generalised epilepsy attending a tertiary referral unit. J.Neurol.Neurosurg.Psychiatry 1995;59(4):384-7.

39. Raymond AA, Halpin SF, Alsanjari N, Cook MJ, Kitchen ND, Fish DR et al. Dysembryoplastic neuroepithelial tumor. Features in 16 patients. Brain 1994;117 (Pt 3):461-75.

40. Duncan JS, Sagar HJ. Seizure characteristics, pathology, and outcome after temporal lobectomy. Neurology 1987;37(3):405-9.

41. Duncan JS. Temporal lobe epilepsy. In: Sander J.W., Walker M.C., Smalls J.E., editors. Epilepsy 2005: From Neuron to NICE - A Practical Guide. 2005. p. 147-51.

42. Geyer JD, Payne TA, Faught E, Drury I. Postictal nose-rubbing in the diagnosis, lateralization, and localization of seizures. Neurology 1999;52(4):743-5.

43. Squire LR, Zola-Morgan S. The medial temporal lobe memory system. Science 1991;253(5026):1380-6.

44. Frisk V, Milner B. The role of the left hippocampal region in the acquisition and retention of story content. Neuropsychologia 1990;28(4):349-59.

45. Smith ML, Milner B. The role of the right hippocampus in the recall of spatial location. Neuropsychologia 1981;19(6):781-93.

46. Hermann BP, Seidenberg M, Schoenfeld J, Davies K. Neuropsychological characteristics of the syndrome of mesial temporal lobe epilepsy. Arch.Neurol. 1997;54(4):369-76.

47. Gleissner U, Helmstaedter C, Elger CE. Right hippocampal contribution to visual memory: a presurgical and postsurgical study in patients with temporal lobe epilepsy. J.Neurol.Neurosurg.Psychiatry 1998;65(5):665-9.

48. Bohbot VD, Allen JJ, Nadel L. Memory deficits characterized by patterns of lesions to the hippocampus and parahippocampal cortex. Ann.N.Y.Acad.Sci. 2000;911:355-68.

49. Elger CE, Helmstaedter C, Kurthen M. Chronic epilepsy and cognition. Lancet Neurol. 2004;3(11):663-72.

50. Aikia M, Salmenpera T, Partanen K, Kalviainen R. Verbal Memory in Newly Diagnosed Patients and Patients with Chronic Left Temporal Lobe Epilepsy. Epilepsy Behav. 2001;2(1):20-7.

51. Lespinet V, Bresson C, N'Kaoua B, Rougier A, Claverie B. Effect of age of onset of temporal lobe epilepsy on the severity and the nature of preoperative memory deficits. Neuropsychologia 2002;40(9):1591-600.

52. Helmstaedter C, Kurthen M, Lux S, Reuber M, Elger CE. Chronic epilepsy and cognition: a longitudinal study in temporal lobe epilepsy. Ann.Neurol. 2003;54(4):425-32.

53. Thompson PJ, Duncan JS. Cognitive decline in severe intractable epilepsy. Epilepsia 2005;46(11):1780-7.

54. Kanner AM, Nieto JC. Depressive disorders in epilepsy. Neurology 1999;53(5 Suppl 2):S26-S32.

55. Kanner AM, Stagno S, Kotagal P, Morris HH. Postictal psychiatric events during prolonged video-electroencephalographic monitoring studies. Arch.Neurol. 1996;53(3):258-63.

56. Logsdail SJ, Toone BK. Post-ictal psychoses. A clinical and phenomenological description. Br.J.Psychiatry 1988;152:246-52.

57. Robertson MM, Trimble MR, Townsend HR. Phenomenology of depression in epilepsy. Epilepsia 1987;28(4):364-72.

58. Blumer D. Dysphoric disorders and paroxysmal affects: recognition and treatment of epilepsy-related psychiatric disorders. Harv.Rev.Psychiatry 2000;8(1):8-17.

59. Onuma T, Adachi N, Ishida S, Katou M, Uesugi S. Prevalence and annual incidence of psychosis in patients with epilepsy. Psychiatry Clin.Neurosci. 1995;49(3):S267-S268.

60. Sherwin I. Psychosis associated with epilepsy: significance of the laterality of the epileptogenic lesion. J.Neurol.Neurosurg.Psychiatry 1981;44(1):83-5.

61. Shorvon SD. The Routine EEG. In: Dam M, Gram L, editors. Comprehensive Epileptology. New York: Raven Press; 1990. p. 321-38.

62. Duncan JS. Imaging and epilepsy. Brain 1997;120 (Pt 2):339-77.

63. Jackson GD, Berkovic SF, Tress BM, Kalnins RM, Fabinyi GC, Bladin PF. Hippocampal sclerosis can be reliably detected by magnetic resonance imaging. Neurology 1990;40(12):1869-75.

64. von Oertzen J, Urbach H, Blumcke I, Reuber M, Traber F, Peveling T et al. Time-efficient T2 relaxometry of the entire hippocampus is feasible in temporal lobe epilepsy. Neurology 2002;58(2):257-64.

65. Berkovic SF, Andermann F, Olivier A, Ethier R, Melanson D, Robitaille Y et al. Hippocampal sclerosis in temporal lobe epilepsy demonstrated by magnetic resonance imaging. Ann.Neurol. 1991;29(2):175-82.

66. von Oertzen J, Urbach H, Jungbluth S, Kurthen M, Reuber M, Fernandez G et al. Standard magnetic resonance imaging is inadequate for patients with refractory focal epilepsy. J.Neurol.Neurosurg.Psychiatry 2002;73(6):643-7.

67. Jack CR, Jr., Sharbrough FW, Twomey CK, Cascino GD, Hirschorn KA, Marsh WR et al. Temporal lobe seizures: lateralization with MR volume measurements of the hippocampal formation. Radiology 1990;175(2):423-9.

68. Cook MJ, Fish DR, Shorvon SD, Straughan K, Stevens JM. Hippocampal volumetric and morphometric studies in frontal and temporal lobe epilepsy. Brain 1992;115 (Pt 4):1001-15.

69. Van Paesschen W, Revesz T, Duncan JS, King MD, Connelly A. Quantitative neuropathology and quantitative magnetic resonance imaging of the hippocampus in temporal lobe epilepsy. Ann.Neurol. 1997;42(5):756-66.

70. Trenerry MR, Jack CR, Jr., Ivnik RJ, Sharbrough FW, Cascino GD, Hirschorn KA et al. MRI hippocampal volumes and memory function before and after temporal lobectomy. Neurology 1993;43(9):1800-5.

71. Jackson GD, Connelly A, Duncan JS, Grunewald RA, Gadian DG. Detection of hippocampal pathology in intractable partial epilepsy: increased sensitivity with quantitative magnetic resonance T2 relaxometry. Neurology 1993;43(9):1793-9.

72. Woermann FG, Barker GJ, Birnie KD, Meencke HJ, Duncan JS. Regional changes in hippocampal T2 relaxation and volume: a quantitative magnetic resonance imaging study of hippocampal sclerosis. J.Neurol.Neurosurg.Psychiatry 1998;65(5):656-64.

73. Liu RS, Lemieux L, Bell GS, Hammers A, Sisodiya SM, Bartlett PA et al. Progressive neocortical damage in epilepsy. Ann.Neurol. 2003;53(3):312-24.

74. Briellmann RS, Berkovic SF, Syngeniotis A, King MA, Jackson GD. Seizure-associated hippocampal volume loss: a longitudinal magnetic resonance study of temporal lobe epilepsy. Ann.Neurol. 2002;51(5):641-4.

75. Fuerst D, Shah J, Shah A, Watson C. Hippocampal sclerosis is a progressive disorder: a longitudinal volumetric MRI study. Ann.Neurol. 2003;53(3):413-6.

76. Rugg-Gunn FJ, Eriksson SH, Symms MR, Barker GJ, Duncan JS. Diffusion tensor imaging of cryptogenic and acquired partial epilepsies. Brain 2001;124(Pt 3):627-36.

77. Rugg-Gunn FJ, Boulby PA, Symms MR, Barker GJ, Duncan JS. Whole-brain T2 mapping demonstrates occult abnormalities in focal epilepsy. Neurology 2005;64(2):318-25.

78. Rugg-Gunn FJ, Eriksson SH, Boulby PA, Symms MR, Barker GJ, Duncan JS. Magnetization transfer imaging in focal epilepsy. Neurology 2003;60(10):1638-45.

79. Rugg-Gunn FJ, Boulby PA, Symms MR, Barker GJ, Duncan JS. Imaging the neocortex in epilepsy with double inversion recovery imaging. Neuroimage. 2006; 31:39-50.

80. Theodore WH, Newmark ME, Sato S, Brooks R, Patronas N, De La PR et al. [18F]fluorodeoxyglucose positron emission tomography in refractory complex partial seizures. Ann.Neurol. 1983;14(4):429-37.

81. Engel J, Jr., Henry TR, Risinger MW, Mazziotta JC, Sutherling WW, Levesque MF et al. Presurgical evaluation for partial epilepsy: relative contributions of chronic depth-electrode recordings versus FDG-PET and scalp-sphenoidal ictal EEG. Neurology 1990;40(11):1670-7.

82. Koepp MJ, Hammers A, Labbe C, Woermann FG, Brooks DJ, Duncan JS. 11C-flumazenil PET in patients with refractory temporal lobe epilepsy and normal MRI. Neurology 2000;54(2):332-9.

83. Hammers A, Koepp MJ, Labbe C, Brooks DJ, Thom M, Cunningham VJ et al. Neocortical abnormalities of [11C]-flumazenil PET in mesial temporal lobe epilepsy. Neurology 2001;56(7):897-906.

84. Hammers A, Koepp MJ, Hurlemann R, Thom M, Richardson MP, Brooks DJ et al. Abnormalities of grey and white matter [11C]flumazenil binding in temporal lobe epilepsy with normal MRI. Brain 2002;125(Pt 10):2257-71.

85. Hammers A, Koepp MJ, Richardson MP, Hurlemann R, Brooks DJ, Duncan JS. Grey and white matter flumazenil binding in neocortical epilepsy with normal MRI. A PET study of 44 patients. Brain 2003;126(Pt 6):1300-18.

86. Stefan H, Bauer J, Feistel H, Schulemann H, Neubauer U, Wenzel B et al. Regional cerebral blood flow during focal seizures of temporal and frontocentral onset. Ann.Neurol. 1990;27(2):162-6.

87. Van Paesschen W, Dupont P, Van Driel G, Van Billoen H, Maes A. SPECT perfusion changes during complex partial seizures in patients with hippocampal sclerosis. Brain 2003;126(Pt 5):1103-11.

88. Wieser HG, Muller RU. Neocortical temporal seizures. In: Wieser HG, Elger CE, editors. Presurgical Evaluation of Epileptics: Basis, Techniques, Implications. Berlin: Springer-Verlag; 1987. p. 252-66.

89. Walker MC, Sander JW. The impact of new antiepileptic drugs on the prognosis of epilepsy: seizure freedom should be the ultimate goal. Neurology 1996;46(4):912-4.

90. Penfield W, Flanigin H. Surgical therapy of temporal lobe seizures. AMA.Arch.Neurol.Psychiatry 1950;64(4):491-500.

91. Berkovic SF, McIntosh AM, Kalnins RM, Jackson GD, Fabinyi GC, Brazenor GA et al. Preoperative MRI predicts outcome of temporal lobectomy: an actuarial analysis. Neurology 1995;45(7):1358-63.

92. Spencer SS. The relative contributions of MRI, SPECT, and PET imaging in epilepsy. Epilepsia 1994;35 Suppl 6:S72-S89.

93. Baxendale SA, Van Paesschen W, Thompson PJ, Duncan JS, Harkness WF, Shorvon SD. Hippocampal cell loss and gliosis: relationship to preoperative and postoperative memory function. Neuropsychiatry Neuropsychol.Behav.Neurol. 1998;11(1):12-21.

94. Sabsevitz DS, Swanson SJ, Morris GL, Mueller WM, Seidenberg M. Memory outcome after left anterior temporal lobectomy in patients with expected and reversed Wada memory asymmetry scores. Epilepsia 2001;42(11):1408-15.

95. Kirsch HE, Walker JA, Winstanley FS, Hendrickson R, Wong ST, Barbaro NM et al. Limitations of Wada memory asymmetry as a predictor of outcomes after temporal lobectomy. Neurology 2005;65(5):676-80.

96. Sass KJ, Spencer DD, Kim JH, Westerveld M, Novelly RA, Lencz T. Verbal memory impairment correlates with hippocampal pyramidal cell density. Neurology 1990;40(11):1694-7.

97. Loring DW, Murro AM, Meador KJ, Lee GP, Gratton CA, Nichols ME et al. Wada memory testing and hippocampal volume measurements in the evaluation for temporal lobectomy. Neurology 1993;43(9):1789-93.

98. Baxendale S. The role of functional MRI in the presurgical investigation of temporal lobe epilepsy patients: a clinical perspective and review. J.Clin.Exp.Neuropsychol. 2002;24(5):664-76.

99. Wiebe S, Blume WT, Girvin JP, Eliasziw M. A randomized, controlled trial of surgery for temporal-lobe epilepsy. N.Engl.J.Med. 2001;345(5):311-8.

100. Wieser HG, Blume WT, Fish D, Goldensohn E, Hufnagel A, King D et al. ILAE Commission Report. Proposal for a new classification of outcome with respect to epileptic seizures following epilepsy surgery. Epilepsia 2001;42(2):282-6.

101. Harkness WFJ, McEvoy A. Methods of Epilepsy Surgery. In: Sander J.W., Walker M.C., Smalls J.E., editors. Epilepsy 2005. From Neuron to NICE - A practical Guide to Epilepsy. 10 ed. 2005. p. 453-60.

102. Baxendale S. Amnesia in temporal lobectomy patients: historical perspective and review. Seizure. 1998;7(1):15-24.

103. Scoville WB, Milner B. Loss of recent memory after bilateral hippocampal lesions. 1957. J.Neuropsychiatry Clin.Neurosci. 2000;12(1):103-13.

104. Penfield W, Milner B. Memory deficit produced by bilateral lesions in the hippocampal zone. AMA.Arch.Neurol.Psychiatry 1958;79(5):475-97.

105. Warrington EK, Duchen LW. A re-appraisal of a case of persistent global amnesia following right temporal lobectomy: a clinico-pathological study. Neuropsychologia 1992;30(5):437-50.

106. Loring DW, Hermann BP, Meador KJ, Lee GP, Gallagher BB, King DW et al. Amnesia after unilateral temporal lobectomy: a case report. Epilepsia 1994;35(4):757-63.

107. Nathan PW, Smith MC. Normal mentality associated with a maldeveloped "rhinencephalon". J.Neurol.Neurosurg.Psychiatry 1950;13(3):191-7.

108. Kapur N, Prevett M. Unexpected amnesia: are there lessons to be learned from cases of amnesia following unilateral temporal lobe surgery? Brain 2003;126(Pt 12):2573-85.

109. Ivnik RJ, Sharbrough FW, Laws ER, Jr. Effects of anterior temporal lobectomy on cognitive function. J.Clin.Psychol. 1987;43(1):128-37.

110. Spiers HJ, Burgess N, Maguire EA, Baxendale SA, Hartley T, Thompson PJ et al. Unilateral temporal lobectomy patients show lateralized topographical and episodic memory deficits in a virtual town. Brain 2001;124(Pt 12):2476-89.

111. Chelune GJ. Hippocampal adequacy versus functional reserve: predicting memory functions following temporal lobectomy. Arch.Clin.Neuropsychol. 1995;10(5):413-32.

112. Chelune GJ, Naugle RI, Luders H, Awad IA. Prediction of cognitive change as a function of preoperative ability status among temporal lobectomy patients seen at 6-month follow-up. Neurology 1991;41(3):399-404.

113. Kneebone AC, Chelune GJ, Dinner DS, Naugle RI, Awad IA. Intracarotid amobarbital procedure as a predictor of material-specific memory change after anterior temporal lobectomy. Epilepsia 1995;36(9):857-65.

114. Jokeit H, Ebner A, Holthausen H, Markowitsch HJ, Moch A, Pannek H et al. Individual prediction of change in delayed recall of prose passages after left-sided anterior temporal lobectomy. Neurology 1997;49(2):481-7.

115. Helmstaedter C, Elger CE. Cognitive consequences of two-thirds anterior temporal lobectomy on verbal memory in 144 patients: a three-month follow-up study. Epilepsia 1996;37(2):171-80.

116. Hermann BP, Wyler AR, Somes G, Berry AD, III, Dohan FC, Jr. Pathological status of the mesial temporal lobe predicts memory outcome from left anterior temporal lobectomy. Neurosurgery 1992;31(4):652-6.

117. Sass KJ, Westerveld M, Buchanan CP, Spencer SS, Kim JH, Spencer DD. Degree of hippocampal neuron loss determines severity of verbal memory decrease after left anteromesiotemporal lobectomy. Epilepsia 1994;35(6):1179-86.

118. Baxendale SA, Thompson PJ, Kitchen ND. Postoperative hippocampal remnant shrinkage and memory decline: a dynamic process. Neurology 2000;55(2):243-9.

119. Martin RC, Sawrie SM, Knowlton RC, Bilir E, Gilliam FG, Faught E et al. Bilateral hippocampal atrophy: consequences to verbal memory following temporal lobectomy. Neurology 2001;57(4):597-604.

120. Rausch R, Crandall PH. Psychological status related to surgical control of temporal lobe seizures. Epilepsia 1982;23(2):191-202.

121. Glosser G, Zwil AS, Glosser DS, O'Connor MJ, Sperling MR. Psychiatric aspects of temporal lobe epilepsy before and after anterior temporal lobectomy. J.Neurol.Neurosurg.Psychiatry 2000;68(1):53-8.

122. Ring HA, Moriarty J, Trimble MR. A prospective study of the early postsurgical psychiatric associations of epilepsy surgery. J.Neurol.Neurosurg.Psychiatry 1998;64(5):601-4.

123. Hermann BP, Wyler AR, Somes G. Preoperative psychological adjustment and surgical outcome are determinants of psychosocial status after anterior temporal lobectomy. J.Neurol.Neurosurg.Psychiatry 1992;55(6):491-6.

124. Bladin PF. Psychosocial aspects of epilepsy and of epilepsy surgery. Clin.Exp.Neurol. 1992;29:49-61.

125. Trimble MR. Behaviour changes following temporal lobectomy, with special reference to psychosis. J.Neurol.Neurosurg.Psychiatry 1992;55(2):89-91.

126. Christodoulou C, Koutroumanidis M, Hennessy MJ, Elwes RD, Polkey CE, Toone BK. Postictal psychosis after temporal lobectomy. Neurology 2002;59(9):1432-5.

127. Jones JE, Berven NL, Ramirez L, Woodard A, Hermann BP. Long-term psychosocial outcomes of anterior temporal lobectomy. Epilepsia 2002;43(8):896-903.

128. Jezzard P, Clare S. Sources of distortion in functional MRI data. Hum.Brain Mapp. 1999;8(2-3):80-5.

129. Jezzard P, Balaban RS. Correction for geometric distortion in echo planar images from B0 field variations. Magn Reson.Med. 1995;34(1):65-73.

130. Hutton C, Bork A, Josephs O, Deichmann R, Ashburner J, Turner R. Image distortion correction in fMRI: A quantitative evaluation. Neuroimage. 2002;16(1):217-40.

131. Niendorf T. On the application of susceptibility-weighted ultra-fast low-angle RARE experiments in functional MR imaging. Magn Reson.Med. 1999;41(6):1189-98.

132. Deichmann R, Josephs O, Hutton C, Corfield DR, Turner R. Compensation of susceptibility-induced BOLD sensitivity losses in echo-planar fMRI imaging. Neuroimage. 2002;15(1):120-35.

133. Deichmann R, Gottfried JA, Hutton C, Turner R. Optimized EPI for fMRI studies of the orbitofrontal cortex. Neuroimage. 2003;19(2 Pt 1):430-41.

134. Ogawa S, Lee TM, Kay AR, Tank DW. Brain magnetic resonance imaging with contrast dependent on blood oxygenation. Proc.Natl.Acad.Sci.U.S.A 1990;87(24):9868-72.

135. Logothetis NK. The underpinnings of the BOLD functional magnetic resonance imaging signal. J.Neurosci. 2003;23(10):3963-71.

136. Villringer A, Dirnagl U. Coupling of brain activity and cerebral blood flow: basis of functional neuroimaging. Cerebrovasc.Brain Metab Rev. 1995;7(3):240-76.

137. Friston KJ, Holmes AP, Worsley KJ, Poline JB, Frith CD, Frackowiak RS. Statistical parametric maps in functional imaging: a general linear approach. Hum.Brain Mapp. 1995;2:189-210.

138. Talairach J, Tournoux P. Co-planar stereotaxic atlas of the human brain. Stuttgart: Thieme; 1988.

139. Josephs O, Henson RN. Event-related functional magnetic resonance imaging: modelling, inference and optimization. Philos.Trans.R.Soc.Lond B Biol.Sci. 1999;354(1387):1215-28.

140. Basser PJ, Mattiello J, LeBihan D. MR diffusion tensor spectroscopy and imaging. Biophys.J. 1994;66(1):259-67.

141. Pierpaoli C, Basser PJ. Toward a quantitative assessment of diffusion anisotropy. Magn Reson.Med. 1996;36(6):893-906.

142. Wheeler-Kingshott CA, Hickman SJ, Parker GJ, Ciccarelli O, Symms MR, Miller DH et al. Investigating cervical spinal cord structure using axial diffusion tensor imaging. Neuroimage. 2002;16(1):93-102.

143. Jones DK, Simmons A, Williams SC, Horsfield MA. Non-invasive assessment of axonal fiber connectivity in the human brain via diffusion tensor MRI. Magn Reson.Med. 1999;42(1):37-41.

144. Alexander DC, Barker GJ, Arridge SR. Detection and modeling of non-Gaussian apparent diffusion coefficient profiles in human brain data. Magn Reson.Med. 2002;48(2):331-40.

145. Parker GJ, Alexander DC. Probabilistic Monte Carlo based mapping of cerebral connections utilising whole-brain crossing fibre information. Lecture Notes in Computer Science 2003;2737:684-95.

146. Tuch DS, Reese TG, Wiegell MR, Makris N, Belliveau JW, Wedeen VJ. High angular resolution diffusion imaging reveals intravoxel white matter fiber heterogeneity. Magn Reson.Med. 2002;48(4):577-82.

147. Tuch DS. Q-ball imaging. Magn Reson.Med. 2004;52(6):1358-72.

148. Tournier JD, Calamante F, Gadian DG, Connelly A. Direct estimation of the fiber orientation density function from diffusion-weighted MRI data using spherical deconvolution. Neuroimage. 2004;23(3):1176-85.

149. Jansons KM, Alexander DC. Persistent Angular Structure: new insights from diffusion MRI data. Dummy version. Inf.Process Med.Imaging 2003;18:672-83.

150. Le Bihan D, Mangin JF, Poupon C, Clark CA, Pappata S, Molko N et al. Diffusion tensor imaging: concepts and applications. J Magn Reson.Imaging 2001;13(4):534-46.

151. Mori S, Crain BJ, Chacko VP, van Zijl PC. Three-dimensional tracking of axonal projections in the brain by magnetic resonance imaging. Ann.Neurol. 1999;45(2):265-9.

152. Conturo TE, Lori NF, Cull TS, Akbudak E, Snyder AZ, Shimony JS et al. Tracking neuronal fiber pathways in the living human brain. Proc.Natl.Acad.Sci.U.S.A 1999;96(18):10422-7.

153. Basser PJ, Pajevic S, Pierpaoli C, Duda J, Aldroubi A. In vivo fiber tractography using DT-MRI data. Magn Reson.Med. 2000;44(4):625-32.

154. Poupon C, Clark CA, Frouin V, Regis J, Bloch I, Le Bihan D et al. Regularization of diffusion-based direction maps for the tracking of brain white matter fascicles. Neuroimage. 2000;12(2):184-95.

155. Parker GJ, Wheeler-Kingshott CA, Barker GJ. Estimating distributed anatomical connectivity using fast marching methods and diffusion tensor imaging. IEEE Trans.Med.Imaging 2002;21(5):505-12.

156. Parker GJ, Stephan KE, Barker GJ, Rowe JB, MacManus DG, Wheeler-Kingshott CA et al. Initial demonstration of in vivo tracing of axonal projections in the macaque brain and comparison with the human brain using diffusion tensor imaging and fast marching tractography. Neuroimage. 2002;15(4):797-809.

157. Sethian JA. A fast marching level set method for monotonically advancing fronts. Proc.Natl.Acad.Sci.U.S.A 1996;93(4):1591-5.

158. Ciccarelli O, Parker GJ, Toosy AT, Wheeler-Kingshott CA, Barker GJ, Boulby PA et al. From diffusion tractography to quantitative white matter tract measures: a reproducibility study. Neuroimage. 2003;18(2):348-59.

159. Parker GJ, Haroon HA, Wheeler-Kingshott CA. A framework for a streamline-based probabilistic index of connectivity (PICo) using a structural interpretation of MRI diffusion measurements. J Magn Reson.Imaging 2003;18(2):242-54.

160. Behrens TE, Woolrich MW, Jenkinson M, Johansen-Berg H, Nunes RG, Clare S et al. Characterization and propagation of uncertainty in diffusion-weighted MR imaging. Magn Reson.Med. 2003;50(5):1077-88.

161. Behrens TE, Johansen-Berg H, Woolrich MW, Smith SM, Wheeler-Kingshott CA, Boulby PA et al. Non-invasive mapping of connections between human thalamus and cortex using diffusion imaging. Nat.Neurosci. 2003;6(7):750-7.

162. Jones DK. Determining and visualizing uncertainty in estimates of fiber orientation from diffusion tensor MRI. Magn Reson.Med. 2003;49(1):7-12.

163. Rye DB. Tracking neural pathways with MRI. Trends Neurosci. 1999;22(9):373-4.

164. Broca P. Reamrques sur le siege de la faculte du langage articule; suivies d'une observation d'aphemie. Bulletin de la Societe Anatomique de Paris 1861;6:330-57.

165. Wernicke C. Der aphasiche Symptomenkomplex. Breslau, Poland: 1874.

166. Price CJ. The anatomy of language: contributions from functional neuroimaging. J.Anat. 2000;197 Pt 3:335-59.

167. Fernandez G, Specht K, Weis S, Tendolkar I, Reuber M, Fell J et al. Intrasubject reproducibility of presurgical language lateralization and mapping using fMRI. Neurology 2003;60(6):969-75.

168. Schlosser MJ, Aoyagi N, Fulbright RK, Gore JC, McCarthy G. Functional MRI studies of auditory comprehension. Hum.Brain Mapp. 1998;6(1):1-13.

169. Lehericy S, Cohen L, Bazin B, Samson S, Giacomini E, Rougetet R et al. Functional MR evaluation of temporal and frontal language dominance compared with the Wada test. Neurology 2000;54(8):1625-33.

170. Gaillard WD, Balsamo L, Xu B, McKinney C, Papero PH, Weinstein S et al. fMRI language task panel improves determination of language dominance. Neurology 2004;63(8):1403-8.

171. Gaillard WD, Balsamo L, Xu B, Grandin CB, Braniecki SH, Papero PH et al. Language dominance in partial epilepsy patients identified with an fMRI reading task. Neurology 2002;59(2):256-65.

172. Adcock JE, Wise RG, Oxbury JM, Oxbury SM, Matthews PM. Quantitative fMRI assessment of the differences in lateralization of language-related brain activation in patients with temporal lobe epilepsy. Neuroimage. 2003;18(2):423-38.

173. Liegeois F, Connelly A, Cross JH, Boyd SG, Gadian DG, Vargha-Khadem F et al. Language reorganization in children with early-onset lesions of the left hemisphere: an fMRI study. Brain 2004;127(Pt 6):1229-36.

174. Woermann FG, Jokeit H, Luerding R, Freitag H, Schulz R, Guertler S et al. Language lateralization by Wada test and fMRI in 100 patients with epilepsy. Neurology 2003;61(5):699-701.

175. Friston KJ, Price CJ, Fletcher P, Moore C, Frackowiak RS, Dolan RJ. The trouble with cognitive subtraction. Neuroimage. 1996;4(2):97-104.

176. Price CJ, Friston KJ. Cognitive conjunction: a new approach to brain activation experiments. Neuroimage. 1997;5(4 Pt 1):261-70.

177. Risse GL, Gates JR, Fangman MC. A reconsideration of bilateral language representation based on the intracarotid amobarbital procedure. Brain Cogn 1997;33(1):118-32.

178. Serafetinides Ea, Hoare Rd, Driver M. Intracarotid Sodium Amylobarbitone And Cerebral Dominance For Speech And Consciousness. Brain 1965;88:107-30.

179. Rasmussen T, Milner B. The role of early left-brain injury in determining lateralization of cerebral speech functions. Ann.N.Y.Acad.Sci. 1977;299:355-69.

180. Pujol J, Deus J, Losilla JM, Capdevila A. Cerebral lateralization of language in normal left-handed people studied by functional MRI. Neurology 1999;52(5):1038-43.

181. Springer JA, Binder JR, Hammeke TA, Swanson SJ, Frost JA, Bellgowan PS et al. Language dominance in neurologically normal and epilepsy subjects: a functional MRI study. Brain 1999;122 (Pt 11):2033-46.

182. Janszky J, Mertens M, Janszky I, Ebner A, Woermann FG. Left-sided interictal epileptic activity induces shift of language lateralization in temporal lobe epilepsy: an fMRI study. Epilepsia 2006;47(5):921-7.

183. Janszky J, Jokeit H, Heinemann D, Schulz R, Woermann FG, Ebner A. Epileptic activity influences the speech organization in medial temporal lobe epilepsy. Brain 2003;126(Pt 9):2043-51.

184. Thivard L, Hombrouck J, du Montcel ST, Delmaire C, Cohen L, Samson S et al. Productive and perceptive language reorganization in temporal lobe epilepsy. Neuroimage. 2005;24(3):841-51.

185. Berl MM, Balsamo LM, Xu B, Moore EN, Weinstein SL, Conry JA et al. Seizure focus affects regional language networks assessed by fMRI. Neurology 2005;65(10):1604-11.

186. Weber B, Wellmer J, Reuber M, Mormann F, Weis S, Urbach H et al. Left hippocampal pathology is associated with atypical language lateralization in patients with focal epilepsy. Brain 2006;129:346-51.

187. Briellmann RS, Labate A, Harvey AS, Saling MM, Sveller C, Lillywhite L et al. Is language lateralization in temporal lobe epilepsy patients related to the nature of the epileptogenic lesion? Epilepsia 2006;47(5):916-20.

188. Benson RR, FitzGerald DB, LeSueur LL, Kennedy DN, Kwong KK, Buchbinder BR et al. Language dominance determined by whole brain functional MRI in patients with brain lesions. Neurology 1999;52(4):798-809.

189. Jayakar P, Bernal B, Santiago ML, Altman N. False lateralization of language cortex on functional MRI after a cluster of focal seizures. Neurology 2002;58(3):490-2.

190. Ramsey NF, Sommer IE, Rutten GJ, Kahn RS. Combined analysis of language tasks in fMRI improves assessment of hemispheric dominance for language functions in individual subjects. Neuroimage. 2001;13(4):719-33.

191. Rutten GJ, Ramsey NF, van Rijen PC, Noordmans HJ, van Veelen CW. Development of a functional magnetic resonance imaging protocol for intraoperative localization of critical temporoparietal language areas. Ann.Neurol. 2002;51(3):350-60.

192. FitzGerald DB, Cosgrove GR, Ronner S, Jiang H, Buchbinder BR, Belliveau JW et al. Location of language in the cortex: a comparison between functional MR imaging and electrocortical stimulation. AJNR Am.J.Neuroradiol. 1997;18(8):1529-39.

193. Schlosser MJ, Luby M, Spencer DD, Awad IA, McCarthy G. Comparative localization of auditory comprehension by using functional magnetic resonance imaging and cortical stimulation. J.Neurosurg. 1999;91(4):626-35.

194. Pouratian N, Bookheimer SY, Rex DE, Martin NA, Toga AW. Utility of preoperative functional magnetic resonance imaging for identifying language cortices in patients with vascular malformations. J.Neurosurg. 2002;97(1):21-32.

195. Desmond JE, Sum JM, Wagner AD, Demb JB, Shear PK, Glover GH et al. Functional MRI measurement of language lateralization in Wada-tested patients. Brain 1995;118 (Pt 6):1411-9.

196. Binder JR, Swanson SJ, Hammeke TA, Morris GL, Mueller WM, Fischer M et al. Determination of language dominance using functional MRI: a comparison with the Wada test. Neurology 1996;46(4):978-84.

197. Hertz-Pannier L, Gaillard WD, Mott SH, Cuenod CA, Bookheimer SY, Weinstein S et al. Noninvasive assessment of language dominance in children and adolescents with functional MRI: a preliminary study. Neurology 1997;48(4):1003-12.

198. Yetkin FZ, Swanson S, Fischer M, Akansel G, Morris G, Mueller W et al. Functional MR of frontal lobe activation: comparison with Wada language results. AJNR Am.J.Neuroradiol. 1998;19(6):1095-8.

199. Carpentier A, Pugh KR, Westerveld M, Studholme C, Skrinjar O, Thompson JL et al. Functional MRI of language processing: dependence on input modality and temporal lobe epilepsy. Epilepsia 2001;42(10):1241-54.

200. Sabbah P, Chassoux F, Leveque C, Landre E, Baudoin-Chial S, Devaux B et al. Functional MR imaging in assessment of language dominance in epileptic patients. Neuroimage. 2003;18(2):460-7.

201. Davies KG, Bell BD, Bush AJ, Hermann BP, Dohan FC, Jr., Jaap AS. Naming decline after left anterior temporal lobectomy correlates with pathological status of resected hippocampus. Epilepsia 1998;39(4):407-19.

202. Saykin AJ, Stafiniak P, Robinson LJ, Flannery KA, Gur RC, O'Connor MJ et al. Language before and after temporal lobectomy: specificity of acute changes and relation to early risk factors. Epilepsia 1995;36(11):1071-7.

203. Hermann BP, Perrine K, Chelune GJ, Barr W, Loring DW, Strauss E et al. Visual confrontation naming following left anterior temporal lobectomy: a comparison of surgical approaches. Neuropsychology. 1999;13(1):3-9.

204. Devinsky O, Perrine K, Llinas R, Luciano DJ, Dogali M. Anterior temporal language areas in patients with early onset of temporal lobe epilepsy. Ann.Neurol. 1993;34(5):727-32.

205. Schwartz TH, Devinsky O, Doyle W, Perrine K. Preoperative predictors of anterior temporal language areas. J.Neurosurg. 1998;89(6):962-70.

206. Sabsevitz DS, Swanson SJ, Hammeke TA, Spanaki MV, Possing ET, Morris GL, III et al. Use of preoperative functional neuroimaging to predict language deficits from epilepsy surgery. Neurology 2003;60(11):1788-92.

207. Noppeney U, Price CJ, Duncan JS, Koepp MJ. Reading skills after left anterior temporal lobe resection: an fMRI study. Brain 2005;128(Pt 6):1377-85.

208. Voets NL, Adcock JE, Flitney DE, Behrens TE, Hart Y, Stacey R et al. Distinct right frontal lobe activation in language processing following left hemisphere injury. Brain 2006;129(Pt 3):754-66.

209. Ojemann JG, Akbudak E, Snyder AZ, McKinstry RC, Raichle ME, Conturo TE. Anatomic localization and quantitative analysis of gradient refocused echo-planar fMRI susceptibility artifacts. Neuroimage. 1997;6(3):156-67.

210. Greicius MD, Krasnow B, Boyett-Anderson JM, Eliez S, Schatzberg AF, Reiss AL et al. Regional analysis of hippocampal activation during memory encoding and retrieval: fMRI study. Hippocampus 2003;13(1):164-74.

211. Lipschutz B, Friston KJ, Ashburner J, Turner R, Price CJ. Assessing study-specific regional variations in fMRI signal. Neuroimage. 2001;13(2):392-8.

212. Price CJ, Friston KJ. Scanning patients with tasks they can perform. Hum.Brain Mapp. 1999;8(2-3):102-8.

213. Craik FIM, Lockhart RS. Levels of processing: A framework for memory. J Verbal Learning and Verbal Behaviour 1972;11:671-84.

214. Kelley WM, Miezin FM, McDermott KB, Buckner RL, Raichle ME, Cohen NJ et al. Hemispheric specialization in human dorsal frontal cortex and medial temporal lobe for verbal and nonverbal memory encoding. Neuron 1998;20(5):927-36.

215. Demb JB, Desmond JE, Wagner AD, Vaidya CJ, Glover GH, Gabrieli JD. Semantic encoding and retrieval in the left inferior prefrontal cortex: a functional MRI study of task difficulty and process specificity. J.Neurosci. 1995;15(9):5870-8.

216. Wagner AD, Schacter DL, Rotte M, Koutstaal W, Maril A, Dale AM et al. Building memories: remembering and forgetting of verbal experiences as predicted by brain activity. Science 1998;281(5380):1188-91.

217. Buckner RL, Kelley WM, Petersen SE. Frontal cortex contributes to human memory formation. Nat.Neurosci. 1999;2(4):311-4.

218. Golby AJ, Poldrack RA, Brewer JB, Spencer D, Desmond JE, Aron AP et al. Material-specific lateralization in the medial temporal lobe and prefrontal cortex during memory encoding. Brain 2001;124(Pt 9):1841-54.

219. Binder JR, Bellgowan PS, Hammeke TA, Possing ET, Frost JA. A comparison of two FMRI protocols for eliciting hippocampal activation. Epilepsia 2005;46(7):1061-70.

220. Fernandez G, Weyerts H, Schrader-Bolsche M, Tendolkar I, Smid HG, Tempelmann C et al. Successful verbal encoding into episodic memory engages the posterior hippocampus: a parametrically analyzed functional magnetic resonance imaging study. J.Neurosci. 1998;18(5):1841-7.

221. Buckner RL, Bandettini PA, O'Craven KM, Savoy RL, Petersen SE, Raichle ME et al. Detection of cortical activation during averaged single trials of a cognitive task using functional magnetic resonance imaging. Proc.Natl.Acad.Sci.U.S.A 1996;93(25):14878-83.

222. Dale AM. Optimal experimental design for event-related fMRI. Hum.Brain Mapp. 1999;8(2-3):109-14.

223. Konishi S, Yoneyama R, Itagaki H, Uchida I, Nakajima K, Kato H et al. Transient brain activity used in magnetic resonance imaging to detect functional areas. Neuroreport 1996;8(1):19-23.

224. Zarahn E, Aguirre G, D'Esposito M. A trial-based experimental design for fMRI. Neuroimage. 1997;6(2):122-38.

225. Wagner AD, Koutstaal W, Schacter DL. When encoding yields remembering: insights from event-related neuroimaging. Philos.Trans.R.Soc.Lond B Biol.Sci. 1999;354(1387):1307-24.

226. Kapur S, Craik FI, Tulving E, Wilson AA, Houle S, Brown GM. Neuroanatomical correlates of encoding in episodic memory: levels of processing effect. Proc.Natl.Acad.Sci.U.S.A 1994;91(6):2008-11.

227. Shallice T, Fletcher P, Frith CD, Grasby P, Frackowiak RS, Dolan RJ. Brain regions associated with acquisition and retrieval of verbal episodic memory. Nature 1994;368(6472):633-5.

228. Wagner AD, Poldrack RA, Eldridge LL, Desmond JE, Glover GH, Gabrieli JD. Material-specific lateralization of prefrontal activation during episodic encoding and retrieval. Neuroreport 1998;9(16):3711-7.

229. Iidaka T, Sadato N, Yamada H, Yonekura Y. Functional asymmetry of human prefrontal cortex in verbal and non-verbal episodic memory as revealed by fMRI. Brain Res.Cogn Brain Res. 2000;9(1):73-83.

230. Aguirre GK, Detre JA, Alsop DC, D'Esposito M. The parahippocampus subserves topographical learning in man. Cereb.Cortex 1996;6(6):823-9.

231. Stern CE, Corkin S, Gonzalez RG, Guimaraes AR, Baker JR, Jennings PJ et al. The hippocampal formation participates in novel picture encoding: evidence from functional magnetic resonance imaging. Proc.Natl.Acad.Sci.U.S.A 1996;93(16):8660-5.

232. Tulving E, Kapur S, Craik FI, Moscovitch M, Houle S. Hemispheric encoding/retrieval asymmetry in episodic memory: positron emission tomography findings. Proc.Natl.Acad.Sci.U.S.A 1994;91(6):2016-20.

233. Nyberg L. PET studies of encoding and retrieval: the HERA model. Psychonomic Bull.Rev. 1996;3:135-48.

234. Tulving E, Markowitsch HJ, Craik FE, Habib R, Houle S. Novelty and familiarity activations in PET studies of memory encoding and retrieval. Cereb.Cortex 1996;6(1):71-9.

235. Haxby JV, Ungerleider LG, Horwitz B, Maisog JM, Rapoport SI, Grady CL. Face encoding and recognition in the human brain. Proc.Natl.Acad.Sci.U.S.A 1996;93(2):922-7.

236. Fletcher PC, Henson RN. Frontal lobes and human memory: insights from functional neuroimaging. Brain 2001;124(Pt 5):849-81.

237. Dolan RJ. Emotion, cognition, and behavior. Science 2002;298(5596):1191-4.

238. Adolphs R, Cahill L, Schul R, Babinsky R. Impaired declarative memory for emotional material following bilateral amygdala damage in humans. Learn.Mem. 1997;4(3):291-300.

239. Strange BA, Henson RN, Friston KJ, Dolan RJ. Brain mechanisms for detecting perceptual, semantic, and emotional deviance. Neuroimage. 2000;12(4):425-33.

240. Schacher M, Haemmerle B, Woermann FG, Okujava M, Huber D, Grunwald T et al. Amygdala fMRI lateralizes temporal lobe epilepsy. Neurology 2006;66(1):81-7.

241. Lepage M, Habib R, Tulving E. Hippocampal PET activations of memory encoding and retrieval: the HIPER model. Hippocampus 1998;8(4):313-22.

242. Gabrieli JD, Brewer JB, Desmond JE, Glover GH. Separate neural bases of two fundamental memory processes in the human medial temporal lobe. Science 1997;276(5310):264-6.

243. Schacter DL, Wagner AD. Medial temporal lobe activations in fMRI and PET studies of episodic encoding and retrieval. Hippocampus 1999;9(1):7-24.

244. Richardson MP, Strange BA, Duncan JS, Dolan RJ. Preserved verbal memory function in left medial temporal pathology involves reorganisation of function to right medial temporal lobe. Neuroimage. 2003;20 Suppl 1:S112-S119.

245. Strange BA, Fletcher PC, Henson RN, Friston KJ, Dolan RJ. Segregating the functions of human hippocampus. Proc.Natl.Acad.Sci.U.S.A 1999;96(7):4034-9.

246. Strange BA, Otten LJ, Josephs O, Rugg MD, Dolan RJ. Dissociable human perirhinal, hippocampal, and parahippocampal roles during verbal encoding. J.Neurosci. 2002;22(2):523-8.

247. Zeineh MM, Engel SA, Thompson PM, Bookheimer SY. Dynamics of the hippocampus during encoding and retrieval of face-name pairs. Science 2003;299(5606):577-80.

248. Eldridge LL, Engel SA, Zeineh MM, Bookheimer SY, Knowlton BJ. A dissociation of encoding and retrieval processes in the human hippocampus. J.Neurosci. 2005;25(13):3280-6.

249. Detre JA, Maccotta L, King D, Alsop DC, Glosser G, D'Esposito M et al. Functional MRI lateralization of memory in temporal lobe epilepsy. Neurology 1998;50(4):926-32.

250. Dupont S, Van de Moortele PF, Samson S, Hasboun D, Poline JB, Adam C et al. Episodic memory in left temporal lobe epilepsy: a functional MRI study. Brain 2000;123 (Pt 8):1722-32.

251. Dupont S, Samson Y, Van de Moortele PF, Samson S, Poline JB, Adam C et al. Delayed verbal memory retrieval: a functional MRI study in epileptic patients with structural lesions of the left medial temporal lobe. Neuroimage. 2001;14(5):995-1003.

252. Dupont S, Samson Y, Van de Moortele PF, Samson S, Poline JB, Hasboun D et al. Bilateral hemispheric alteration of memory processes in right medial temporal lobe epilepsy. J.Neurol.Neurosurg.Psychiatry 2002;73(5):478-85.

253. Bellgowan PS, Binder JR, Swanson SJ, Hammeke TA, Springer JA, Frost JA et al. Side of seizure focus predicts left medial temporal lobe activation during verbal encoding. Neurology 1998;51(2):479-84.

254. Roland PE, Eriksson L, Stone-Elander S, Widen L. Does mental activity change the oxidative metabolism of the brain? J Neurosci. 1987;7(8):2373-89.

255. Jokeit H, Okujava M, Woermann FG. Memory fMRI lateralizes temporal lobe epilepsy. Neurology 2001;57(10):1786-93.

256. Golby AJ, Poldrack RA, Illes J, Chen D, Desmond JE, Gabrieli JD. Memory lateralization in medial temporal lobe epilepsy assessed by functional MRI. Epilepsia 2002;43(8):855-63.

257. Richardson MP, Strange BA, Dolan RJ. Encoding of emotional memories depends on amygdala and hippocampus and their interactions. Nat.Neurosci. 2004;7(3):278-85.

258. Richardson MP, Strange BA, Thompson PJ, Baxendale SA, Duncan JS, Dolan RJ. Pre-operative verbal memory fMRI predicts post-operative memory decline after left temporal lobe resection. Brain 2004;127(Pt 11):2419-26.

259. Richardson MP, Strange BA, Duncan JS, Dolan RJ. Memory fMRI in left hippocampal sclerosis: optimizing the approach to predicting postsurgical memory. Neurology 2006;66(5):699-705.

260. Rabin ML, Narayan VM, Kimberg DY, Casasanto DJ, Glosser G, Tracy JI et al. Functional MRI predicts post-surgical memory following temporal lobectomy. Brain 2004;127(Pt 10):2286-98.

261. Janszky J, Jokeit H, Kontopoulou K, Mertens M, Ebner A, Pohlmann-Eden B et al. Functional MRI predicts memory performance after right mesiotemporal epilepsy surgery. Epilepsia 2005;46(2):244-50.

262. Maccotta L, Buckner RL, Gilliam FG, Ojemann JG. Changing Frontal Contributions to Memory Before and After Medial Temporal Lobectomy. Cereb.Cortex 2006.

263. Young MP. Objective analysis of the topological organization of the primate cortical visual system. Nature 1992;358(6382):152-5.

264. Hilgetag CC, O'Neill MA, Young MP. Indeterminate organization of the visual system. Science 1996;271(5250):776-7.

265. Burgel U, Schormann T, Schleicher A, Zilles K. Mapping of histologically identified long fiber tracts in human cerebral hemispheres to the MRI volume of a reference brain: position and spatial variability of the optic radiation. Neuroimage. 1999;10(5):489-99.

266. Di Virgilio G, Clarke S, Pizzolato G, Schaffner T. Cortical regions contributing to the anterior commissure in man. Exp.Brain Res. 1999;124(1):1-7.

267. Rolls ET. Hippocampo-cortical and cortico-cortical backprojections. Hippocampus 2000;10(4):380-8.

268. Witter MP, Van Hoesen GW, Amaral DG. Topographical organization of the entorhinal projection to the dentate gyrus of the monkey. J.Neurosci. 1989;9(1):216-28.

269. Van Hoesen GW, Pandya DN, Butters N. Cortical afferents to the entorhinal cortex of the Rhesus monkey. Science 1972;175(29):1471-3.

270. Insausti R, Amaral DG, Cowan WM. The entorhinal cortex of the monkey: II. Cortical afferents. J.Comp Neurol. 1987;264(3):356-95.

271. Pandya DN, Kuypers HG. Cortico-cortical connections in the rhesus monkey. Brain Res. 1969;13(1):13-36.

272. Martin-Elkins CL, Horel JA. Cortical afferents to behaviorally defined regions of the inferior temporal and parahippocampal gyri as demonstrated by WGA-HRP. J.Comp Neurol. 1992;321(2):177-92.

273. Amaral DG, Price JL. Amygdalo-cortical projections in the monkey (Macaca fascicularis). J.Comp Neurol. 1984;230(4):465-96.

274. Suzuki WA, Amaral DG. Perirhinal and parahippocampal cortices of the macaque monkey: cortical afferents. J.Comp Neurol. 1994;350(4):497-533.

275. Dejerine J. Anatomie des Centres Nerveux. Paris: 1895.

276. Catani M, Jones DK, Donato R, Ffytche DH. Occipito-temporal connections in the human brain. Brain 2003;126(Pt 9):2093-107.

277. Mesulam M. Imaging connectivity in the human cerebral cortex: the next frontier? Ann.Neurol. 2005;57(1):5-7.

278. Guye M, Parker GJ, Symms M, Boulby P, Wheeler-Kingshott CA, Salek-Haddadi A et al. Combined functional MRI and tractography to demonstrate the connectivity of the human primary motor cortex in vivo. Neuroimage. 2003;19(4):1349-60.

279. Toosy AT, Ciccarelli O, Parker GJ, Wheeler-Kingshott CA, Miller DH, Thompson AJ. Characterizing function-structure relationships in the human visual system with functional MRI and diffusion tensor imaging. Neuroimage. 2004;21(4):1452-63.

280. Parker GJ, Luzzi S, Alexander DC, Wheeler-Kingshott CA, Ciccarelli O, Lambon Ralph MA. Lateralization of ventral and dorsal auditory-language pathways in the human brain. Neuroimage. 2005;24(3):656-66.

281. Catani M, Jones DK, Ffytche DH. Perisylvian language networks of the human brain. Ann.Neurol. 2005;57(1):8-16.

282. Amunts K, Schleicher A, Burgel U, Mohlberg H, Uylings HB, Zilles K. Broca's region revisited: cytoarchitecture and intersubject variability. J.Comp Neurol. 1999;412(2):319-41.

283. Shapleske J, Rossell SL, Woodruff PW, David AS. The planum temporale: a systematic, quantitative review of its structural, functional and clinical significance. Brain Res.Brain Res.Rev. 1999;29(1):26-49.

284. Good CD, Johnsrude I, Ashburner J, Henson RN, Friston KJ, Frackowiak RS. Cerebral asymmetry and the effects of sex and handedness on brain structure: a voxel-based morphometric analysis of 465 normal adult human brains. Neuroimage. 2001;14(3):685-700.

285. Pujol J, Lopez-Sala A, Deus J, Cardoner N, Sebastian-Galles N, Conesa G et al. The lateral asymmetry of the human brain studied by volumetric magnetic resonance imaging. Neuroimage. 2002;17(2):670-9.

286. Toga AW, Thompson PM. Mapping brain asymmetry. Nat.Rev.Neurosci. 2003;4(1):37-48.

287. Polyak S. The Vertebrate Visual System. Chicago: University of Chicago Press; 1957. p. 405-9.

288. Ebeling U, Reulen HJ. Neurosurgical topography of the optic radiation in the temporal lobe. Acta Neurochir.(Wien.) 1988;92(1-4):29-36.

289. Sisodiya SM, Moran N, Free SL, Kitchen ND, Stevens JM, Harkness WF et al. Correlation of widespread preoperative magnetic resonance imaging changes with unsuccessful surgery for hippocampal sclerosis. Ann.Neurol. 1997;41(4):490-6.

290. Moran NF, Lemieux L, Kitchen ND, Fish DR, Shorvon SD. Extrahippocampal temporal lobe atrophy in temporal lobe epilepsy and mesial temporal sclerosis. Brain 2001;124(Pt 1):167-75.

291. Diehl B, Najm I, LaPresto E, Prayson R, Ruggieri P, Mohamed A et al. Temporal lobe volumes in patients with hippocampal sclerosis with or without cortical dysplasia. Neurology 2004;62(10):1729-35.

292. Stefan H, Feichtinger M, Pauli E, Schafer I, Eberhardt KW, Kasper BS et al. Magnetic resonance spectroscopy and histopathological findings in temporal lobe epilepsy. Epilepsia 2001;42(1):41-6.

293. Keller SS, Mackay CE, Barrick TR, Wieshmann UC, Howard MA, Roberts N. Voxel-based morphometric comparison of hippocampal and extrahippocampal abnormalities in patients with left and right hippocampal atrophy. Neuroimage. 2002;16(1):23-31.

294. Concha L, Beaulieu C, Gross DW. Bilateral limbic diffusion abnormalities in unilateral temporal lobe epilepsy. Ann.Neurol. 2005;57(2):188-96.

295. Van Paesschen W, Sisodiya S, Connelly A, Duncan JS, Free SL, Raymond AA et al. Quantitative hippocampal MRI and intractable temporal lobe epilepsy. Neurology 1995;45(12):2233-40.

296. Oldfield RC. The assessment and analysis of handedness: the Edinburgh inventory. Neuropsychologia 1971;9(1):97-113.

297. Coughlan, A. K. and Hollows, S. E. The Adult Memory and Information Processing Battery. 1985. Leeds (UK), Psychology Department, St. James' Hospital.

298. Baxendale SA, Van Paesschen W, Thompson PJ, Connelly A, Duncan JS, Harkness WF et al. The relationship between quantitative MRI and neuropsychological functioning in temporal lobe epilepsy. Epilepsia 1998;39(2):158-66.

299. Boulby PA, Symms M, Barker GJ. A simple method for matching distortions in functional and structural data. Proc. Int. Soc. Magn. Res. Med. 2004; 2196.

300. Snodgrass JG, Vanderwart M. A standardized set of 260 pictures: norms for name agreement, image agreement, familiarity, and visual complexity. J.Exp.Psychol.[Hum.Learn.] 1980;6(2):174-215.

301. Gaillard WD. Functional MR imaging of language, memory, and sensorimotor cortex. Neuroimaging Clin.N.Am. 2004;14(3):471-85.

302. Friston KJ, Fletcher P, Josephs O, Holmes A, Rugg MD, Turner R. Event-related fMRI: characterizing differential responses. Neuroimage. 1998;7(1):30-40.

303. Duvernoy HM. The Human Hippocampus. Seconded. Berlin Heidelberg New York: Springer; 1998.

304. Grill-Spector K, Knouf N, Kanwisher N. The fusiform face area subserves face perception, not generic within-category identification. Nat.Neurosci. 2004;7(5):555-62.

305. Pierpaoli C, Jezzard P, Basser PJ, Barnett A, Di Chiro G. Diffusion tensor MR imaging of the human brain. Radiology 1996;201(3):637-48.

306. Tusa RJ, Ungerleider LG. The inferior longitudinal fasciculus: a reexamination in humans and monkeys. Ann.Neurol. 1985;18(5):583-91.

307. McKeefry DJ, Zeki S. The position and topography of the human colour centre as revealed by functional magnetic resonance imaging. Brain 1997;120 (Pt 12):2229-42.

308. Sereno MI, Dale AM, Reppas JB, Kwong KK, Belliveau JW, Brady TJ et al. Borders of multiple visual areas in humans revealed by functional magnetic resonance imaging. Science 1995;268(5212):889-93.

309. Insausti R, Juottonen K, Soininen H, Insausti AM, Partanen K, Vainio P et al. MR volumetric analysis of the human entorhinal, perirhinal, and temporopolar cortices. AJNR Am.J.Neuroradiol. 1998;19(4):659-71.

310. Bohnen NI, O'Brien TJ, Mullan BP, So EL. Cerebellar changes in partial seizures: clinical correlations of quantitative SPECT and MRI analysis. Epilepsia 1998;39(6):640-50.

311. Shin WC, Hong SB, Tae WS, Seo DW, Kim SE. Ictal hyperperfusion of cerebellum and basal ganglia in temporal lobe epilepsy: SPECT subtraction with MRI coregistration. J Nucl.Med. 2001;42(6):853-8.

312. Harkness WFJ. Methods of Epilepsy Surgery. In: Sander J.W. WMCSJE, editor. Epilepsy 2003 from synapse to society. A practical Guide to Epilepsy. 9 ed. 2003. p. 453-60.

313. Rasmussen AT. The extent of recurrent geniculo-calcarine fibres (loop of Archambault and Meyer) as demonstrated by gross brain dissection. Anat Rec 1943;85:277-84.

314. Guenot M, Krolak-Salmon P, Mertens P, Isnard J, Ryvlin P, Fischer C et al. MRI assessment of the anatomy of optic radiations after temporal lobe epilepsy surgery. Stereotact.Funct.Neurosurg. 1999;73(1-4):84-7.

315. Krolak-Salmon P, Guenot M, Tiliket C, Isnard J, Sindou M, Mauguiere F et al. Anatomy of optic nerve radiations as assessed by static perimetry and MRI after tailored temporal lobectomy. Br.J Ophthalmol. 2000;84(8):884-9.

316. Kier EL, Staib LH, Davis LM, Bronen RA. MR imaging of the temporal stem: anatomic dissection tractography of the uncinate fasciculus, inferior occipitofrontal fasciculus, and Meyer's loop of the optic radiation. AJNR Am.J Neuroradiol. 2004;25(5):677-91.

317. Clark CA, Barrick TR, Murphy MM, Bell BA. White matter fiber tracking in patients with space-occupying lesions of the brain: a new technique for neurosurgical planning? Neuroimage. 2003;20(3):1601-8.

318. Kirchhoff BA, Wagner AD, Maril A, Stern CE. Prefrontal-temporal circuitry for episodic encoding and subsequent memory. J.Neurosci. 2000;20(16):6173-80.

319. Pihlajamaki M, Tanila H, Hanninen T, Kononen M, Mikkonen M, Jalkanen V et al. Encoding of novel picture pairs activates the perirhinal cortex: an fMRI study. Hippocampus 2003;13(1):67-80.

320. Friston KJ, Zarahn E, Josephs O, Henson RN, Dale AM. Stochastic designs in event-related fMRI. Neuroimage. 1999;10(5):607-19.

321. Corkin S, Amaral DG, Gonzalez RG, Johnson KA, Hyman BT. H. M.'s medial temporal lobe lesion: findings from magnetic resonance imaging. J Neurosci. 1997;17(10):3964-79.

322. Fernandez G, Effern A, Grunwald T, Pezer N, Lehnertz K, Dumpelmann M et al. Real-time tracking of memory formation in the human rhinal cortex and hippocampus. Science 1999;285(5433):1582-5.

323. Otten LJ, Henson RN, Rugg MD. Depth of processing effects on neural correlates of memory encoding: relationship between findings from across- and within-task comparisons. Brain 2001;124(Pt 2):399-412.

324. Otten LJ, Henson RN, Rugg MD. State-related and item-related neural correlates of successful memory encoding. Nat.Neurosci. 2002;5(12):1339-44.

325. Fletcher PC, Stephenson CM, Carpenter TA, Donovan T, Bullmorel ET. Regional brain activations predicting subsequent memory success: an event-related fMRI study of the influence of encoding tasks. Cortex 2003;39(4-5):1009-26.

326. Maril A, Simons JS, Mitchell JP, Schwartz BL, Schacter DL. Feeling-of-knowing in episodic memory: an event-related fMRI study. Neuroimage. 2003;18(4):827-36.

327. Stark CE, Squire LR. When zero is not zero: the problem of ambiguous baseline conditions in fMRI. Proc.Natl.Acad.Sci.U.S.A 2001;98(22):12760-6.

328. Perrett DI, Smith PA, Potter DD, Mistlin AJ, Head AS, Milner AD et al. Neurones responsive to faces in the temporal cortex: studies of functional organization, sensitivity to identity and relation to perception. Hum.Neurobiol. 1984;3(4):197-208.

329. Damasio AR, Damasio H, Van Hoesen GW. Prosopagnosia: anatomic basis and behavioral mechanisms. Neurology 1982;32(4):331-41.

330. Gorno-Tempini ML, Price CJ, Josephs O, Vandenberghe R, Cappa SF, Kapur N et al. The neural systems sustaining face and proper-name processing. Brain 1998;121 (Pt 11):2103-18.

331. Kanwisher N, McDermott J, Chun MM. The fusiform face area: a module in human extrastriate cortex specialized for face perception. J Neurosci. 1997;17(11):4302-11.

332. Nakamura K, Kawashima R, Sato N, Nakamura A, Sugiura M, Kato T et al. Functional delineation of the human occipito-temporal areas related to face and scene processing. A PET study. Brain 2000;123 (Pt 9):1903-12.

333. Ungerleider LG, Mishkin M. Two cortical visual systems. In: Ingle DJ, Goodale MA, Mansfield RJW, editors. Analysis of Visual Behaviour. Cambridge, MA: MIT Press; 1982. p. 549-80.

334. Szaflarski JP, Holland SK, Schmithorst VJ, Dunn RS, Privitera MD. High-resolution functional MRI at 3T in healthy and epilepsy subjects: hippocampal activation with picture encoding task. Epilepsy Behav. 2004;5(2):244-52.

335. Robinson S, Windischberger C, Rauscher A, Moser E. Optimized 3 T EPI of the amygdalae. Neuroimage. 2004;22(1):203-10.

336. Ward NS, Brown MM, Thompson AJ, Frackowiak RS. Neural correlates of outcome after stroke: a cross-sectional fMRI study. Brain 2003;126(Pt 6):1430-48.

337. Blasi V, Young AC, Tansy AP, Petersen SE, Snyder AZ, Corbetta M. Word retrieval learning modulates right frontal cortex in patients with left frontal damage. Neuron 2002;36(1):159-70.

338. Weiller C, Isensee C, Rijntjes M, Huber W, Muller S, Bier D et al. Recovery from Wernicke's aphasia: a positron emission tomographic study. Ann.Neurol. 1995;37(6):723-32.

339. Heiss WD, Kessler J, Thiel A, Ghaemi M, Karbe H. Differential capacity of left and right hemispheric areas for compensation of poststroke aphasia. Ann.Neurol. 1999;45(4):430-8.

340. Johansen-Berg H, Dawes H, Guy C, Smith SM, Wade DT, Matthews PM. Correlation between motor improvements and altered fMRI activity after rehabilitative therapy. Brain 2002;125(Pt 12):2731-42.

341. Brazdil M, Chlebus P, Mikl M, Pazourkova M, Krupa P, Rektor I. Reorganization of language-related neuronal networks in patients with left temporal lobe epilepsy - an fMRI study. Eur.J.Neurol. 2005;12(4):268-75.

342. Powell HW, Koepp MJ, Symms MR, Boulby PA, Salek-Haddadi A, Thompson PJ et al. Material-specific lateralization of memory encoding in the medial temporal lobe: blocked versus event-related design. Neuroimage. 2005;27(1):231-9.

343. Warburton E, Price CJ, Swinburn K, Wise RJ. Mechanisms of recovery from aphasia: evidence from positron emission tomography studies. J.Neurol.Neurosurg.Psychiatry 1999;66(2):155-61.

344. Filippi M, Rocca MA. Cortical reorganisation in patients with MS. J.Neurol.Neurosurg.Psychiatry 2004;75(8):1087-9.

345. Reddy H, Bendahan D, Lee MA, Johansen-Berg H, Donaghy M, Hilton-Jones D et al. An expanded cortical representation for hand movement after peripheral motor denervation. J.Neurol.Neurosurg.Psychiatry 2002;72(2):203-10.

346. Golby A, Silverberg G, Race E, Gabrieli S, O'Shea J, Knierim K et al. Memory encoding in Alzheimer's disease: an fMRI study of explicit and implicit memory. Brain 2005;128(Pt 4):773-87.

347. Baxendale S, Thompson P, Harkness W, Duncan J. Predicting memory decline following epilepsy surgery: a multivariate approach. Epilepsia 2006;In press.

348. Baxendale S, Thompson P. Defining meaningful postoperative change in epilepsy surgery patients: measuring the unmeasurable? Epilepsy Behav. 2005;6(2):207-11.

349. Powell, H. W., Richardson, M. P., Thompson, P. J., Symms, M., Duncan, J., and Koepp, M. J. Reorganisation of verbal and non-verbal memory in unilateral temporal lobe epilepsy: An event-related study. Epilepsia 45(Suppl. 7), 292. 2004.

350. Engman E, Andersson-Roswall L, Svensson E, Malmgren K. Non-parametric evaluation of memory changes at group and individual level following temporal lobe resection for pharmaco-resistant partial epilepsy. J.Clin.Exp.Neuropsychol. 2004;26(7):943-54.

351. Sawrie SM, Martin RC, Kuzniecky R, Faught E, Morawetz R, Jamil F et al. Subjective versus objective memory change after temporal lobe epilepsy surgery. Neurology 1999;53(7):1511-7.

352. Morris JS, Frith CD, Perrett DI, Rowland D, Young AW, Calder AJ et al. A differential neural response in the human amygdala to fearful and happy facial expressions. Nature 1996;383(6603):812-5.

353. Vuilleumier P, Armony JL, Driver J, Dolan RJ. Effects of attention and emotion on face processing in the human brain: an event-related fMRI study. Neuron 2001;30(3):829-41.

354. Breiter HC, Etcoff NL, Whalen PJ, Kennedy WA, Rauch SL, Buckner RL et al. Response and habituation of the human amygdala during visual processing of facial expression. Neuron 1996;17(5):875-87.

355. Whalen PJ, Rauch SL, Etcoff NL, McInerney SC, Lee MB, Jenike MA. Masked presentations of emotional facial expressions modulate amygdala activity without explicit knowledge. J.Neurosci. 1998;18(1):411-8.

356. Lichtheim L. On aphasia. Brain 1885;7:433-84.

357. Ludwig E, Klinger J. Atlas Cerebri Humani. Basel: 1956.

358. Geschwind N. The organization of language and the brain. Science 1970;170(961):940-4.

359. Galaburda AM, LeMay M, Kemper TL, Geschwind N. Right-left asymmetrics in the brain. Science 1978;199(4331):852-6.

360. Geschwind N, Levitsky W. Human brain: left-right asymmetries in temporal speech region. Science 1968;161(837):186-7.

361. Habib M, Robichon F, Levrier O, Khalil R, Salamon G. Diverging asymmetries of temporo-parietal cortical areas: A reappraisal of Geshwind/Galaburda theory. Brain Language 1995;48:238-58.

362. Galaburda AM, Sanides F, Geschwind N. Human brain. Cytoarchitectonic left-right asymmetries in the temporal speech region. Arch.Neurol. 1978;35(12):812-7.

363. Barrick TR, Mackay CE, Prima S, Maes F, Vandermeulen D, Crow TJ et al. Automatic analysis of cerebral asymmetry: an exploratory study of the relationship between brain torque and planum temporale asymmetry. Neuroimage. 2005;24(3):678-91.

364. Johansen-Berg H, Behrens TE, Sillery E, Ciccarelli O, Thompson AJ, Smith SM et al. Functional-anatomical validation and individual variation of diffusion tractography-based segmentation of the human thalamus. Cereb.Cortex 2005;15(1):31-9.

365. Beauchamp MS, Argall BD, Bodurka J, Duyn JH, Martin A. Unraveling multisensory integration: patchy organization within human STS multisensory cortex. Nat.Neurosci. 2004;7(11):1190-2.

366. Beauchamp MS, Lee KE, Argall BD, Martin A. Integration of auditory and visual information about objects in superior temporal sulcus. Neuron 2004;41(5):809-23.

367. van Atteveldt N, Formisano E, Goebel R, Blomert L. Integration of letters and speech sounds in the human brain. Neuron 2004;43(2):271-82.

368. Hikosaka K, Iwai E, Saito H, Tanaka K. Polysensory properties of neurons in the anterior bank of the caudal superior temporal sulcus of the macaque monkey. J.Neurophysiol. 1988;60(5):1615-37.

369. Marinkovic K, Dhond RP, Dale AM, Glessner M, Carr V, Halgren E. Spatiotemporal dynamics of modality-specific and supramodal word processing. Neuron 2003;38(3):487-97.

370. Rademacher J, Burgel U, Geyer S, Schormann T, Schleicher A, Freund HJ et al. Variability and asymmetry in the human precentral motor system. A cytoarchitectonic and myeloarchitectonic brain mapping study. Brain 2001;124(Pt 11):2232-58.

371. Anderson B, Southern BD, Powers RE. Anatomic asymmetries of the posterior superior temporal lobes: a postmortem study. Neuropsychiatry Neuropsychol.Behav.Neurol. 1999;12(4):247-54.

372. Watkins KE, Paus T, Lerch JP, Zijdenbos A, Collins DL, Neelin P et al. Structural asymmetries in the human brain: a voxel-based statistical analysis of 142 MRI scans. Cereb.Cortex 2001;11(9):868-77.

373. Buchel C, Raedler T, Sommer M, Sach M, Weiller C, Koch MA. White matter asymmetry in the human brain: a diffusion tensor MRI study. Cereb.Cortex 2004;14(9):945-51.

374. Hutsler J, Galuske RA. Hemispheric asymmetries in cerebral cortical networks. Trends Neurosci. 2003;26(8):429-35.

375. Hickok G, Poeppel D. Towards a functional neuroanatomy of speech perception. Trends Cogn Sci. 2000;4(4):131-8.

376. Wise RJ, Scott SK, Blank SC, Mummery CJ, Murphy K, Warburton EA. Separate neural subsystems within 'Wernicke's area'. Brain 2001;124(Pt 1):83-95.

377. Matsumoto R, Nair DR, LaPresto E, Najm I, Bingaman W, Shibasaki H et al. Functional connectivity in the human language system: a cortico-cortical evoked potential study. Brain 2004;127(Pt 10):2316-30.

378. Powell HW, Guye M, Parker GJ, Symms MR, Boulby P, Koepp MJ et al. Noninvasive in vivo demonstration of the connections of the human parahippocampal gyrus. Neuroimage. 2004;22(2):740-7.

379. Hermann B, Seidenberg M. Executive system dysfunction in temporal lobe epilepsy: effects of nociferous cortex versus hippocampal pathology. J.Clin.Exp.Neuropsychol. 1995;17(6):809-19.

380. Nucifora PG, Verma R, Melhem ER, Gur RE, Gur RC. Leftward asymmetry in relative fiber density of the arcuate fasciculus. Neuroreport 2005;16(8):791-4.

381. Werring DJ, Toosy AT, Clark CA, Parker GJ, Barker GJ, Miller DH et al. Diffusion tensor imaging can detect and quantify corticospinal tract degeneration after stroke. J.Neurol.Neurosurg.Psychiatry 2000;69(2):269-72.

382. Shimony JS, Burton H, Epstein AA, McLaren DG, Sun SW, Snyder AZ. Diffusion Tensor Imaging Reveals White Matter Reorganization in Early Blind Humans. Cereb.Cortex 2005.

383. Rovaris M, Gass A, Bammer R, Hickman SJ, Ciccarelli O, Miller DH et al. Diffusion MRI in multiple sclerosis. Neurology 2005;65(10):1526-32.

384. Eriksson SH, Rugg-Gunn FJ, Symms MR, Barker GJ, Duncan JS. Diffusion tensor imaging in patients with epilepsy and malformations of cortical development. Brain 2001;124(Pt 3):617-26.